

Universiteit
Leiden
The Netherlands

Understanding disease suppressive soils: molecular and chemical identification of microorganisms and mechanisms involved in soil suppressiveness to Fusarium culmorum of wheat

Ossowicki, A.S.

Citation

Ossowicki, A. S. (2021, June 1). *Understanding disease suppressive soils: molecular and chemical identification of microorganisms and mechanisms involved in soil suppressiveness to Fusarium culmorum of wheat*. Retrieved from https://hdl.handle.net/1887/3180746

Version:	Publisher's Version
License:	Licence agreement concerning inclusion of doctoral thesis in the Institutional Repository of the University of Leiden
Downloaded from:	https://hdl.handle.net/1887/3180746

Note: To cite this publication please use the final published version (if applicable).

Cover Page



Universiteit Leiden



The handle https://hdl.handle.net/1887/3180746 holds various files of this Leiden University dissertation.

Author: Ossowicki, A.S.
Title: Understanding disease suppressive soils: molecular and chemical identification of microorganisms and mechanisms involved in soil suppressiveness to Fusarium culmorum of wheat
Issue Date: 2021-06-01



Understanding disease suppressive soils

Molecular and chemical identification of microorganisms and mechanisms involved in soil suppressiveness to *Fusarium culmorum* of wheat

Adam Ossowicki

NIOO
NEDERLANDS INSTITUUT VOOR ECOLOGIE (NIOO-KNAW)
NETHERLANDS INSTITUTE OF ECOLOGY (NIOO-KNAW)

Understanding disease suppressive soils

Molecular and chemical identification of microorganisms and mechanisms involved in soil suppressiveness to Fusarium culmorum of wheat

Adam Stanisław Ossowicki

Promotoren

Prof.dr. J.M. Raaijmakers

Prof.dr. P. Garbeva (Netherlands Institute of Ecology; NIOO-KNAW)

Promotiecommissie

Prof.dr. G.P. van Wezel

Prof.dr.ir. T.M. Bezemer

Dr. D.E. Rozen

Prof. dr. G.B. de Deyn (Wageningen University and Research)

Prof. dr. G.A. Kowalchuk (Universiy of Utrecht)

Dr. M. Haubjerg Nicolaisen (University of Copenhagen)

Understanding disease suppressive soils

Molecular and chemical identification of microorganisms and mechanisms involved in soil suppressiveness to Fusarium culmorum of wheat

Proefschrift

ter verkrijging van

de graad van doctor aan de Universiteit Leiden,

op gezag van rector magnificus prof.dr.ir. H. Bijl,

volgens besluit van het college voor promoties

te verdedigen op dinsdag 1 Juni 2021

klokke 13.45 uur

door

Adam Stanisław Ossowicki

geboren te Gdynia, Polen

in 1988

Copyright© 2021, Adam Stanisław Ossowicki
Understanding disease suppressive soils: molecular and chemical identification of microorganisms and mechanisms involved in soil suppressiveness to Fusarium culmorum of wheat
The research described in this thesis was performed at the Department of Microbial Ecology, NIOO-KNAW, Wageningen, The Netherlands; Adam Ossowicki was supported by NWO ALWGR. 2015.1b grant.
Cover painting: Emma Lodes
Design: Adam Ossowicki
Printed by: Proefschriftmaken
This is NIOO Thesis Number 187
ISBN: 978-94-6423-290-5

This dissertation, or parts of, may be reproduced freely for scientific and educational purposes as long as the source of the material is acknowledged.

The sky is not always blue, especially when it rains.

Nie zawsze niebo jest niebieskie, szczególnie kiedy pada deszcz.

T. Pełczyński

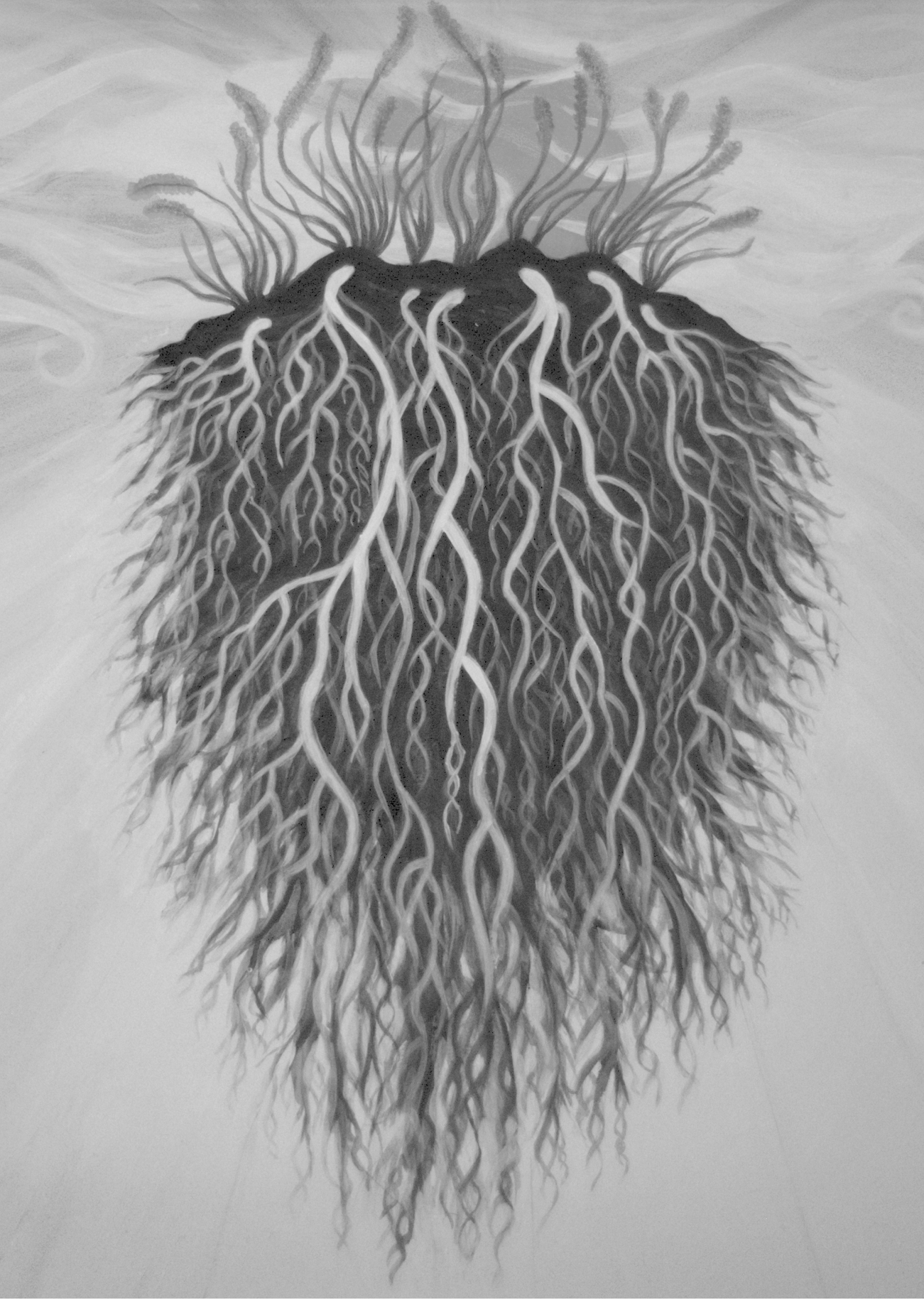


Table of Contents

Chapter 1

General introduction and thesis outline 9

Chapter 2

Microbial and volatile profiling of soils suppressive to *Fusarium culmorum* of wheat 25

Chapter 3

Dissecting disease-suppressive rhizosphere microbiomes by functional amplicon sequencing and 10X metagenomics 63

Chapter 4

Deciphering the microbiome of disease suppressive soils by dilution-to-extinction 93

Chapter 5

Impact of plastic mulch film residues on soil microbiome, disease suppressiveness, and plant growth 131

Chapter 6

General and summarizing discussion 151

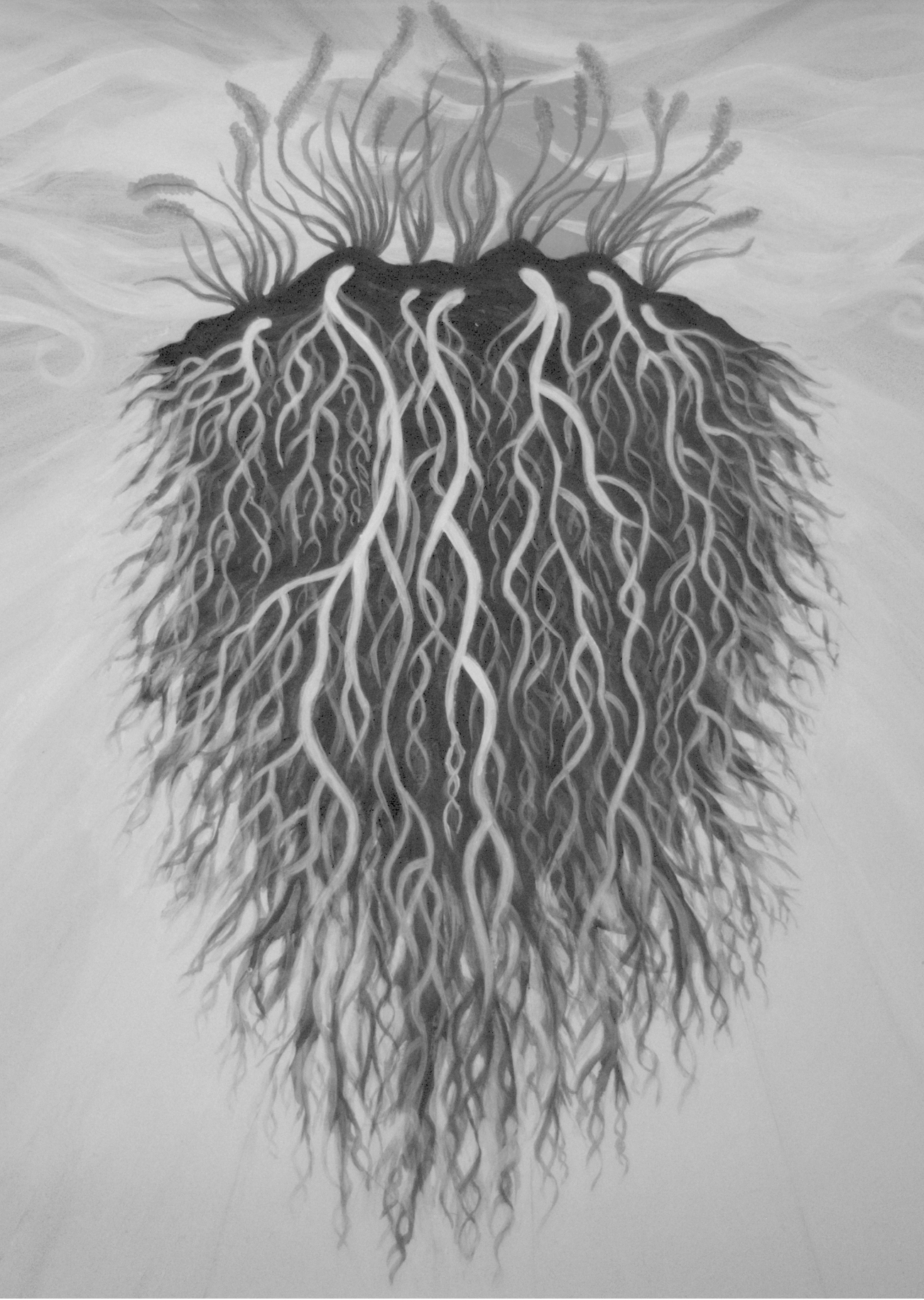
References 163

Summary 190

Streszczenie 193

Curriculum Vitae 195

Publications 196



Chapter 1

General introduction and thesis outline

A part of this chapter in modified version was submitted for publication

Soil – a habitat of microbes

Soil – the thin top layer of the Earth's surface – is so common that often we do not think about it as an ecosystem with diverse life support functions. On a global scale, soil supports life on our planet by cleaning our drinking water, degrading toxic compounds, recycling of nutrients, and protecting plants from pests and diseases. These functions of this fascinating yet highly complex and heterogeneous world beneath our feet are largely governed by microorganisms with an estimated number of around 10^9 bacteria cells and up to 50,000 bacterial taxa in just one gram of soil (Roesch et al., 2007; Wagg et al., 2014). Together with other (micro)organisms like fungi, archaea, protists and viruses they constitute an enormous richness of microbial life (Tecon and Or, 2017). Soil environments can be remarkably diverse depending on their geographic location and the history of land use, but they are typically composed of a solid fraction (minerals), organic matter, live organisms, and water or gas-filled pores (Díaz-Zorita et al., 2002; Tecon and Or, 2017). A large contribution to the heterogeneity of the soil environments comes from the formation of aggregates with different physical and chemical characteristics (Rillig et al., 2017). Is it easy to be a microorganism in the soil? Certainly, living in the soil offers a variety of resources and diverse niches that are colonized cooperatively or in competition with other organisms (Pande and Kost, 2017; Vos et al., 2013). For more than three hundred years, we isolate and grow soil bacteria under laboratory conditions. Already thousands of bacterial species have been catalogued and preserved, but this is just the tip of the iceberg: most likely the vast majority of soil microorganisms do not survive extraction from their natural environments or can be cultivated in artificial media (Hofer, 2018; Pande and Kost, 2017). Despite these limitations, however, new sequencing technologies have enabled us to explore the unculturable and yet unknown fraction of the soil microbiome.

Microbial life at the interface between soil and plants

Plant roots live in a close relationship with soil microbes and both sides of this relationship rely on each other. Plants recruit microorganisms from the reservoir present in the soil, creating a specialized environment around their roots. This specific ecosystem, called the rhizosphere, is strongly influenced by root exudates containing various substrates that can constitute up to 40% of the plant's fixed carbon (D. L. Jones et al., 2009; Rillig and Mummey, 2006). Compared to the bulk soil (i.e. soil without plant roots), the microbial communities in the rhizosphere are substantially more numerous (approximately 10 to 100-fold higher) but taxonomically less diverse; this is called the rhizosphere effect (Bakker et al., 2013; Mendes et al., 2013; Minz et al., 2013). The rhizosphere communities are a subset of the microbes residing in the soil possibly complemented with endophytic microorganisms residing inside the germinating seeds, and their composition depends on the plant species or even genotype within a given plants species (Berg and Smalla, 2009; Hartmann et al.,

2009). What kinds of microbes do plants select in the rhizosphere? From an evolutionary perspective, plants are expected to recruit and support microorganisms that are beneficial for their growth, development and health. Hence, various rhizosphere microorganisms have been identified that exhibit beneficial functions for plants such as promoting germination of seeds (13), nutrient acquisition (Brussaard, 2012; *Soil Microbiology, Ecology and Biochemistry*, 2015), growth promotion via the production of phytohormones (Babalola, 2010; MacMillan, 2001; Saleem et al., 2007; Sousa and Olivares, 2016), inducing the plant's systemic resistance to infection (Bakker et al., 2003; Haas and Défago, 2005; Harman et al., 2004; Pieterse et al., 2014; Sousa and Olivares, 2016; Zehnder et al., 2001), or protecting directly against infectious root pathogens (Haas and Défago, 2005; Raaijmakers et al., 2002; Raaijmakers and Mazzola, 2012; Sousa and Olivares, 2016). This latter group of pathogenic microorganisms also responds to root exudates as cues for locating a host plant for infection. Hence, it has been postulated that soil-borne pathogens and parasites have hijacked the signals that the plant developed to recruit beneficial microbes (Al-Babili and Bouwmeester, 2015; López-Ráez and Bouwmeester, 2008). Thus, there is a fragile equilibrium between the attraction of pathogenic and beneficial microorganisms. The major challenge of modern agriculture is to steer soil and rhizosphere microbiomes in such a way that they provide beneficial functions for crops while at the same time they ward off the pathogenic (micro)organisms. To this end, we need a deeper understanding of soil functioning, microbe-microbe and microbe-plant interactions (Mendes et al., 2013).

Plant pathogenic microorganisms – a threat to food security

Wheat constitutes more than 40% of all cultivated cereals in Europe and, in 2018, approximately 700 million tons of a total of 2,7 billion tons of cereals produced worldwide, providing approximately 20% of the calories intake by humans ("Food and Agriculture Organisation of the United Nations," 2020). To meet the demand of a growing human population, farming has become even more intensified with less diversity and more fertilizers and pesticides. Multi-hectare monocultures are still the preferred crop production system, but make food security highly vulnerable to pests and diseases (Ramankutty et al., 2018). Infections, once initialized, can quickly spread, taking a serious toll on yield because of genetically uniform crop species (McDonald and Stukenbrock, 2016). For wheat, it is estimated that up to 23% of the yield is lost due to diseases (Savary et al., 2019). Plant pathogenic fungi have a great share in these economic losses. In particular fungal pathogens from the genus *Fusarium* are major yield-limiting factors and also cause hazards to human and animal health via the contamination of food products with mycotoxins (Antonissen et al., 2014; Dean et al., 2012; Scherm et al., 2013).

Fusarium species are commonly found in soils worldwide and are often associated with plants. While most of the members are saprophytes, several species are considered the

most devastating soil-borne plant pathogens (Dean et al., 2012, p. 10; Moretti, 2009). *Fusarium* pathogens can infect more than 100 plant species but few pathogens, mostly *F. graminearum, F. pseudograminearum and F. culmorum*, are widespread in cereals, mostly in wheat and barley. Among the disease symptoms caused by Fusaria one can find Fusarium head blight (FHB), Fusarium root rot (FRR), stem rot, stunting, wilting due to fungal colonization of the vascular tissues or due to enzymatic degradation of the plant cell wall. One of the most important problem in cereals affected by Fusaria is the contamination with mycotoxins that are poisonous for humans, animals, and not suitable for malting (Antonissen et al., 2014; Dean et al., 2012; Goswami and Kistler, 2004; Nielsen et al., 2014). The species used in experimental work described in this thesis is *Fusarium culmorum*. The most common symptoms caused by this pathogen in cereals are FRR and FHB (Fig. 1). Root rot occurs already in the early stages of plant development, one or two weeks after germination, but *Fusarium* infection may even lead to pre-emergence seedling blight. The most prevalent mycotoxins produced by *F. culmorum* are deoxynivalenol, nivalenol, fusarenone and their derivatives. The mycotoxin profile is a basis of dividing the pathogen into chemotypes. In severely affected plant tissues, the fungus produces characteristic pink-red coloration caused by sporulating mycelium, a phenotype that is also observed in *in-vitro* cultures (Fig. 1). The macroconidia produced by *F. culmorum* are curved, between 25 to 50 µm long (Fig. 1) and easily spread by rain, wind, insects, and animals. Fusaria are difficult to eradicate because they stay viable in post-harvest plant debris in the soil even after a few seasons, waiting for a suitable host.

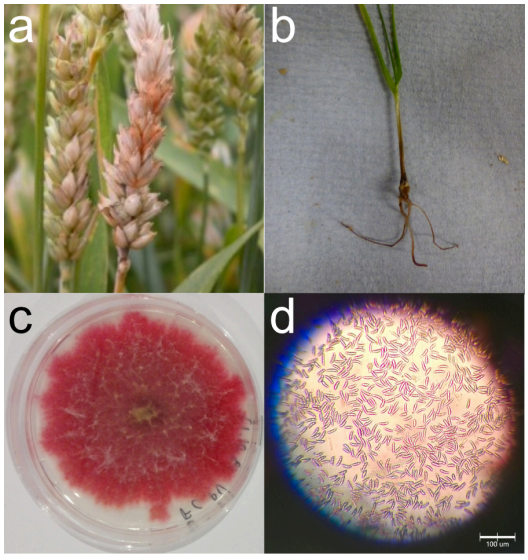


Figure 1. Characteristic disease symptoms on wheat plants caused by Fusarium culmorum: Fusarium Head Blight (a) and Fusarium Root Rot (b). Fusarium culmorum PV growing on agar media (c) and its macroconidia under light microscope (c). Photo (a) adopted from fyi.extension.wisc.edu

Soil suppressiveness - a sustainable alternative for controlling fungal diseases

The environmental impact of agriculture is already pushing the limits of Earth's resource boundaries (Campbell et al., 2017) and conventional, high-input agriculture aggravates this even further (Ramankutty et al., 2018). One of the alternatives and a big step towards sustainable agriculture is using what nature has to offer. Already for more than 100 years (Atkinson, 1892) it has been recognized that some agricultural soils are suppressive to specific soil-borne diseases including diseases caused by *Fusarium* (Alabouvette, 1986). In such soils, susceptible plants do not get diseased or only little despite the presence of a virulent pathogen and conditions that allow infection (Deacon, 1984). The nature of this phenomenon is, in most cases, microbiological and the physical and chemical properties of these soils may affect the onset and magnitude of the suppressiveness (Andrade et al., 1994; Carrion et al., 2018; Cha et al., 2016; Cook and Rovira, 1976; Duijff et al., 1999; Weller et al., 2002a; Wiseman et al., 1996). Soil disease suppressiveness has been defined as general and specific depending on the range of pathogens it protects from. General suppressiveness reduces the disease development of various pathogens and is present at some level in most soils as a result of the metabolic activity of the microbial community. The protective effect of general suppression is not transferable by soil transplantation. Specific disease suppressiveness, on the other hand, targets a specific pathogen and can be

transferred to a nonsuppressive (i.e. conducive) soil by transplantation. The protective effect is the result of the activity of select members within the soil or root-associated microbiome that are enriched in response to a disease outbreak (for review: (Alabouvette, 1986; Garbeva et al., 2004; Gomes Exposito et al., 2017; Hornby, 1983; Kwak and Weller, 2013; Schlatter et al., 2017a)). Understanding the microorganisms and mechanisms involved in disease suppressiveness can be exploited for developing new and sustainable management practices in agriculture. To this end, we need to disentangle the network of interactions in the soil- or root-associated microbiome and find the responsible microorganisms and underlying microbial traits.

Examples of suppressive soils and the microbes and mechanisms involved

Take-all decline soils

The fungus *Gaeumannomyces graminis* var. *tritici* (GGT) causes take-all disease in wheat, barley, and other cereals. Typical GGT-symptoms are brown to black lesions of root system, stunting and yellowing, the heads appear white, not producing seeds. Affected plants die prematurely within circular patches in the field. The pathogen is difficult to control by chemical pesticides, and there are also no GGT-resistant varieties of cereals yet. Soils suppressive to GGT are referred to as take-all decline (TAD) soils and are found worldwide (Kwak and Weller, 2013). TAD soils were found in the USA (Cook and Rovira, 1976; Raaijmakers and Weller, 1998), Netherlands (Bergsma-Vlami et al., 2005; Gerlagh, 1968), three different areas in Montana, USA (Andrade et al., 1994), in volcanic soils in Chile (Duran et al., 2017) and on the South Island, New Zealand (Chng et al., 2015). In most of these studies, disease suppressiveness was eliminated by pasteurization and could be transferred to a conducive soil by transplantation of 1% (w/w) of the suppressive soil. Microbiome analysis of TAD soils from Washington State (USA) and the Netherlands revealed that the suppressiveness is associated with enriched populations of fluorescent Pseudomonads that inhibit the growth of the pathogen by the production of 2,4-diacetylphloroglucinol (2,4-DAPG), also hydrogen cyanide and cyclic lipopeptides were suggested to have a role in suppressiveness (Kwak and Weller, 2013; Raaijmakers and Weller, 1998). Another proposed mode of action has its basis in the low abundance of bioavailable iron in soils where Pseudomonads compete with pathogen producing siderophores, nevertheless it was not experimentally proven. There is also evidence that 2,4-DAPG can induce systemic resistance of plants, which can constitute another mode of action of Pseudomonads in TAD soils. Nevertheless, so far this latter mechanism was only shown for *Arabidopsis thaliana* (Chae et al., 2020).

Rhizoctonia-suppressive soils

Dutch agricultural fields near Hoeven and Zwaagdijk in the Netherlands were identified as suppressive to *Rhizoctonia solani* AG2. The biological nature of suppressiveness was confirmed by heat sterilization and soil transplantation (Mendes et al., 2011). Comparative taxonomic and functional analyses between suppressive and conducive soils further revealed the importance of rhizospheric *Pseudomonadaceae* and *Burkholderiaceae,* and of endophytic *Flavobacteriaceae* and *Chitinophagaceae* in suppressiveness. Subsequent transposon mutagenesis of selected isolates from the suppressive soils led to the identification of the chlorinated lipopeptide thanamycin as a key metabolite in Rhizoctonia control by *Pseudomonas* strain SH-C52 (Mendes et al., 2011; Watrous et al., 2012), antifungal volatiles by *Burkholderia, Paraburkholderia* (Carrion et al., 2018) and *Streptomyces* (V. Cordovez et al., 2015), and a chemically unidentified compound of endophytic *Flavobacterium* (Carrión et al., 2019). Carrion et al. (2019) also reconstructed a synthetic community which was able to provide enhanced protection of sugar beet from the pathogen (Carrión et al., 2019). Moreover, in the Greenlandic potato fields, suppressiveness to *Rhizoctonia solani* AG3 was observed with no significant disease symptoms for even 50 years. Bioassays with agricultural soil from Inneruulalik demonstrated that the damping-off symptoms caused by *R. solani* on tomato were indeed minor and the disease suppressive effect was eliminated by sterilization and transferred to conducive soil by a soil transplant. Detailed *in-vitro* analysis of a bacterial strain collection from this suppressive soil revealed a *Pseudomonas fluorescens* strain In5 with strong antifungal activity towards *R. solani* AG3. In a microcosm experiment, where strain In5 was introduced to the soil, Michelsen *et al.* showed protective effects at In5 population densities less than 1% of the bacterial community (Michelsen et al., 2015). Genomic and metabolomic analysis of strain In5 revealed a gene cluster and corresponding metabolite, referred to as nunamycin, which were highly similar to the BGC and thanamycin compound identified in *Pseudomonas* SH-C52 from the Dutch *Rhizoctonia*-suppressive soil described above.

Different anastomosis group *Rhizoctionia solani* - AG8 is a pathogen of grain crops, mostly wheat and barley, causing root rot and stunting of seedlings called bare patch disease. The pathogen is difficult to control because of its wide host range, lack of resistant crop varieties and the survival structures referred to as sclerotia (Barnett et al., 2017; Cook et al., 2002). Suppressive soils to *R. solani* AG8 were identified for the first time in South Australia (Roget, 1995) and confirmed as (micro)biological in nature and transferable (Wiseman et al., 1996). Using a high throughput screening with an *in-vitro* pathosystem, Barnett et al. isolated a variety of fungal and bacterial strains assigned to *Aspergillus*, *Cylindrocarpon*, *Trichoderma*, *Bacillus*, *Paenibacillus*, *Microbacterium*, *Streptomyces, Pandoraea*, *Brevibacterium*, *Chryseobacterium*, *Phyllobacterium* and *Pseudomonas* able to provide protection against *R. solani* AG8 and growth promotion of wheat (Barnett et al., 2017). Later

metatranscriptomics analysis revealed higher expression of oxidative stress related genes and polyketide cyclases in suppressive soil compared to the conducive soil, indicating possible mechanisms of suppression (Hayden et al., 2018). Moreover, a metabolomics approach using liquid chromatography and nuclear magnetic resonance to discriminate between suppressive and non-suppressive soils to AG8 indicated antifungal secondary metabolites macrocarpals to be soil suppressiveness biomarkers (Hayden et al., 2019). Another *R. solani* AG8 suppressive soil was recognized in the Pacific Northwest of the USA where Schillinger and Paulitz demonstrated that bare patch disease can be suppressed by natural microflora in long-term cropping systems (Schillinger and Paulitz, 2013). In a subsequent study the role of bacterial communities was found instrumental in developing disease suppressiveness with higher frequencies of *Acidobacteria* and *Gemmatimonas* in the rhizosphere of healthy plants (Yin et al., 2013).

Fusarium-suppressive soils

Fusarium oxysporum infects many vegetables and fruits causing wilting. Based on the host range, the pathogen is further classified as *formae speciales* (*f. sp.*). Symptomatic plants show chlorosis, necrosis, premature leaf drop, stunting and damping-off as a result of the fungus colonizing their vascular system (Bosland, 1988). Fusarium wilt suppressive soils of strawberry were identified in South Korea (Cha et al., 2016), and of banana in Northern Hainan Island, China (Ou et al., 2019). The Fusarium-suppressive soils in the Châteaurenard region in France has been studied since the 1970s. Also, in that case, suppressiveness was eliminated by sterilization and transferred to conducive soil by a transplant of 1-2% (w/w). Two of the key microorganisms associated with suppressiveness of the Châteaurenard soil are non-pathogenic *Fusarium oxysporum* and fluorescent *Pseudomonas* species. The major mechanisms are competition for organic carbon and for iron. These two mechanisms complement each other, the production of siderophores by Pseudomonads regulates the availability of iron, while the availability of iron is proportional to the intensity of competition for carbon between pathogenic and non-pathogenic Fusaria (Alabouvette, 1999, 1986; Alabouvette et al., 2009; Cha et al., 2016; Lemanceau et al., 1992; Mazurier et al., 2009, 2009; Siegel-Hertz et al., 2018a).

Disentangling the microbiome of suppressive soils by perturbation

To resolve the functioning of microbial communities in disease-suppressive soils is challenging because of the taxonomic and functional complexity as well as the spatial-temporal dynamics of root-associated microbiomes. Nevertheless, there is a fragile balance in their functioning in response to external factors that we can use to our advantage in studying the microbial and mechanistic basis of suppressive soils. Perturbation is a promising tool to disentangle microbial communities and understand their functions. By

applying a selective pressure that perturbs the microbiome, we can generate a compositional shift and a simplification of a complex microbial community in a controlled way. This simplification reduces the microbiome diversity, disrupts the activity of specific members of the microbiome and/or alters the communication and interactions within the microbiome and between the microbiome, the plant and the pathogen. Perturbation methods are culture-independent and therefore the preferred choice for soil microbiome analyses where the majority of taxa appear to be unculturable. Here, I present an overview of different microbiome perturbation approaches, in particular selective heat, selective biocides and dilution-to-extinction (Fig. 2).

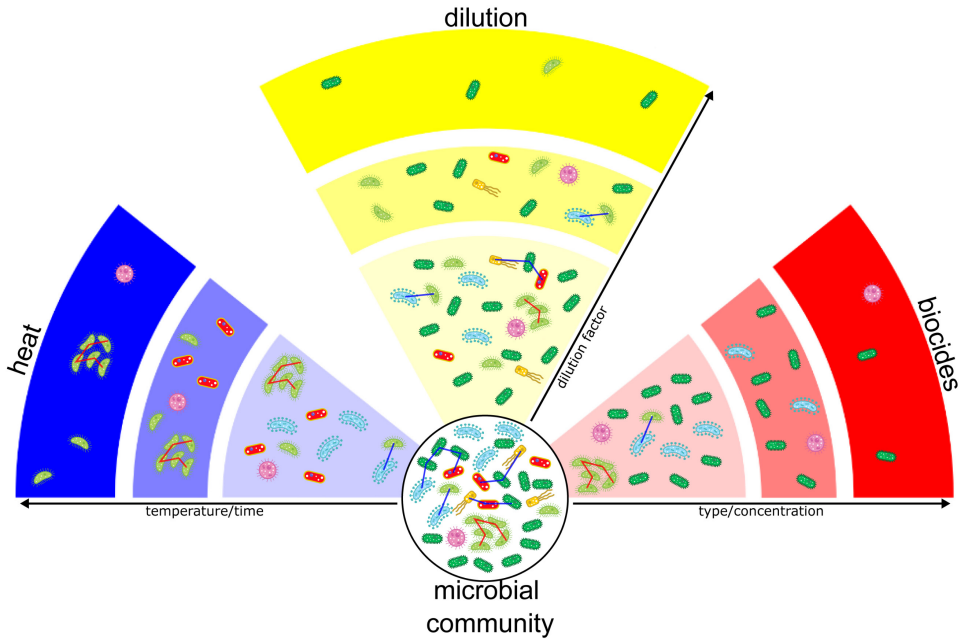


Figure 2. A schematic representation of three perturbation techniques and their effect on a soil microbiome. The original microbial community is presented in the circle. It is composed of six bacterial species with different abundance, from highly abundant (dark green), to rare species (pink). The interactions between bacteria are represented as lines connecting microbes, intraspecific with red and interspecific with blue lines. The intensity of the perturbation grows outwards from the inner circle and is represented in three levels with gradually darker colours. As we can see on the figure, regardless of the perturbation technique used, the microbial community gets simplified, the number of species decreases, and the interactions are disturbed. Blue part - *heat can be used for sterilization, but when applied in sublethal temperature and exposure times it can result in a subset of the original community that is composed of mostly organisms with higher*

resilience to changing temperature and organisms able to produce some heat resistance survival forms (e.g., spores). Red part - *Some groups of microorganisms can be eliminated from the original microbial community by the application of biocides in specific concentrations. That treatment will eliminate the groups of bacteria that are susceptible to the compound. We can also attempt to engineer the microbiome using a combination of antibiotics if the presence of antibiotic resistance genes in a microbial community is known from molecular studies. Yellow part - The dilution-to-extinction technique where the microbial community is distributed stochastically in a series of dilutions. This technique is unspecific and the presence of the groups of microorganisms in consecutive dilutions mostly depends on their initial abundance.*

Heat treatment

Elevated temperatures cause substantial mortality (30-60%) in a microbial community and leaves empty niches ready to be colonized by those microorganisms that survived the heat. The mortality rate depends on the method used to elevate the temperature and exposure time. Firmicutes, Actinobacteria and other Gram-positive bacterial phyla forming survival structures are typically the first to recover from elevated temperatures. The second bacterial phyla to colonize the new environment is Proteobacteria, which typically consists of fast-growing bacterial genera able to quickly multiply and use a broad spectrum of nutritional resources. The community structure in a heat-treated soil microbiome, measured as diversity and evenness, is unlikely to come back to the initial point even weeks after the disturbance (Jurburg et al., 2017a, 2017b). Riah-Anglet et al. (2015) further investigated the functions of microbial communities after a heat stress by measuring enzymatic activity. Their experiment showed substantial changes in functions and taxa composition. Soil microbiomes did not fully restore their β-glucosidase, cellulase, N-acetyl-glucosaminidase, and dehydrogenase activities within 4 weeks after the heat disturbance, which was associated with decreased abundance of Actinobacteria, Acidobacteria and Planctomycetes. They also showed, based on a marker-gene copy number study, that soil fungal communities are more susceptible to the heat stress than bacteria, and that the physical parameters and chemical composition of the soil have a major impact on the perturbed community (Riah-Anglet et al., 2015). The effect of heat treatment on microbiome assembly in a suppressive soil was investigated by Van der Voort et al (2016) indicating heat tolerance and growth rate of bacteria as key traits influencing rearrangement of microbial community after the perturbation. This paper also suggested that elimination of suppressiveness to *R. solani* by heat treatment was associated with a decrease in abundance of three Actinobacteria families: Streptomycetaceae, Micrococcaceae and Mycobacteriaceae (van der Voort et al., 2016). The effect of a heat shock on rare soil taxa was examined by Kurm et al., providing an indication that low

abundance taxa can benefit from the disturbance. In their study, taxa classified as rare (< 0,01% relative abundance) increased their relative abundance even to above 1% (Kurm et al., 2019).

Biocides

Chemical substances used for control of potentially harmful living organisms in medicine, agriculture and industry are collectively named biocides. We can include in that group pesticides (e.g., fungicides, insecticides) and antimicrobials (e.g., antibiotics). The majority of studies on biocides concerns the impact of antibiotics on gut microbiome and human health (for review: (Blaser, 2016; Francino, 2016; Schwartz et al., 2020)). The influence of biocides on soil and rhizosphere microbiomes has been mostly studied in the context of antibiotic and fungicide spills into the environment from anthropogenic sources, like agriculture and industry (Cycoń et al., 2019). Nevertheless, the application of biocides is also a valuable tool for investigating the functionalities of soil microbiomes. Recently, Dong et al. (2020) described the impact of different classes of antibiotics on soil bacteriomes and the stability of antibiotics in the soil (Dong et al., 2020). Their study showed the minor effect of easily degradable antibiotics on soil bacteria communities, the significant growth inhibition of phyla Firmicutes and Bacteroidetes by nalidixic acid and of the phyla Firmicutes, Bacteroidetes and Cyanobacteria by tetracycline. These two antibiotics also have a negative impact on overall bacteria diversity. It is also worth noting that tetracycline, ceftriaxone and nalidixic acid caused an increase in the relative abundance of some classes of *Proteobacteria*. In recent work Lee et al. investigated the effect of vancomycin on biological disease suppression to bacterial wilt disease caused by *Ralstonia solanacearum*. Their results show that vancomycin alter microbial community of suppressive soil via disturbing the protective effect conferred by Firmicutes and Actinobacteria (Lee et al., 2020). Using biocides to perturbate the soil microbiome in a controlled way depends a lot on experimental setup. One should take into consideration following factors: stability of the biocides, dispersion in the system, heat or light resistance, and impact of by-products of metabolism and degradation.

Dilution-to-extinction

The dilution technique allows us to perturbate the microbiome in an untargeted way. Diluted microbial communities contain a subset of the original one that is smaller as the dilution factor increases. Between consecutive dilutions, members of the microbiome (species) distribute stochastically, reducing the diversity and possibly losing some species. Most of the soil microbiome dilution experiments described to date use sterile water or water-based buffer to extract the microbial community and later as a diluent (Chen et al., 2020; Garland and Lehman, 1999; Hol et al., 2015; Korenblum et al., 2020; Peter et al., 2011;

Yan et al., 2017; Zegeye et al., 2019). This way, the communities are serially diluted up to 10^9 times depending on the study. Microbiome dilutions are mostly introduced to a sterile soil and incubated for a certain time before any further testing. It is also possible to dilute the soil microbiome without extraction using sterile soil as a diluent.

Studies published to date, show the decrease of taxonomic and functional diversity along the dilution series. For example, Yan et al. compared the taxonomic structure of the diluted soil microbial community before introducing it to the soil and after 8 weeks of incubation in the soil. They showed that microbiome dilution leads to a significant change in microbiome assembly over time, but its structure cannot be predicted based on the taxonomic composition of the inoculum (Yan et al., 2015). In the follow-up study, Yan et al. analyzed the functional potential of the microbiome over the dilution series using *in-silico* function prediction and showed the relative stability of functions in the rhizosphere. They indicated the strong selective power of the rhizosphere towards general functions (Yan et al., 2017). The changes in various soil/plant traits and functions were also measured in diluted microbial communities by sequencing-independent methods. The carbon source respiration tests showed a non-linear reduction in the number of the utilized carbon sources in diluted soil microbiomes. Serial dilution of a chitin-enriched soil microbial community revealed the importance of initial community complexity on the future stability of microbiome (Zegeye et al., 2019). The impact of the soil microbiome dilution on plants was also investigated. Chen et al. indicated that the loss of bacterial diversity, being a result of the dilution, may have a negative correlation with plant productivity, using lettuce as a model (Chen et al., 2020). Another study investigated how the root microbiome modulates the systemic induction of root exudation of metabolites in tomato. Authors showed that the reduction of microbiome diversity and composition, obtained by dilution-to-extinction, resulted in exudation of particular metabolite profiles. They demonstrated that the rhizosphere microbiome assembly drives the systemically induced exudation process at the molecular and chemical level (Korenblum et al., 2020). The only study, at least to our knowledge, that used the dilution-to-extinction approach in relation to plant protection against pathogens is the study by Hol et al. They diluted microbial communities from agricultural soils and tested these in the context of volatile-mediated inhibition of plant pathogens (Hol et al., 2015). They showed that emission of volatile compounds in soil was one of the factors contributing to overall soil disease suppressiveness. The role of volatiles in *Fusarium*-suppressive soils is also addressed in the second chapter of this thesis.

Dilution-to-extinction proved to be a good tool to manipulate natural soil microbiomes. Unlike other methods, it allows us to manipulate the diversity of a community and track diversity-related microbiome characteristics like, network structure or functional redundancy. In combination with -omics techniques dilution-to-extinction makes a powerful tool to investigate the mechanisms of soil functions.

Other methods used for microbiome perturbation

In recent years we see fast advances in genome editing tools based on CRISPR-Cas system. This method can be used to edit genomes microorganisms, control gene expression, modulate the production of metabolites and proteins and specifically eliminate members of the microbiome (Ramachandran and Bikard, 2019). So far, targeted microbiome perturbation using CRISPR-Cas editing capabilities were successfully used for microbiome studies for strain-specific depletion in mouse gut microbiome (Lam et al., 2020). In the field of plant-microbe interactions, it was used in the work of Carrion et al., where a specific gene cluster in a member of the plant protective synthetic community was perturbated in a targeted way using a SpyCas9-mediated system. This community was able to protect sugar beet from *Rhizoctonia solani,* but partially lost this ability after the elimination of a specific gene encoding a NRPS/PKS biosynthetic gene cluster (Carrión et al., 2019)**.** A totally different approach to study soil microbiome functions was presented recently by Naylor et al. where a soil microbiome was enriched in functions by using different nutritional and growth conditions. This work presents an intriguing set of different "functional modules" and their implications for the bacteria community (Naylor et al., 2020).

In conclusion, various perturbation methods have proven to be a valuable tool to manipulate natural soil and plant-associated microbiomes. These methods allow us to manipulate the diversity of a microbial community and track diversity-related microbiome characteristics like, network structure or functional redundancy. In combination with different -omics techniques, perturbation presents a powerful tool to deconstruct the functionalities of soil and plant microbiomes and to disentangle the microbes and mechanisms responsible for specific soil functions, including disease suppressiveness.

Thesis outline

The overall aim of my thesis is to disentangle the microorganisms and mechanisms involved in disease suppressiveness to *Fusarium culmorum* of wheat. To this end I integrated various approaches and techniques to identify the taxonomic groups of bacteria, their biosynthetic gene clusters and metabolites associated with this intriguing microbiome-associated plant phenotype.

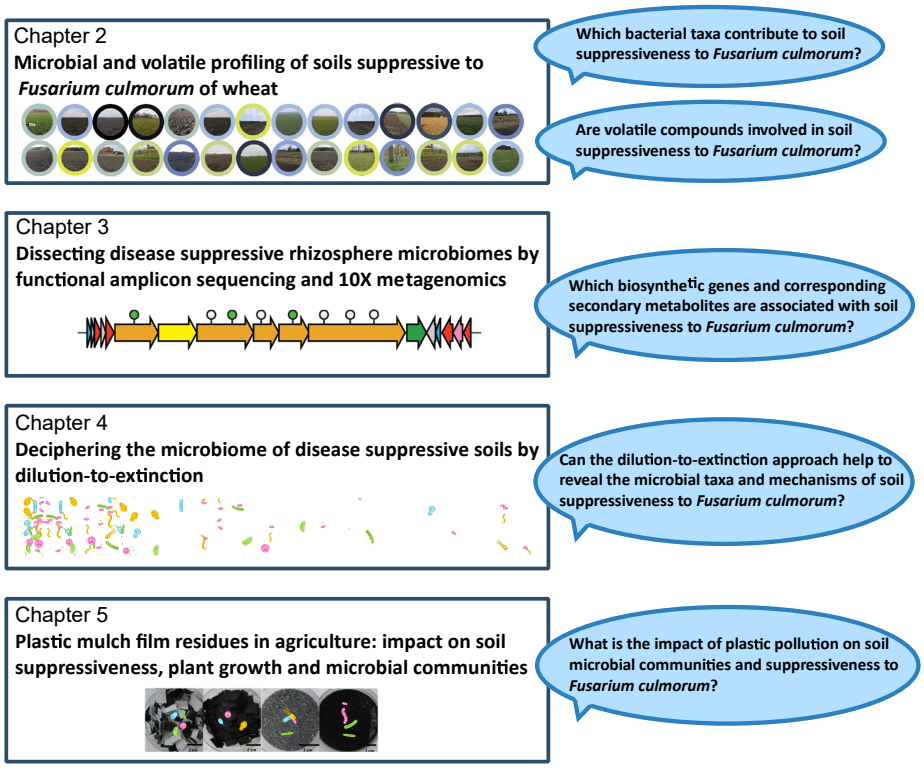


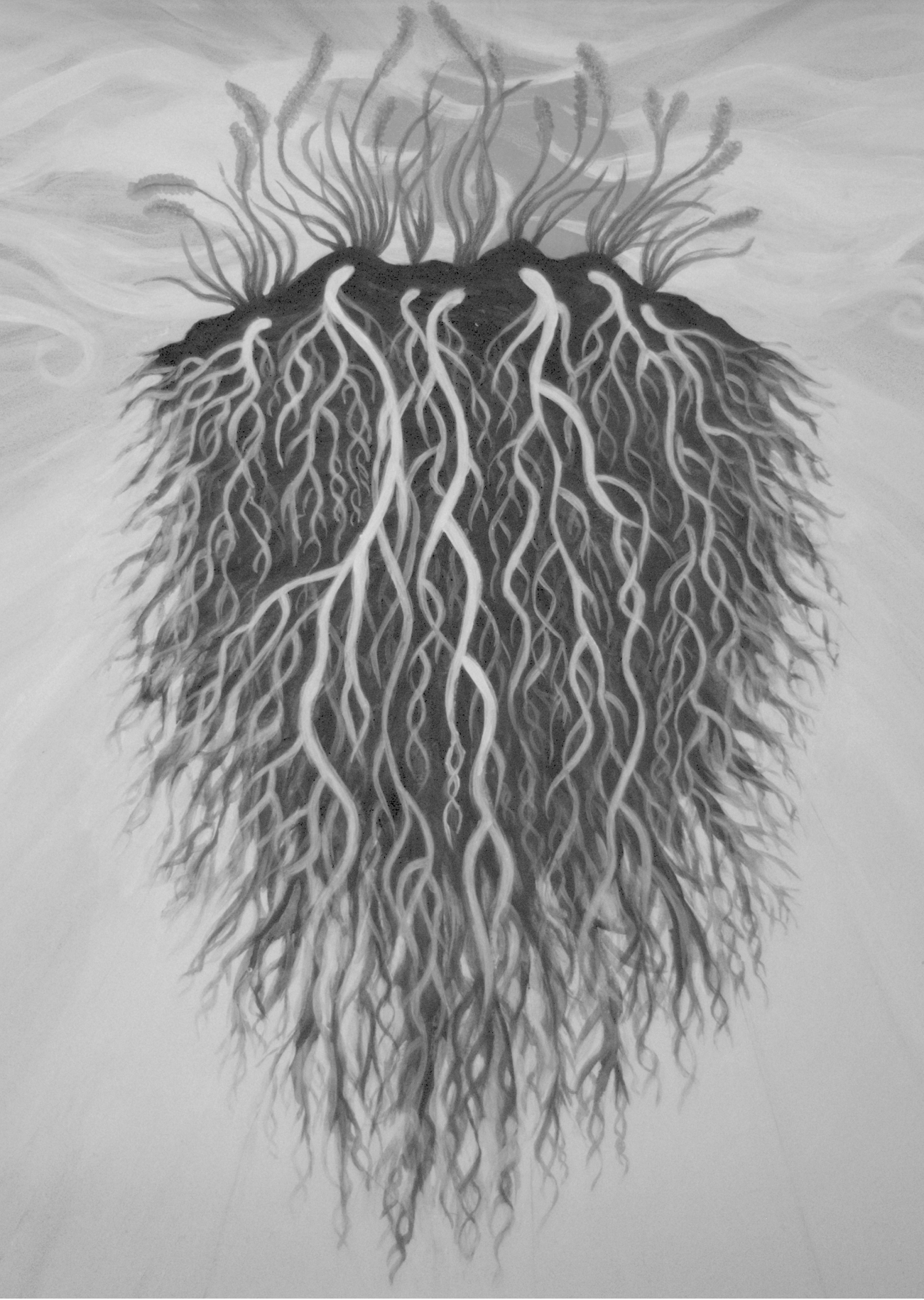
Fig. 3. Thesis outline with the main research questions addressed in each chapter

The first chapter of my thesis introduces the topic of suppressive soils and describes its importance for sustainable agriculture and food security. In **the second chapter**, we built and characterized a collection of diverse soil samples and evaluated their disease suppressiveness to *Fusarium culmorum,* an economically important fungal root pathogen of wheat. Subsequently, we analyzed the taxonomic diversity of the soil and rhizosphere microbiomes as well as the emitted volatile profiles of these soils. In **chapter 3,** we extended the approach of taxonomic profiling of bacteria in suppressive soils by adopting an extensive functional amplicon analysis focusing on adenylation domains of non-ribosomal peptide

synthetases and polyketide synthases. These domains are parts of biosynthetic gene clusters encoding modular enzymes used by microorganisms to synthetize non-ribosomal peptides and polyketides, metabolites that are often associated with disease suppressiveness. In **chapter 4,** we make use of the dilution-to-extinction approach to further deconstruct the microbiome of one of the *Fusarium*-suppressive soil. A combination of deep metagenomic sequencing and phenotypic analysis of diluted microbiomes gave additional insight into the microbes and putative functions by which the plants are protected from *Fusarium* root rot. In **chapter 5,** we evaluated the impact of plastic mulching film debris on wheat growth and suppressiveness to *Fusarium culmorum* and how this is reflected in changes in the microbial community of the suppressive soil.

Key questions addressed in this thesis:

- Which bacterial taxa contribute to soil suppressiveness to *Fusarium culmorum*?
- Are volatile compounds involved in soil suppressiveness to *Fusarium culmorum*?
- Which biosynthetic genes and corresponding secondary metabolites are associated with soil suppressiveness to *Fusarium culmorum*?
- Can the dilution-to-extinction approach help to reveal the microbial taxa and mechanisms of soil suppressiveness to *Fusarium culmorum*?
- What is the impact of plastic pollution on soil microbial communities and suppressiveness to *Fusarium culmorum*?



Chapter 2

Microbial and volatile profiling of soils suppressive to *Fusarium culmorum* of wheat

Adam Ossowicki[1*], Vittorio Tracanna[2*], Marloes L. C. Petrus[3], Gilles van Wezel[3], Jos M. Raaijmakers[1,3], Marnix H. Medema[2#] and Paolina Garbeva[1#]

1. Department of Microbial Ecology, Netherlands Institute of Ecology (NIOO-KNAW), Wageningen, The Netherlands
2. Bioinformatics Group, Wageningen University, Wageningen, The Netherlands
3. Institute of Biology, University of Leiden, Leiden, The Netherlands

Published in Proceedings of the Royal Society B
https://doi.org/10.1098/rspb.2019.2527

Abstract

In disease-suppressive soils, microbiota protect plants from root infections. Bacterial members of this microbiota have been shown to produce specific molecules that mediate this phenotype. To date, however, studies have focused on individual suppressive soils and the degree of natural variability of soil suppressiveness remains unclear. Here, we screened a large collection of field soils for suppressiveness to *F. culmorum* using wheat (*Triticum aestivum*) as a model host plant. A high variation of disease suppressiveness was observed, with 14% showing a clear suppressive phenotype. The microbiological basis of suppressiveness to *F. culmorum* was confirmed by gamma-sterilization and soil transplantation. Amplicon sequencing revealed diverse bacterial taxonomic compositions and no specific taxa were found exclusively enriched in all suppressive soils. Nonetheless, co-occurrence network analysis revealed that two suppressive soils shared an overrepresented bacterial guild dominated by various *Acidobacteria*. In addition, our study revealed that volatile emission may contribute to suppression, but not for all suppressive soils. Our study raises new questions regarding the possible mechanistic variability of disease suppressive phenotypes across physicochemically different soils. Accordingly, we anticipate that larger-scale soil profiling, along with functional studies, will enable a deeper understanding of disease suppressive microbiomes.

Introduction

The phenomenon of soil disease suppressiveness has been recognized for almost a century and was first defined by Cook and Baker (Cook and Baker, 1983) as soils where a particular soil-borne disease does not develop, despite the presence of the virulent pathogen, a susceptible host and favorable conditions for disease development. Physical and chemical properties of the soil can play a role in this phenomenon, but in many cases disease suppressiveness is microbial in nature (Andrade et al., 2011; Cha et al., 2016; Weller et al., 2002b; Wiseman et al., 1996).

Two types of soil suppressiveness can be distinguished, namely general and specific. General suppression is effective against a range of pathogens, whereas specific suppression operates against only one or a few of them. General soil suppressiveness is a result of the activity of the overall soil microbial community, whereas specific soil suppressiveness is due to the concerted action of specific microbial genera that interfere at some stage of the life cycle of the soil-borne pathogen. Specific soil suppressiveness can be eliminated by selective heat treatments and is transferable to a conducive soil by mixing in a small amount (1-10%) of suppressive soil (for review: (Mazzola, 2002; Schlatter et al., 2017a)).

For many suppressive soils the microorganisms and mechanisms have not been elucidated. Some of the best-studied suppressive soils to date are the take-all-decline (TAD) soils, where

root disease of wheat or barley caused by the fungal pathogen *Gaeumanomyces graminis* var. *tritici* is suppressed (Cook and Rovira, 1976; Duran et al., 2017; Hornby, 1983). Suppressiveness to take-all disease is, at least in part, due to the enrichment of populations of root-associated *Pseudomonas* spp. producing the antifungal polyketide 2,4-diacetylphloroglucinol (2,4-DAPG) (Kwak et al., 2011; Raaijmakers et al., 1999; Raaijmakers and Weller, 1998; Weller et al., 2002b). For Fusarium-wilt-suppressive soils, the microbes and mechanisms identified so far involve non-pathogenic *Fusarium oxysporum* and *Pseudomonas* species that, in a complementary manner, compete with pathogenic *F. oxysporum* for carbon and iron(Alabouvette, 1986; Duijff et al., 1999; Siegel-Hertz et al., 2018b). Recent studies on soils suppressive to *Rhizoctonia* damping-off disease of sugar beet revealed the involvement of multiple bacterial genera belonging to the Pseudomonadaceae, Streptomycetaceae and Burkholderiacea*e*. The suppression was linked to the production of antifungal lipopeptide thanamycin by *Pseudomonas* and to the production of volatile metabolites by *Streptomyces* spp*.* and *Paraburkholderia graminis* (Carrion et al., 2018; Viviane Cordovez et al., 2015; Duran et al., 2017). Volatiles are low-molecular-mass metabolites involved in long-distance interactions with potent antimicrobial activities (Cho et al., 2017; Garbeva et al., 2014a, 2011; Ossowicki et al., 2017). For example, the effects of volatiles emitted from 50 agricultural soils on two soil-borne pathogenic fungi (*F. oxysporum, R. solani*) and a plant pathogenic oomycete (*Pythium intermedium*) have recently been studied (van Agtmaal et al., 2018). This work showed that most soils emit volatiles that inhibit hyphal growth, but the extent of growth inhibition per soil differed strongly for the three pathogens.

To date, most studies on suppressive soils have been limited to a single field soil. Except for the case of the TAD soils (Landa et al., 2002), it is currently unclear how widespread suppressiveness to specific pathogens is as a biological phenomenon. Furthermore, it is not established yet whether suppression is mediated by one or multiple taxa and mechanisms across various suppressive soils. Finally, the role of volatiles in soil suppressiveness in the presence of both the pathogen and the host plant is yet unexplored.

In this study, we screened a large collection of field soils for suppressiveness to *Fusarium culmorum*, a ubiquitous soil-borne fungus causing foot rot, root rot and Fusarium head blight of different cereals, in particular wheat and barley (Wiese, 1987). Using wheat (*Triticum aestivum*) as the host plant, we found *F. culmorum* suppressiveness in 4 out of 28 soils.

We hypothesised that 1) soils suppressive to *F. culmorum* have similar rhizobacterial community compositions with specific enriched taxa, 2) volatile compounds contribute to disease suppression against *F. culmorum,* and 3) disease-suppressive soils have similar volatile profiles. We anticipated that specific rhizobacterial taxa and volatiles correlate with

soil suppressiveness against *F. culmorum*. However, our comparative analysis of bacterial rhizosphere microbiome composition of suppressive and non-suppressive (conducive) soils, along with volatile profiling, indicates that the phenomenon may be mediated by different rhizobacterial genera across these soils and that volatiles may contribute to the suppressive phenotype only for a limited number of soils.

Materials and Methods

Soil collection

In order to examine soil disease suppressiveness to *F. culmorum*, 28 sites in the Netherlands and Germany were chosen based on information on soil type and crop rotation. The sites included 25 arable fields, 2 pastures and 1 forest. The arable fields included sites with wheat present in crop rotation over the last three years and sites without wheat present in the available history of the field.

Soil samples were collected in the period from January to April 2017 from 3-meter squares located in the middle of each agricultural field/pasture. In this area, top soil cores of approximately 30 cm deep were extracted. Samples were air-dried in room temperature, homogenized, sieved through 4 mm sieve and stored at 4°C. Heavy clay-type soils were additionally flaked using a jaw-crusher (Type BB-1, Retsch, Germany) after drying. Soil physical and chemical parameters were measured as described in Supplementary material part I.

Wheat growth conditions and pathogen inoculation

All the greenhouse experiments were performed in growth cabinets (MC 1750 VHO-EVD, Snijders Labs) in 20°C day and night, photoperiod 12h day /12h night and 60 % relative humidity. In all the experiments, surface-sterilized and pre-germinated wheat seeds (JB Asano from Agrifirm, Netherlands) were used. Plants were watered every second day and weekly supplemented with 0.5 Hoagland solution (1ml per 80 cc of the soil, 0.5M $Ca(NO_3)_2{\cdot}4H_2O$, 1M KNO_3, 1M KH_2PO_4, 0.5M $MgSO_4{\cdot}7H_2O$ and 98.6 mM ferric EDTA).

As a standard substrate, we used a dune soil collected near Bergharen, the Netherlands (BS) (Schulz-Bohm et al., 2015). Before use, BS was air-dried, sieved and gamma-sterilized (Synergy Health Ede B.V., the Netherlands). Sub-samples of eight soils from the collection were gamma-sterilized as well in the same conditions for later use.

Prior to screening for disease suppressiveness, all soils were “activated” in order to induce microbial activity in a so-called microbiome activation step. For this, soils hosted the growth of wheat for two weeks in the conditions indicated above. After this, plants, including their whole root system, were removed and the remaining soil with activated microbiome was mixed properly.

The soil-borne pathogen *Fusarium culmorum* PV (Blom et al., 2011) was grown on 1/2 PDA media (Oxoid, the Netherlands) and maintained in continuous culture. For plant inoculation, the fungus was transferred to 1/4 PDA and grown for 2 weeks in 20°C. After the incubation, 6mm plugs were cut from the border zone of *Fusarium* hyphae and mixed with the growth substrate (1 plug per 10 cc). Controls without pathogen were inoculated with sterile 1/4 PDA plugs. At the end of the experiments disease symptoms were assessed and plants were used for rhizosphere DNA extraction and sequencing analysis (see Supplementary material part I).

Disease suppressiveness screening

Initial disease suppressiveness screening was performed in propagation trays containing 140 single pots (Teku, the Netherlands) each containing 38cc of soil per pot. In order to minimize the physicochemical differences between the 28 soils, after the activation step (described in paragraph above) the natural soil was mixed 2:1:1 in volume with sterile BS soil and sterile vermiculite (Agra-vermiculite, the Netherlands). The soil was inoculated with *Fusarium* or mock-inoculated with agar plugs, and one seedling was placed in the center of each pot. Plants were grown in ten replicates per treatment and, after three weeks, disease symptoms were assessed (see Supplementary material part I). As a control, we used BS mixed with vermiculite 3:1 in volume.

Confirmation of disease suppressiveness with soils sterilization

Four suppressive and four conducive soils were selected to confirm the previously observed levels of suppressiveness. The confirmation test was performed identically as the screening test but the system was scaled up to 380 cc soil per pot (7x7x8 cm, Teku, the Netherlands) with three plants in each. An additional treatment was included - sterilized soil inoculated with pathogen. Sterile BS, vermiculite mix was used as a control. All the treatments had an additional control without pathogen.

Transplantation assay

To assess whether soil suppressiveness is transferable, we mixed natural soils in proportions 1:9 and 3:7 in volume with a conducive substrate consisting of sterile BS and vermiculite. This experiment was also performed with 380 cc soil per pot (7x7x8 cm), each containing three plants, in treatments with and without the addition of the pathogen. Sterile BS and vermiculite mixture was used as a control.

Sequencing and bioinformatics analysis

Rhizosphere DNA extraction, sequencing, 16S rRNA amplicon data processing and analysis are described in Supplementary material part I.

Effects of soil-emitted volatiles on fungal growth

Assays were performed as previously described by Garbeva et al. (Garbeva et al., 2014a) with small modifications, see Supplementary material part I.

Effects of soil-emitted volatile compounds on disease suppression

The eight soils selected in the suppressiveness screening were tested for their ability to induce soil suppressiveness via volatiles. For this, the modified method described by (Park et al., 2015) was used. Briefly, wheat plants growing in conducive soil mixed with *F. culmorum* plugs were exposed to volatiles emitted by soil present in the compartment below the pot. To avoid any physical contact, compartments were separated and sealed with sterile nylon mesh (Sefar, Switzerland) and paper medical tape as described above. The scheme of the system is shown on figure 3B. Four pots per treatment with three plants per pot were grown for three weeks; afterwards, disease symptoms were assessed.

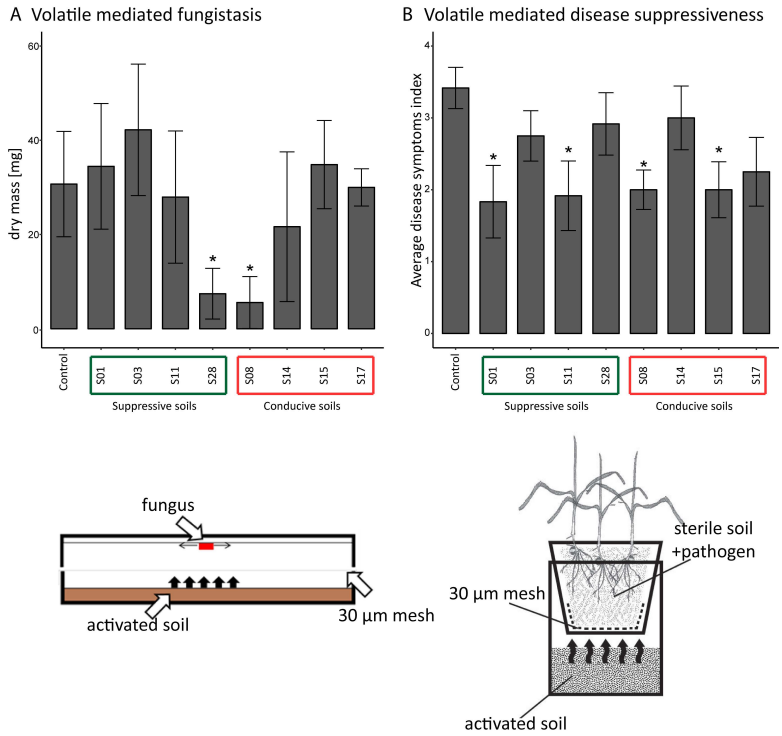


Figure 1. The effect of the volatiles emitted by eight prioritized soils on Fusarium culmorum growth (fungistasis) and disease suppression. (A) Average dry mass of the fungus with standard deviation, the statistically significant differences between treatments and control (based on ANOVA and Tuckey post-hoc test p<0.05) are indicated

by asterisk. (B) Average symptoms index with standard error. The statistically significant differences between treatments and control (based on chi-square test p<0.05) are indicated by asterisk.

Volatile trapping and GC-MS analysis

Volatile compounds were trapped using steel trap containing 150 mg Tenax TA and 150 mg Carbopack B (Markes International Ltd, Llantrisant, UK) and measured using GC-QTOF system. Statistical data analysis was performed using MetaboAnalyst 4.0 software (http://www.metaboanalyst.ca/MetaboAnalyst (Chong et al., 2018)). For details of Volatile trapping and GC-MS analysis, see Supplementary material part I.

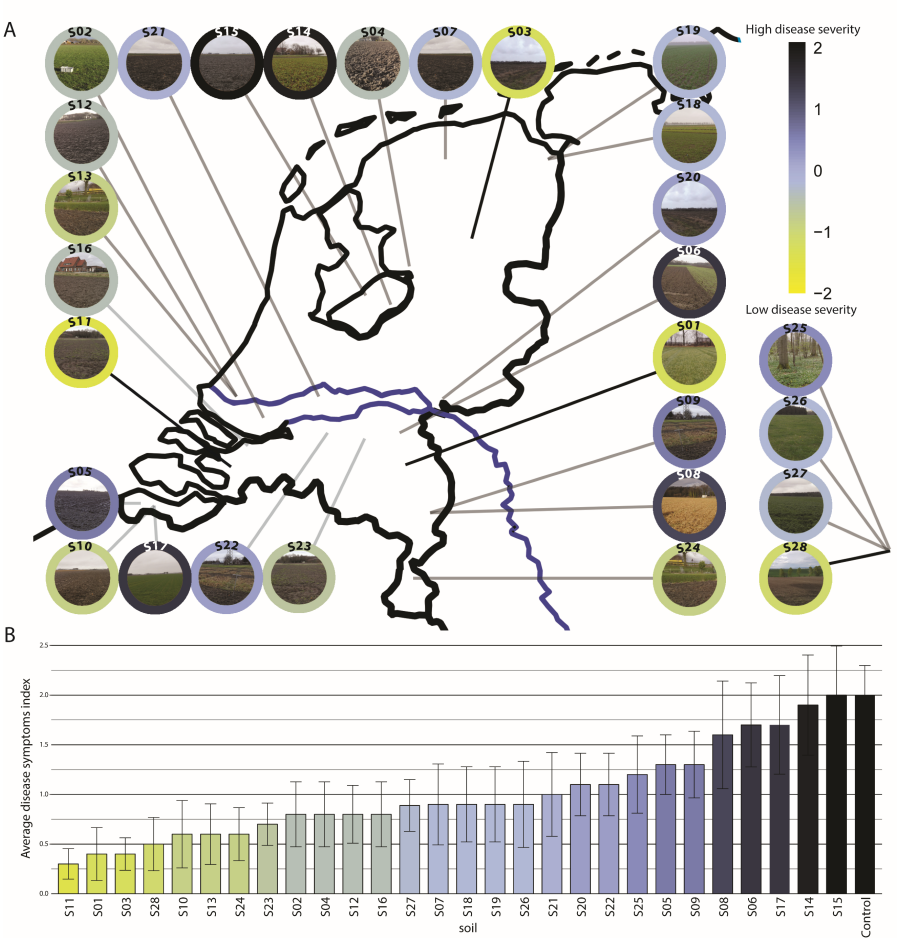


Figure 2. Results of the phenotypic screening towards soil suppressiveness to F. culmorum in 28 soils. (A) Map showing locations of 28 sampling sites and the results of the screening. The color of the outer circle around the photos represents the z-score

transformed average disease symptoms value. Low disease severity indicates soil suppressiveness (yellow color). (B) Bar graph showing average disease symptoms indexes with standard errors.

Results

Identification of soils suppressive to *F. culmorum*

A collection of 28 soils of diverse geographical origins (figure 1A), soil types and agricultural histories (table S1) was screened for disease suppressiveness against *F. culmorum* in greenhouse pot experiments. The disease symptoms of the plants grown in each of the soils were examined three weeks after pathogen inoculation. Overall, high variation in disease suppressiveness was observed between the 28 soils, while being largely consistent between replicates. The disease symptoms across the collection varied from mild or no infection to severe disease. Four soils (S01, S03, S11 and S28 - yellow color, figure 1) showed the lowest level of disease severity with an average score below 0.5 and were considered suppressive (figure 1). Four soils revealed high disease severity with average disease symptoms above 1.5 (S08, S14, S15 and S17 – black color, figure 1) and were considered conducive.

Disease suppression is independent of soil physicochemical properties

In order to investigate phenotypic variation across multiple soil types, our collection included soils from 25 arable fields, 2 pastures and 1 forest, representing different soil types, ranging from sands to heavy clays, with diverse pH (5.3 to 7.8) and C/N ratio (8.8 to 17.5). All physicochemical parameters and field history are summarized in Table S1. No clear correlations between the level of disease suppressiveness and physicochemical parameters and field history were found. Based on canonical correspondence analysis of the 28 soils, there was no separation between disease-suppressive and conducive soils (figure S1, yellow and black dots accordingly). Only weak Pearson correlations were found between physicochemical parameters and disease severity (figure S2). Also, no relevant correlations were found between disease severity and soil pH and C/N ratio (0.24 and 0.25 respectively).

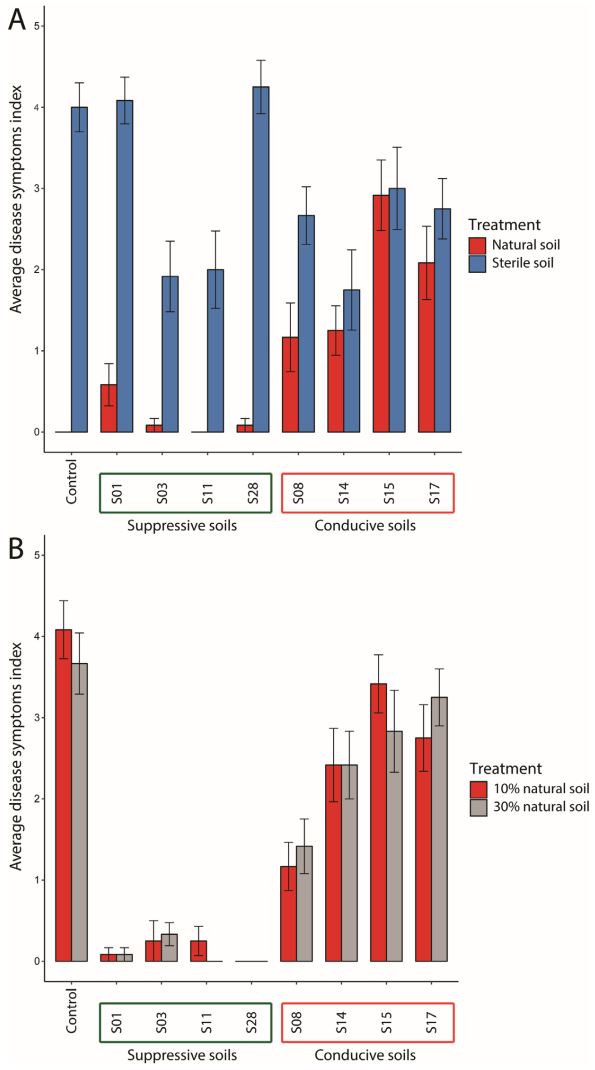


Figure 3. Disease symptoms observed in wheat inoculated with Fusarium culmorum grown in eight prioritized soils. (A) Natural and gamma-sterilized soil with sterile BS soil/vermiculite mix as a control (B) 10% and 30% in volume of natural soil mixed with standardized sterile substrate or with sterile BS soil as a control. The bar indicates the average of the disease symptoms index, with the error bars representing the standard error.

Disease suppressiveness has a microbial basis

Based on the results from the initial screening, a set of eight soils was selected for confirmation assays and further analysis. This included the four soils with the highest level of disease suppressiveness (S01, S03, S11 and S28) and the four conducive soils showing the most contrasting phenotypes (S08, S14, S15 and S17). For the four suppressive soils, low average disease indices were again observed (figure 2A, red bars) but after gamma sterilization, disease indices increased significantly (figure 2A, blue bars). For the four conducive soils, except for S08, gamma sterilization did not substantially enhance disease severity. Furthermore, the results revealed that suppressiveness to *F. culmorum* is

transferable (figure 2B). Mixing 10% or 30% of the suppressive soil (S01, S03, S11 and S28) in a conducive background soil transferred suppressiveness. There was no significant difference in the level of suppression between the transfer of 10% and 30% suppressive soil. Collectively, our data suggest that the microbial community contributes to the suppressive phenotype.

Volatile-mediated inhibition of fungal growth and disease suppression is observed for suppressive and conducive soils

To determine the role of volatile compounds in disease suppression and antifungal activity, the eight selected soils were tested in two experimental systems: i) hyphal growth of *Fusarium* on artificial media exposed to soil volatiles, and ii) plants growing in conducive soil inoculated with the pathogen exposed to soil volatiles (figure 4 A, B and Supplementary material part I). The first assay revealed that only two soils (S28 suppressive and S08 conducive) emitted volatiles that significantly reduced growth of the fungus compared to the control. When plants were exposed to soil volatiles, disease suppression was observed for four out of eight soils (figure 4 B). Again, these included both suppressive (S01, S11) and conducive (S08, S15) soils. Subsequent analysis of volatile profiles emitted by these eight soils did not reveal clear separation between suppressive and conducive soils (figure S3). Interestingly, several suppressive and conducive soils (S03, S08, S11 and S14) revealed very similar volatile profiles. These results suggest that volatiles are not a common mechanism of soil suppressiveness to *F. culmorum*.

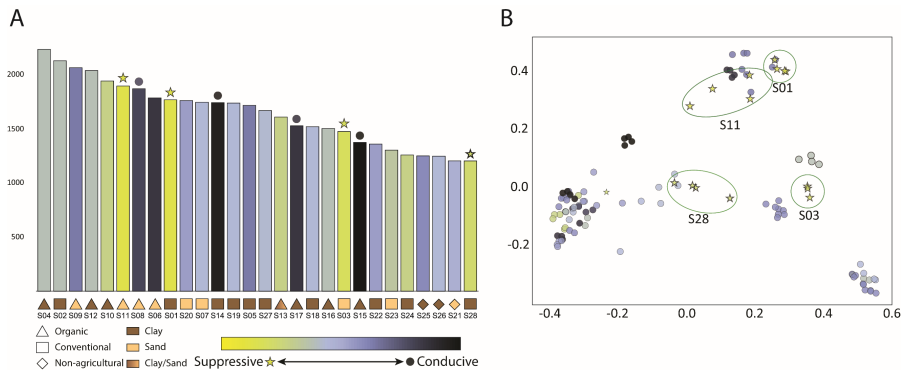


Figure 4. Characteristics of rhizosphere bacterial communities across all 28 soils. (A) Bar plot representing the alpha diversity using the rarefied unique ASV counts. Samples are sorted according to their alpha diversity score and color-coded according to suppressive phenotype. (B) PCoA based on Unweighted UniFrac distance between samples. Circles highlight the suppressive sample replicates clustered together.

Microbial profiling of *F. culmorum*-suppressive soils

To investigate possible links between the rhizobacterial community composition and the disease suppressive phenotype, extensive 16S sequencing was performed for all 28 soils (see Supplementary material part I). The rhizobacterial communities showed large variation between samples and even between replicates of the same samples, as can be seen from the inter- and intra-sample Jaccard similarity of 0.056 (sd = 0.033) and 0.346 (sd = 0.057) respectively. Based on the alpha- and beta-diversity, there were no significant community differences between suppressive and conducive soils. Beta-diversity for all sample pairs was calculated with unweighted UniFrac, which shows consistent grouping for soil sample replicates (figure 4B). Subsequent PCoA analysis of the rhizobacterial community composition of the suppressive and conducive soils indicated that the different suppressive soils have diverse taxonomic compositions and did not group together (figure 4B). This was also the case when calculating community diversity of the samples within specific taxonomic groups (Supplementary figures S4). As for alpha diversity, Wilcoxon rank-sum test showed no significant association between observed ASVs ($p=0.74$) or Shannon diversity ($p=0.07$) and soil suppressiveness. The suppressive soils included both the most and the least diverse communities. The soils from organic farms were associated with higher bacterial diversity compared to the soils from conventional farms and to the non-agricultural soils (figure 4A). Again, there was no consistent correlation between soil suppressiveness and alfa- or beta-diversity.

To establish whether the disease-suppressive phenotypes were mediated by specific rhizobacterial taxon or by multiple taxa, 16S amplicon data were analyzed in more depth. To reveal if one or more individual abundant amplicon sequence variants (ASVs) could be associated with disease suppressiveness, we inspected the presence-absence patterns of all ASVs that were significantly enriched in suppressive soils (figure 5). No individual ASV appeared to be exclusively present in all suppressive samples compared to the conducive samples (figure S5). Random forest classifiers trained on their taxonomic profiles could not predict the suppressive soil phenotype in a leave-one-out analysis. The results were not significantly different when the same analysis was performed using OTU-level clustering of ASVs (at 97% identity).

Co-occurrence network analysis indicates bacterial communities enriched in rhizosphere microbiomes of suppressive soils

To investigate whether specific combinations of ASVs are associated with disease suppressiveness (in subsets of the four suppressive soils), we calculated Spearman correlations between ASV occurrences across all 28 soils and constructed a co-occurrence network from the most highly correlating ASVs in the correlation matrix (see Supplementary material part I). The resulting network (figure 6A) consists of 928 nodes (comprising 21% of

all 4,322 ASVs), distributed across 37 subnetworks. The ASVs in the network that were significantly enriched in suppressive soils are indicated by squares with black border in figure 6B. The subnetworks are taxonomically diverse, with no network being taxonomically homogeneous, even at the phylum level. Interestingly, one of the connected components was found to be particularly associated with the suppressive phenotype. Within this connected component, 7 out of the 163 ASVs were strongly enriched in suppressive soils and these were part of a more densely connected subcomponent comprising 60 ASVs that comprised 6 out of the 7 abovementioned ones. Taxonomic assignments of the suppression-associated subnetwork displayed an overrepresentation of ASVs belonging to different Acidobacteria, namely Blastocatellales and members of subgroup 6, compared to the overall community composition ($p=0.0003$, Fisher exact test, figure 6b). Moreover, several of these Acidobacteria displayed characteristics of being hub taxa in these subnetworks based on their high betweenness centrality. In addition, 11 of the 60 ASVs in the suppressive-associated network were exclusively present in two suppressive soils (figure 6C), 7 of which were taxonomically assigned to Acidobacteria.

Discussion

F. culmorum is an economically important fungal plant pathogen that causes disease in many cereal and non-cereal crops. However, little is known about the occurrence and distribution of soil suppressiveness to this pathogen. To our knowledge, this study is the first to screen for disease suppressiveness in a large collection of diverse soils. Although a high variation in the level of disease suppressiveness was observed between the soils, 14% of the tested soils revealed a clear suppressive phenotype. Interestingly, no physicochemical parameter such as soil type, field history, pH, C/N ratio or content and concentration of bioavailable Fe, K, Mg, P, S correlated with the observed suppressive phenotype. In previous work, physicochemical soil parameters such as soil type, moisture, pH, organic matter and microelements content have been more commonly associated with general disease suppressiveness (Hoper and Alabouvette, 1996; Janvier et al., 2007).

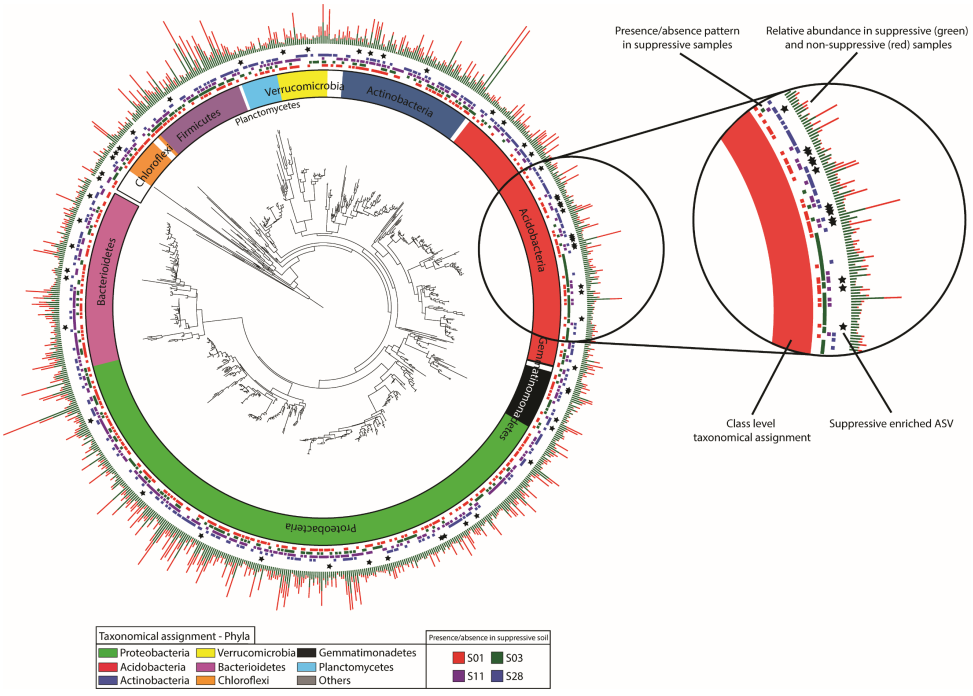


Figure 5. Phylogenetic tree of all ASVs consistently detected in one or more suppressive rhizosphere samples. The rings, from the inside to the outside, represent 1) the taxonomical assignment of the ASVs at the phylum level, 2) the presence/absence patterns of ASVs in the four different suppressive soils, 3) indications (with starts) of ASVs strongly enriched in suppressive samples, and 4) the average cumulative normalized abundance of each ASV in suppressive (green) versus non-suppressive (red) samples. The results show that all ASVs enriched in suppressive samples are specific to a subset of the suppressive soils, while none of the ASVs that occur throughout all suppressive soils are significantly enriched in suppressive versus non-suppressive soils.

In our study, the microbiological basis of specific suppressiveness to *F. culmorum* was revealed by two independent approaches: gamma-sterilization and soil transplantation eliminated and conferred suppressiveness, respectively, and confirmed that suppressiveness to *F. culmorum* was not linked to soil physicochemical parameters but rather to the soil (micro)biome.

Along with the soil, the plant itself is an important determinant of the structure of soil microbial communities and disease suppressiveness. Hence, the strength of disease suppressiveness is attributed to all players in the tripartite relationship of plant-soil-microorganisms (Garbeva et al., 2004). Considering this, in the present study, all

experiments included a “microbiome activation step” by growing wheat for 2 weeks prior screening for disease suppressiveness. The application of plants provides substrates for growth via root exudates and space for the soil microbial community. Several studies have associated disease-suppressive phenotypes to individual bacterial groups based on their relative enrichment compared to a conducive phenotype (Donn et al., 2014; Schlatter et al., 2017a; Yin et al., 2013). However, rhizosphere microbiomes are highly diverse (Charlop-Powers et al., 2015) and multiple differences may exist even between physicochemical similar soils. In the present study, 28 different soils were examined and no individual bacterial taxon was found to be exclusively present or enriched in all suppressive soils. Bacterial taxonomic groups that were more prevalent in some of the suppressive soils were not prevalent in other suppressive soils.

Many studies have aimed to understand the relationship between microbial diversity and disease suppressiveness. However, both low (Mehrabi et al., 2016) and high (Garbeva et al., 2004) community diversity have been associated with soil suppressiveness. Here, we found suppressive samples with both high and low community richness, which suggests community diversity is not the key driver of soil suppressiveness to *Fusarium culmorum*. Community evenness is correlated with the phenotype but the strength of this association is not strong enough ($p=0.07$) to warrant speculations on its role in disease suppressiveness. To our surprise, no ASVs or OTU-level ASV clusters were found to be shared uniquely between the microbial communities of all four suppressive soils, or to be differentially abundant across all these four soils. The fact that random forest classifiers were unable to accurately predict suppressive phenotypes in a leave-one-out analysis of the soils suggests that i) the suppressive phenotypes are mediated by different taxonomic groups across the different suppressive soils and/or ii) that rhizobacteria do not play a major role in suppressiveness to *F. culmorum*. Many functional elements that are known to be able to drive disease suppression (such as biosynthetic gene clusters for secondary metabolites) are often strain-specific and are frequently transferred horizontally across species (Medema et al., 2014). Hence, it is still possible that the same or similar functional elements could drive the suppressiveness across all four soils, while being undetectable by 16S sequencing due to its limited resolution or due to the elements being encoded in the genomes of diverse bacterial taxa.

Representatives of a range of bacterial groups can carry out functions that result in the suppression of soil-borne diseases. For example, several *Bacillus*, *Pseudomonas*, *Streptomyces* or *Flavobacterium* species are well known to play role in suppression of various soil-borne plant pathogens (Cha et al., 2016; Chapelle et al., 2016; Donn et al., 2014; Garbeva et al., 2006; Kwak et al., 2018). However, various previous studies indicate that many of these bacteria reveal antimicrobial activities only as results of interspecific interaction networks (Garbeva et al., 2011; Traxler et al., 2013; Tyc et al., 2017, 2014). The

correlation-based network analysis performed here revealed complex inter-sample connections between individual bacterial taxa that are likely interacting either directly or indirectly, based on their observed co-occurrence. One of the network components provided insights into a bacterial guild that is potentially associated with disease suppressiveness to *Fusarium culmorum*. Multiple ASVs were found to be exclusively present in two distinct disease suppressive microbiomes, while additionally being strongly correlated with another sub-community of ASVs that also consistently occurred in a conducive microbiome. Interestingly, most of these ASVs belonged to *Acidobacteria*. We observe an over-representation of *Acidobacteria* in the suppression associated network when compared to the general community composition (Fisher exact test, p=0.0003). This phylum has previously been associated with *Rhizoctonia solani* bare patch (Yin et al., 2013) and has been shown to harbor diverse species with a large specialized metabolic potential that could be involved in interactions with fungi (Crits-Christoph et al., 2018). Based on their specific enrichment, the identified bacterial guild might represent the suppressive core at the base of the phenotype for two of the four suppressive samples (soils S01 and S11). Further shotgun sequencing efforts as well as microbiological and biochemical analysis are needed to clarify the functional roles of these organisms. Furthermore, one should bear in mind that in addition to the bacterial community structure, the expression of functional genes conferring suppressiveness to soil-borne pathogens might be dependent on interactions with other soil microorganisms such as fungi, protists and viruses.

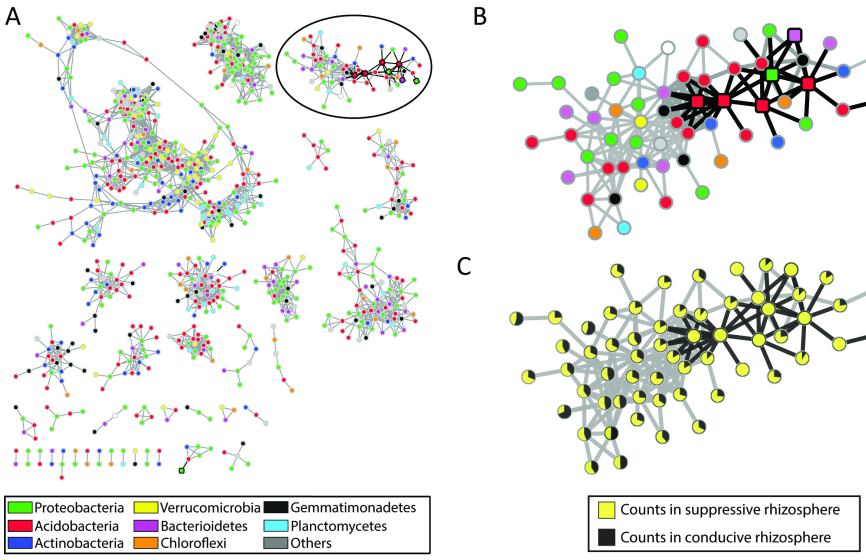


Figure 6. Co-occurrence network analysis of rhizosphere bacteria across samples. A) Complete network of correlated ASVs using Spearman correlation. Nodes represent

individual ASVs; edges link ASVs which had a correlation score above a given threshold. The node color indicates the taxonomical annotation at the phylum level. Edges of ASVs that are significantly enriched in suppressive samples are highlighted black as the respective nodes. B) Zoomed in view of a subnetwork of interest, which shows a number of ASVs associated with the suppressive phenotype indicated by squares with black border, along with its taxonomical distribution. C) Normalized counts ratio between conducive (yellow) and suppressive (black) samples for ASVs from the network in panel B.

Frequently, the germination and growth of plant pathogenic fungi are negatively affected by direct or indirect contact with soils (without the presence of a host plant). This phenomenon is named soil fungistasis (Garbeva et al., 2011; Watson and Ford, 1972) and is often associated with general disease suppressiveness. Whereas abiotic soil factors can be involved, the major cause of fungistasis is biological since it is strongly reduced after soil sterilization, which is analogous to the soil disease suppressiveness. Recent studies revealed that microbial volatiles play important roles in both soil fungistasis as well as disease suppressiveness (Effmert et al., 2012; van Agtmaal et al., 2018). Our study did not reveal any congruence between volatile-mediated soil fungistasis and disease suppressiveness. Volatile-mediated soil suppressiveness was observed only with four soils, including both two suppressive and two conducive soils. This indicates that, even though volatile emission is one of the factors that may contribute to disease suppressiveness to *F. culmorum*, it is not a general one. Apparently, other (complementary) factors and mechanisms are needed to develop a full protective potential against *F. culmorum*. Alternatively, it might be that suppressiveness across the four soils is mediated by different mechanisms, involving volatiles in some cases but not in others. This could also explain the lack of commonly enriched taxa across the four suppressive soils.

In conclusion, we discovered several agricultural soils that protect wheat plants from *Fusarium culmorum* infections through a microbial component. Moreover, these suppressive soils revealed different bacterial taxonomic patterns and diversity, as well as variable degrees of antifungal volatile emissions. These observations reject the hypothesis that specific rhizobacterial taxa and specific volatiles correlate with suppressiveness of *F. culmorum.*

Co-occurrence network analysis suggested that two of the suppressive samples share a similar microbial basis of the phenotype through a uniquely overrepresented bacterial guild dominated by *Acidobacteria*. Of course, taxonomic profiling alone cannot provide definitive answers on the actual biological mechanisms responsible for the suppressive phenotype. Accordingly, we anticipate our work to lay the foundation for a combination of functional metagenomics along with microbiological and biochemical analyses, in order to elucidate the functional mechanisms behind soil suppressiveness to *F. culmorum* in the near future.

Supplementary material

Material and methods

Soil physical and chemical parameters

Soil physical and chemical parameters were measured in triplicate using three independent sub-samples. The soil pH was measured in water and soil organic matter content was determined by loss of ignition, both using standard laboratory methods. Bioavailable iron, potassium, magnesium, phosphorus and sulfur were extracted using 0,01M $CaCl_2$ (VWR, Netherlands) and concentrations were measured with ICP-OES (iCAP 6500 ICP-OES Duo ,Thermo Scientific). Carbon and nitrogen content were determined using an Element Analyser (Flash EA 1112 ,Thermo Scientific).

Disease symptoms assessment

To assess disease symptoms, the wheat plants were carefully removed, the excess of soil was shaken and roots were cleaned in water. The root system was visually inspected for brown/black lesions or rotting, and the stem base/coleoptile was inspected for rotting and the presence of pink-white fungal hyphae. Plants were scored for disease symptoms from 0-5: 0- healthy plants; 1- one or two dark lesions on the roots up to 10 mm; 2- lesions bigger than 10 mm; 3- large lesions on the roots and/or stem base rot; 4- visible pink-white fungal hyphae on the stem with shoot discoloration, extensive root lesions, or stem base rot (at least two of this symptoms); and 5- dead plants (for examples see figure S6). Statistical differences in disease symptoms between treatments and control were assessed using the chi-square test, with an alpha cutoff of $p<0.05$.

Rhizosphere DNA extraction and sequencing

At the end of the experiments, plants were gently removed from the trays. Soil loosely adhering to the roots was removed by shaking. The roots with surrounding soil were placed on a sterile filter in a laminar flow cabinet and the soil particles adhering to the roots were collected using a brush. DNA was immediately isolated using a DNeasy PowerSoil Kit (QIAGEN, the Netherlands) according to manufactures protocol using 0.25 g of rhizosphere soil. Samples were additionally purified using DNeasy PowerClean cleanup kit (QIAGEN, the Netherlands). Sequencing of the bacterial V3-V4 region of the 16S rRNA gene (with primers 16S_V3-341F 5'-CCTACGGGNGGCWGCAG and 16S_V4-785R 5'-GACTACHVGGGTATCTAATCC (Herlemann et al., 2011)) was performed at BaseClear (Leiden, the Netherlands) using Illumina MiSeq in 4 biological replicates per treatment.

Amplicon assembly and taxonomical assignment

The 16S rRNA gene sequencing yielded a total of 4,966,035 reads, sequencing depths for all samples is reported in table S2. Reads were quality-filtered using a sliding window approach of five nucleotides and a Phred score threshold of 30 (Bolger et al., 2014). Forward and reverse reads were then truncated at 280 and 220 bp in length, respectively. The Dada2 (B. J. Callahan et al., 2016) pipeline from Qiime2 (Caporaso et al., 2010) was used to denoise and obtain amplicon sequence variants (ASVs) from demultiplexed reads for all 112 samples. Reads that did not overlap were removed from the rest of the analysis. To remove sequences derived from errors that were not corrected during the DADA2 denoising step, ASVs that had fewer than 20 amplicons mapped across all samples and that appeared in less than 4 different samples were removed from further analysis. This resulted in 4,322 reliable ASVs across the 112 samples, while still retaining over 80% of the sequencing information. Taxonomic assignment was performed in Qiime2 using a Bayesian classifier (Bokulich et al., 2018; Pedregosa et al., 2011) built for the primer pairs used in this study (341F and 805R) on the SILVA release 132 database ref NR 99. The resulting feature count tables were logCSS-normalized in R using the metagenomeSeq library (Paulson et al., 2013). Alpha/beta diversity and clustering of samples using different metrics were calculated with Qiime2 and python skbio library.

Principal coordinate analysis of the amplicon data

Principal coordinate analysis (PCoA) was performed in Qiime2 using Bray-Curtis dissimilarity, Jaccard index, weighted UniFrac and unweighted Unifrac (Lozupone and Knight, 2005). Weighted and unweighted UniFrac distances were calculated in a Python script for all individual bacterial taxonomy groups to reveal existing correlations within taxonomic groups that were being masked by other features. Code for these analyses is available at (https://git.wageningenur.nl/users/traca001/groups).

Identification of suppressive rhizosphere-associated ASVs

ASVs enriched in suppressive and conducive soils were determined with FitZig (Paulson et al., 2013) using the suppressive phenotype as model matrix for hypothesis testing. A strict filter was applied to select ASVs of interest; we consider enriched only ASVs which yielded a p-value below ($p<10^{-10}$) and which occur in at least two different suppressive soil samples (replicates).

Random forest prediction of suppressive soil

Multiple random forest classifiers were built to predict soil phenotype based on its community composition. The classifiers are built with python scikit-learn library bootstrapping the selection of suppressive and conducive samples used to train and test

the model. For each classifier, 3 suppressive and 12 conducive samples are randomly chosen and the remaining samples are used to test the classifier predictions. None of the suppressive sample phenotype could be correctly predicted by the classifier.

Co-occurrence network analysis

Spearman's rank correlation coefficient was calculated using the normalized feature table for all ASV pairs across all samples. Clusters of highly correlated ASVs were obtained by applying a static threshold that preserved only correlations above 0.8, corresponding to approximately 1% of the nonzero interactions. Clusters which contained suppression-associated ASVs as determined by FitZig were further investigated to identify suppression-specific ASV clusters. Network visualization was performed in Cytoscape (Shannon et al., 2003); nodes in the network represent the different ASVs and edges were drawn between pairs of ASVs having a Spearman correlation score above the 0.8 threshold.

Effects of soil-emitted volatiles on fungal growth

To investigate the antifungal activity of the volatiles emitted by eight selected soils on the growth of Fusarium culmorum PV, the bottom-top approach was applied as described previously by Garbeva et al., (Garbeva et al., 2014b) with small modifications. The top part of the experimental system contained a Petri dish with 20 ml of 1/2 PDA medium and a 6 mm Fusarium culmorum PV plug placed in the center, whereas 30 g of soil was added at the bottom. The two parts where separated with a 30 µm sterile nylon mesh (Sefar, Switzerland) to allow exchange of volatile compounds but prevent exchange of spores and soil particles. The whole system was fixed together with paper medical tape (Kruidvat, the Netherlands). The scheme of the system is shown on figure 3A. After seven days at 20°C in the dark, fungal hyphae were harvested, lyophilized and weighed. Every treatment was replicated five times.

Volatile trapping and GC-MS analysis

Volatiles emitted by the eight suppressive and conducive soils were collected in a steel trap with 150 mg Tenax TA and 150 mg Carbopack B (Markes International Ltd, Llantrisant, UK). A perforated steel tube was placed in the glass pot with tested soil mixed with F. culmorum PV agar plugs. The pre-germinated wheat seedling was introduced to this system and after one week of growth, the steel trap was connected to tubes present in the soil for 16h. Every soil was tested in three independent biological replicates. After removing, traps were capped and stored at 4°C until GC-Q-TOF analysis. Volatiles were desorbed from the traps using an automated thermodesorption unit (model UnityTD-100, Markes International Ltd., Llantrisant, UK) at 210°C for 12 min (Helium flow 50 mL/min) and trapped on the cold trap at -10°C. The trapped volatiles were introduced into the GC-QTOF (model Agilent 7890B GC

and the Agilent 7200AB QTOF, Santa Clara, USA) by heating the cold trap for 3 min to 280°C with the split ratio set to 1:10. The column used was a 30 × 0.25 mm DB-5MS UI, film thickness 0.25 µm (122-5532UI, Agilent J&W, USA). Temperature program used was as follows: 39°C for 2 min, from 39°C to 95°C at 3.5°C/min, then to 165°C at 6°C/min, to 250°C at 15°C/min and finally to 300°C at 40°C/min, hold 20 min. The volatiles were detected by the MS operating at 70 eV in EI mode. Mass spectra were acquired in full scan mode (30–400 amu, 4 scans/s). For the volatilomics analysis, the acquired raw mass spectrometry (MS) data was extracted to m/z format using MassHunter Qualitative Analysis Software V B.07.00 (Agilent Technologies, Santa Clara, CA, USA). The m/z data was processed with MZMine V 2.36 (Copyright © 2005–2012 MZmine Development Team, (Pluskal et al., 2010)) as described in (Lankenau et al., 2015) to create an m/z and peak intensity table that could be used as input file for MetaboAnalyst 4.0 software (http://www.metaboanalyst.ca/MetaboAnalyst (Chong et al., 2018)). Before the statistical analysis, the data was filtered using Interquantile range (IQR) and normalized by the log transformation with automatic scaling.

Table S1. Table presenting physical and chemical characteristics of the soils and the crops grown in the fields in 3 seasons before the collection

soil	pH	SD	OM	SD	Fe	SD	K	SD	Mg	SD	P	SD	S	SD	C	SD	N	SD	C:N	soil type	2016	2015	2014
BS	7.53	0.05	0.24	0.04	0.19	0.01	2.02	0.32	0.00	0.00	0.11	0.03	0.00	0.00	0.05	0.01	0.00	0.00	NA	Sand	-	-	-
S01	6.22	0.17	3.46	0.35	0.09	0.00	34.00	0.92	163.19	1.75	1.40	0.01	1.29	0.08	2.31	0.18	0.14	0.01	16.50	Sand	-	-	-
S02	6.75	0.04	3.81	0.08	0.03	0.00	86.66	2.38	36.86	0.79	0.89	0.02	2.50	0.15	1.60	0.08	0.11	0.01	14.55	Clay	Wheat	Potatoes	Wheat
S03	5.28	0.27	5.49	0.68	0.45	0.06	59.95	2.29	56.74	2.11	2.69	0.08	2.60	0.16	3.77	1.13	0.26	0.10	14.50	Sand	Winter wheat	Winter wheat	Winter wheat
S04	7.30	0.30	3.10	0.29	0.02	0.00	117.12	1.20	56.49	0.25	1.53	0.05	7.21	0.99	2.11	0.02	0.13	0.00	16.23	Clay	Wheat	Onions	Lucerne
S05	6.47	0.10	3.56	0.37	0.16	0.00	109.72	2.16	74.87	1.58	7.76	0.32	1.29	0.18	1.99	0.53	0.16	0.04	12.44	Clay	Winter wheat	Potatoes	Winter wheat
S06	7.58	0.02	3.51	0.40	0.05	0.00	223.26	1.92	84.60	0.92	2.62	0.08	12.23	0.85	2.72	1.11	0.19	0.10	14.32	Sandy loam	Rye	Leaf vegetables	Winter wheat
S07	7.58	0.06	4.32	0.36	0.03	0.00	82.92	1.74	61.11	0.43	1.66	0.05	5.57	0.07	2.92	0.11	0.18	0.01	16.22	Sand	Winter wheat	Potatoes	Winter wheat
S08	6.87	0.06	2.81	0.51	0.08	0.00	181.54	3.76	109.68	1.70	16.23	0.05	1.14	0.05	1.94	0.24	0.16	0.01	12.13	Sand	Spring wheat	Pattison/ yakon	Pattison/ yakon
S09	6.87	0.18	3.26	0.32	0.06	0.01	174.31	1.13	113.01	0.78	3.06	0.07	1.26	0.22	1.35	0.14	0.12	0.01	11.25	Sand	Spring wheat	Onions	Sweet corn
S10	7.49	0.04	2.92	0.44	0.02	0.00	97.07	2.67	70.88	0.54	1.12	0.07	2.96	0.05	2.62	0.13	0.16	0.01	16.38	Clay	Spelt	Peas	Beetroot/pumpkins
S11	7.28	0.19	3.48	0.47	0.11	0.00	68.77	1.10	56.43	0.58	5.43	0.04	1.17	0.15	1.99	0.88	0.16	0.07	12.44	Sand	Luzerne/grass	Luzerne/grass	Barley
S12	7.75	0.01	3.81	0.32	0.02	0.00	233.38	0.68	83.72	0.95	1.06	0.01	9.00	0.29	2.03	0.35	0.14	0.04	14.50	Clay	Celery	Cabbage	Grass clover
S13	7.55	0.14	7.03	0.25	0.04	0.00	207.13	4.04	122.52	1.44	3.40	0.12	7.57	0.06	3.82	0.01	0.34	0.00	11.24	Clay	Grass clover	Grass clover	Red cabbage
S14	7.61	0.05	5.04	0.35	0.04	0.00	82.49	4.08	98.91	4.04	0.70	0.06	8.61	0.08	2.35	0.14	0.15	0.01	15.67	Sandy clay	Winter wheat	Beetroot	Potatoes
S15	7.82	0.05	3.77	0.63	0.02	0.00	45.83	0.53	60.60	0.52	0.90	0.05	5.95	0.06	1.91	0.08	0.11	0.01	17.36	Clay	Potatoes	Grass clover	Onions
S16	7.63	0.12	2.91	0.57	0.03	0.00	53.60	0.85	78.47	0.42	5.61	0.17	2.79	0.21	2.33	1.44	0.18	0.13	12.94	Clay	Luzerne	Potatoes	Carrots
S17	7.75	0.06	4.23	0.79	0.01	0.00	87.17	2.45	74.54	0.80	1.03	0.04	2.27	0.06	2.63	0.05	0.15	0.00	17.53	Clay	Potatoes	Spelt	Pumpkins
S18	7.69	0.06	7.53	0.94	0.02	0.00	53.59	0.56	113.54	0.51	1.49	0.06	5.80	0.37	2.30	0.02	0.24	0.00	9.58	Clay	Winter wheat	Winter wheat	Winter wheat
S19	7.73	0.02	5.38	0.50	0.02	0.01	63.09	0.68	104.28	2.48	1.50	0.01	5.00	0.28	2.35	0.02	0.24	0.00	9.79	Clay	Winter wheat	Winter wheat	Sugar beet
S20	7.30	0.16	8.00	0.21	0.10	0.00	234.45	3.76	299.63	6.42	2.69	0.02	6.98	0.41	3.25	0.65	0.36	0.10	9.03	Sand	Maize	Maize	Winter wheat
S21	5.56	0.12	20.59	1.00	0.82	0.07	58.82	4.26	484.44	14.16	4.86	0.10	24.70	0.13	9.30	0.39	1.04	0.03	8.94	Sand	Pasture	Pasture	Pasture
S22	6.50	0.10	3.02	0.48	0.03	0.01	74.84	1.84	237.38	3.52	0.87	0.09	3.67	0.15	2.65	0.10	0.30	0.01	8.83	Clay	Maize	Winter wheat	Sugar beet
S23	5.92	0.39	4.50	0.50	0.47	0.04	51.98	1.52	122.23	3.32	11.88	0.27	4.03	0.29	1.92	0.60	0.17	0.05	11.29	Sand	Grass clover	Maize	Maize
S24	7.27	0.06	6.15	0.38	0.02	0.00	76.47	1.19	66.70	0.61	2.58	0.12	5.24	0.45	0.98	0.07	0.11	0.00	8.91	Clay	Wheat	Beetroot	Wheat
S25	5.35	0.15	7.34	0.55	0.24	0.04	57.68	12.82	83.30	3.25	1.26	0.05	5.61	1.70	3.17	0.03	0.26	0.01	12.19	Clay	Forest	Forest	Forest
S26	5.76	0.05	8.54	1.92	0.12	0.01	27.52	2.83	113.43	0.69	1.41	0.14	3.50	0.46	3.13	0.12	0.32	0.01	9.78	Clay	Pasture	Pasture	Pasture
S27	7.05	0.04	7.86	0.94	0.04	0.01	52.66	2.86	98.95	2.37	0.85	0.04	4.53	0.47	3.21	0.14	0.31	0.01	10.35	Clay	Winter rape	Winter wheat	Winter rape
S28	7.13	0.07	3.29	0.12	0.02	0.00	71.36	0.44	160.26	2.70	0.79	0.02	1.74	0.24	1.52	0.01	0.17	0.00	8.94	Clay	Winter wheat	Winter wheat	Winter rape

* to highlight the differences in the measured parameters, pH values are colored from red to blue, showing low to high values respectively.
Other parameters: organic matter content (OM), content of bioavailable elements (Fe, K, Mg, P, S), total carbon (C) and nitrogen (N) are colored with green bars according to their normalized values. Presented values are average of three replicates with standard deviations (SD).
Column “soil”: soil samples in the collection S01 to S28 and BS: “Bergharen soil” used as a standard substrate in the study.

Table S2. Sequencing depths for all rhizosphere samples, the value following underscore indicates the replicate number.

sample-id	input	filtered	denoised	merged	non-chimeric
S01_1	41725	33607	33607	17264	16866
S01_2	45462	36178	36178	19858	19373
S01_3	41822	33415	33415	17196	16778
S01_4	49352	39531	39531	25025	23379
S02_1	53186	42592	42592	23199	22708
S02_2	42743	33988	33988	17520	17061
S02_3	54037	42031	42031	24111	23450
S02_4	43360	34930	34930	19538	19008
S03_1	44954	36506	36506	20855	19746
S03_2	42219	33757	33757	19801	18422
S03_3	46183	36515	36515	18537	17677
S03_4	46941	38080	38080	26964	21045
S04_1	49195	39946	39946	22155	21807
S04_2	49236	39690	39690	21736	21295
S04_3	47442	38178	38178	18923	18293
S04_4	49544	39379	39379	21418	21023
S05_1	49240	39988	39988	22254	21030
S05_2	48264	39067	39067	22833	19870
S05_3	49934	39348	39348	21713	20461
S05_4	39082	31770	31770	15274	14745
S06_1	36164	28958	28958	14296	13856
S06_2	42717	33193	33193	17723	17161
S06_3	45214	36400	36400	19923	19316
S06_4	48268	39142	39142	22538	21914
S07_1	53097	43001	43001	24869	23953
S07_2	45927	36549	36549	20537	19901
S07_3	63205	50499	50499	28516	27743
S07_4	33926	23095	23095	11884	11526
S08_1	46293	36945	36945	19611	18169
S08_2	44794	35469	35469	17577	17171
S08_3	49441	39931	39931	20719	20031
S08_4	37841	30283	30283	15807	15425
S09_1	50458	40629	40629	20554	19966

S09_2	49480	40250	40250	21995	20986
S09_3	52163	41629	41629	21864	21281
S09_4	42913	34941	34941	20271	19325
S10_1	46209	37005	37005	19507	18922
S10_2	50250	40050	40050	22734	21712
S10_3	48066	38386	38386	20345	19824
S10_4	49532	39101	39101	21937	21262
S11_1	56437	45456	45456	23637	22725
S11_2	39385	31551	31551	17438	16721
S11_3	53460	42318	42318	25257	21916
S11_4	50498	40678	40678	23542	22765
S12_1	45994	36824	36824	20278	19617
S12_2	51667	41515	41515	21963	21437
S12_3	45604	36075	36075	18933	18300
S12_4	51902	41044	41044	21966	21488
S13_1	51177	36785	36785	19145	18648
S13_2	41781	24407	24407	11186	10807
S13_3	49981	35778	35778	18301	17694
S13_4	52143	36067	36067	19093	18040
S14_1	43642	34264	34264	16925	16489
S14_2	48616	35195	35195	17718	17067
S14_3	44910	35575	35575	19273	18733
S14_4	46545	37762	37762	19310	18766
S15_1	42858	34576	34576	21410	19796
S15_2	44762	36195	36195	21763	20477
S15_3	47422	37758	37758	22556	20948
S15_4	40163	32478	32478	19295	17778
S16_1	37249	29402	29402	17735	15462
S16_2	42173	33561	33561	19422	17928
S16_3	45586	35797	35797	19070	18582
S16_4	47442	37272	37272	20494	19546
S17_1	51215	40873	40873	23147	22687
S17_2	36361	28296	28296	15250	14910
S17_3	46849	35967	35967	21923	20765
S17_4	34766	27361	27361	15537	14981
S18_1	41336	32946	32946	20058	19553

S18_2	40194	32632	32632	22587	20284
S18_3	42221	33277	33277	20019	19251
S18_4	46846	37084	37084	22159	21539
S19_1	46160	37438	37438	20790	19621
S19_2	50469	40792	40792	25392	24178
S19_3	48494	38879	38879	22395	21824
S19_4	47951	38527	38527	21996	21417
S20_1	47183	38076	38076	21987	20928
S20_2	42260	34401	34401	18843	17951
S20_3	50901	40503	40503	24416	23098
S20_4	46791	37990	37990	21608	20737
S21_1	41015	33565	33565	20978	19475
S21_2	42477	34136	34136	22696	20685
S21_3	40303	32376	32376	20665	18926
S21_4	48019	38702	38702	25304	23038
S22_1	40909	32639	32639	18592	17702
S22_2	41907	33008	33008	19844	19022
S22_3	39314	30697	30697	16937	16152
S22_4	38281	29928	29928	16296	15277
S23_1	40319	31358	31358	18190	17451
S23_2	37341	29756	29756	16975	16319
S23_3	44530	34840	34840	24350	23209
S23_4	32947	26534	26534	17998	15700
S24_1	33962	27307	27307	18314	16753
S24_2	28800	21596	21596	12698	12206
S24_3	37292	29303	29303	17886	17219
S24_4	34107	27271	27271	15776	15092
S25_1	49186	38629	38629	23479	22078
S25_2	34056	27924	27924	17522	16205
S25_3	33382	26871	26871	16546	15777
S25_4	46462	37279	37279	23340	22028
S26_1	44438	35281	35281	24243	22827
S26_2	35931	28941	28941	18414	17321
S26_3	41725	33546	33546	21393	20124
S26_4	38662	30842	30842	19765	18296
S27_1	43453	34538	34538	18675	17996

S27_2	36183	29045	29045	16110	15616
S27_3	35734	29053	29053	17498	16072
S27_4	45394	36708	36708	20020	19196
S28_1	36616	29403	29403	17577	16093
S28_2	31889	26103	26103	15858	14455
S28_3	34760	27914	27914	16259	15566
S28_4	45368	36476	36476	21778	20336

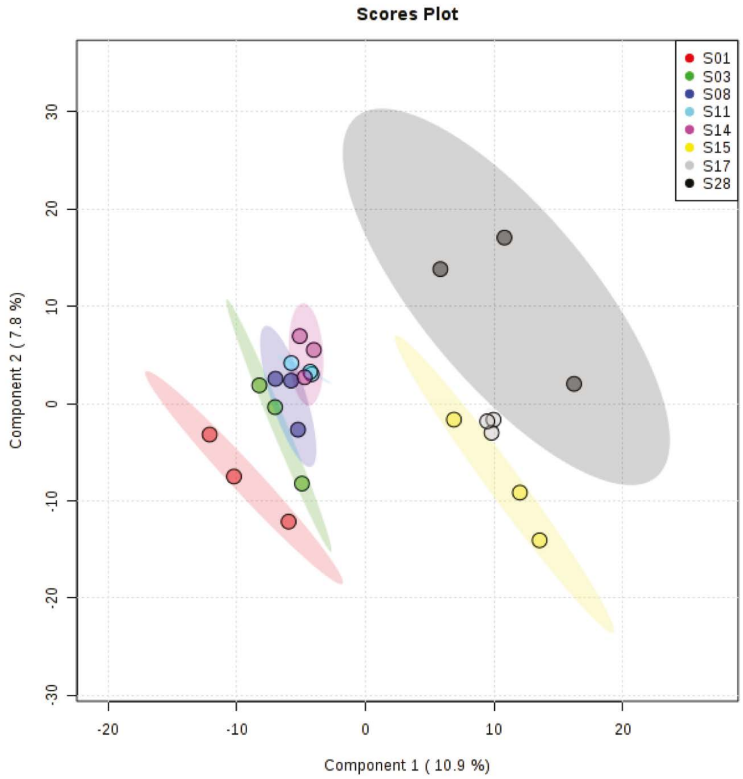
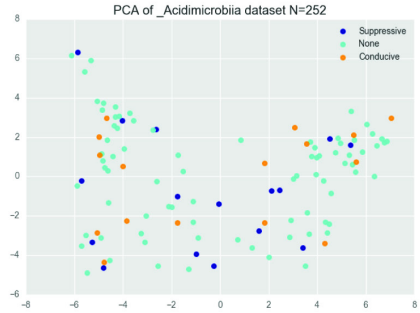
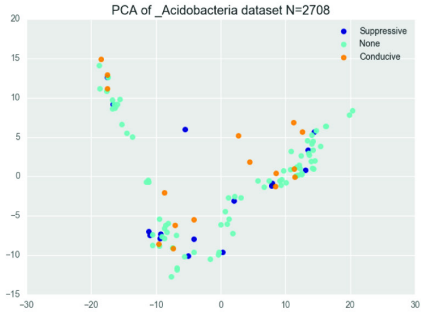
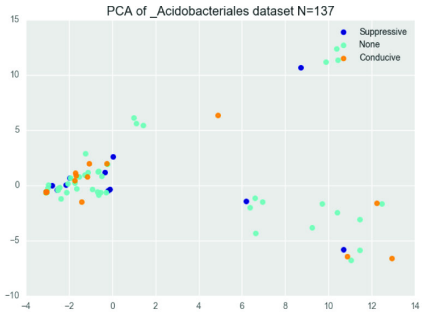
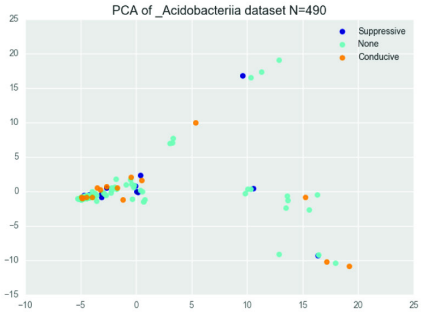


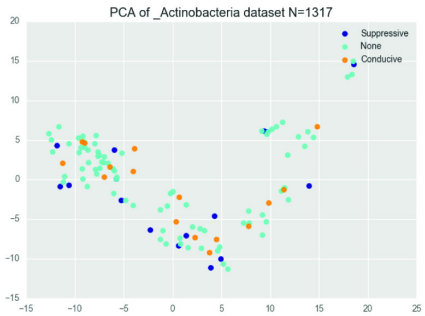
Figure S3. PCoA plot showing GC-MS profiles of volatile compounds emitted by eight soils, four suppressive (S01, S03, S11 and S28) and four conducive (S08, S14, S15 and S17) soils.

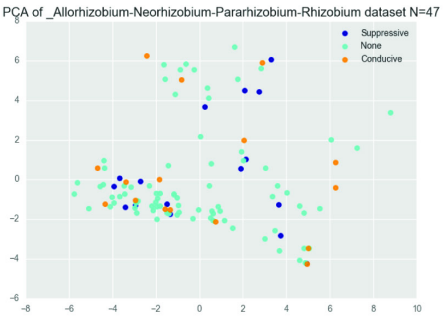

PCA of _Acidimicrobiia dataset N=252
Suppressive
None
Conducive

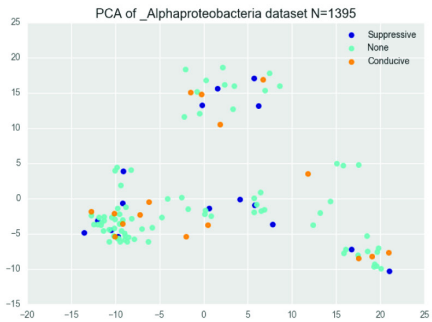

PCA of _Acidobacteria dataset N=2708
Suppressive
None
Conducive

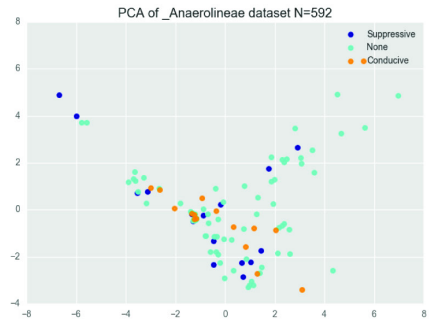

PCA of _Acidobacteriales dataset N=137
Suppressive
None
Conducive

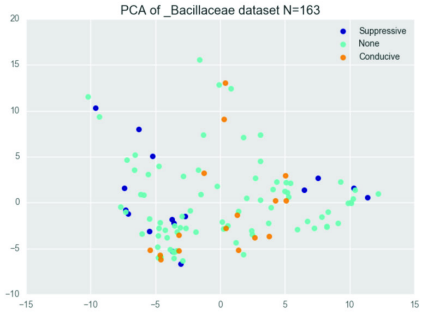

PCA of _Acidobacteriia dataset N=490
Suppressive
None
Conducive

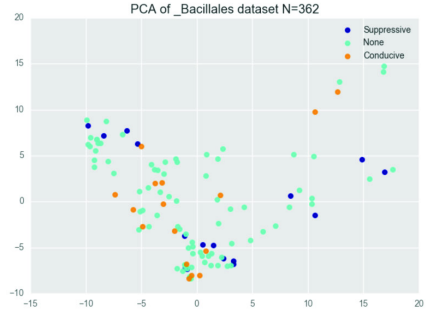

PCA of _Actinobacteria dataset N=1317
Suppressive
None
Conducive

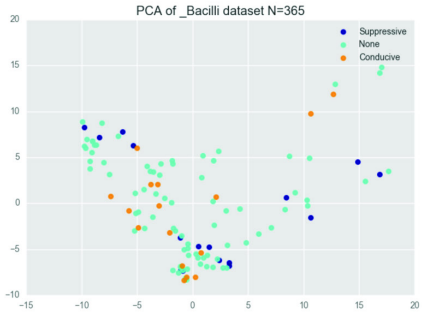

PCA of _Allorhizobium-Neorhizobium-Pararhizobium-Rhizobium dataset N=47
Suppressive
None
Conducive

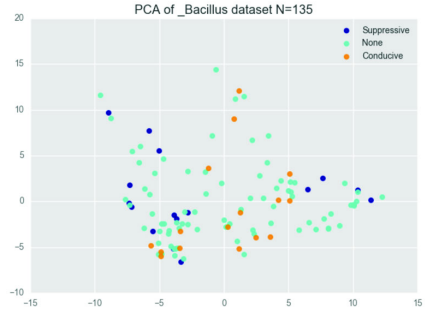

PCA of _Alphaproteobacteria dataset N=1395
Suppressive
None
Conducive

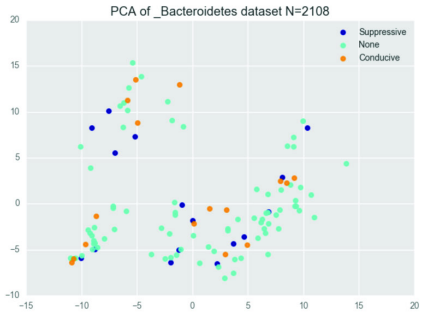

PCA of _Anaerolineae dataset N=592
Suppressive
None
Conducive

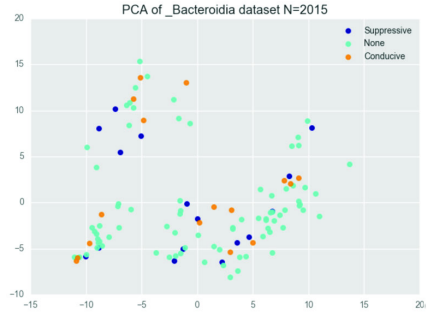

PCA of _Bacillaceae dataset N=163
Suppressive
None
Conducive

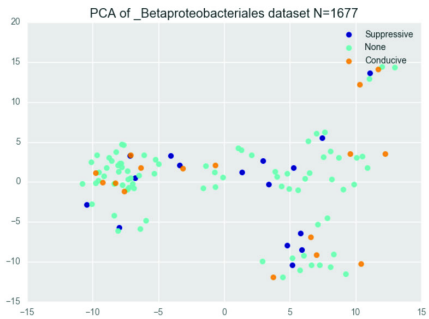

PCA of _Bacillales dataset N=362
Suppressive
None
Conducive

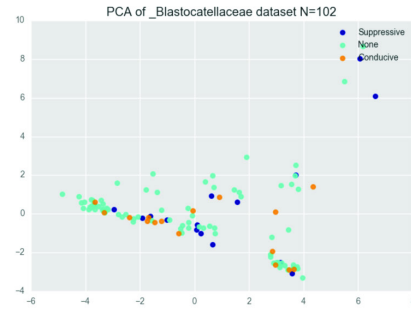

PCA of _Bacilli dataset N=365
Suppressive
None
Conducive

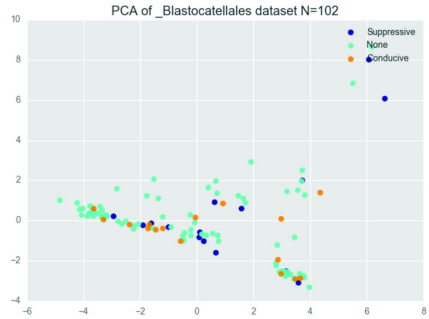

PCA of _Bacillus dataset N=135
Suppressive
None
Conducive

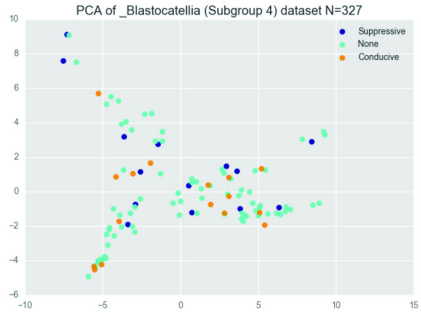

PCA of _Bacteroidetes dataset N=2108
Suppressive
None
Conducive

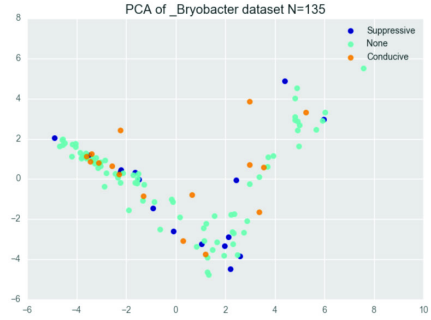

PCA of _Bacteroidia dataset N=2015
Suppressive
None
Conducive

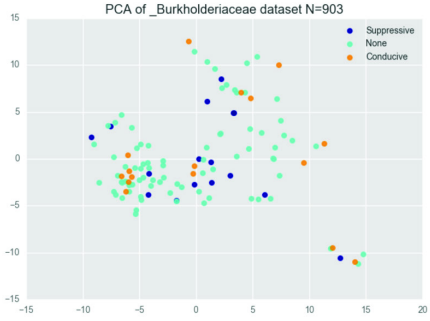

PCA of _Betaproteobacteriales dataset N=1677
Suppressive
None
Conducive

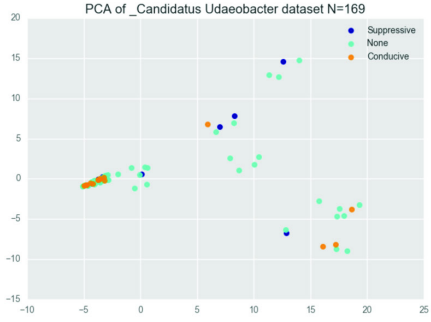

PCA of _Blastocatellaceae dataset N=102
Suppressive
None
Conducive

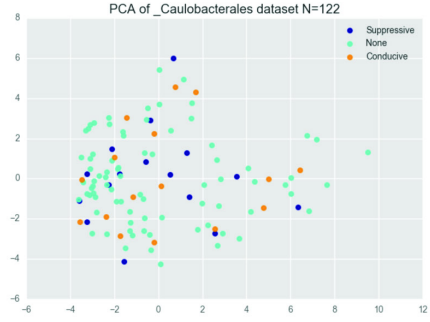

PCA of _Blastocatellales dataset N=102
Suppressive
None
Conducive

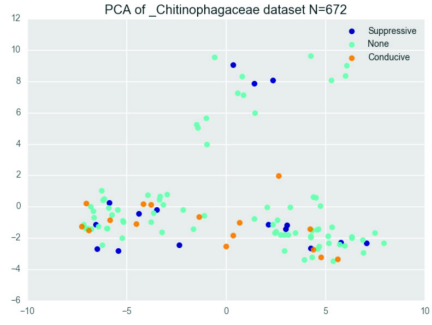

PCA of _Blastocatellia (Subgroup 4) dataset N=327
Suppressive
None
Conducive

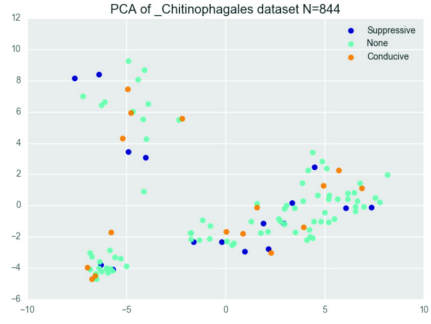

PCA of _Bryobacter dataset N=135
Suppressive
None
Conducive

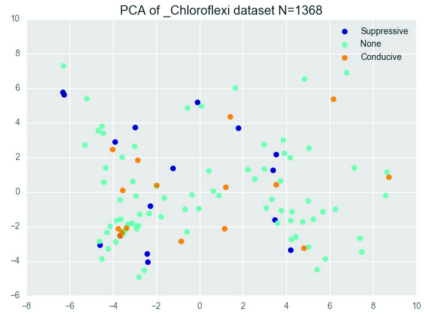

PCA of _Burkholderiaceae dataset N=903
Suppressive
None
Conducive

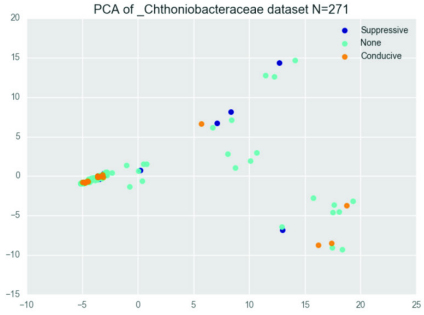

PCA of _Candidatus Udaeobacter dataset N=169
Suppressive
None
Conducive

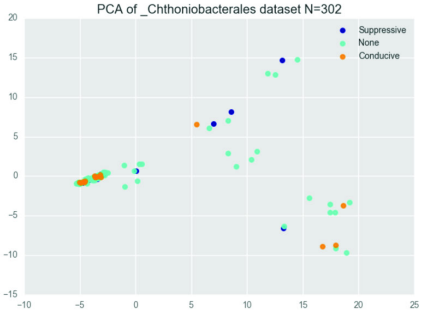

PCA of _Caulobacterales dataset N=122
Suppressive
None
Conducive

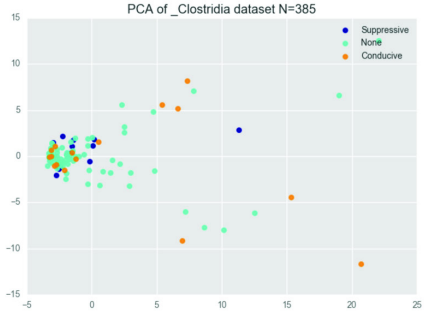

PCA of _Chitinophagaceae dataset N=672
Suppressive
None
Conducive

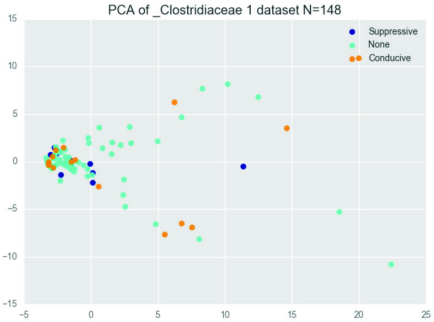

PCA of _Chitinophagales dataset N=844
Suppressive
None
Conducive

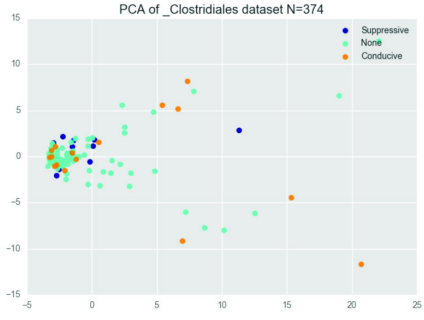

PCA of _Chloroflexi dataset N=1368
Suppressive
None
Conducive

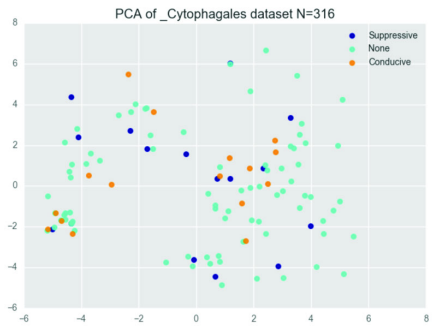

PCA of _Chthoniobacteraceae dataset N=271
Suppressive
None
Conducive

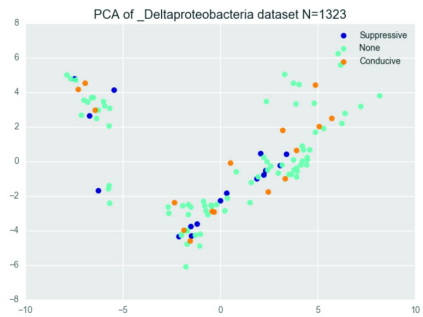

PCA of _Chthoniobacterales dataset N=302
Suppressive
None
Conducive

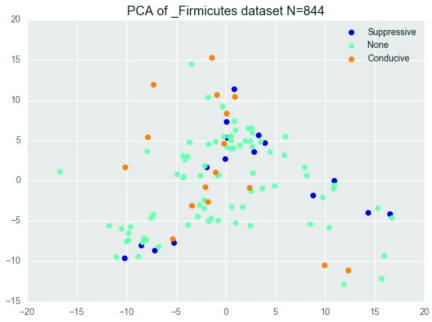

PCA of _Clostridia dataset N=385
Suppressive
None
Conducive

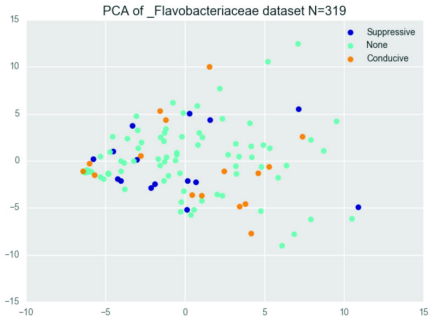

PCA of _Clostridiaceae 1 dataset N=148
Suppressive
None
Conducive

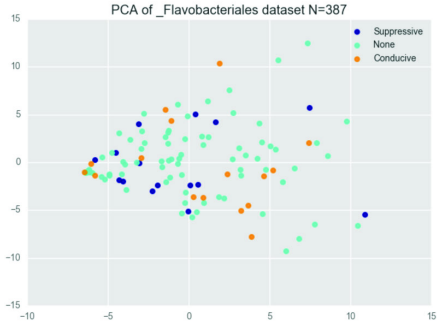

PCA of _Clostridiales dataset N=374
Suppressive
None
Conducive

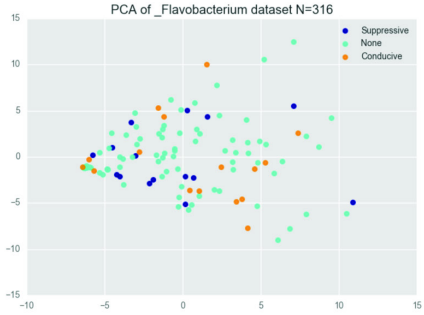

PCA of _Cytophagales dataset N=316
Suppressive
None
Conducive

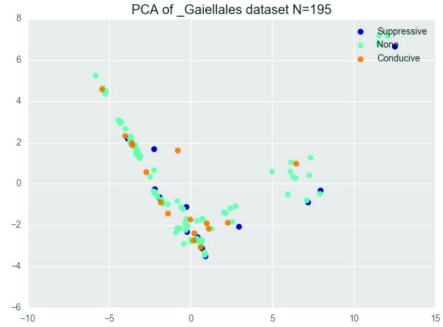

PCA of _Deltaproteobacteria dataset N=1323
Suppressive
None
Conducive

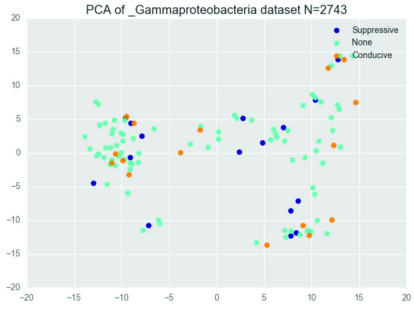

PCA of _Firmicutes dataset N=844
Suppressive
None
Conducive

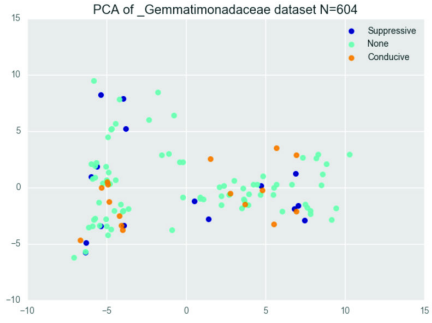

PCA of _Flavobacteriaceae dataset N=319
Suppressive
None
Conducive

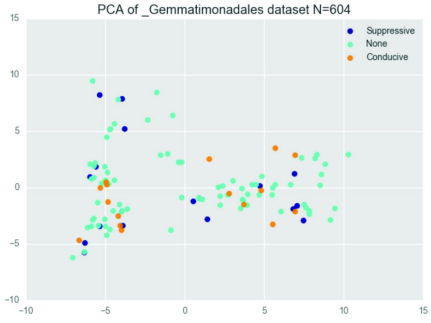

PCA of _Flavobacteriales dataset N=387
Suppressive
None
Conducive

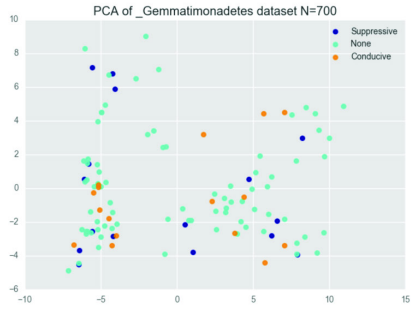

PCA of _Flavobacterium dataset N=316
Suppressive
None
Conducive

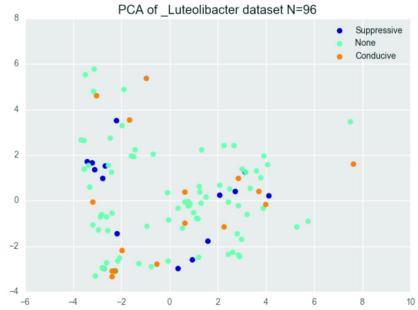

PCA of _Gaiellales dataset N=195
Suppressive
None
Conducive

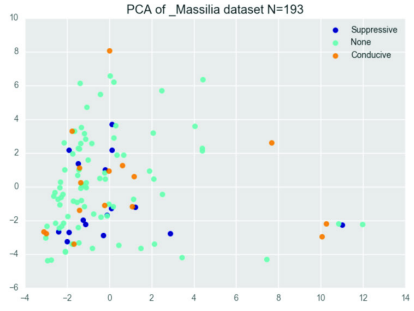

PCA of _Gammaproteobacteria dataset N=2743
Suppressive
None
Conducive

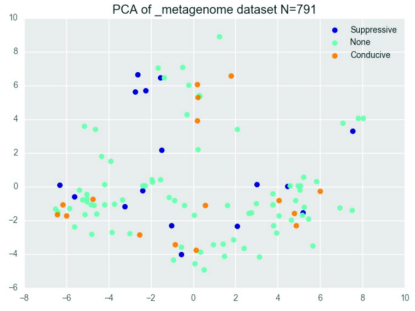

PCA of _Gemmatimonadaceae dataset N=604
Suppressive
None
Conducive

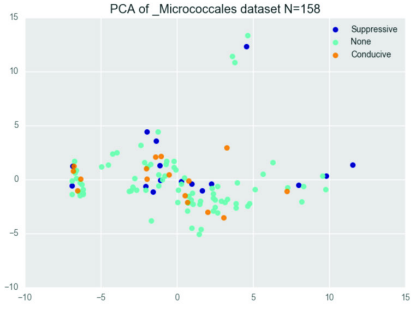

PCA of _Gemmatimonadales dataset N=604
Suppressive
None
Conducive

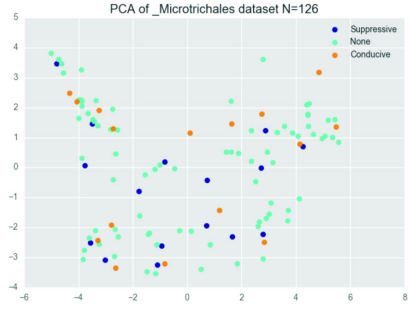

PCA of _Gemmatimonadetes dataset N=700
Suppressive
None
Conducive

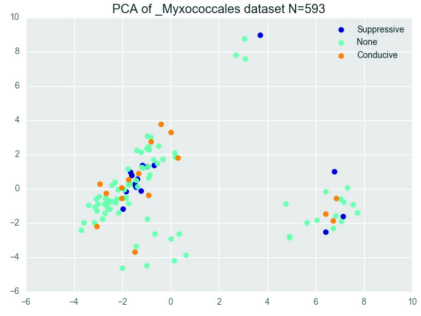

PCA of _Luteolibacter dataset N=96
Suppressive
None
Conducive

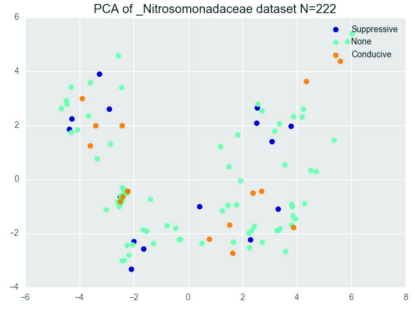

PCA of _Massilia dataset N=193
Suppressive
None
Conducive

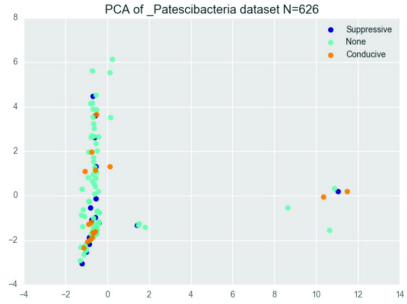

PCA of _metagenome dataset N=791
Suppressive
None
Conducive

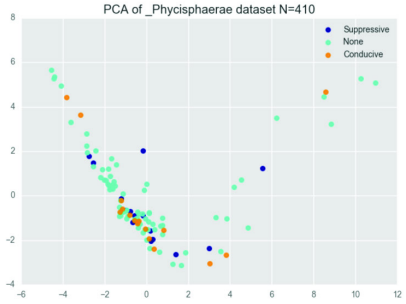

PCA of _Micrococcales dataset N=158
Suppressive
None
Conducive

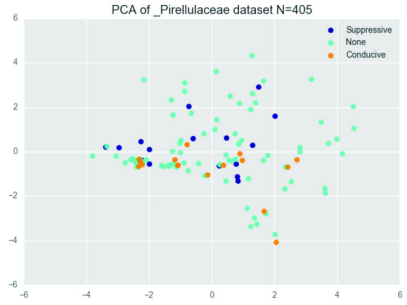

PCA of _Microtrichales dataset N=126
Suppressive
None
Conducive

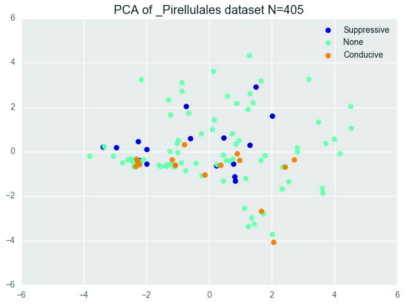

PCA of _Myxococcales dataset N=593
Suppressive
None
Conducive

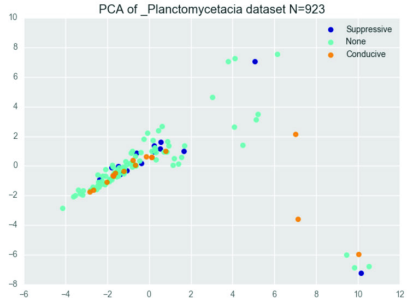

PCA of _Nitrosomonadaceae dataset N=222
Suppressive
None
Conducive

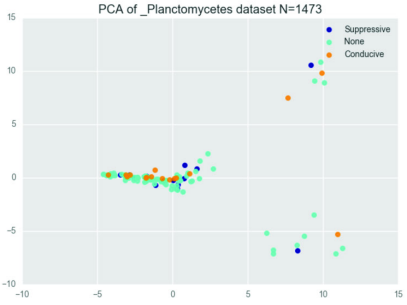

PCA of _Patescibacteria dataset N=626
Suppressive
None
Conducive

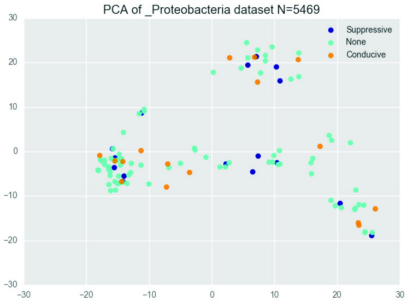

PCA of _Phycisphaerae dataset N=410
Suppressive
None
Conducive

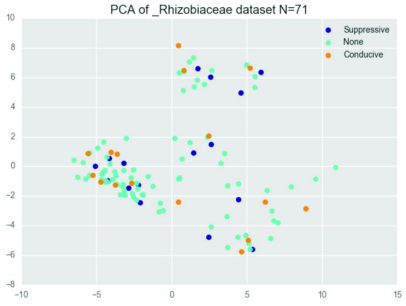

PCA of _Pirellulaceae dataset N=405
Suppressive
None
Conducive

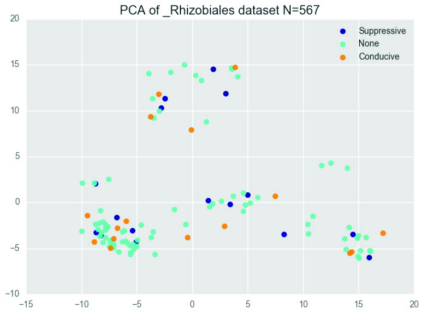

PCA of _Pirellulales dataset N=405
Suppressive
None
Conducive

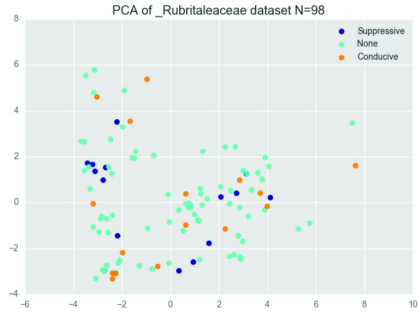

PCA of _Planctomycetacia dataset N=923
Suppressive
None
Conducive


PCA of _Planctomycetes dataset N=1473
Suppressive
None
Conducive

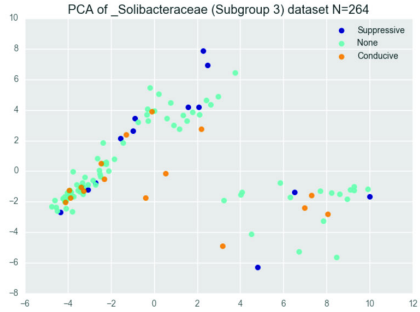

PCA of _Proteobacteria dataset N=5469
Suppressive
None
Conducive

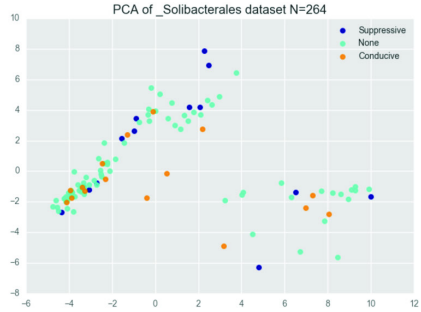

PCA of _Rhizobiaceae dataset N=71
Suppressive
None
Conducive

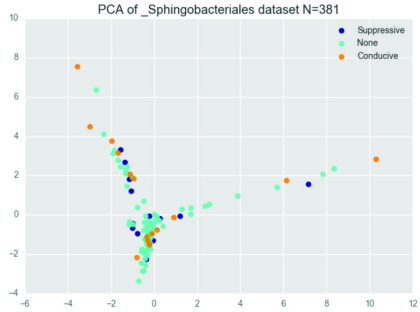

PCA of _Rhizobiales dataset N=567
Suppressive
None
Conducive

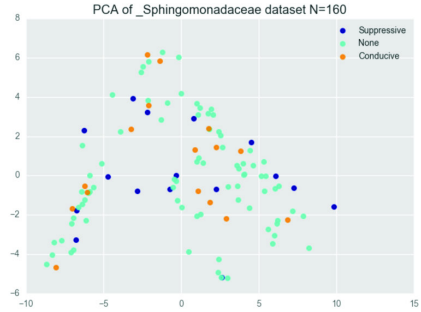

PCA of _Rubritaleaceae dataset N=98
Suppressive
None
Conducive

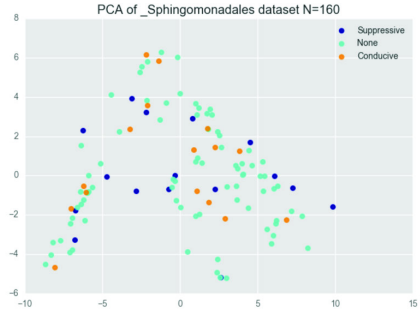

PCA of _SC-I-84 dataset N=238
Suppressive
None
Conducive

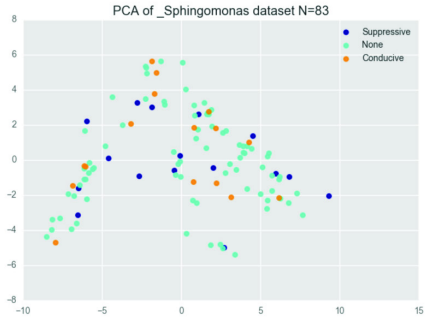

PCA of _Solibacteraceae (Subgroup 3) dataset N=264
Suppressive
None
Conducive

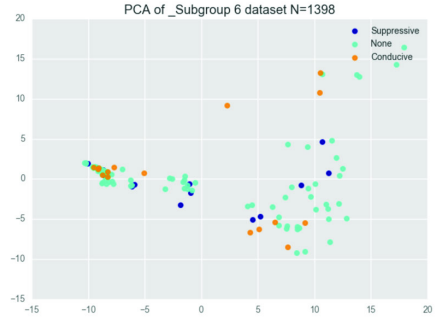

PCA of _Solibacterales dataset N=264
Suppressive
None
Conducive

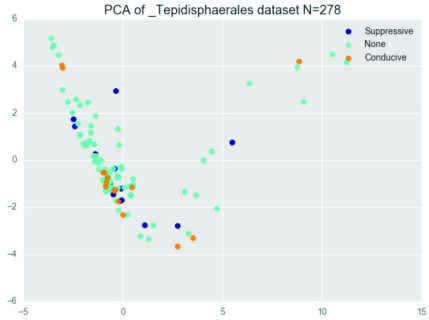

PCA of _Sphingobacteriales dataset N=381
Suppressive
None
Conducive

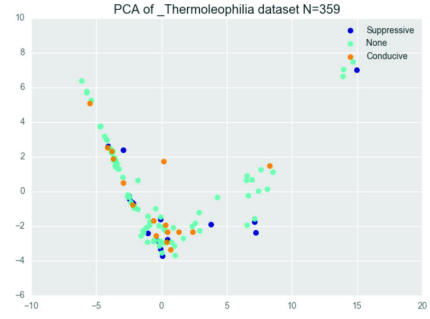

PCA of _Sphingomonadaceae dataset N=160
Suppressive
None
Conducive

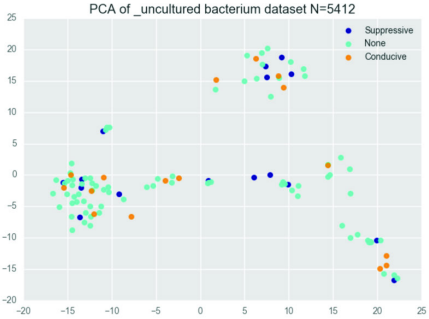

PCA of _Sphingomonadales dataset N=160
Suppressive
None
Conducive

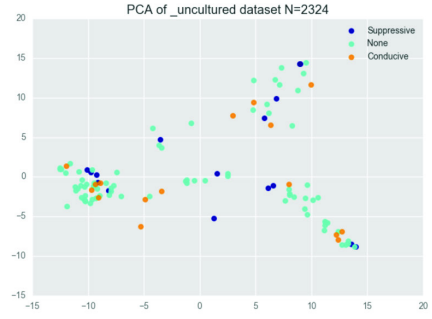

PCA of _Sphingomonas dataset N=83
Suppressive
None
Conducive

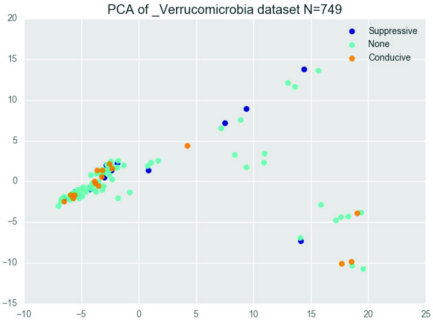

PCA of _Subgroup 6 dataset N=1398
Suppressive
None
Conducive

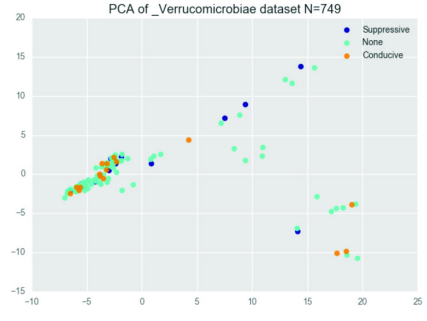

PCA of _Tepidisphaerales dataset N=278
Suppressive
None
Conducive


PCA of _Thermoleophilia dataset N=359
Suppressive
None
Conducive


PCA of _uncultured bacterium dataset N=5412
Suppressive
None
Conducive


PCA of _uncultured dataset N=2324
Suppressive
None
Conducive


PCA of _Verrucomicrobia dataset N=749
Suppressive
None
Conducive


PCA of _Verrucomicrobiae dataset N=749
Suppressive
None
Conducive

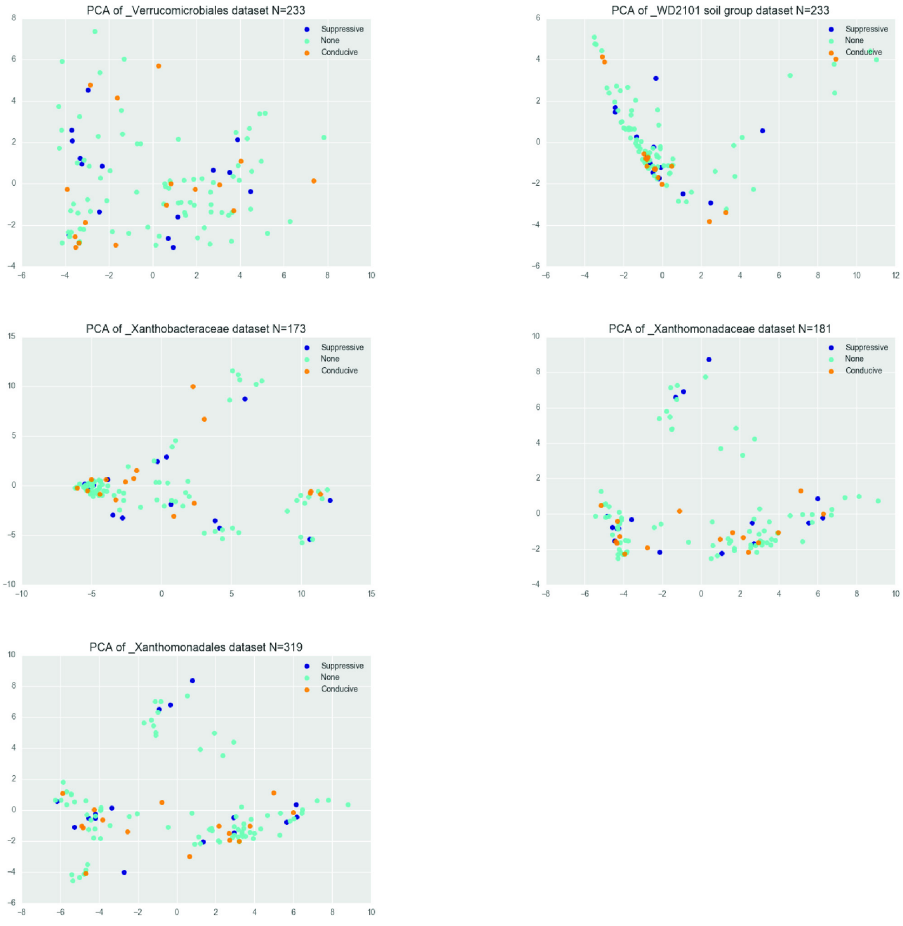


Figure S4. PCA plots of different taxonomy groups. The number of ASVs used for the component analysis is reported on top of each plot together with the taxonomic group represented in the figure.

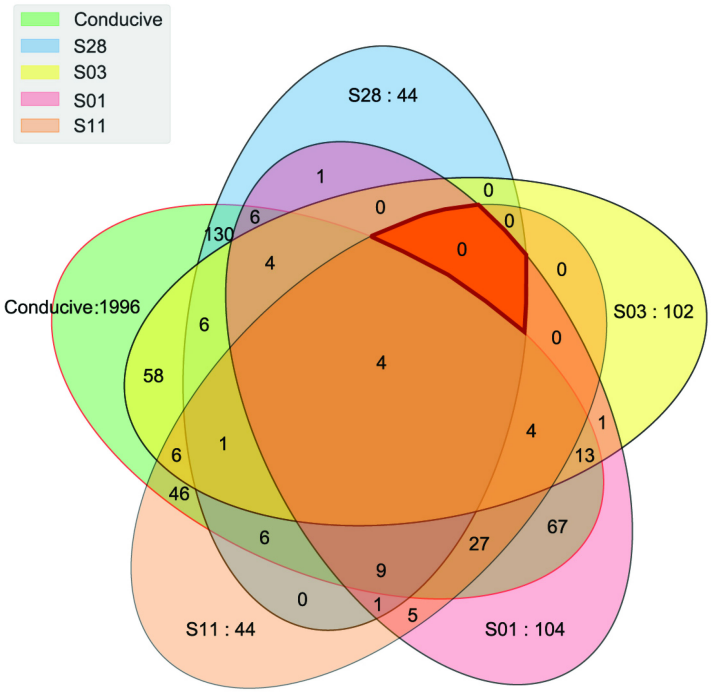


Figure S5. Presence-absence patterns of consistent ASVs. Venn diagram representing the ASVs which consistently appear in all replicates for each of the suppressive samples (S01, S03, S11 and S28) and the conducive samples (here grouped under "conducive").

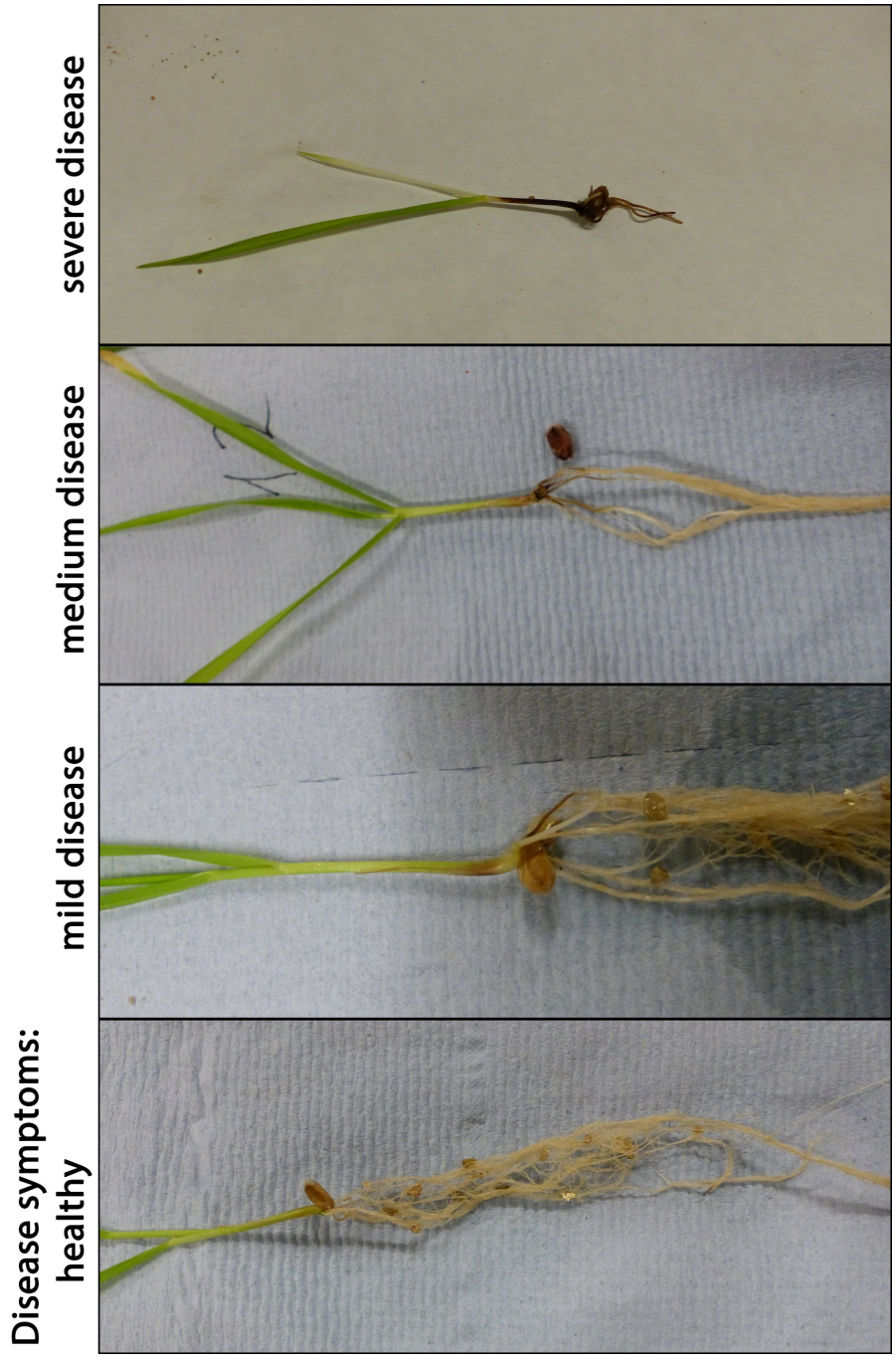
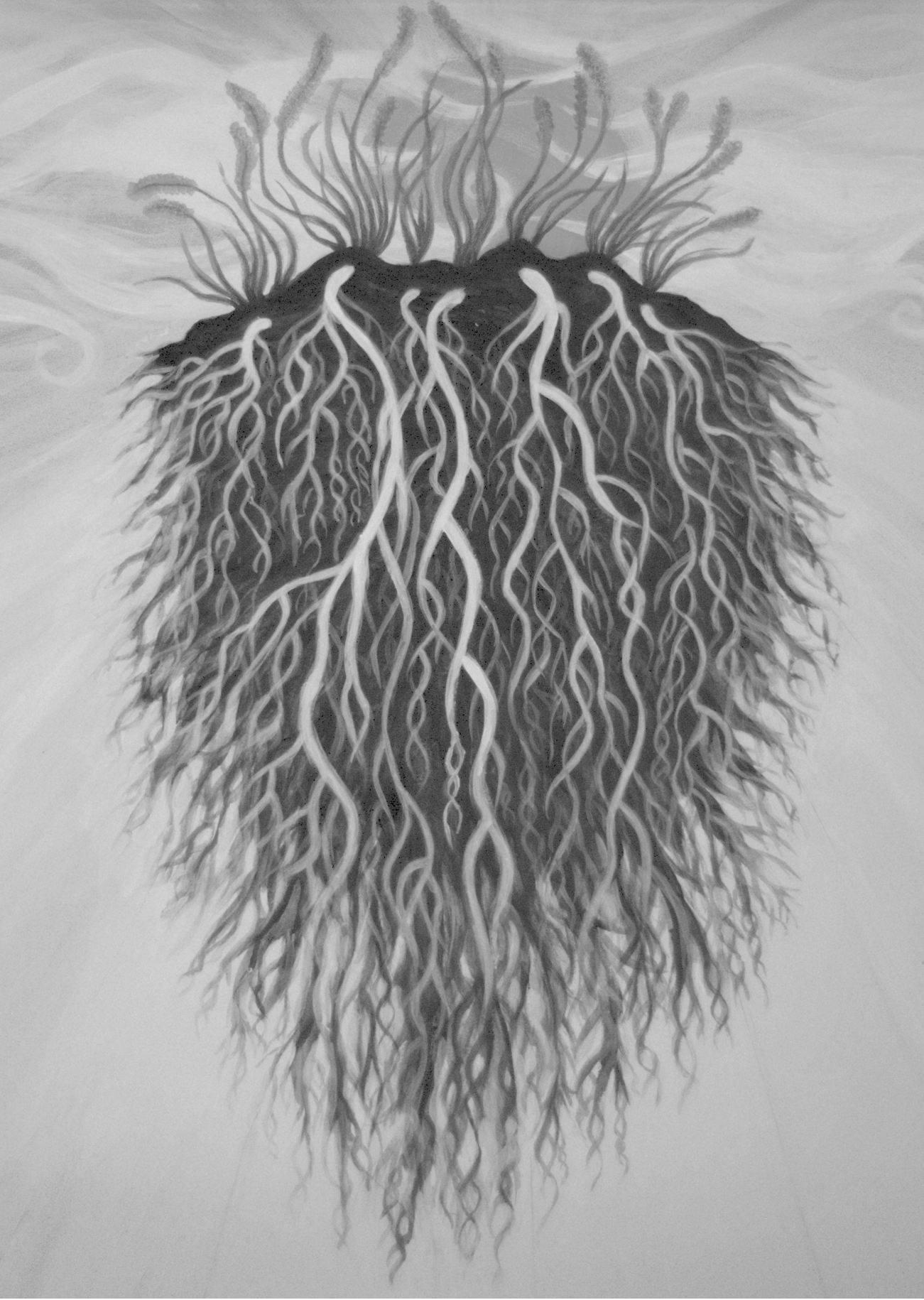


Figure S6. Examples of healthy and diseased plants obtained in the screening with disease scores indicated in brackets.



Chapter 3

Dissecting disease-suppressive rhizosphere microbiomes by functional amplicon sequencing and 10X metagenomics

Vittorio Tracanna[1]*, Adam Ossowicki[2]*, Marloes L. C. Petrus[3], Sam Overduin[1], Barbara R. Terlouw[1], George Lund[4], Serina L. Robinson[5], Sven Warris[6], Elio G. W. M. Schijlen[6], Gilles P. van Wezel[2,3], Jos M. Raaijmakers[2,3], Paolina Garbeva[2], Marnix H. Medema[1]

1. Bioinformatics Group, Wageningen University and Research, Wageningen, The Netherlands
2. Microbial Ecology, Netherlands Institute of Ecology (NIOO-KNAW), Wageningen, The Netherlands
3. Microbial Biotechnology, Leiden Institute of Biology, Leiden, The Netherlands
4. Biointeractions and Crop Protection, Rothamsted Research, Harpenden, United Kingdom
5. BioTechnology Institute, University of Minnesota-Twin Cities, MN, USA
6. Bioscience, Wageningen University and Research, Wageningen, The Netherlands
*: contributed equally to this work

A revised version was accepted for publication in mSystems

Abstract

Disease-suppressive soils protect plants against soil-borne fungal pathogens that would otherwise cause root infections. Soil suppressiveness is, in most cases, mediated by the antagonistic activity of the microbial community associated with the plant roots. Considering the enormous taxonomic and functional diversity of the root-associated microbiome, identification of microbial genera and mechanisms underlying this phenotype is challenging. One approach to unravel the underlying mechanisms is to identify metabolic pathways enriched in the disease-suppressive microbial community, in particular pathways that encode natural products with antifungal properties. An important class of these natural products are peptides produced by Non-Ribosomal Peptide Synthetases (NRPSs). Here, we adopted functional amplicon sequencing of NRPS-associated Adenylation domains (A-domains) to a collection of eight soils that are suppressive or nonsuppressive (i.e., conducive) to *Fusarium culmorum*, a fungal root pathogen of wheat. To identify functional elements in the root-associated bacterial community, we developed an open-source pipeline, referred to as dom2BGC, for amplicon annotation and putative gene cluster reconstruction through analyzing A-domain co-occurrence across samples. We applied this pipeline to rhizosphere communities from four disease-suppressive and four conducive soils and found significant similarities in NRPS repertoires between suppressive soils when compared to conducive soils. Specifically, several siderophore biosynthetic gene clusters were consistently associated with suppressive soils, hinting at competition for iron as a potential mechanism of suppression. Finally, to validate dom2BGC and to allow more unbiased functional metagenomics, we performed 10X metagenomic sequencing of one suppressive soil, leading to the identification of multiple gene clusters potentially associated with the disease-suppressive phenotype.

Importance

Soil-borne plant pathogenic fungi continue to be a major threat to agriculture and horticulture. The genus *Fusarium* in particular is one of the most devastating groups of soil-borne fungal pathogens for a wide range of crops. Our approach to develop novel sustainable strategies to control this fungal root pathogen is to explore and exploit an effective, yet poorly understood naturally occurring protection, i.e. disease-suppressive soils. After screening 28 agricultural soils, we recently identified four soils that were suppressive to root disease of wheat caused by *Fusarium culmorum*. We also confirmed, via sterilization and transplantation, that the microbiomes of these soils play a significant role in the suppressive phenotype. By adopting NRPS functional amplicon screening of suppressive and conducive soils, we here show how computationally driven comparative analysis of combined functional amplicon and metagenomic data can unravel putative mechanisms underlying microbiome-associated plant phenotypes.

Introduction

Cereals are a staple food for the human population, with wheat as the most widely consumed cereal crop worldwide. It is estimated that up to 40% of crop yields are lost due to weeds, pests and diseases ("Food and Agriculture Organisation of the United Nations," 2020). Pathogenic fungi are one of the major threats to agriculture. The genus *Fusarium* in particular is one of the most devastating groups of pathogens for a wide range of crops, including wheat (Dean et al., 2012; Valverde-Bogantes et al., 2019). *Fusarium culmorum* causes root rot and head blights in wheat and barley. It can kill plants at early stages of development or reduce their fitness and contaminate the grain with an arsenal of mycotoxins. Intriguingly, in some agricultural soils, root rot caused by *Fusarium culmorum* does not occur or only little (5). This so-called soil disease suppressiveness is a phenomenon where plants show strongly reduced disease symptoms despite the presence of a virulent pathogen and conditions favourable for disease development (Hornby, 1983). It is now well established that the soil and root microbiome are essential for disease suppressiveness. In recent work, we performed an extensive screening of 28 soils for their suppressiveness to *F. culmorum* (Ossowicki et al., 2020). We identified and confirmed, via sterilization and transplantation, that in four tested soils the microbiome is associated with suppressiveness to *F. culmorum*. Subsequent comparative taxonomic analysis of the root-associated bacterial communities, aimed to identify differences in abundance or absence/presence patterns of specific genera, revealed only limited commonalities between the four suppressive soils. The overall aim of this study was to adopt a functional approach to generate hypotheses regarding putative mechanisms associated with the disease-suppressive phenotype.

Many microbe-microbe interactions are mediated by specialized metabolites with diverse functions, including inhibition of fungal growth (Raaijmakers and Mazzola, 2012). The production of these bioactive compounds is often encoded by biosynthetic gene clusters (BGCs): groups of physically clustered genes that encode molecular machineries such as Non-Ribosomal Peptide Synthetases (NRPSs) and PolyKetide Synthases (PKSs), which enzymatically assemble complex metabolites. Importantly, these BGCs are often discontinuously distributed across taxa due to high rates of horizontal gene transfer (Medema et al., 2014). Additionally, there may be functional redundancy, due to overlapping biological activities between the products of different BGCs. Therefore, looking at BGC distribution patterns may help explain microbiome-associated phenotypes for which no clear taxonomic associations are identified. PKS and NRPS enzymes are often organized in multi-domain modules, which each contain a set of enzymatic domains that extend the growing peptide or polyketide chain with a specific monomer during enzymatic assembly. Functional amplicon sequencing can target such domains using oligoprimers to amplify DNA

from BGCs. Because the sequencing is highly selective, even BGCs from lowly abundant microorganisms can be detected by this technology (Hover et al., 2018; Owen et al., 2013).

Here, we use NRPS amplicon screening for comparative functional analyses of a set of four suppressive and four conducive agricultural soils in the presence and absence of the pathogen *F. culmorum*. To facilitate this analysis, we introduce dom2BGC, a pipeline for extensive annotation of BGC-related amplicons (2020). The amplicons are annotated based on similarity to domains in MIBiG and antiSMASH-DB, two large natural product BGC databases. For NRPS adenylation (A) domains, substrate specificities are predicted based on a newly built random forest classifier trained on the amplified region of these domains. When multiple samples are available, dom2BGC creates a co-occurrence network to aid in detection of groups of amplicons that jointly originate from known or related BGCs. We apply dom2BGC and validate the annotation and clustering results with the high-quality metagenome of a selected sample enhanced using 10X-based read clouds. The results show siderophore BGCs as key candidates associated with disease suppressiveness of the soils against *F. culmorum*. The linked-read metagenomic dataset further revealed several additional BGCs that, based on their predicted functions, may be involved in the disease-suppressive phenotype. This study exemplifies how computationally driven analysis of combined functional amplicon and metagenomic data can unravel new candidate BGCs for further investigation and help to develop new hypotheses regarding the mechanisms underlying important microbiome-associated phenotypes.

Materials and Methods

Soil collection

Eight soil samples: S01, S03, S08, S11, S14, S15, S17 and S28 were collected from 3-meter squares located at the centre of each agricultural field in January-April 2017. In this area, topsoil cores of approximately 30 cm deep were collected. Soils were air-dried at room temperature, homogenized, sieved through a 4mm mesh sieve and stored at 4°C. Soil S28 was additionally flaked after drying using a jaw-crusher (Type BB-1, Retsch, Germany). Detailed descriptions of the soil samples are included in our previous study (Ossowicki et al., 2020).

Disease suppressiveness assay and A-domains amplification

Wheat growth conditions, pathogen inoculation, the suppressiveness assay, A-domains amplification and sequencing are described in detail in supplementary methods. Briefly, wheat seedlings were transferred to substrate containing one of the eight tested soils and challenged with pathogenic *Fusarium culmorum* PV. After three weeks, wheat plants were

inspected for disease symptoms together with rhizosphere DNA isolation. NRPS adenylation domains were amplified using 3F and A7R primers (Ayuso-Sacido and Genilloud, 2005).

A-domain amplicon preparation

Barcoding and sequencing of the A-domain amplicons was performed at BaseClear (Leiden, the Netherlands) using Illumina MiSeq, which generated 843,536 paired-end reads of 250 bp in length per read. Sequences were de-multiplexed and adapters trimmed using Qiime2 (Bolyen et al., 2019, p. 2). Quality filtering and denoising was done with Dada2 (Benjamin J Callahan et al., 2016). Nucleotide sequences were translated to amino acid sequences with transeq from the EMBOSS suite (Rice et al., 2000). Forward sequences were aligned with the AMP-binding domain hidden Markov model (HMM) profile PF00501 from the pfam database [version 27] (El-Gebali et al., 2019) using hmmsearch from the HMMer package [version 3.1] (Wheeler and Eddy, 2013). The output table was parsed to retain only the conserved amino acids in the sequence corresponding to "match" states with the HMM profile. Protein sequences shorter than 66 amino acids were discarded. The resulting pre-aligned amplicon sequences from the natural source are referred to as nAMPs (natural amplicons) to distinguish them from the *in silico* amplicons used for their annotation.

10X metagenome

DNA extraction, sequencing and the assembly are described in detail in the supplementary methods. Briefly, 10X Genomics Chromium was used to generate a read cloud library from high quality rhizosphere DNA and subsequently sequenced on an Illumina NovaSeq 6000.

Feature extraction from amplicons for substrate specificity prediction

These methods, including substrate specificity prediction model training and tuning, are described in detail in the supplementary methods.

Dom2BGC pipeline - Generation of *in silico* amplicons

To generate a reference dataset of NRPS functional amplicons, A-domain sequences were extracted from BGCs from a variety of reference databases. Hmmsearch with default parameters was used to detect the A-domains, and the domain regions targeted by the oligoprimers were extracted from the matched sequences using HMM profile match coordinates. This process creates *in silico* amplicons which are pre-aligned to the nAMPs, which allows for quick matching between nAMPs and *in silico* AMPs using pairwise identity. Annotations available for *in silico* amplicons are stored to be transferred to any nAMPs matching with it. Currently supported annotations include, where available, the taxonomy of the source organism, the BGC type annotation based on antiSMASH predictions, and the

name of the natural product for which the production is encoded in the BGC (for domains extracted from MIBiG entries, (Kautsar et al., 2020)).

Dom2BGC pipeline - Amplicon matching and annotation

Each nAMP is matched to an in-silico amplicon if it shares 90% or more of its amino acid sequence with the reference. For nAMPs matching to multiple in-silico AMPs within a reference database, all entries are recorded. In case of multiple nAMPs matching an individual in-silico amplicon, all matched nAMPs are grouped for evaluation of presence-absence patterns and abundance of the in-silico amplicon.

In dom2bgc, amplicons are taxonomically annotated at the lowest rank available. In case of annotation to a reference BGC with a different taxonomic annotation, dom2BGC assigns the amplicon to the lowest common ancestor of the matching references. In addition, information from the reference cluster on the gene cluster family is passed on to the matching amplicon. This annotation is based on antiSMASH classification rules for predicted gene clusters. Possible annotations include NRPS, lipopeptides, hybrid PKS and more. In case of an amplicon matching with reference clusters belonging to different gene cluster families, dom2BGC reports all matches.

Dom2BGC pipeline - Co-occurrence network creation and analysis

Pairwise co-occurrence patterns of nAMPs are calculated using Spearman rank correlation of presence-absence patterns using numpy meshgrid. To filter out spurious relationships, the correlation network contains only the strongest correlations in the 99^{th} percentile among abundant nAMPs. In the resulting network, amplicons are nodes and edges are drawn based on co-occurrence. Clustering within the network to define BGC hubs is performed with DBscan. These BGC hubs, comprising highly correlated nAMPs, are inspected for nAMP annotation enrichment. Cluster nodes and first-degree neighbors annotated to the same reference gene cluster are further selected as putative gene clusters. Networks are visualized in Cytoscape (Shannon et al., 2003) and putative clusters are reported in a separate tab separated file.

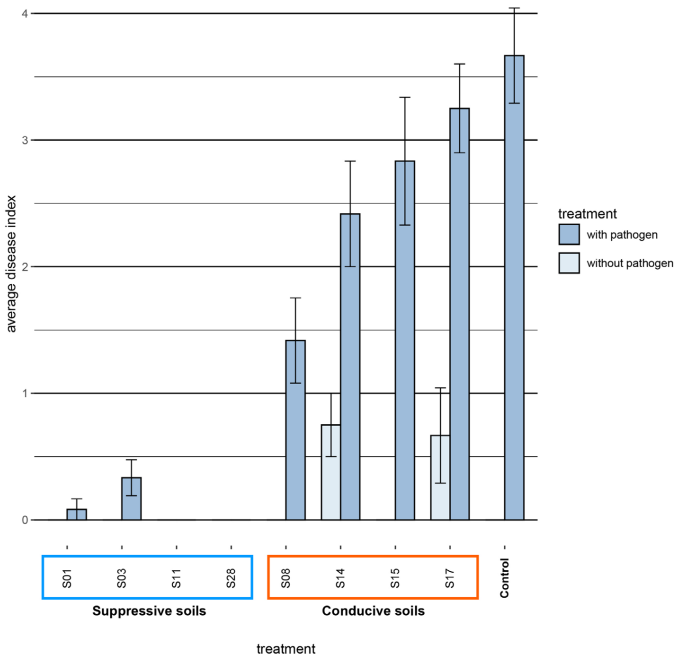


Figure 1. Disease index of Fusarium root rot disease of wheat grown in eight different agricultural soils. Four soils (S01, S03, S11, S28) were classified as disease suppressive and four soils (S08, S14, S15, S17) as disease conducive. Dark blue - inoculated with F. culmorum, light blue – non-inoculated, sterile BS dune soil was used as a control. The bar indicates the average disease index, with the error bars representing the standard error of the mean (n=12).

Results and Discussion

Identification of disease- suppressive agricultural soils

In our previous study (Ossowicki et al., 2020), we tested 28 diverse field soils from the Netherlands and Germany for disease suppressiveness against *F. culmorum* root rot of wheat. Based on these results we selected four disease-suppressive (S01, S03, S11 and S28) and four disease-conducive (S08, S14, S15 and S17) soils for further analysis. For the amplicon-based analyses of the rhizosphere microbiome, we again performed disease suppressiveness assays on these eight soils. We observed no disease symptoms in two inoculated suppressive soils (S11 and S28), and only low levels of disease in the other two inoculated suppressive soils (S01 and S03). This clearly contrasts with the four conducive soils, where disease levels varied from moderate (S08) to high (S14, S15 and S17, Fig.1). In two of the conducive soils (S14 and S17), we also identified some mild disease symptoms in treatments without addition of the pathogen, indicating the presence of indigenous populations of *F. culmorum* or of other pathogens causing similar disease symptoms (Fig. 1, light blue bars). Altogether, these results confirm and extend the results of our previous study and show a clear distinction in phenotype between the four suppressive and the four conducive soils.

Functional amplicon sequencing uncovers novel NRPS domains from low-abundant bacteria in rhizosphere microbial communities

As our previous 16S rRNA-based analysis of taxonomic similarities and differences between and across conducive and suppressive soils revealed that no taxa were unequivocally linked to disease suppression (Ossowicki et al., 2020), we turned to functional amplicon sequencing to assess whether this could point to metabolites or classes of metabolites associated with the suppressive phenotype. The selective amplification of functional domains allows capturing biosynthetic diversity found within a complex soil sample. Specifically, we used PCR amplification of A-domains of NRPSs, which are involved in the production of several types of bioactive molecules that have been previously linked to disease suppression, such as lipopeptides and siderophores. In NRPSs, the role of A-domains is to recognise and activate amino acid substrates that are incorporated into the growing peptide (Martínez-Núñez and López, 2016). Based on their sequence, it is possible to predict their amino acid specificity and match them to databases of known or predicted BGCs.

Functional amplicon sequencing of adenylation domains across the four suppressive and four conducive soils produced 4,181,437 raw reads across all samples, which were used to identify association patterns of A-domains across suppressive and conducive soils. One replicate from suppressive soil S28 (FC.1, supplementary Fig.S1) was removed from further analysis, because it produced significantly fewer reads compared to other samples (12,380 reads while the rest of the samples average 61,132 reads). Processing of the reads resulted in 3,396,393 reads mapping to 51,912 unique domains. Rarefaction analysis revealed that for most samples, diversity was sufficiently covered at ~30,000 reads per sample (Supplementary Table.S1).

To facilitate linking amplicon sequences to specific BGCs, we generated a high-quality shotgun metagenome assembly of one sample from the rhizosphere microbiome of plants grown in soil S11. This soil was chosen because of its strong disease suppression in this study as well as in our previous experiments (Ossowicki et al., 2020). To increase assembly contiguity, we made use of 10X linked read sequencing technology, which is able to generate much more contiguous contigs compared to what is possible with conventional metagenomics with comparable coverage. We used the dedicated cloudSPAdes 10X linked reads assembler on these data, which resulted in an assembly size of 2.2Gb and an N50 of 2.8Kb for contigs above 1Kb, with the largest contig measuring 1.3 Mb. Compared to the metaSPAdes equivalent assembly, which does not make use of the linked read information, we observed a considerable improvement in the N50 and assembly size for contigs above 5Kb (7.3Kb for regular metaSPAdes assembly and 20.2Kb for cloudSPAdes) which makes the cloudSPAdes assembly more suited to obtain complete NRPS BGCs (Meleshko et al., 2019).

Functional amplicon sequencing of A-domains can achieve better coverage of domains from rare BGCs compared to metagenomics with the same sequencing volume. This is reflected by the higher diversity of domains found in natural amplicons (nAMPs), with 40,005 unique amplicons at the protein level, compared to the shotgun assembly that yielded 8,762 unique *in silico* amplicons. Remarkably, we observed that the number of unique sequences present in all our samples surpasses the diversity contained in antiSMASH-DB (24,085 AMPs) - the largest available annotated database for natural product-encoding BGCs that contains sequence data for 32,548 BGCs from 24,776 microbial genomes. To highlight the importance of environmental sampling efforts, we further matched the nAMP sequences to *in silico* amplicons from antiSMASH-DB. We found that most sequences could be matched at or above 70% identity. However, there are 162 instances of A-domains with < 30% amino acid sequence identity to their closest representative in the database. These domains, while still matching the Pfam domain, can potentially harbor novel functions, such as incorporation of different amino acids, or may simply belong to rare and uncharted BGCs. The percentage identity of nAMPs to the closest antiSMASH-DB AMP follows a normal distribution, with a peak to the right accounted for by (near-)perfect matches to previously sequenced clusters (Fig. 2A).

To evaluate the impact of the primer bias on the observed amplicon diversity, we performed an inverse analysis by identifying the closest match of *in silico* amplicons from antiSMASH-DB to the nAMPs from the soil, as the first is not affected by primer bias. The results revealed a bimodal distribution (Fig. 2B and supplementary table S2). The leftmost mode includes amplicons not present in the samples, as well as amplicons that might be present in the samples but absent in the nAMPs set because of their poor match to the primer sequences. Still, the majority of the *in silico* amplicons from antiSMASH-DB had a match in our sample above 60% sequence identity. This indicated that the primer bias, despite being present, does not prevent the majority of the known sequence diversity of adenylation domains to be represented in the functional amplicon data. These results confirm the high value of functional amplicon sequencing studies in charting the biosynthetic potential of environmental niches. Based on these results we see that with limited primer bias we can still get substantial coverage of nAMPs.

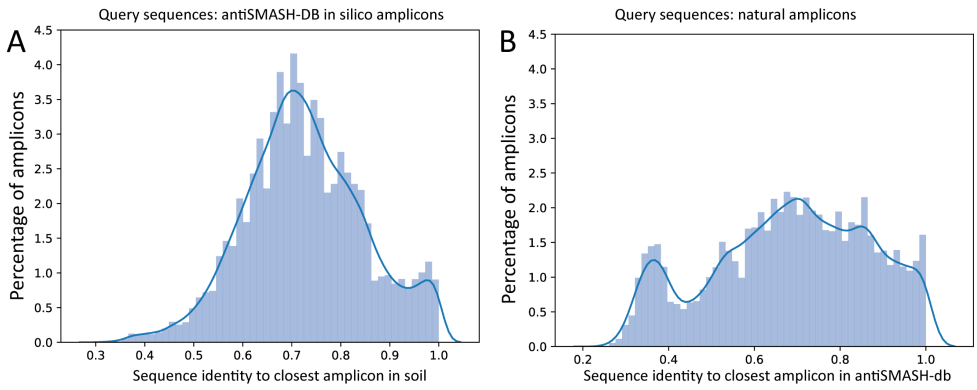


Figure 2. Sequence distance between nAMPs and antismash-DB in silico amplicons. A) Histogram showing the distribution of best matches (as in highest percentage identity at protein level) between each nAMP and the antiSMASH-DB in silico amplicon database. B) Histogram showing the distribution of best matches (as in highest percentage identity at protein level) between each antiSMASH-DB in silico amplicon and the nAMPs.

The dom2BGC pipeline facilitates automated annotation and networking of functional amplicons

Current tools for the annotation of functional amplicons (eSNaPD (Reddy et al., 2014), NaPDoS ("The Natural Product Domain Seeker NaPDoS: A Phylogeny Based Bioinformatic Tool to Classify Secondary Metabolite Gene Diversity," n.d.)) have limited applications or rely on laborious processes which require expensive laboratory automation of BAC clone library approaches (CONKAT-seq (Libis et al., 2019)). To harness the potential of A-domain functional amplicons in soils, we developed dom2BGC, a pipeline to add taxonomical, functional and product annotation to amplicon sequences and validate some of the predicted clusters using shotgun metagenomics assembly data. Within dom2BGC (Fig. 3), amplicons are matched to antiSMASH-DB and MIBiG, two natural product BGC databases, and annotations are transferred to the query amplicons when hits are reported above a user-set threshold (default: 95% identity). Diversity measurements and community structure relationships between samples are calculated and visualized in a series of automatically generated figures (examples: Fig.2, Fig.5 - network). Finally, a co-occurrence network of amplicons across the samples is created. Neighboring amplicons mapping onto domains of known clusters from antiSMASH-DB or MIBiG are considered as domains which potentially belong to the same original cluster. This information can then be used in designing further experiments to validate the putative functions of the identified clusters.

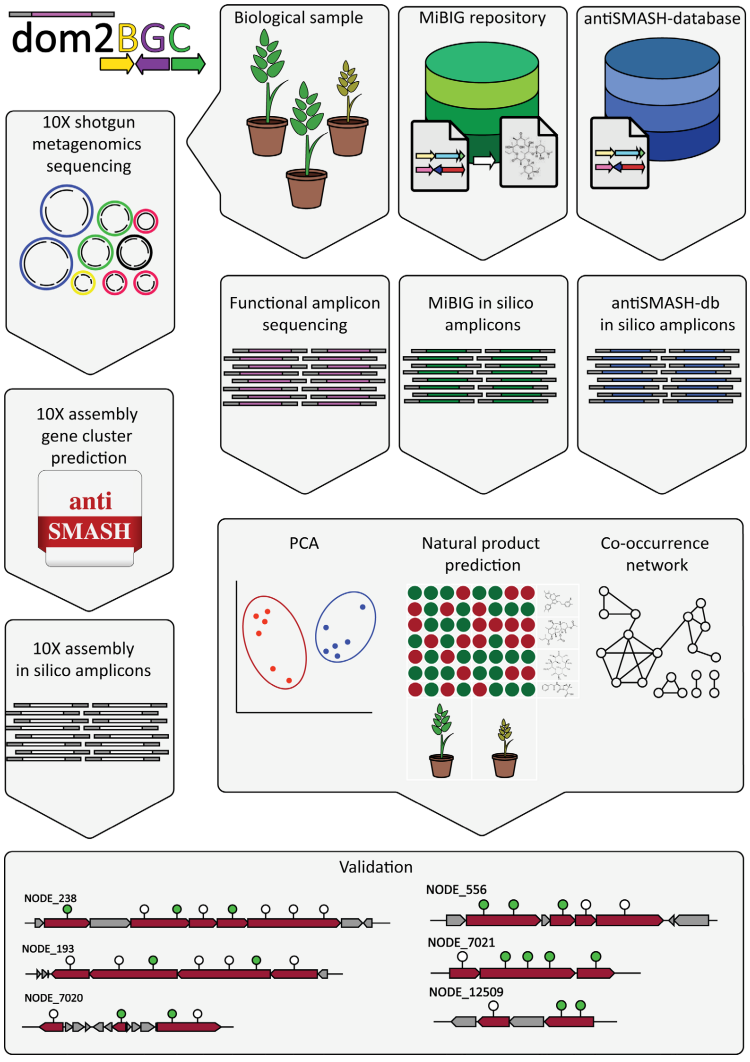


Figure 3. The dom2BGC annotation pipeline and validation process. Amplified sequences from the rhizosphere are translated to nAMPs as per methods section and have been annotated through comparison with in silico amplicons from MiBIG and antiSMASH databases. Richness and community composition measures are used to assess their associations with phenotype and treatments. Co-occurrence patterns of amplicons which share similarity to the same reference BGCs were used to predict presence of (homologues of) known BGCs. Finally, in this study, a shotgun metagenomic assembly from one of the soil samples was used to confirm the presence of these predicted gene clusters from the amplicon data.

To identify known natural product BGCs in the microbial communities, a total of 3,239 *in silico* amplicons were generated from MIBiG products entries (MAMPs – MIBiG amplicons). 1,312 unique nAMPs, corresponding to 8% of the total, were matched and associated to a BGC for a known natural product. Notably, the most abundant known BGC annotated encodes the biosynthesis of pyoverdine; this NRPS gene cluster is widespread among *Pseudomonas* species which are also common members of the rhizosphere. Still, even for MIBiG entries with a perfect match and consistent coverage across samples, not all the A-domains present in the reference cluster could be amplified. This illustrates how functional amplicon sequencing provides deep coverage of biosynthetic diversity across microbiome samples, but also misses certain domains because of mismatches between oligo-primers and the target sequence or other PCR biases. This is partially balanced by the fact that most NRPS gene clusters encode multiple A-domains, which increases the chance that at least one of these regions is amplified. As for database coverage, 119 out of 860 entries with an adenylation domain in MIBiG had at least one amplicon from our data mapping to one of its domains above 90% amino acid identity. This is testament to the extensive natural product potential of soil microbial communities.

To investigate the taxonomical and gene cluster class distributions of nAMPS, a total of 40,211 *in silico* amplicons were generated from antiSMASH-DB BGCs (aSAMPs) and used to annotate 5,531 nAMPs (corresponding to 29,9% of total reads), linking them to 1,443 different BGCs. This annotation rate constitutes about a 4-fold increase compared to the numbers of nAMPs that could be annotated using MIBiG as reference.

Disease-suppression is not associated with increased adenylation domain diversity but shows distinct community structure

There is great need for diagnostic tools to assess the disease-suppressive potential of agricultural soils based on their microbial and functional composition. In a recently published paper, Yuan et al. (Yuan et al., 2020) explored in a meta-analysis the potential of 16S and ITS amplicons as predictors of disease occurrence. Since A-domain functional amplicon data showed more distinctive patterns than 16S data between soils with conducive and suppressive phenotypes (5), we set out to explore if it might be feasible to use functional amplicon sequencing as a diagnostic tool of disease suppressiveness. To test the possible association of within-sample amplicon diversity measures with the suppressive phenotype, we calculated within-sample richness, evenness and phylogenetic diversity for all samples based on observed unique amplicons, Simpson-e and Faith-PD, respectively. Wilcoxon rank-sum tests showed no significant association of alpha diversity measures with the presence of the pathogen nor with the suppressive phenotype for any of these metrics (Fig.4A).

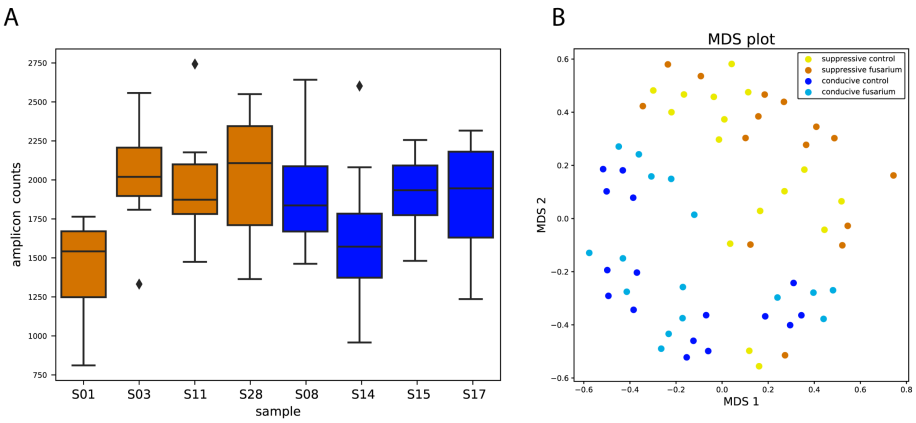


Figure 4. Community diversity and composition. A) Adenylation domain richness across suppressive (orange bars) and conducive (blue bars) soils, calculated as unique sequences. B) Visualization of the adenylation domain community composition with multidimensional scaling.

Several studies have associated overall microbial species richness or evenness in the soil and rhizosphere with disease suppressiveness (Chaparro et al., 2012; Garbeva et al., 2004; Janvier et al., 2007; Larkin, 2015; van Bruggen et al., 2015). In other studies, however, this was not the case, and suppressiveness was associated with the abundance/enrichment of specific genera or functions (Carrión et al., 2019; Mendes et al., 2011). Here, we note that suppressive soils were both among the most and least diverse in terms of NRPS A-domains, which highlights the importance of availability of samples from multiple sources that share the same phenotype before drawing conclusions on the role of community diversity in disease suppression.

In a multi-dimensional scaling (MDS) analysis, suppressive soils did form a distinct group based on their community profile (Fig.4, panel B) with significant grouping, suggesting that similar community NRPS profiles can indeed be associated with the suppressive phenotype based on unweighted Unifrac (PERMANOVA, p-value=0.010; ANOSIM, p-value=0.010). This could indicate that the observed phenotype is caused by a single or limited number of pathway(s), not detectable with overall richness or abundance measurements, that directly interfere with a pathogen's ability to colonize the rhizosphere, initiate root penetration and disease.

Thus, it appears that sequencing A-domain community composition has the potential to become a predictive tool for diagnosing soil suppressiveness. Nevertheless, we should emphasize that our study is based on only one host-pathogen system (wheat and *Fusarium culmorum*) and a collection of eight soils. Still, the fact that the production of compounds

by NRPS and PKS enzymes play crucial roles in other disease-suppressive soils (Carrión et al., 2019; Duijff et al., 1999, 1994; Hayden et al., 2018; Kinkel et al., 2012; Michelsen et al., 2015; Raaijmakers and Weller, 1998; Scher M., 1982; Weller et al., 2002a; Zhao et al., 2018) supports this proposition. This method has to be further developed and validated in the future through the inclusion of more host-pathogen systems and soils suppressive to other soil-borne fungal pathogens.

Suppressive soils are enriched in cyclic-peptide-associated A-domains

Adenylation domains activate and incorporate specific amino acids in the growing nonribosomal peptide during synthesis by an NRPS assembly line. The substrate specificity for different A-domains is determined by a restricted number of residues in their sequence (Stachelhaus et al., 1999). A-domains incorporate a large variety of both proteogenic and non-proteogenic amino acids, which facilitate the structural diversity of the final peptide products. We reasoned that prediction of the substrate specificities of the domain amplicons detected in suppressive and conducive rhizosphere samples could provide new insights into the abundance and diversity of different products, and trained a classifier to predict these specificities (see Methods). Intriguingly, we found predicted threonine-specific domains to be significantly more common in suppressive soils versus conducive (rank-sum test p-value<0.001, full result table in Supplementary table S3). This is particularly interesting as threonine is an amino acid commonly involved in lactone ring formation of cyclic and branched cyclic (lipo)peptides. Such peptides have a large variety of natural functions, which encompass, among others, the induction of systemic resistance in plants to fungal infection and direct antifungal activity (Cawoy et al., 2015; Geudens and Martins, 2018; Kruijt et al., 2009; Mm et al., 2014; Omoboye et al., 2019b, 2019a, p. 3; Oni et al., n.d.; Raaijmakers et al., 2010; Raaijmakers and Mazzola, 2012).

Reconstruction of 31 gene clusters from amplicon data using domain annotation and co-occurrence pattern analysis

Co-occurrence of domains across the soil samples was used to build a pairwise co-occurrence matrix as described in methods. A strict filter was applied to remove spurious correlations, creating in a co-occurrence network containing 1,618 amplicons. Associations of co-occurring amplicons into putative BGCs were predicted only for co-occurring amplicons which share annotation to one or multiple references; this resulted in the reconstruction of 31 gene clusters (supplementary table S4). These clusters belonged to multiple taxonomical groups, namely *Pseudomonas*, *Delftia*, *Streptomyces*, *Variovorax*, *Burkholderia* and *Collimonas*. In order to validate putative network clusters, we generated 8,762 *in silico* amplicons from our 10X shotgun metagenome-assembly as described above. Two of the 31 reconstructed gene clusters could be matched to known gene cluster

products predicted from the metagenome: the BGCs for nunamycin and delftibactin from *Pseudomonas* and *Delftia* respectively, as shown in Figures 5 and 6.

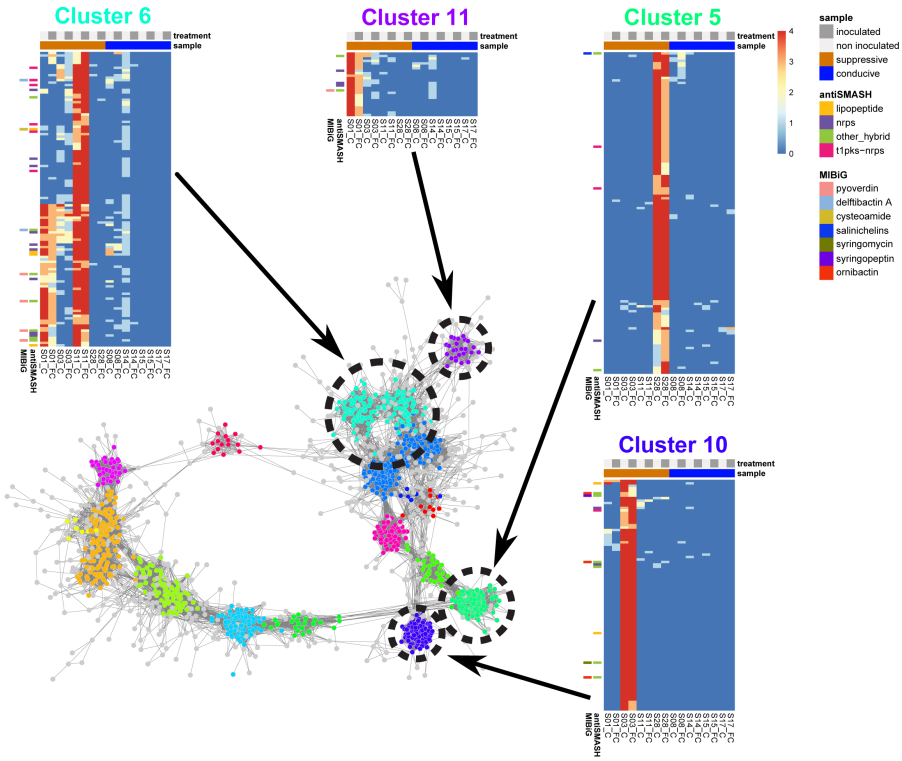


Figure 5. Domain co-occurrence network showing clusters associated with soil suppressiveness. For each of the four clusters (5, 6, 10 and 11), a heatmap shows distribution of A-domains across the samples. The heatmap colour scale represents the number of replicates in which the A-domain occurs (from dark blue – absent to red – present in all four replicates. Upper colour bars in the heatmaps describes samples – light grey – non-inoculated, dark grey – inoculated with pathogen and disease suppressiveness – orange – suppressive, blue - conducive. The left side of each heatmap shows which A-domains were annotated using the MiBIG or antiSMASH databases with colour bars. Colour of the bars indicate a compound or compound class shown in the legend.

Overview of the BGCs associated with suppressive soils

Next, we identified in more detail the BGCs detected in the wheat rhizosphere microbiome from suppressive soil S11. To this end, we used antiSMASH to identify BGCs in the 10X shotgun metagenome assembly of this soil. This resulted in 991 predicted BGCs from multiple GCFs associated with various known compounds. Notable compounds include siderophores like turnerbactin, delftibactin, fimsbactin, xanthoferrin and amonabactin, lipopeptides like nunamycin/nunapeptin and brabantamide (Barghouthi et al., 1989; Bohac et al., 2019; Han et al., 2013; Michelsen et al., 2015, 2015; Pandey et al., 2017; Schmidt et al., 2014; Tejman-Yarden et al., 2019), and known antifungal compounds like 2,4-diacetylphloroglucinol (Raaijmakers and Weller, 1998). This array of candidate clusters offered an initial insight into putative mechanisms associated with the disease-suppressive phenotype, in which one or multiple compounds may inhibit simultaneously or sequentially the growth of the invading pathogen and suppress root infection.

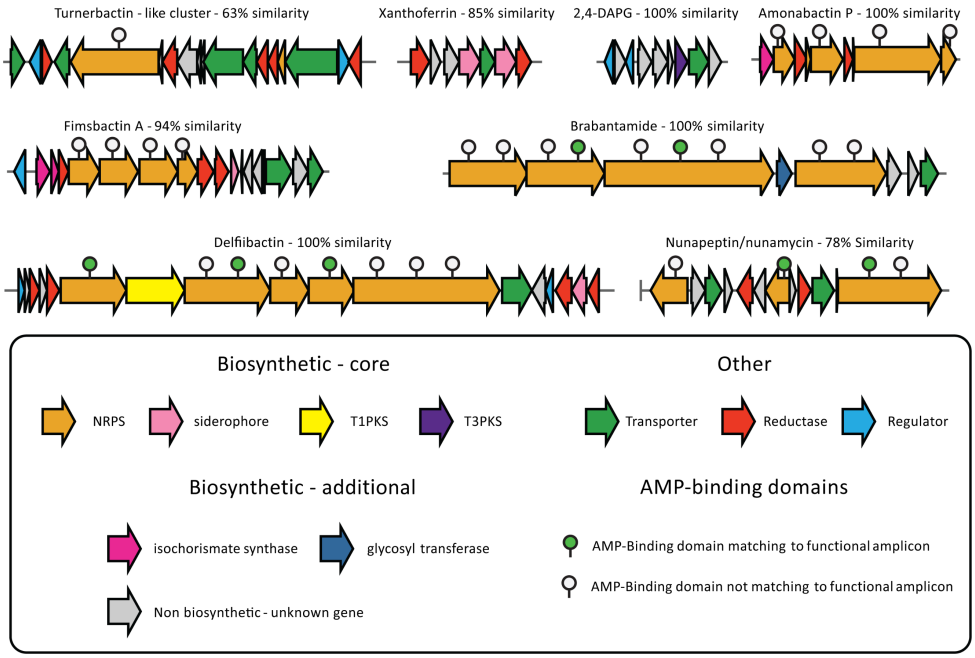


Figure 6. Selection of known BGCs predicted in the rhizosphere metagenome of suppressive soil S11. Arrows represent predicted genes and are colour-coded based on their annotated function. AMP-binding domains matching to functional amplicons are highlighted as described in the legend.

Analysis of siderophores and lipopeptides associated with observed phenotypes

As expected, our MIBiG-based annotations show that a considerable portion of the amplicons (955 out of 5,531) mapped to *Pseudomonas* A-domains. A-domains from this study could be mapped to BGCs belonging to 68 different genera and 208 bacterial species (Supplementary table S2). With these taxonomic annotations obtained from dom2BGC, it was possible to identify taxonomic patterns of adenylation domains associated with soil disease suppressiveness. Multiple species known for their biosynthetic potential and for involvement in disease suppressiveness in other systems were significantly enriched in suppressive soils at high taxonomical resolution (Supplementary table S4). This suggests that these bacteria, which were previously found to exhibit antifungal activity, might also play a role in the disease suppressiveness against *F. culmorum* in wheat.

DBscan clustering of the A-domain co-occurrence network produced 16 clusters. Among these clusters, 4 were associated with at least one suppressive soil. The most interesting subnetwork (Fig. 5, cluster 6) has amplicons associated with suppressive soil S11 and partially with soil S01, with some amplicons present across three suppressive soils. Three separate domain clusters were reconstructed within this subnetwork, with all three matching BGCs encoding the production of known siderophores, namely pyoverdine from *Pseudomonas*, scabichelin from *Streptomyces* and delftibactin from *Delftia*. All of these were associated with suppressive soil S11 and the last one with suppressive soil S01 as well. Siderophores are a group of secondary metabolites produced by microorganisms in iron-limited environments like soil. These metabolites form complexes with insoluble iron, facilitating the uptake of this iron by microorganisms. Often, competition for iron is a central process in soil systems with neutral to high pH (Haas and Défago, 2005; Kloepper et al., 1980; Kramer et al., 2020; Lemanceau et al., 1993; Saha et al., 2016). Siderophores and competition for iron were found to be involved in soil disease suppression mechanisms against Fusarium wilt (Alabouvette, 1986; Baker et al., 1986; Duijff et al., 1999, 1994; Scher M., 1982) , *take-all* disease in wheat (Lemanceau et al., 2009; Verbon et al., 2017) and damping-off of sugar beet (Carrión et al., 2019).

The concentration of soluble iron in eight tested soils, as assayed in our previous study (Ossowicki et al., 2020), ranged from 0.01 mg/kg in soil S17 to 0.11 mg/kg in soil S11 with the exception of soil S03, where the concentration was much higher and reached 0.45 mg/kg. The high iron concentration in soil S03 can be explained by its low pH (5.28), which increases the solubility of oxidized iron. All other soils have a neutral pH (7.13 to 7.82) or are only slightly acidic (soils S01 and S08, pH 6.22 and 6.87, respectively) (supplementary table S5 and (Ossowicki et al., 2020)). We observe that the broad presence of siderophores is not limited to environments with a low availability of iron. Those results do not indicate a simple connection between the concentration of soluble iron and soil disease

suppressiveness against *F. culmorum*. Nevertheless, the production of siderophores is so widespread among microorganisms is soil systems that we can consider it as primary process in ecosystem functioning consequently indispensable for soil disease suppressiveness.

The network hub associated with suppressive soil S03 (Fig. 5, cluster 10) contains three predicted reconstructed gene clusters taxonomically assigned to *Burkholderia*, *Collimonas* and *Pseudomonas*. The *Burkholderia* and *Collimonas* clusters matched to multimodular NRPSs with no known associated natural product, while the reconstructed cluster from *Pseudomonas* matched to the syringafactin BGC. Finally, the pyoverdine BGC from *Pseudomonas* was recovered from a smaller amplicon subnetwork (Fig. 5, cluster 11). While the consistent recovery of the pyoverdine BGC in multiple hubs is expected given its ubiquity in rhizosphere-associated pseudomonads, the recovery of the delftibactin and scabichelin BGCs and their association to two suppressive soils emphasize the contribution of different kinds of siderophores in disease suppression. Our results were further confirmed by the prediction of a delftibactin BGC in the associated shotgun metagenome assembly from soil S11 with antiSMASH, which has an almost perfect match with the delftibactin BGC in MiBIG (Fig.6). The largest suppressive-sample-associated subnetwork by number of amplicons (Fig. 5, cluster 5) possesses an individual cluster matching the scabichelin BGC from *Streptomyces scabies*. This siderophore has been found to be produced by previously reported *Fusarium*-suppressive strains (del Barrio-Duque et al., 2019). The reconstruction of separate instances of the same BGC suggest that the underlying amplicons belong to variants of the scabichelin cluster present in different rhizosphere communities.
All in all, the results suggest an association of siderophore BGCs with the disease-suppressive phenotype across the soils studied. They also point to a possible functional redundancy that should be validated in future work: in some soils, a suppressive function might be mediated through the production of some siderophores (e.g., delftibactin), while in other soils the same function might be mediated by other natural products (e.g., scabichelin).

Based on the MIBiG database, 15 lipopeptides were annotated in our samples. Figure S2 presents the distribution of these compounds among suppressive and conducive soils. Interestingly, most annotated lipopeptides are much more abundant in conducive soils, especially in soil S17. Many of these lipopeptides are connected to bacterial plant pathogens and act like pathogenicity factors (for example: syringafactin, tolaasin, sessilin), while others have been implicated in soil disease suppressiveness and antagonistic interactions with fungi (for example: nunamycin and thanamycin) or breaking down bacterial biofilms (for

example: WLIP, entolysin, putisolvin and xantholysin A). Many of the A domains that are part of NRPS BGCs of plant pathogenic bacteria are also part of NRPS BGCs of non-pathogenic bacteria (Girard et al., 2020). Isolation of the bacteria harbouring these BGCs and subsequent genetic, genomic, transcriptomic and mutational analyses will be needed to determine the identity as well as any functional significance of these BGCs in suppressiveness.

Conclusions

Our study provides novel insights into the NRPS AMP-binding domain diversity of agricultural rhizosphere samples. Remarkably, the set of unique amplicons from this rhizosphere collection equals the level of diversity of adenylation domains found across all publicly available genomes. Annotation rates for nAMPs were generally low, which highlights the incredible potential of plant-associated microbiomes for discovering novel natural products. We report significant community structure overlap among suppressive rhizobacterial adenylation domains profiles, and generated new hypotheses regarding possible roles for siderophores in disease suppression against *Fusarium culmorum*. We also developed a pipeline for taxonomic and functional annotation of NRPS amplicons without the requirement of a BAC-clone library. The dom2BGC pipeline can be extended to and currently supports annotation of any natural product-associated domain that occurs multiple times within a BGC, and to some extent for any BGC-associated domain. We validated the amplicon clustering results by reconstructing the delftibactin BGC, a siderophore associated with suppressive soils using a combination of amplicon sequencing and novel 10X genomics shotgun metagenomics sequencing. We conclude that combining functional amplicon sequencing and shotgun metagenomics highlighted represents a powerful approach to probe complex microbiome-associated plant phenotypes and to generate new hypotheses on the functional roles of microbial metabolites in microbe-microbe and microbe-host interactions.

Data availability

Raw sequence data that support the findings of this study have been deposited in NCBI under project number PRJNA670155.

Supplementary material

Table S1. Read counts per sample table pre and post filtering.

Sample-ID	Raw counts	Filtered counts
S01-30-C-1_38060-A01	61522	56356
S01-30-C-2_38060-B01	69249	63627
S01-30-C-3_38060-C01	93329	86633
S01-30-C-4_38060-D01	88579	81528
S01-30-FC-1_38060-E01	73573	68386
S01-30-FC-3_38060-G01	59679	54557
S01-30-FC-4_38060-H01	54754	50564
S03-30-C-1_38060-A02	49444	45627
S03-30-C-2_38060-B02	59744	55266
S03-30-C-3_38060-C02	45294	42639
S03-30-C-4_38060-D02	55966	51235
S03-30-FC-1_38060-E02	69574	66177
S03-30-FC-2_38060-F02	72277	66783
S03-30-FC-3_38060-G02	56285	51549
S03-30-FC-4_38060-H02	54935	49470
S08-30-C-1_38060-A05	57233	53380
S08-30-C-2_38060-B05	66362	61590
S08-30-C-3_38060-C05	64633	60426
S08-30-C-4_38060-D05	82370	77089
S08-30-FC-1_38060-E05	68239	64447
S08-30-FC-2_38060-F05	89136	82245
S08-30-FC-3_38060-G05	69234	63569
S08-30-FC-4_38060-H05	56346	51398
S11-30-C-1_38060-A03	56932	53328
S11-30-C-2_38060-B03	72236	67006
S11-30-C-3_38060-C03	60323	56541
S11-30-C-4_38060-D03	76486	72089
S11-30-FC-1_38060-E03	65674	62059
S11-30-FC-2_38060-F03	69165	63976
S11-30-FC-3_38060-G03	61222	57484
S11-30-FC-4_38060-H03	62399	58216

S14-30-C-1_38060-A06	65009	60765
S14-30-C-2_38060-B06	70802	65514
S14-30-C-3_38060-C06	64070	59514
S14-30-C-4_38060-D06	54727	50559
S14-30-FC-1_38060-E06	72434	66960
S14-30-FC-2_38060-F06	81112	71312
S14-30-FC-3_38060-G06	59644	55225
S14-30-FC-4_38060-H06	64895	58831
S15-30-C-1_38060-A07	59465	53857
S15-30-C-2_38060-B07	68717	62513
S15-30-C-3_38060-C07	75261	69264
S15-30-C-4_38060-D07	74238	68226
S15-30-FC-1_38060-E07	83840	77529
S15-30-FC-2_38060-F07	85701	77805
S15-30-FC-3_38060-G07	60580	56114
S15-30-FC-4_38060-H07	69506	63197
S17-30-C-1_38060-A08	56302	51984
S17-30-C-2_38060-B08	78187	67847
S17-30-C-3_38060-C08	85159	76649
S17-30-C-4_38060-D08	80787	74714
S17-30-FC-1_38060-E08	73688	69596
S17-30-FC-2_38060-F08	76891	70879
S17-30-FC-3_38060-G08	63541	59126
S17-30-FC-4_38060-H08	61208	56702
S28-30-C-1_38060-A04	54744	49232
S28-30-C-2_38060-B04	72221	65227
S28-30-C-3_38060-C04	48818	43892
S28-30-C-4_38060-D04	69285	63359
S28-30-FC-1_38060-E04	14606	12380
S28-30-FC-2_38060-F04	85430	78041
S28-30-FC-3_38060-G04	54205	50309
S28-30-FC-4_38060-H04	54170	49003
Total:	3459604	3396393

Table S2. Statistic tests for Figure 2B

Phenotype, permanova	
method name	PERMANOVA
test statistic name	pseudo-F
sample size	63
number of groups	2
test statistic	4.9766
p-value	0.0010
number of permutations	999
Name: PERMANOVA results, dtype: object	
Treatment, permanova	
method name	PERMANOVA
test statistic name	pseudo-F
sample size	63
number of groups	2
test statistic	0.8660
p-value	0.6890
number of permutations	999
Name: PERMANOVA results, dtype: object	
Phenotype, anosim	
method name	ANOSIM
test statistic name	R
sample size	63
number of groups	2
test statistic	0.3529
p-value	0.0010
number of permutations	999
Name: ANOSIM results, dtype: object	
Treatment, anosim	
method name	ANOSIM
test statistic name	R
sample size	63
number of groups	2
test statistic	-0.0008
p-value	0.4030
number of permutations	999
Name: ANOSIM results, dtype: object	

Table S3. Cumulative relative abundance of predicted amino acid substrates in suppressive and conducive rhizosphere soils. Rank sum statistics is calculated using relative counts of appearances of amplicons annotated to the monomer for calculating ranks.

Substrate specificity	Cumulative relative abundance suppressive	Cumulative relative abundance conducive	Rank sums statistic	Rank sums	p-value
ala	0,1136	0,1355	0,8383	-2,3834	0,0203
asn	0,0077	0,0064	1,2166	-0,5024	0,6172
asp	0,0013	0,0004	3,5484	2,2128	0,0307
cys	0,0810	0,0864	0,9370	-3,3174	0,0015
dab	0,0006	0,0005	1,0138	2,5104	0,0148
gln	0,0341	0,0373	0,9149	2,5214	0,0144
glu	0,0009	0,0011	0,8449	-2,9170	0,0050
gly	0,2195	0,2234	0,9825	-0,8890	0,3776
leu	0,0122	0,0065	1,8587	3,4547	0,0010
phe	0,0015	0,0015	1,0138	0,1616	0,8722
pro	0,0271	0,0238	1,1377	-0,1885	0,8512
ser	0,2781	0,2843	0,9782	-1,2785	0,2060
thr	**0,2103**	**0,1817**	**1,1569**	**4,8296**	**9,83E-06**
tyr	0,0122	0,0109	1,1152	0,6348	0,5280

Table S4 Annotated MIBig clusters with counts in all suppressive and all conducive soils

cluster	suppressive counts	conducive counts
BGC0000438_AAF99707.2	5499	58
BGC0000438_AAO72425.1	4836	47
BGC0000437_AAY37655.1	4834	47
BGC0001416_KPN93063.1	4367	86
BGC0001416_KPN90376.1	4417	234
BGC0001721_AUD11994.1	3824	0
BGC0000984_ABX37383.1	2021	167
BGC0000984_ABX37382.1	1987	137
BGC0001346_AOA33122.1	1503	72
BGC0000438_AAO72424.1	1493	78
BGC0000437_AAY37654.1	1482	78
BGC0000437_AAY37653.1	1443	55
BGC0001842_ABA73955.1	1668	409
BGC0001980_QDF82255.1	1698	474

BGC0001509_WP	1987	800
BGC0000435_AAO56329.1	925	0
BGC0001567_WP	1142	473
BGC0001312_CAY48788.1	418	208
BGC0001416_KPN93064.1	276	76
BGC0000305_BAC67535.1	376	263
BGC0001752_ctg1	409	308
BGC0001984_QED55423.1	76	3
BGC0001519_WP	105	35
BGC0000305_BAC67536.1	142	77
BGC0001331_WP	37	0
BGC0001332_WP	31	6
BGC0000443_AED90003.1	26	3
BGC0000429_AEA30273.1	27	5
BGC0001999_WP	42	23
BGC0000425_AFH75321.1	96	78
BGC0001806_APU91750.1	96	78
BGC0001330_WP	24	6
BGC0000425_AFH75320.1	98	81
BGC0000429_AEA30272.1	18	1
BGC0000447_CCJ67639.1	100	83
BGC0000447_CCJ67638.1	100	83
BGC0001389_AHZ34242.1	96	80
BGC0001389_AHZ34241.1	96	80
BGC0000371_BAH33409.1	34	20
BGC0000431_EFE73312.1	14	0
BGC0000315_CAB38518.1	13	0
BGC0001370_ALV82356.1	13	0
BGC0000437_AAY37647.1	14	2
BGC0001192_AJM89738.1	19	8
BGC0001153_AEZ51520.1	19	8
BGC0001192_AJM89735.1	19	8
BGC0000408_ACA97580.1	19	8
BGC0000403_AFJ14794.1	19	8
BGC0000408_ACA97576.1	19	8

BGC0001153_AEZ51516.1	19	8
BGC0002014_WP	13	2
BGC0001715_CUX79061.1	16	6
BGC0001715_CUX79060.1	16	6
BGC0000429_AEA30274.1	13	4
BGC0001657_BAV56270.1	9	0
BGC0000461_AEP18655.1	5	0
BGC0000461_AEP18656.1	4	0
BGC0001042_ACY06285.1	20	16
BGC0001370_ALV82384.1	3	0
BGC0000315_CAB38517.1	3	0
BGC0001763_BBA20967.1	5	2
BGC0001620_ASX95241.1	5	2
BGC0001214_AJV88375.1	2	0
BGC0001984_QED55421.1	2	0
BGC0000418_AIE77059.1	1	0
BGC0002001_WP	5	5
BGC0000311_CAC48361.1	4	5
BGC0000955_CCA29203.1	0	1
BGC0000341_ABD65958.1	0	2
BGC0000359_AAZ55900.1	0	2
BGC0000385_AEH59099.1	0	2
BGC0000385_AEH59100.1	0	2
BGC0001462_OLZ52457.1	0	2
BGC0000419_AIG79241.1	0	2
BGC0001416_KPN90369.1	0	2
BGC0001459_OKA09423.1	0	2
BGC0001460_EME52990.1	0	2
BGC0000311_CAC48360.1	0	2
BGC0001460_EME52989.1	0	3
BGC0000326_AAK81826.1	0	3
BGC0001975_QBG38784.1	2	5
BGC0001459_OKA09424.1	1	5
BGC0000354_CAM56770.1	31	35
BGC0000393_ABF87031.1	0	4

BGC0000455_AEI58866.1	0	5
BGC0001792_WP	0	8
BGC0000463_AGM14934.1	11	28
BGC0000333_ABW00331.1	0	22
BGC0000447_CCJ67637.1	131	156
BGC0001368_WP	1	26
BGC0000289_CAD91212.1	3	31
BGC0000440_CAE53352.1	2	31
BGC0000441_CAG15011.1	2	31
BGC0001178_AGS77309.1	2	31
BGC0001806_APU91751.1	22	52
BGC0000425_AFH75322.1	15	50
BGC0000413_AAY93356.2	5	41
BGC0000413_AAY93354.1	5	41
BGC0001389_AHZ34243.1	31	73
BGC0000344_CAK15814.1	41	89
BGC0000463_AGM14933.1	41	89
BGC0000344_CAK15815.1	41	89
BGC0001838_AFJ23826.1	38	89
BGC0000439_AHH53506.1	0	66
BGC0001838_AFJ23825.1	15	82
BGC0000411_ABW17377.1	51	119
BGC0000411_ABW17376.1	47	139
BGC0001842_ABA73956.1	279	417
BGC0001980_QDF82259.1	325	477
BGC0001767_ctg1	2438	2651
BGC0000325_CAB53322.1	100	342
BGC0001312_CAY48789.1	124	400
BGC0000389_ABH06369.2	159	444
BGC0000423_CBG75492.1	2445	2741
BGC0000349_CAM02313.1	2291	2589
BGC0000389_ABH06368.2	268	611
BGC0001211_WP	2448	2820
BGC0000413_AAY93445.1	52510	73141

Table S5. Chemical properties of tested soils

	S01	S03	S11	S28
pH	6,22 SD 0,17	5,28 SD 0,27	7,28 SD 0,19	7,13 SD 0,07
OM [%]	3,46 SD 0,35	5,49 SD 0,68	3,48 SD 0,47	3,29 SD 0,12
Fe [mg/kg]	0,09 SD 0	0,45 SD 0,06	0,11 SD 0	0,02 SD 0
K [mg/kg]	34 SD 0,92	59,95 SD 2,29	68,77 SD 1,1	71,36 SD 0,44
Mg [mg/kg]	163,19 SD 1,75	56,74 SD 2,11	56,43 SD 0,58	160,26 SD 2,7
P [mg/kg]	1,4 SD 0,01	2,69 SD 0,08	5,43 SD 0,04	0,79 SD 0,02
S [mg/kg]	1,29 SD 0,08	2,6 SD 0,16	1,17 SD 0,15	1,74 SD 0,24
C [%]	2,31 SD 0,18	3,77 SD 1,13	1,99 SD 0,88	1,52 SD 0,01
N [%]	0,14 SD 0,01	0,26 SD 0,1	0,16 SD 0,07	0,17 SD 0
C:N	16,5	14,5	12,44	8,94

	S08	S14	S15	S17
pH	6,87 SD 0,06	7,61 SD 0,05	7,82 SD 0,05	7,75 SD 0,06
OM [%]	2,81 SD 0,51	5,04 SD 0,35	3,77 SD 0,63	4,23 SD 0,79
Fe [mg/kg]	0,08 SD 0	0,04 SD 0	0,02 SD 0	0,01 SD 0
K [mg/kg]	181,54 SD 3,76	82,49 SD 4,08	45,83 SD 0,53	87,17 SD 2,45
Mg [mg/kg]	109,68 SD 1,7	98,91 SD 4,04	60,6 SD 0,52	74,54 SD 0,8
P [mg/kg]	16,23 SD 0,05	0,7 SD 0,06	0,9 SD 0,05	1,03 SD 0,04
S [mg/kg]	1,14 SD 0,05	8,61 SD 0,08	5,95 SD 0,06	2,27 SD 0,06
C [%]	1,94 SD 0,24	2,35 SD 0,14	1,91 SD 0,08	2,63 SD 0,05
N [%]	0,16 SD 0,01	0,15 SD 0,01	0,11 SD 0,01	0,15 SD 0
C:N	12,13	15,67	17,36	17,53

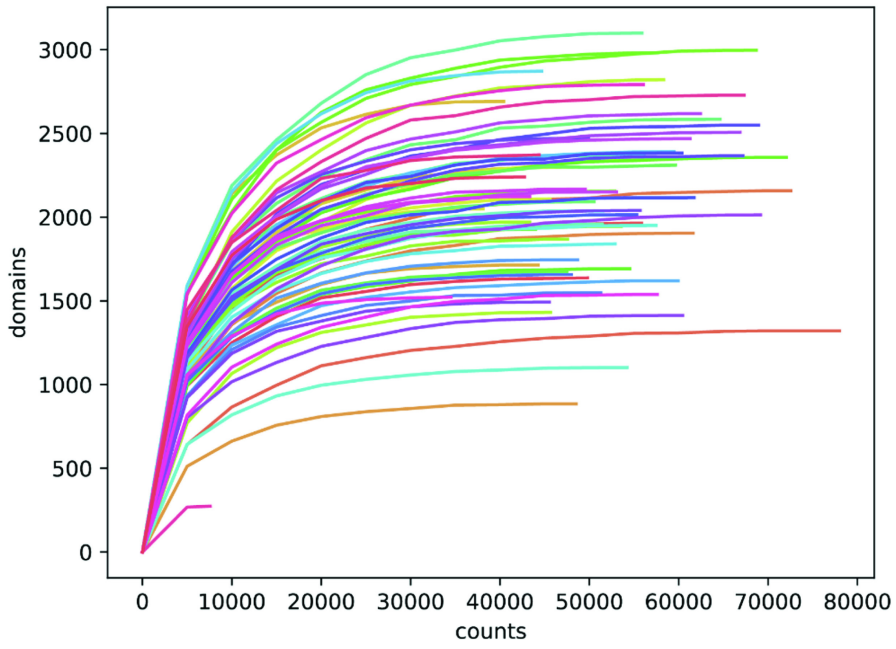


Figure S1. Rarefaction analysis of rhizosphere A-domain amplicons. Samples rarefaction analysis showing number of unique amp-binding domains (ordinate) at different rarefaction points (abscissa). One sample was clearly an outlier (pink arrow on the bottom) and was removed from the analysis.

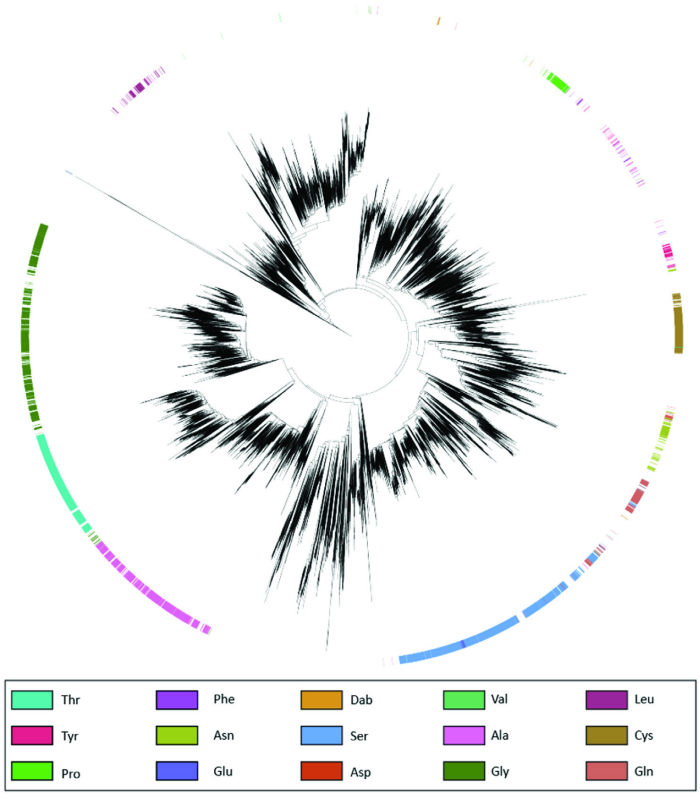
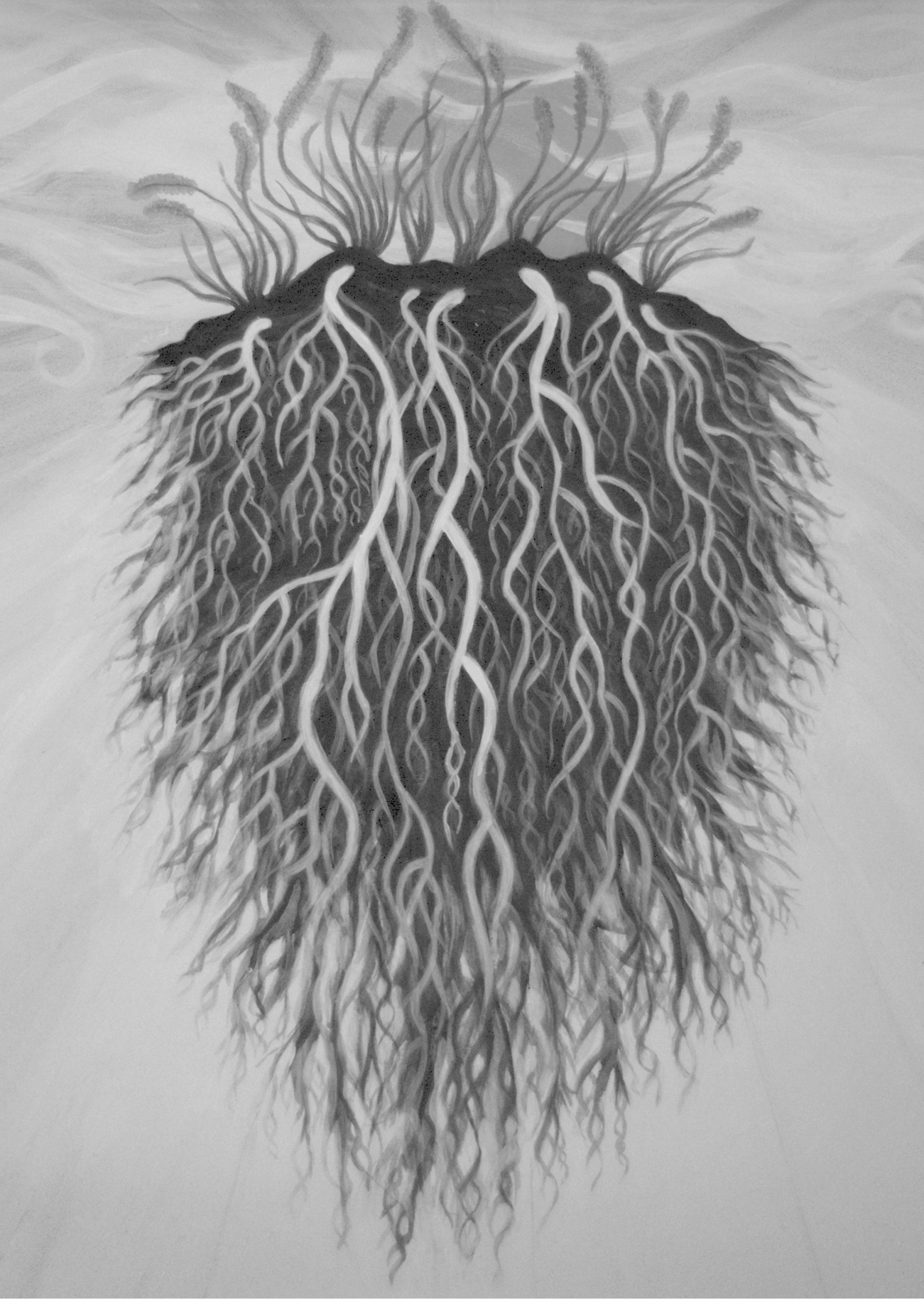


Figure S2. – Phylogeny tree of the natural amplicons analyzed in this study. On the outer ring, colors represent predicted amino acid specificity and amino acid group specificity as detailed in supplementary material.



Chapter 4

Deciphering the microbiome of disease suppressive soils by dilution-to-extinction

Adam Ossowicki[1]*, Vittorio Tracanna[2]*, Somayah S. Elsayed[3], Elio G. W. M. Schijlen[4], Mirna Baak[5], Walter Pirovano[5], Gilles P. van Wezel[1,3], Jos M. Raaijmakers[1,3], Marnix H. Medema[2], Paolina Garbeva[1]

1. Microbial Ecology, Netherlands Institute of Ecology (NIOO-KNAW), Wageningen, The Netherlands
2. Bioinformatics Group, Wageningen University and Research, Wageningen, The Netherlands
3. Microbial Biotechnology, Leiden Institute of Biology, Leiden, The Netherlands
4. Bioscience, Wageningen University and Research, Wageningen, The Netherlands
5. BaseClear, Leiden, The Netherlands
*: contributed equally to this work

Abstract

In disease-suppressive soils, root-associated microbiomes provide plant protection against infections by specific soil-borne plant pathogens. Previously, we screened a large number of soils for suppressiveness to *Fusarium culmorum* of wheat and revealed that soil S11 showed a consistent and high level of suppressiveness that was associated with the rhizosphere microbiome. In this study, we used a dilution-to-extinction approach to investigate the underlying mechanisms of microbiome-mediated disease suppressiveness to *F. culmorum*. Our results show that disease suppressiveness can be transferred to a sterile soil by introducing the microbiome extracted from the rhizosphere of wheat grown in suppressive soil S11. Introducing different dilutions of this S11 rhizosphere microbiome into the sterile soil revealed a nonlinear relationship between the dilution factor and the level of disease suppressiveness. At low microbiome dilution, disease was significantly suppressed relative to the untreated control, but the suppressive effect was lost at higher dilutions (100X and higher). Shotgun metagenomic sequencing and reconstruction of 96 metagenome assembled genomes from the rhizosphere microbiota of the different dilutions revealed changes in microbiome composition and functions. We observed a reduction in microbial diversity along the dilution trajectory with an increase in the relative abundance of the Proteobacteria and Bdellovibrionota, and a decrease in the relative abundances of Streptomycetales, Acidobacteria and Verrucomicrobiota. Analysis of the occurrences of KEGG orthologs showed enrichment for 143 orthologs in the suppressive conditions and included terms associated with iron uptake, chitinases and components of the type 6 secretion system. Nine metagenome-assembled genomes were associated with the diminished suppressive phenotype, including a high-quality genome from the bacterial genus *Labilithrix* that contains multiple novel biosynthetic gene clusters. Collectively, this study exemplifies the high added value of dilution-to-extinction to deconstruct a naturally occurring microbiome-associated plant phenotype, i.e., disease suppressiveness. Deciphering the mechanisms and microbial consortia involved in suppressive soils is highly instrumental for the development of new disease management strategies for sustainable agriculture.

Introduction

The thin layer of soil surrounding and influenced by plant roots - the rhizosphere – is populated by diverse microbial communities recruited from the soil microbiome by root exudates (Berg and Smalla, 2009; Morella et al., 2020). Rhizosphere microbes often confer beneficial functions to plants, such as nutrient acquisition, production of phytohormones and protection against biotic and abiotic stresses (Cordovez et al., 2019). Hence, changes in the composition of the rhizosphere microbiome can positively or negatively affect plant

growth and health. For ages, people have recognized that some soils are better for cultivation of particular crops, but only in the last decades we started to understand how microbes present in a soil contribute to better yields and protection from diseases. In so-called disease suppressive soils, the level of disease is low to absent, despite the presence of a virulent pathogen and a susceptible host plant (Raaijmakers and Mazzola, 2011). For most disease-suppressive soils, the protection provided to the plant is mediated by activities of specific members of the soil and rhizosphere microbiota (for reviews see:(Gomes Exposito et al., 2017; Schlatter et al., 2017b; Weller et al., 2002a)). Because of the complex diversity and dynamics of the rhizosphere microbiota (Wagg et al., 2014), unravelling the mechanisms by which specific microbial consortia provide protection against diseases is a challenge. Here we integrated dilution-to-extinction (DTE) and metagenomics to disentangle the microbial traits associated with suppressiveness of soils to *Fusarium* root disease of wheat. DTE is a controlled perturbation method leading to a simplified derivative of the initial microbiome and has been used for manipulation of microbiomes of the gut (Kenters et al., 2011; Lagier et al., 2015) and water (Stingl et al., 2008; Yu et al., 2019) to study rare taxa and ecological succession. Manipulation of microbiome structure and diversity by DTE has also successfully been used in several studies of soil microbiomes in the context of the utilization of carbon sources (Garland and Lehman, 1999), fungistasis (Hol et al., 2015), chitin and cellulose degradation (Peter et al., 2011), antibiotic resistance (Chen et al., 2019, 2017) and general functional potential (Yan et al., 2017). A study by Chen et al. (2020) demonstrated, using a DTE approach, the impact of the microbial taxonomic diversity on soil functions and a positive correlation between microbial diversity and crop productivity (Chen et al., 2020). Korenblum et al. (2020) recently used a combination of DTE with metatranscriptomics and metabolomics to investigate how bacteria reprogram metabolism and root exudation in tomato (Korenblum et al., 2020). The study by Hol et al. (2015) revealed by DTE that reduced taxonomic diversity leads to a reduced ability of the soil microbiota to inhibit the growth of fungal plant pathogens *in-vitro* (Hol et al., 2015). Here, we integrated DTE with metagenomics to identify, for the first time, microbiome functions associated *in situ* with disease suppressiveness to *F. culmorum.* Identifying microbial consortia and microbial functions involved in suppressive soils can substantially contribute to developing new sustainable solutions for future agriculture with reduced inputs of fertilizers and chemical pesticides.

In our previous studies, we screened 28 soils for suppressiveness to *F. culmorum* of wheat and identified several suppressive soils. Amplicon sequencing showed that these suppressive soils did not share the same taxonomic patterns, but co-occurrence network analysis revealed at least one common uniquely overrepresented bacterial guild dominated by *Acidobacteria* (Ossowicki et al., 2020). In some of the suppressive soils, we also found an

association between suppressiveness and the abundance of biosynthetic gene clusters (BGCs) encoding the production of siderophores based on NRPS functional amplicon sequencing (Tracanna et al., n.d.). For the work presented here, we chose agricultural soil S11 because it showed the highest and most consistent level of disease suppressiveness and an association of suppressiveness with siderophore BGCs. For the experimental work, we inoculated a sterile soil with different dilutions of soil S11 and planted wheat. Then, we challenged the plants with the fungal pathogen and monitored disease severity and microbiome dynamics by in-depth metagenomic sequencing. We hypothesize that dilution of the suppressive rhizosphere microbiome i) diminishes the abundance of specific microbial taxa and biosynthetic gene clusters (BGCs) involved in disease suppressiveness, ii) diminishes microbial diversity and thereby disturbs the interactions within the microbial consortia responsible for disease suppressiveness.

Results and discussion

Impact of rhizosphere microbiome dilution on disease suppressiveness

In a greenhouse pot experiment, we extracted the microbiome of disease-suppressive soil S11 grown for 2 weeks to wheat. When introduced into a sterile sandy soil, the extracted soil microbiome (ESM) conferred significant suppressiveness to *F. culmorum* infections of wheat in two independent bioassays with sixteen biological replicates (Fig.1). Dilution of the ESM reduced the level of disease suppressiveness in a non-linear manner. At low dilutions (10X, 25X and 50X), the disease was significantly suppressed, but the suppressive effect was lost at higher dilutions (100X, 200X and 400X) (Fig.1).

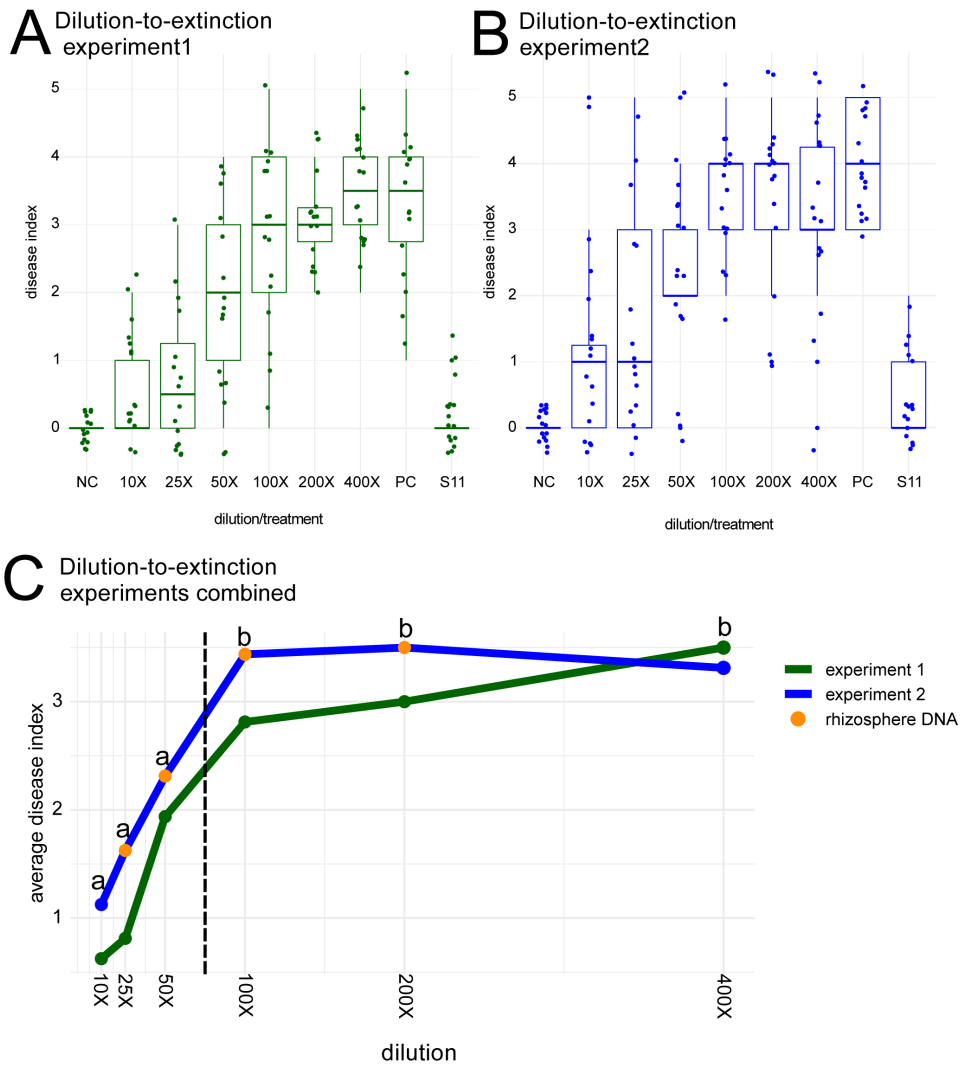


Figure 1. Effects of diluted soil suspensions (10X up to 400X) of disease-suppressive soil S11 on Fusarium culmorum disease severity of wheat plants grown in a sterile soil. Results of two independent experiments (panels A, B) are shown. Disease severity was scored with an index scale ranging from 0 (healthy) to 5 (dead plants). Average disease indices are shown for 16 replicates per treatment. NC is the 'healthy control' where wheat plants are grown in the sterile soil without the pathogen; PC is the 'diseased control' with sterile soil inoculated with the fungal pathogen; S11 is suppressive field soil S11 inoculated with the pathogen. Panel C represents the combined results of the two independent experiments shown in panels A and B. The black dashed line indicates the

transition point in the plant phenotype from suppressive to conducive according to the statistical analyses of the chi-square test; different letters above the data points indicate statistically significant differences. For the metagenome analyses, DNA rhizosphere samples were collected in experiment 2 from the four dilutions indicated by orange dots on the graph.

Dilution-to-extinction is an effective approach to dissect microbiome-associated phenotypes

Following the bioassays, DNA was extracted from the rhizosphere of wheat plants treated with four ESM dilutions that confer phenotypes ranging from disease-suppressive to conducive (non-suppressive). Based on taxonomic classification of the metagenomic reads, the results showed that the rhizosphere microbiomes maintained their overall taxonomic structure at the phylum level over the dilution series (Fig. 2), but the relative abundance of various taxonomic groups significantly changed as a result of the dilution (presented and discussed further below).

The taxonomic distribution was consistent among all five biological replicates of the original extracted ESM and of each of the four dilutions (Fig. S1). According to nonpareil estimation of coverage, the in-depth sequencing efforts for this experiment was able to cover even less abundant and rare members of the rhizosphere microbiota nearly completely (Fig. 3A), providing a basis to deconstruct microbial functions associated with the disease-suppressive plant phenotype while maintaining a similar overall taxonomic composition of the rhizosphere microbiome.

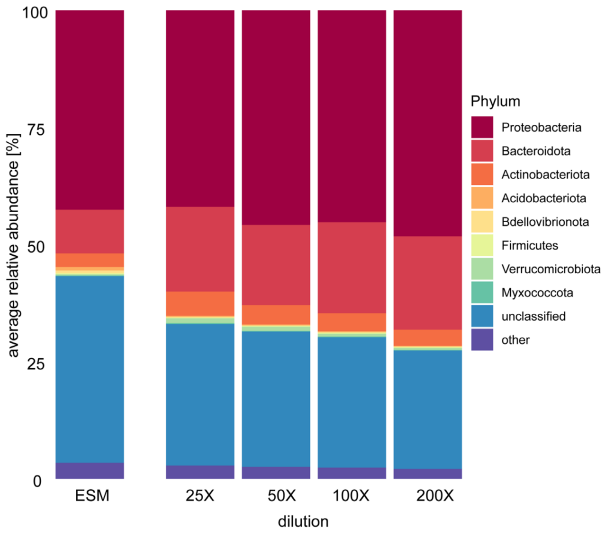


Figure 2. Relative abundance of the bacterial phyla detected in different dilutions of the rhizosphere microbiome of wheat plants grown in Fusarium-suppressive soil S11. ESM represents the extracted soil microbiome, whereas 25X – 200X represent the ESM diluted 25 – 200 times. Taxonomic assignment of the sequence reads was performed using Kraken2 with the GTDB database (Parks et al., 2020; Wood et al., 2019). Averages of 5 replicates are shown.

Changes in microbiome composition and diversity are associated with suppressiveness

Taxonomic annotation at the read level using Kraken2 with the GTDB database (Parks et al., 2020; Wood et al., 2019) showed that the most abundant phyla were Proteobacteria and Bacterioidota. These two phyla together constituted 60 - 68 % of the bacterial community, and their relative share increased at higher ESM dilutions (Fig. 2). Accordingly, the relative abundance of other phyla decreased, except the Bdellovibrionota. *Bdellovibrio* are considered to be potential agents for controlling phytopathogens (Yair et al., 2009; Youdkes et al., 2020), in particular bacterial but not fungal pathogens. The increased relative abundance of Proteobacteria was attributed to the orders of Burkholderiales, Nevskiales, Caulobacterales, Rhizobiales and Sphingomonadales (Fig.4). The relative abundance of Bacterioidota was stable in all the ESM dilutions. Notably, we observed a significant decrease in the relative abundances of taxa previously associated with disease suppressiveness, including the order Streptomycetales (V. Cordovez et al., 2015; Kinkel et al., 2012) and Acidobacteria (Ossowicki et al., 2020; Shen et al., 2015) and Verrucomicrobiota (Chapelle et al., 2016; Navarrete et al., 2015) (Fig.4). In our previous work on comparative taxonomic profiling of disease conducive and disease suppressive soils to *F. culmorum*, including soil S11, co-occurrence network analysis revealed similarities

between the suppressive soils through an overrepresentation of Acidobacteria (Ossowicki et al., 2020). Hence, the results obtained here by metagenomic analysis supports this earlier observation and suggests a potential role of Acidobacteria in suppressiveness to *F. culmorum*. To validate the potential role of Acidobacteria in suppressiveness will require isolation of representative genera and species of this phylum, many of which are still very difficult to culture in laboratory conditions (Costa et al., 2018).

The diversity detected in the twenty rhizosphere metagenomes and in the undiluted ESM was estimated using the database-independent Nonpareil 3 algorithm (Rodriguez-R et al., 2018). The results showed a diversity reduction with increased ESM dilutions (Fig.3B). The major drop in diversity between undiluted ESM and the subsequent dilutions may reflect the selective power of the rhizosphere and the inability of certain groups of microbes to establish and thrive in a sterile soil following inoculation. We noted that the diversity of the rhizosphere metagenomes significantly differed between the lower dilutions (25X and 50X), and the higher dilutions (100X and 200X) (Fig. 3B), which correlates with their contrasting plant phenotypes. In two former studies (Berg et al., 2017; Mallon et al., 2015) it was postulated that the invasion of a pathogen in a biological system, like the rhizosphere, may lead to the extinction of a subset of the resident species, compromising community functioning. It was experimentally shown (from a 'bottom-up' perspective) that reducing the diversity in synthetic bacterial communities made them more susceptible to invading species (Jousset et al., 2011; van Elsas et al., 2012). Our results suggest that the reduced microbial diversity negatively affects disease suppressiveness, supporting the hypothesis that diversity of root-associated microbiomes contributes to plant resilience to biotic stress. In summary, our results showed: i) a reduction in microbial diversity along the ESM dilution trajectory with a concomitant reduction in disease suppressiveness, ii) an increase in the relative abundance of the Proteobacteria and Bdellovibrionota at higher dilutions, and iii)) a decrease in the relative abundances of Streptomycetales, Acidobacteria and Verrucomicrobiota at higher ESM dilutions.

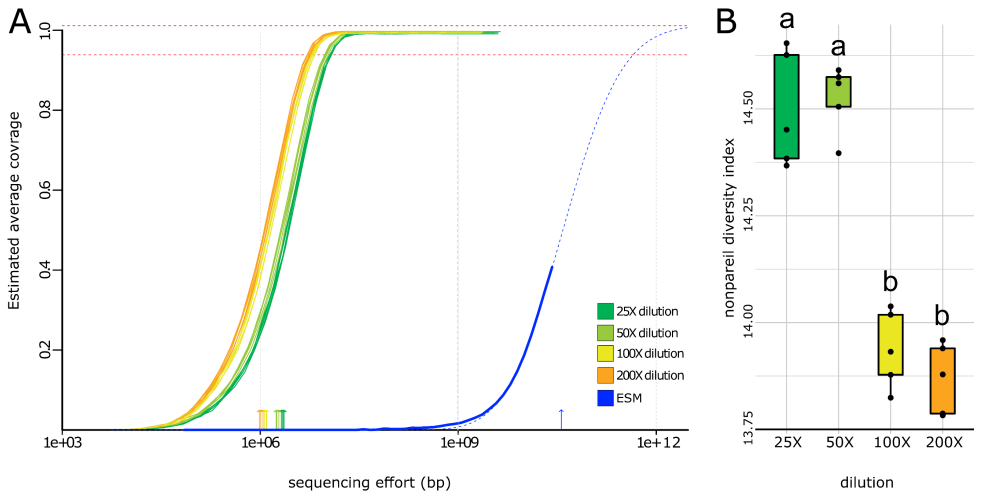


Figure 3. Panel A: estimated sequencing coverage of extracted soil microbiome of suppressive soil S11 (ESM) and rhizosphere microbiomes from different ESM dilutions. ESM coverage for the original extract before inoculation is incomplete (less than 50% of the sequence space is covered) and shows much higher complexity. All the rhizosphere samples cover the genetic diversity of the microbial communities. The curves show a small but consistent separation between low (25X and 50X) and high (100X and 200X) dilutions with lower dilutions displaying higher diversity. Panel B: Effect of diluted suspension of suppressive soil S11 introduced to a sterile soil on genetic diversity of wheat rhizosphere microbiomes expressed as a nonpareil diversity index. The disease symptoms caused by plant pathogen F. culmorum in two lower dilutions 25X and 50X were significantly suppressed compared to higher dilutions 100X and 200X. The significance levels according to ANOVA and Tukey post-hoc test with $p > 0.001$ are indicated by different letters. Full results are presented in Table S1.

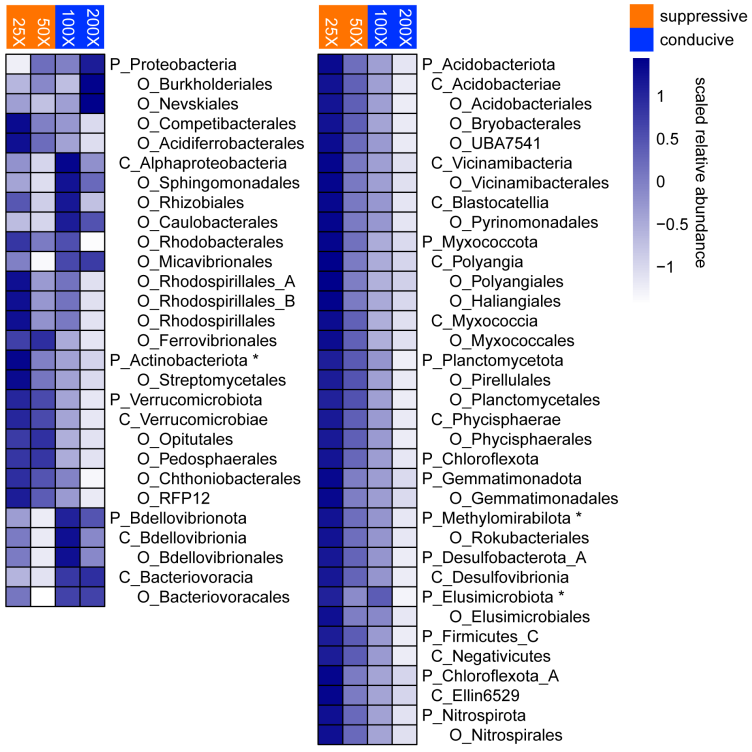


Figure 4. Significant changes in the relative abundance of the rhizosphere bacterial taxa between suppressive soil S11 dilutions exibiting a Fusarium-suppressive (25X and 50X) or a non-suppressive phenotype (100X and 200X). Relative abundance is scaled in rows (z-score), and the name of the taxonomic level is indicated by capital letters: P – Phylum, C – Class, O – Order. The significance of the change in abundance evaluated according to DESeq2 analysis with an adjusted p value < 0,05. The change in relative abundance of taxa marked with an asterisk is not statistically significant, and they are shown to indicate the phylum of lower taxonomic levels. Low abundant taxa (<1%) are not shown on the figure for the clarity of presentation. All the taxa significantly changing abundance are shown in table S2.

Genes associated with iron uptake, chitinase activity and T6SS secretion systems are enriched in disease-suppressive rhizosphere microbiomes

Co-assembly of all rhizosphere metagenome reads (8,214,787,741 reads, 953,849,270,414 Gb) yielded a total of 327,947 contigs above 5 Kb in length with an N50 of 11.908 Kb and total assembly size of 3.638 Gb. The co-assembly strategy was chosen to improve the overall coverage for each organism in the niche, as significant overlap was expected for all samples derived from the same ESM. The KEGG ortholog (KO) functional annotation of diluted

rhizosphere metagenomes reflected the functional potential of the microbial community. As expected in a rhizosphere metagenome, there was a large variety of KEGG orthologous groups (KO groups) with 11,459 unique entries. When investigating a general functional profile of the rhizosphere communities (top and second-level KEGG ortholog categories) across the dilution series showed no statistically significant changes (see supplementary material). To find associations between individual KEGG orthologue groups and the suppressive phenotype, we then separated metagenomic contigs in two categories based on a DESeq2 enrichment test between the lower two dilution points (25X and 50X) versus the two higher dilution points (100X and 200X). Occurrences of KO group annotations for genes of putative suppressiveness-associated contigs were grouped together and tested versus counts in the rest of the assembly. A Fisher's exact test of the occurrences of KEGG orthologs showed enrichment for 143 orthologs after multiple testing correction. Among those, we found terms associated with iron uptake like TonB [ko:K03832] and bacterioferritin [ko:K03594], chitinases [ko:K01183] and components of the Type VI Secretion System (T6SS) [ko:K11894]. Competition for iron was also identified as a potential mechanism of suppression of *F. culmorum* in our previous amplicon-based analyses of nonribosomal peptide synthetase (NRPS) genes (Tracanna et al., n.d.) and previously also for soils suppressive to Fusarium oxysporum (Lemanceau et al., 2009; Mazurier et al., 2009; Siegel-Hertz et al., 2018a; Tamietti and Alabouvette, 1986). The enrichment of NRPS genes involved in siderophore biosynthesis discovered here with untargeted metagenome analysis corroborates our earlier results and highlights the possible contribution of competition for iron in disease suppressiveness to *F. culmorum*.

Chitinases are enzymes involved in degradation of polymeric chitin and often associated with bacteria-fungi interactions (Lacombe-Harvey et al., 2018; Veliz et al., 2017). Production of chitinases was recognized as a potential control mechanism in a soil suppressive to club-root disease of cabbage (Hjort et al., 2014). Also, in a recent study on suppressiveness to *Rhizoctonia solani*, Carrion at al. found the expression of chitinases significantly upregulated in disease-suppressive consortia of root endophytic bacteria (Carrion et al., 2019). However, the enrichment of chitinases in *F. culmorum* suppressive rhizosphere may be related to saprophytic activity of bacteria as well as direct antagonism against the pathogen. Additional experiments are needed to test and validate those scenarios.

T6SS is used by gram-negative bacteria to deliver effectors such as toxins and other pathogenicity factors (Coulthurst, 2013; Records, 2011). T6SS is known to mediate bacteria-bacteria interaction. Nevertheless, some studies suggested a role of T6SS in antagonistic activity of bacteria against fungi (Monjarás Feria and Valvano, 2020; Trunk et al., 2018). While we cannot exclude the incidental enrichment of T6SS components with taxonomic

changes in the microbiome this opens the possibility of a direct inhibition of *F. culmorum* by members of the microbial community which are diminished across dilutions.

Biosynthetic gene clusters and metagenome-assembled genomes associated with suppressiveness

Secondary metabolites are often associated with direct antagonistic activity against fungal pathogens, which can result in disease suppression (Gomez-Exposito et al., 2017; Kwak and Weller, 2013; Schlatter et al., 2017). Microorganisms produce an incredible diversity of bioactive compounds, the production of which is encoded in biosynthetic gene clusters (BGCs). In this study, we identified 42,170 differentially abundant contigs using the DESeq2 package. AntiSMASH prediction of BGCs within this set of contigs yielded 504 BGCs of various classes (Fig.5). Statistical analysis of the distribution of BGC classes in this set versus the whole metagenome showed the enrichment of BGC classes encoding melanin, aryl polyenes and ladderanes in the lower dilutions (Table S4). Melanins in fungi are mainly associated with virulence and protection against physical and chemical stresses (Cordero and Casadevall, 2017). However, they can also be produced extracellularly by diverse bacterial taxa including Streptomycetes which were already found to decrease in abundance at higher ESM dilutions (Fig.4) (El-Naggar and El-Ewasy, 2017). Accordingly, the melanin clusters found in this group share high similarity to other melanin BGCs found in multiple *Streptomyces* strains. Melanins appear to have a role in root colonization by Streptomycetes (Chewning et al., 2019) and considering the relationship between rhizosphere population density and disease suppression (Johnson, 1994; Raaijmakers and Weller, 1998), melanins may indirectly contribute to the disease-suppressive phenotype by increasing the fitness of key microbes involved in suppression of the pathogen. The enrichment of aryl polyenes and ladderanes is discussed in supplementary material.

Considering that BGC classes are generally broad and functionally heterogeneous, we focused our attention on specific gene clusters for which the abundance strongly correlates with the changes in the suppressive phenotype. Among them, we noted delftibactin, pyoverdine, myxochelin and unknown siderophores, including NRPS containing TonB-dependent siderophore receptor) as well as multiple fragments or analogs of BGCs encoding metabolites with reported antifungal properties such as caniferolides (Pérez-Victoria et al., 2019) and Kutznerides (Dong Zhang et al., 2020). Full antiSMASH results can be accessed online ("AntiSMASH results," 2021). However, given such a large collection of potential targets, which in most cases cannot be associated to previously characterized gene clusters in the MIBiG database, we first prioritized those BGCs present in the metagenome-assembled genomes (MAGs) as it can provide additional genomic and taxonomic context (Fig. 5). Manual curation of individual bins resulted in a collection of 96 MAGs. Then, we analyzed the MAG collection looking for BGCs that become differentially abundant along

the ESM dilution trajectory. This resulted in 9 MAGs that were strongly associated with disease suppressiveness and belonged to the bacterial families Burkholderiaceae, Acidimicrobiaceae, Verrucomicrobiaceae, and Polyangiales (Fig. 5 and Fig. 6). Among the 9 MAGs, the ones assigned to the genera *Labilithrix* (Polyangiales) and *Prosthecobacter* (Verrucomicrobiaceae) belong to taxa that displayed a significant decrease in abundance at higher dilutions (table S2). We then linked the KEGG orthologues enriched genes to the MAGs and found that out of the 9 MAGs, only the *Labilithrix* bin contained genes from the previously discussed categories such as chitinase, siderophores associated genes and core T6SS associated genes (Fig. 8). Additionally, we found multiple copies of the T6SS component FHA (Forkhead-associated domain) that was enriched in the dilutions with a suppressive phenotype within the same *Labilithrix* MAG. One particular multimodular NRPS gene cluster stood out, as it is predicted to encode a peptide with 11 modules, does not have a thioesterase termination domain in the BGC region and lies on a contig edge suggesting that it is a fragment of an even larger BGC (Fig. 7). AntiSMASH clusterblast and knownclusterblast results showed little to no similarity to previously encountered and classified clusters, including those from its closest representative in the NCBI database. *Labilithrix* and closely related bacteria were, so far, never associated with disease suppressiveness but have been recognized as producers of antibacterial, antifungal and antiviral agents (Mulwa et al., 2018; Weissman and Müller, 2009; Yamamoto et al., 2014). Future experiments on this genus should aim at the identification of BGCs expressed on roots of wheat challenged with *F. culmorum* and the expression levels correlating with the disease suppressive phenotype. Additionally, previous studies successfully established synthetic communities from disease suppressive endosphere isolates that were able to reproduce the suppressive phenotype (Carrión et al., 2019). Here, we describe a set of 9 MAGs which constitute suitable candidates for initial leads in this direction.

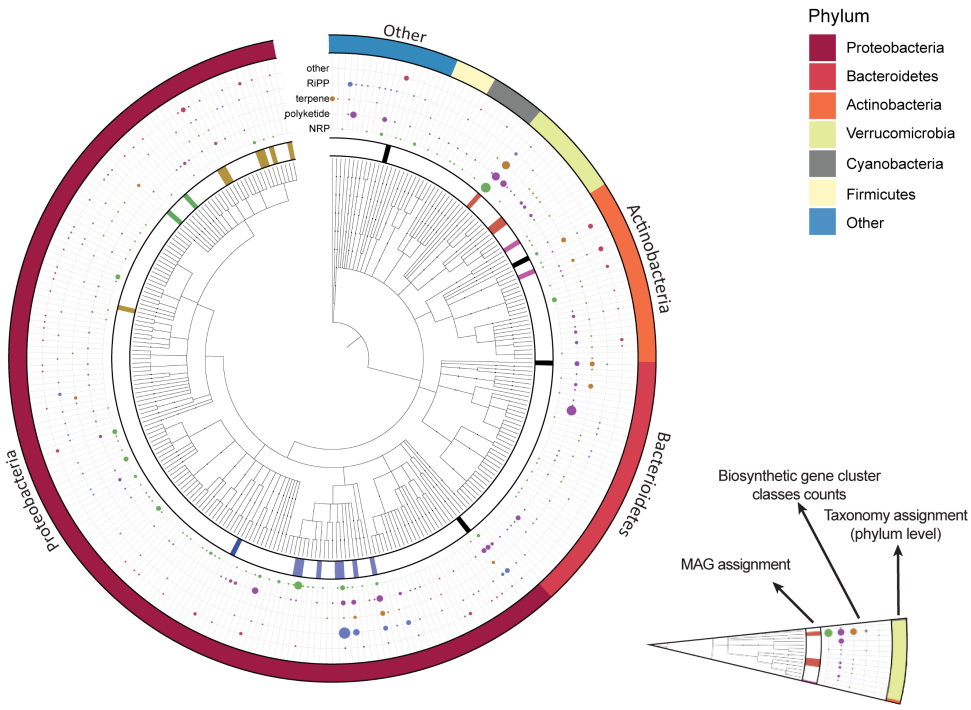


Figure 5. Taxonomical representation of 504 differentially abundant contigs containing biosynthetic gene clusters from the dilution metagenomes. A phylogenetic tree based on their taxonomical annotation is used to order the contigs. In this visualization, contigs assigned to the same taxa are grouped together. The innermost circle (MAG assignment) represents the taxonomic groups containing contigs assigned to a specific metagenome-assembled genome. Contigs assigned to the same MAG are marked with the same color (further description in Fig.7 for a color legend) or with black for MAGs containing only one BGC-harboring contig. For example, the contigs assigned to the L. luteola (Polyangiacee) MAG at approximately 180 degrees are shown in blue both in this inner ring and in Fig 7. Further, the major antiSMASH -predicted BGC classes in the contigs are indicated with dots. The number of predicted BGC is reflected by the size of the dot. Finally, the outer ring represents the contig taxonomical assignment at the phylum level.

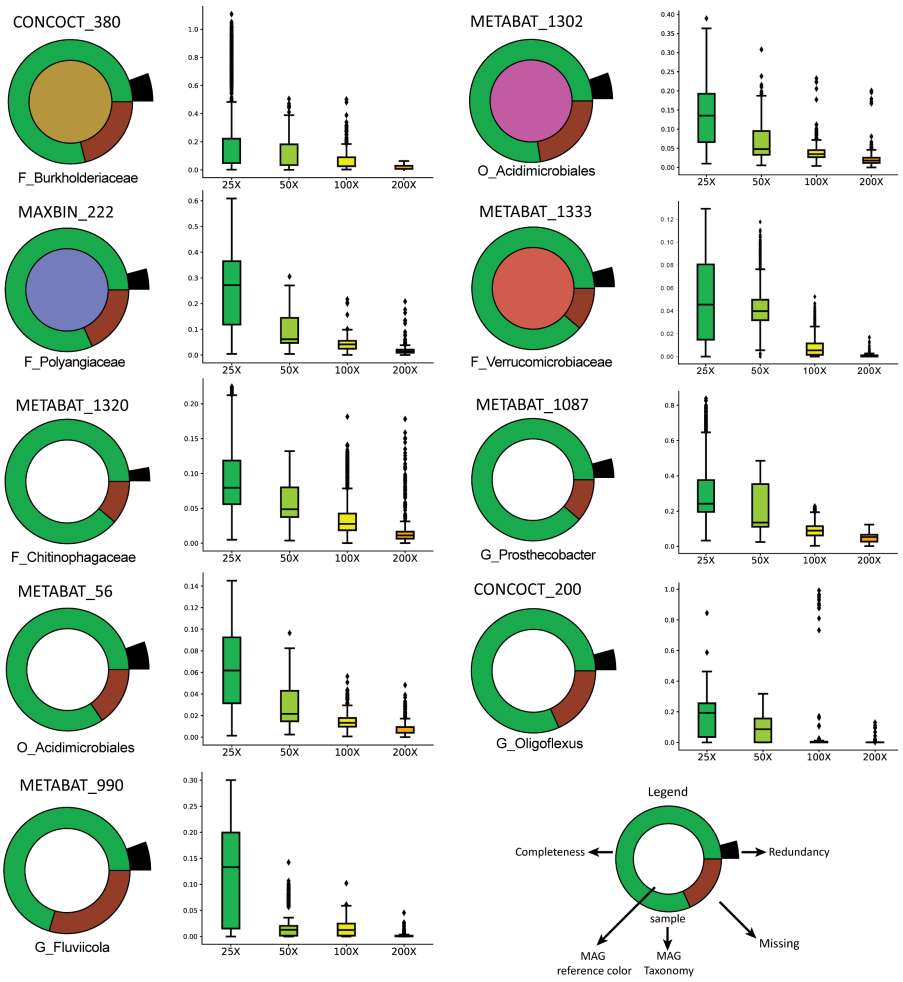


Figure 6. Representation of the MAGs from the metagenome showing significant association with the suppressive phenotype. The MAGs shown here are constituted by 50% or more in length by differentially abundant contigs according to DESeq2 analysis. The ring shows an overview of the MAGs assembly completeness and redundancy. For each MAG, a boxplot shows the abundance of all its contigs across the dilutions. MAG reference colors refer to Fig. 5. The taxonomic levels are inndicated by a capital letters: O – Order,F -family, and G – genus.

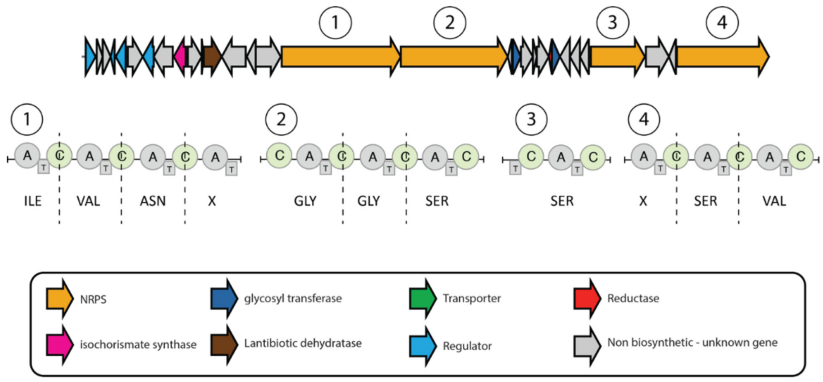


Figure 7. Large NRP gene cluster within Labilithrix MAG with predicted amino acid specificities for each module. The cluster lays on a contig edge and is missing a TE domain and is therefore considered incomplete.

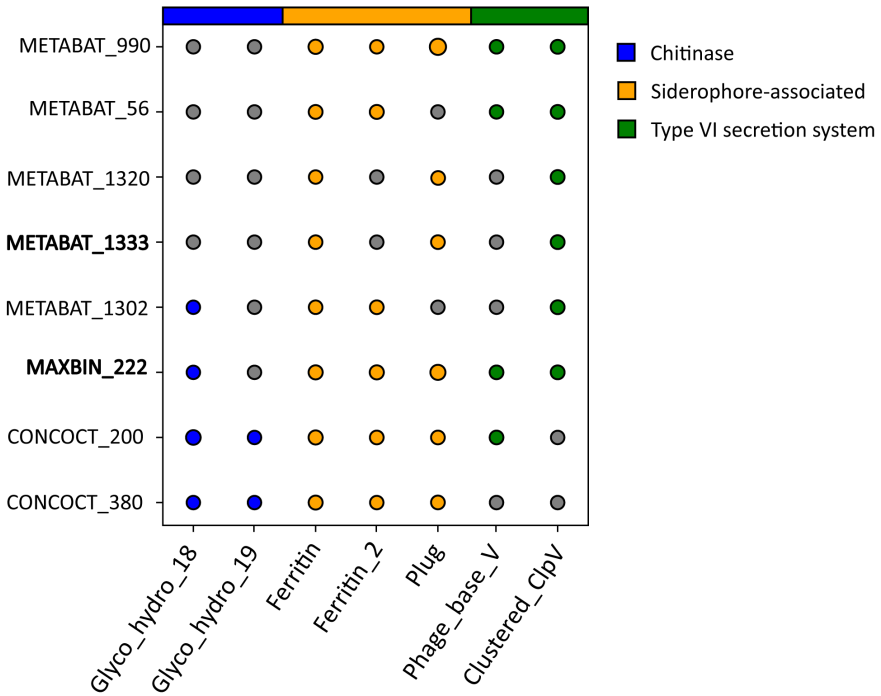


Figure 8. Presence (colored dot) absence (gray dot) patterns of domains contained in KEGG orthologues genes enriched in suppressive dilution points in the MAG collection. Bacterial chitinase families are shown in blue, siderophores associated domains in yellow

and core-representative-components of type VI secretion system in green. Presence of both Phage_base_V and co-occurrence of all 4 ClpV subdomains (AAA, AAA_2, AAA_lid_9 and ClpB_D2-small) on the same contig are considered as minimal requirements for putative presence of type VI secretion system.

Conclusions

We analyzed the microbiome of disease suppressive soil by integrating a dilution-to-extinction approach with shotgun metagenomics. The dilution of the rhizosphere microbial community of the *Fusarium*-suppressive soil led to the decline of the plant protective effect. The dilution effect produced significant changes in the abundance of multiple bacterial taxa and diversity, but these changes could not directly be matched by shifts in the microbiome functional profile. Nevertheless, key BGCs associated with chitin degradation and siderophore biosynthesis were associated with the disease suppressive phenotype. These genes were also detected in the metagenome assembled genomes (MAGs) with yet unknown secondary metabolite production potential. Altogether, this work represents the first example of the dissection of the rhizosphere microbiome of a disease-suppressive soil by using a dilution-to-extinction. This approach could be instrumental in future studies for discovering the mechanisms involved in other soil functions.

Materials and Methods

Soils used in the study

Soil S11 was collected from an agricultural field near Bergen op Zoom, the Netherlands in March 2018. This soil exhibited a high level of disease suppressiveness against *Fusarium culmorum,* which was evaluated in our previous study (Ossowicki et al., 2020). Furthermore, we used a sandy dune soil (BS) collected near Bergharen, the Netherlands (Schulz-Bohm et al., 2015). After collecting soils were air-dried in room temperature, sieved through 4 mm sieve, and stored at 4°C. BS soil was additionally gamma sterilized (Synergy Health Ede B.V., The Netherlands) before use.

Seed preparation and growth conditions

JB Asano wheat seeds (Agrifirm, The Netherlands) were surface sterilized and pre-germinated in order to use in the experiment. Briefly, after surface sterilization with 70% ethanol and 10% bleach, seeds were washed with an excess of sterile water and placed on a wet 1mm paper filter (VWR, the Netherlands). Three-day-old seedlings were transferred to the soil, watered every second day and supplemented weekly with 0,5 Hoagland solution without microelements (0.5 M Ca(NO3)2·4H2O, 1 M KNO3, 1 M KH2PO4, 0.5 M MgSO4·7H2O and 98.6 mM ferric EDTA). Plants were grown in cabinets (MC 1750 VHO-EVD,

Snijders Labs) at 20°C day and night, photoperiod 12 h day/12 h night with 60% relative humidity.

Inoculation and disease suppressiveness evaluation

Soilborne pathogen *F. culmorum* PV (de Boer et al., 1998) was grown on ¼ strength PDA media (Oxoid, The Netherlands) for 2 weeks at 20°C in order to use in the experiment. Where indicated, the pathogen was introduced to the soil before seedling transfer as 6mm mycelium plugs (1 per 10cc of soil). After the experiment wheat plants were gently removed from the soil and cleaned. The disease symptoms on the roots were assessed according at a scale from 0- healthy to 5-severely diseased, like we described before (Ossowicki et al., 2020). Statistical differences in disease symptoms between treatments and control were assessed using the chi-square test, with an alpha cut-off of $p<0.05$.

Microbiome extraction

Wheat plants were grown in four 130 cc pots filled with S11 for two weeks. In order to perform a liquid extraction of the microbiome from the suppressive soil S11, all the glassware, materials and buffer were autoclaved. Plants were gently removed from the pots and the soil with the whole root system was transferred to a glass bottle with 10 volumes of phosphate buffer (10 mM KH_2PO_4, pH=6.5) and 5g of sterile glass beads. These bottles were shaken using an orbital shaker for 1 h at 180 rpm, sonicated for 15 min and shaken again for 1h to detach microorganisms from soil particles. Afterwards, all the extracts were merged in one beaker and sieved through a metal sieve to separate bigger soil particles and roots. Subsequently, extract was briefly centrifuged (1000 x g, 1 min) and the supernatant was filtered again using a Buchner funnel through a filter paper (VWR Grade 415 Filter Paper, VWR the Netherlands). The extract obtained this way was considered a 10X diluted Extracted Soil Microbiome (ESM) because the soil was extracted with 10 volumes of the buffer. In parallel, as a control, the same procedure was applied with the sterile soil BS with a sterile vermiculite (Agra-vermiculite, The Netherlands) in a 1 to 1 volume ration. This way a BS control extract was obtained.

Dilution to extinction - introduction to a sterile soil

In order to optimize the magnitude of the dilution we performed preliminary experiments (data not shown) investigating first, if dilution affects soil disease suppressiveness to *F. culmorum* (the phenotype), and second, at which dilution point the change in phenotype from suppressive to conducive occurs. After the preliminary experiments we chose the dilution steps in such a way that the phenotype tipping point occurs centrally. Compared to the dilution steps used in other studies (Chen et al., 2020; Hol et al., 2015; Korenblum et al., 2020; Yan et al., 2015), we applied a relatively small dilution magnitude. Nevertheless, in

the experimental system we present in this work, these small dilution steps allow us to observe a gradual change of the phenotype.

The 10X dilution of the ESM was serially diluted with phosphate buffer to 25X, 50X, 100X, 200X and 400X and stored at 4°C. The dilution range was determined in a preliminary experiment (data not shown). Plastic, 100 cc pots were filled with the sterile soil BS mixed with sterile vermiculite in a volume ratio of 1 to 1 and with mycelium plugs of *F. culmorum* or sterile ¼ PDA plugs (mock inoculation) according to the treatment. Distinct dilutions of the ESM and the BS control extract were added to pots, 20 ml per day for seven days, before wheat seedlings were introduced. Plants were grown for 3 weeks before the disease assessment and a rhizosphere DNA isolation.

Dilution to extinction - experimental setup

All the dilution treatments and controls consisted sixteen biological replicates, plants were grown in a randomized order to minimize spatial bias. A negative control and a positive control, with and without the pathogen, respectively, were used to control for the infectiousness of the pathogen and the effect of the sterile soil, buffer, and the extraction procedure. The control S11 contained natural suppressive soil S11 with the pathogen introduced to control for the soil disease suppressiveness of the soil that was used for microbiome extraction.

The experiment was performed twice, and the rhizosphere samples used for the DNA extraction were collected in the second experiment from randomly selected replicates.

Rhizosphere DNA extraction

Five out of sixteen replicates were randomly selected for a rhizosphere DNA extraction before the disease assessment. Plants were gently removed from the pots and the soil loosely adhering to the roots was removed by shaking. The whole root system was placed in a 50 ml falcon tube with 25 ml of sterile MQ grade water. The tubes were vortexed, sonicated, and vortexed again, each step for 1 min. Afterwards, the roots were removed with sterile forceps and disease symptoms were assessed on them. The water with extracted rhizosphere was briefly spined down (1000 x g, 1 min) and carefully decanted to a new 50 ml falcon tube. The decanted liquid was frozen at -20 °C and freeze dried overnight (Free zone 12, Labconco the USA). This resulted in forming a white powder in the tube which was collected and extracted using a DNeasy PowerSoil Kit (QIAGEN, the Netherlands) according to the manufacturer's protocol, without applying a bead beating step. Samples were subsequently purified using the DNeasy PowerClean cleanup kit (QIAGEN, the Netherlands).

Data quality control, assembly, mapping and binning

Raw paired sequence reads were quality-checked with (Andrews, 2015) and trimmed using bbduk (Bushnell, n.d.) with a Phred score threshold of 30. Read pairs for which at least one mate was shorter than 150 bp were discarded. Reads for all dilution points were co-assembled in a single assembly using megahit v1.2.9 (Li et al., 2016). Genes were predicted using prodigal v2.6.3 (Hyatt et al., 2010) using the metagenome mode. Reads were mapped back onto the assembly contigs using hisat2 (Kim et al., 2019). BAM files were converted into SAM using samtools v1.7 and rpkm counts were obtained with the mpileup (Li et al., 2009). Binning was performed within anvi'o environment v6.2 (Eren et al., 2015) using DASTOOL (Sieber et al., 2018) refinement of MAXBIN2 v2.2.7 (Wu et al., 2016), CONCOCT v1.1.0 (Qian and Comin, 2019) and METABAT v2.15 (Kang et al., 2019) obtained bins. MAGs with a DASTOOL confidence score >= 0.5 were kept.

Enrichment analysis, biosynthetic gene cluster annotation, reads taxonomy annotation and KEGG functional annotation

Identification of differentially abundant contigs was performed in R using DESeq v1.18.1 (Love et al., 2014, p. 2) looking for enrichment of contigs in the first two dilution points (25X and 50X) versus the higher dilution points (100X and 200X). Contigs with adjusted p-value < 0.05 were considered differentially abundant. Biosynthetic gene clusters were predicted from differentially abundant contigs with a positive fold change using antiSMASH 5.1.2 (Blin et al., 2019) using the prodigal-meta option for gene prediction, --cb-general and --cb-knownclusters for comparison of predicted clusters to antismash-database (Blin et al., 2020) and MIBiG (Kautsar et al., 2020). Quality-trimmed reads were taxonomically annotated using kraken v2.0.8 (Wood et al., 2019) against the GTDB-taxonomy database release 05-RS95 (Parks et al., 2020) KEGG annotation was performed at Baseclear (Leiden, The Netherlands) using the full megahit assembly.

Phylogeny tree construction and annotation

Differentially abundant contigs which had at least one predicted cluster were taxonomically annotated using diamond v 0.9.21 (Buchfink et al., 2015) against the NCBI nr database Oct. 2020 (NCBI Resource Coordinators, 2016). Contigs were assigned to the taxonomical group with the highest cumulative score across the contig. Contigs annotated with the same taxonomy were grouped for tree construction. The list of taxonomic groups was used in NCBI common tree to obtain a tree in PHYLIP format representing the phylogeny relations of the taxonomies present in the differentially abundant contigs with biosynthetic gene clusters shown in Figure 5. Annotation of the tree was done with iTOL (Letunic and Bork, 2019) and is available at https://itol.embl.de/tree/8873156232367181606086331#.

Presence-absence of KEGG orthologs enriched domains in MAGs was determined using hmmsearch v3.1b2 (Mistry et al., 2013) and hmm domains from pfam (El-Gebali et al., 2019) against the different MAGs using trusted cutoffs. Presence of ClpV was determined based on the co-occurrence of all 4 ClpV subdomains (AAA, AAA_2, AAA_lid_9 and ClpB_D2-small) on the same contig. ClpV and Phage_base_V are considered core components of type VI secretion system (Boyer et al., 2009).

Supplementary material

General functional profiles of the rhizosphere microbiomes are resilient to dilution

We grouped KEGG orthologs by their KEGG Orthology hierarchical classification and aggregated their RPKM counts to generate functional profiles for each sample per KO category. Interestingly, no category with a sufficient number of entries was found to be significantly different across the dilutions (Fig. S3), including categories which contain differentially abundant KOs.

From these observations, we deduce that, despite the changes in the taxonomic profiles, the KO functional profiles of the communities are generally stable at the level of these broad categories across dilutions, with no statistical differences (Fig.S3). This may be connected to the strong selective pressure of the environment, which restricts members of the community into a well-defined functional profile. In our experiment, every rhizosphere community occupied highly similar niche; therefore, we can conclude that the general functional profiles could also be highly similar. We can speculate that further dilutions of the ESM inoculum would have a stronger effect on the metabolic profiles, as shown in the work of Yan et al. (Yan et al., 2017). Nevertheless, it would also disturb the community in considerable way and our intention in this experiment was to track the changes in microbial communities related to the change in disease suppressiveness which were shown to be significant between these dilution points. The loss of the suppressive phenotype across the dilutions without significant changes in functional profiles suggests that the origin of this phenomenon is not related to specific community-wide microbiome features but to specific "silver bullets" which cannot be tracked with large scale functional analysis.

Because of the character of KEGG database (Kanehisa et al., 2017) we can only draw conclusions about the general functional profiles of the soil microbial communities. To understand the specialized secondary metabolism of soil microbiomes, which was recognized to be crucial for soil suppressiveness in a number of studies (Gomes Exposito et al., 2017; Kwak and Weller, 2013; Schlatter et al., 2017b), we need to use other approaches. To this end, we decided to expand the functional analysis with prediction and identification of biosynthetic gene clusters (BGC) using antiSMASH pipeline (Blin et al., 2019).

Additional enriched gene cluster classes in suppressive rhizosphere

In addition to melanins, two more BGC product classes were significantly more present in suppressive enriched contigs compared to the rest of the metagenome: aryl polyenes and ladderane. The functional role of aryl polyenes produced by rhizosphere bacteria is so far unknown. This class of antioxidants is similar to carotenoids in structure and biochemical function and likely protect bacteria from reactive oxygen species produced by the plant as a response to infection (Lehmann et al., 2015). The synthesis genes of aryl polyenes are

abundant among Proteobacteria but not in Alphaproteobacteria and Gammaproteobacteria (Schöner et al., 2016). Since Alphaproteobacteria are the main contributors to the increased abundance of whole phylum in high dilutions, it is likely that also the enrichment of the aryl polyene BGCs is related to the abundance of associated taxa. Laddreanes are membrane lipids present in anammoxosomes – intracellular compartments of ammonium-oxidizing bacteria (Hancock and Brown, 2021). Since, these lipids are mostly found in Planctomycetes (Sinninghe Damsté et al., 2005) we can attribute the ladderane BGCs enrichment to the abundance of this group (Fig.4). Ladderanes are predominantly found in marine environments and their role in rhizosphere is unknown. Despite their enrichment in suppressive associated contigs, these biosynthetic gene cluster classes have no known association with antifungal activity nor provide fitness competitive advantage over the pathogen. Therefore, we consider this enrichment incidental to the relative decrease in abundance of the corresponding producing taxonomic groups.

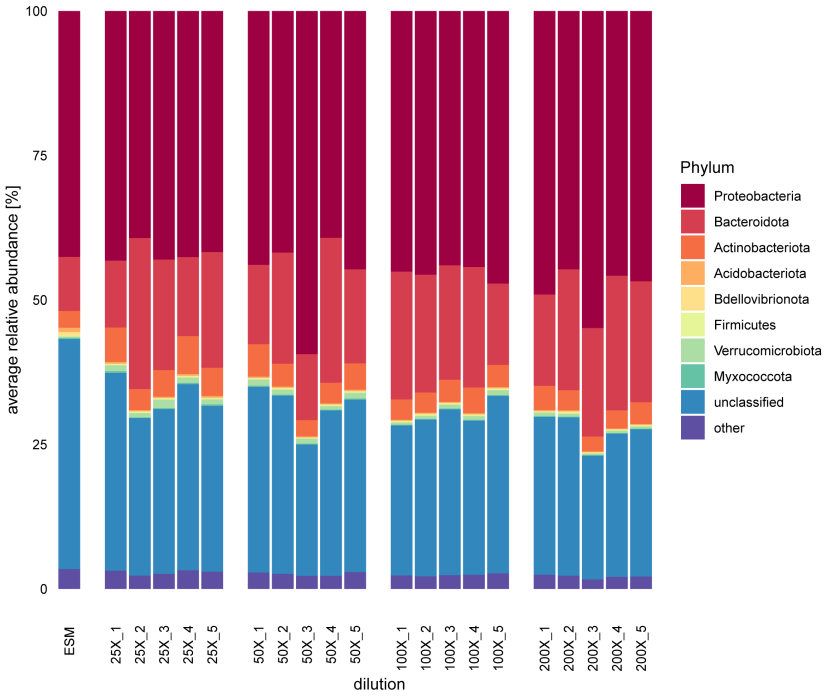


Figure S1. Barplot showing the most abundant phyla in the ESM and rhizosphere across four dilution points in five replicates.

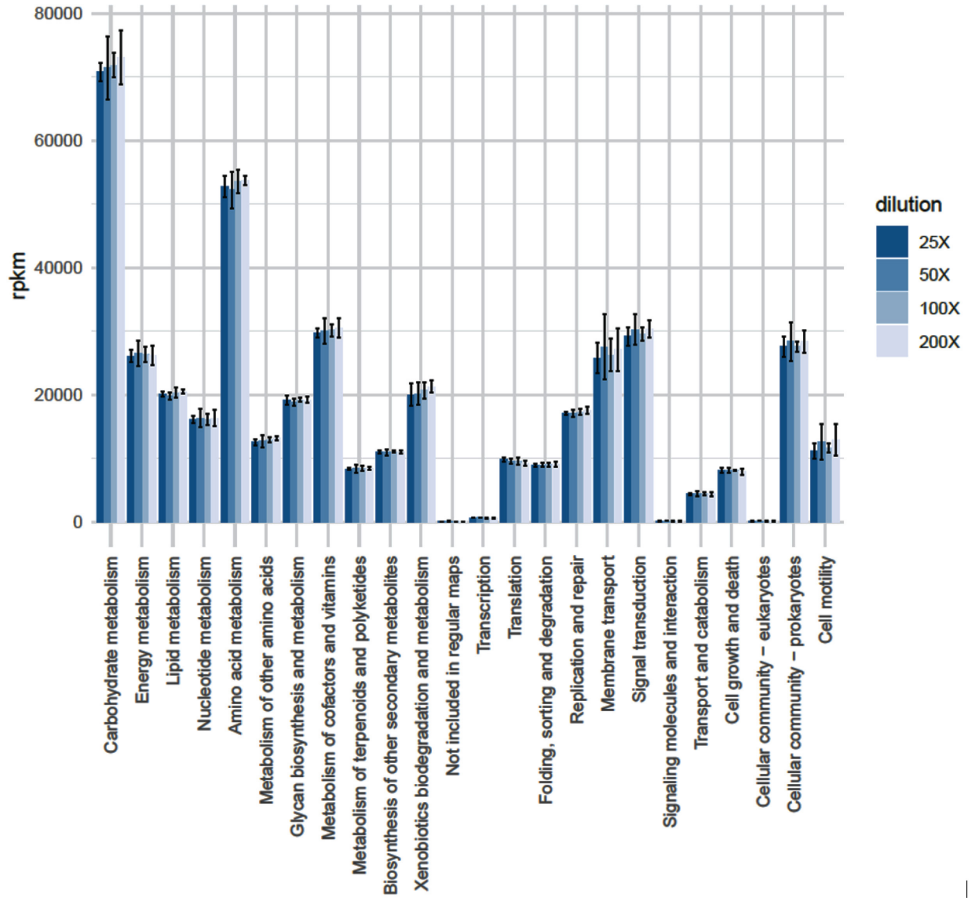


Figure S2. Graph summarising KEGG orthology annotations of rhizosphere metagenomes in four dilutions. The values on y axis are expressed in reads per kilo base per million mapped reads (rpkm). Error bars show the standard deviation of the mean in five replicates.

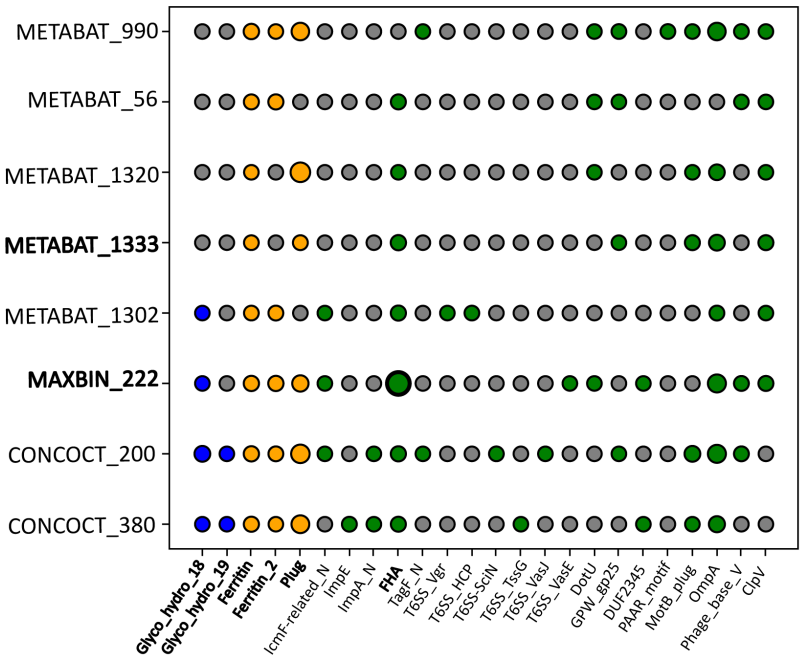


Figure S3. Presence (colored dot) absence (gray dot) patterns of domains contained in KEGG orthologues genes enriched in suppressive dilution points in the MAG collection. Bacterial chitinase families are shown in blue, siderophores associated domains in yellow and components of type VI secretion system in green. ClpV is considered present (last column) if all 4 ClpV subdomains (AAA, AAA_2, AAA_lid_9 and ClpB_D2-small) cooccur on the same contig. FHA domain counts for Labilithrix MAG is shown in bold. Here, multiple core and accessory components of the type VI secretion system are shown.

Table S1. Nonpareil diversity index

	kappa	C	LR	modelR	LRstar	diversity
ESM	0,36975	0,4027322	4,361E+10	0,9994318	1,60E+12	24,86517
25X-1	0,99481	0,9952547	4010631554	0,9965573	2,61E+07	14,62634
25X-2	0,99405	0,9945596	3511713953	0,9967691	2,28E+07	14,45159
25X-3	0,99289	0,9934986	3284871908	0,9971337	1,88E+07	14,38412
25X-4	0,99234	0,9929955	3336073351	0,9970277	1,96E+07	14,36748
25X-5	0,99604	0,9963795	4320103063	0,9966588	2,66E+07	14,65394
50X-1	0,99015	0,9909921	3936582220	0,9968238	2,58E+07	14,57465
50X-2	0,99233	0,9929864	3439318405	0,9969511	2,13E+07	14,39654
50X-3	0,9911	0,9918612	3665552015	0,9967706	2,40E+07	14,50529
50X-4	0,9958	0,99616	3895751514	0,9967257	2,32E+07	14,59096
50X-5	0,99038	0,9912025	3987968934	0,9970652	2,42E+07	14,56012

100X-1	0,99706	0,9973121	2015635523	0,9973075	1,20E+07	13,87775
100X-2	0,99234	0,9929955	2152546737	0,9974004	1,31E+07	13,93182
100X-3	0,99506	0,9954833	2360093190	0,9969755	1,43E+07	14,03799
100X-4	0,99216	0,9928309	1898749915	0,9978125	1,16E+07	13,82418
100X-5	0,99182	0,9925199	2210853791	0,9970134	1,31E+07	14,01849
200X-1	0,99043	0,9912483	2216373822	0,9967982	1,38E+07	13,95889
200X-2	0,99416	0,9946602	1851961914	0,9974601	1,11E+07	13,78291
200X-3	0,99318	0,9937639	2027743164	0,9973221	1,26E+07	13,87862
200X-4	0,99424	0,9947334	1865565389	0,9971779	1,16E+07	13,78712
200X-5	0,99698	0,997239	2092116998	0,9972424	1,35E+07	13,93965

Table S2. Taxonomic groups showing a statistically significant difference between suppressive and conducive phenotype based on deseq2 analysis with adjusted p value (padj) >0.05.

	baseMean	log2FoldChange	lfcSE	stat	pvalue	padj
Phylum						
Chloroflexota_A	39490,725	0,491	0,108	4,533	0,000	0,000
Verrucomicrobiota	1385470,535	0,600	0,138	4,340	0,000	0,000
Nitrospirota	23890,565	0,154	0,036	4,249	0,000	0,000
Bdellovibrionota	222620,736	-0,683	0,162	-4,206	0,000	0,000
Acidobacteriota	368569,397	0,230	0,056	4,134	0,000	0,000
Chloroflexota	112861,105	0,054	0,014	3,913	0,000	0,000
Myxococcota	273855,337	0,304	0,094	3,227	0,001	0,006
Desulfobacterota_A	61305,855	-0,066	0,025	-2,579	0,010	0,034
Firmicutes_C	37613,401	-0,080	0,031	-2,546	0,011	0,034
Planctomycetota	198268,737	0,141	0,056	2,525	0,012	0,034
Proteobacteria	90539661,798	-0,363	0,145	-2,503	0,012	0,034
Gemmatimonadota	112082,072	0,219	0,088	2,487	0,013	0,034
Class						
Alphaproteobacteria	22996742,173	-0,521	0,083	-6,249	0,000	0,000
Vicinamibacteria	111813,239	0,426	0,093	4,564	0,000	0,000
Bacteriovoracia	76844,438	-1,084	0,247	-4,391	0,000	0,000
Acidobacteriae	178419,644	0,092	0,021	4,368	0,000	0,000
Ellin6529	39472,064	0,466	0,108	4,313	0,000	0,000
Verrucomicrobiae	1344083,126	0,594	0,140	4,231	0,000	0,000
Desulfovibrionia	61501,926	-0,088	0,024	-3,616	0,000	0,002
Myxococcia	88014,978	0,246	0,073	3,350	0,001	0,004
Phycisphaerae	48833,733	0,083	0,027	3,125	0,002	0,007
Bdellovibrionia	145735,276	-0,526	0,177	-2,975	0,003	0,010
Blastocatellia	25422,819	0,224	0,076	2,959	0,003	0,010
Polyangia	155993,898	0,332	0,112	2,955	0,003	0,010
Negativicutes	37763,815	-0,102	0,039	-2,641	0,008	0,024
Order						
Acidobacteriales	98538,785	0,115	0,019	6,207	0,000	0,000

Bryobacterales	47288,440	0,194	0,035	5,519	0,000	0,000
Pirellulales	46891,132	0,232	0,044	5,246	0,000	0,000
Rhodospirillales_B	33273,037	-0,160	0,031	-5,185	0,000	0,000
Opitutales	555734,077	1,097	0,220	4,991	0,000	0,000
Nitrospirales	16056,519	0,222	0,045	4,975	0,000	0,000
Sphingomonadales	6161963,173	-0,705	0,143	-4,935	0,000	0,000
Vicinamibacterales	103115,445	0,498	0,103	4,830	0,000	0,000
CSP1-4	34652,118	0,553	0,116	4,779	0,000	0,000
Caulobacterales	4207529,338	-0,572	0,120	-4,767	0,000	0,000
Rhodobacterales	835706,211	-0,171	0,038	-4,504	0,000	0,000
Phycisphaerales	28862,538	0,161	0,038	4,259	0,000	0,000
Rhizobiales	9388973,888	-0,310	0,073	-4,244	0,000	0,000
Rhodospirillales	28924,747	-0,120	0,029	-4,145	0,000	0,000
Myxococcales	88250,073	0,294	0,076	3,853	0,000	0,001
Rhodospirillales_A	38583,001	-0,148	0,039	-3,767	0,000	0,001
Pedosphaerales	136133,148	0,519	0,138	3,758	0,000	0,001
Elusimicrobiales	12380,224	-0,083	0,023	-3,554	0,000	0,002
Micavibrionales	62012,405	-0,579	0,165	-3,506	0,000	0,003
Acidiferrobacterales	11485,584	0,099	0,029	3,453	0,001	0,003
Polyangiales	90226,803	0,506	0,150	3,373	0,001	0,004
Pyrinomonadales	21227,649	0,291	0,089	3,253	0,001	0,006
Haliangiales	14268,707	0,430	0,136	3,164	0,002	0,008
RFP12	12941,743	0,131	0,042	3,118	0,002	0,009
Palsa-1104	20145,003	0,171	0,058	2,954	0,003	0,014
Planctomycetales	23272,475	0,194	0,066	2,928	0,003	0,015
Ferrovibrionales	17106,596	0,422	0,151	2,805	0,005	0,021
Competibacterales	11509,354	-0,093	0,034	-2,745	0,006	0,024
Nevskiales	685807,899	-0,420	0,154	-2,731	0,006	0,025
20CM-4-69-9	12032,020	0,186	0,069	2,711	0,007	0,025
Gemmatimonadales	101811,055	0,246	0,093	2,646	0,008	0,030
Chthoniobacterales	74652,607	0,296	0,113	2,616	0,009	0,031
Bdellovibrionales	145402,464	-0,474	0,185	-2,553	0,011	0,037
Rokubacteriales	69620,443	0,102	0,041	2,480	0,013	0,043
Bacteriovoracales	57229,742	-0,655	0,265	-2,473	0,013	0,043
UBA7541	22119,531	0,097	0,039	2,463	0,014	0,043
Burkholderiales	43343891,188	-0,298	0,122	-2,451	0,014	0,044
Streptomycetales	1466959,322	0,138	0,057	2,422	0,015	0,046
Family						
Koribacteraceae	35374,794	0,165	0,027	6,072	0,000	0,000
Bryobacteraceae	47332,723	0,208	0,039	5,379	0,000	0,000
Nitrospiraceae	14852,896	0,257	0,048	5,395	0,000	0,000
Pirellulaceae	34394,854	0,260	0,050	5,204	0,000	0,000
Opitutaceae	536829,319	1,137	0,226	5,035	0,000	0,000
UBA2999	58261,358	0,563	0,113	4,996	0,000	0,000
Sphingomonadaceae	6160426,173	-0,693	0,144	-4,795	0,000	0,000

Maricaulaceae	23348,656	-0,168	0,035	-4,797	0,000	0,000
CSP1-41	34694,230	0,569	0,118	4,829	0,000	0,000
Magnetospirillaceae	32213,060	-0,153	0,032	-4,732	0,000	0,000
Caulobacteraceae	4104809,357	-0,569	0,124	-4,576	0,000	0,000
SM1A02	21577,933	0,199	0,046	4,311	0,000	0,000
Thalassospiraceae	14696,777	-0,221	0,053	-4,167	0,000	0,000
Rhizobiaceae	4693341,083	-0,536	0,132	-4,071	0,000	0,001
SG8-39	32734,921	0,378	0,095	3,994	0,000	0,001
Pedosphaeraceae	76627,446	0,584	0,147	3,984	0,000	0,001
Myxococcaceae	68699,392	0,346	0,087	3,976	0,000	0,001
Acidobacteriaceae	59741,790	0,104	0,026	3,960	0,000	0,001
Rhodobacteraceae	837358,889	-0,157	0,040	-3,936	0,000	0,001
UBA9959	11274,853	-0,085	0,022	-3,911	0,000	0,001
Akkermansiaceae	133660,860	-0,442	0,120	-3,671	0,000	0,002
AV2	15573,664	0,489	0,139	3,514	0,000	0,004
Polyangiaceae	73382,203	0,558	0,160	3,485	0,000	0,004
GWC2-71-9	42955,815	0,243	0,070	3,479	0,001	0,004
Micavibrionaceae	51138,475	-0,516	0,149	-3,466	0,001	0,004
Rhodospirillaceae	28989,936	-0,106	0,031	-3,413	0,001	0,005
Chitinibacteraceae	23881,359	-0,186	0,055	-3,391	0,001	0,005
Inquilinaceae	13609,211	-0,126	0,038	-3,345	0,001	0,006
Pyrinomonadaceae	21303,299	0,306	0,092	3,322	0,001	0,006
DEV007	19383,070	0,249	0,077	3,252	0,001	0,007
Haliangiaceae	14327,598	0,446	0,137	3,249	0,001	0,007
Demequinaceae	29817,088	0,195	0,060	3,231	0,001	0,008
Phreatobacteraceae	16444,155	-0,265	0,083	-3,194	0,001	0,008
Chitinimonadaceae	11548,946	-0,209	0,066	-3,153	0,002	0,009
Cellulomonadaceae	128381,509	0,223	0,071	3,149	0,002	0,009
UBA10450	41732,871	0,247	0,079	3,149	0,002	0,009
Planctomycetaceae	23343,172	0,209	0,069	3,053	0,002	0,012
Beutenbergiaceae	12593,733	0,185	0,061	3,010	0,003	0,013
Xanthobacteraceae	1526260,733	-0,272	0,092	-2,947	0,003	0,016
Ferrovibrionaceae	17157,291	0,434	0,149	2,915	0,004	0,017
20CM-4-69-91	12069,230	0,202	0,071	2,830	0,005	0,022
Stappiaceae	49373,538	-0,105	0,038	-2,763	0,006	0,027
Nevskiaceae	663860,569	-0,423	0,157	-2,696	0,007	0,032
Ilumatobacteraceae	15569,050	0,335	0,126	2,659	0,008	0,035
UBA1479	9088,574	-0,103	0,039	-2,633	0,008	0,037
UBA75411	21316,019	0,109	0,042	2,614	0,009	0,038
GWA2-73-35	69814,975	0,116	0,045	2,609	0,009	0,038
Streptomycetaceae	1459514,215	0,153	0,060	2,570	0,010	0,041
Bdellovibrionaceae	141832,170	-0,470	0,184	-2,559	0,011	0,042
Fen-1088	14690,777	0,136	0,054	2,515	0,012	0,046
Bacteriovoracaceae	57274,022	-0,643	0,259	-2,488	0,013	0,049

Table S3. Differentially abundant KEGG orthologous (KOs) groups according to bonferroni-corrected exact t-test for occurrence of KOs in differentially abundant contigs versus non differtaially abundant. Only KOs which occurred more often in the first two dilution points are shown here (all oddsratio > 1).

	counts	Total counts	annotation	pvalue	Odds ratio	Bonferroni-corrected pvalue
K01337	167	1216	ko:K01337 E3.4.21.50; lysyl endopeptidase [EC:3.4.21.50]	6,07E-45	3,98	6,95E-41
K21686	192	1563	ko:K21686 prpR; XRE family transcriptional regulator, fatty acid utilization regulator	3,21E-44	3,50	3,68E-40
K03088	2206	42449	ko:K03088 rpoE; RNA polymerase sigma-70 factor, ECF subfamily	5,13E-43	1,37	5,88E-39
K12132	676	10515	ko:K12132 prkC, stkP; eukaryotic-like serine/threonine-protein kinase [EC:2.7.11.1]	1,48E-36	1,72	1,69E-32
K07713	144	1261	ko:K07713 zraR, hydG; two-component system, NtrC family, response regulator HydG	2,85E-30	3,22	3,27E-26
K02456	282	3593	ko:K02456 gspG; general secretion pathway protein G	2,94E-28	2,13	3,37E-24
K03407	236	2818	ko:K03407 cheA; two-component system, chemotaxis family, sensor kinase CheA [EC:2.7.13.3]	1,09E-27	2,29	1,25E-23
K05499	190	2063	ko:K05499 cytR; LacI family transcriptional regulator, repressor for deo operon, udp, cdd, tsx, nupC, and nupG	2,22E-27	2,54	2,54E-23
K03932	217	2788	ko:K03932 lpqC; polyhydroxybutyrate depolymerase	9,71E-22	2,11	1,11E-17
K07114	516	8716	ko:K07114 yfbK; Ca-activated chloride channel homolog	5,34E-21	1,57	6,12E-17
K03559	248	3543	ko:K03559 exbD; biopolymer transport protein ExbD	9,60E-19	1,88	1,10E-14
K03301	83	746	ko:K03301 TC.AAA; ATP:ADP antiporter, AAA family	1,63E-17	3,13	1,87E-13
K03561	154	1938	ko:K03561 exbB; biopolymer transport protein ExbB	1,07E-16	2,16	1,22E-12
K20444	439	7595	ko:K20444 rfbC; O-antigen biosynthesis protein [EC:2.4.1.-]	1,77E-16	1,53	2,03E-12
K02669	174	2316	ko:K02669 pilT; twitching motility protein PilT	2,33E-16	2,03	2,67E-12
K10941	67	555	ko:K10941 fleQ, flrA; sigma-54 dependent transcriptional regulator, flagellar regulatory protein	3,42E-16	3,43	3,92E-12

K02078	226	3386	ko:K02078 acpP; acyl carrier protein	4,66E-15	1,79	5,34E-11
K04767	34	181	ko:K04767 acuB; acetoin utilization protein AcuB	2,09E-14	5,78	2,39E-10
K07011	308	5097	ko:K14652 ribBA; 3,4-dihydroxy 2-butanone 4-phosphate synthase / GTP cyclohydrolase II [EC:4.1.99.12 3.5.4.25]	2,69E-14	1,61	3,09E-10
K02065	188	2804	ko:K02065 mlaF, linL, mkl; phospholipid/cholesterol/gamma-HCH transport system ATP-binding protein	5,56E-13	1,80	6,37E-09
K20276	961	19857	ko:K20276 bapA; large repetitive protein	1,44E-12	1,27	1,65E-08
K03973	116	1494	ko:K03973 pspC; phage shock protein C	2,35E-12	2,10	2,69E-08
K07315	238	3872	ko:K07315 rsbU_P; phosphoserine phosphatase RsbU/P [EC:3.1.3.3]	3,94E-12	1,64	4,51E-08
K12982	57	525	ko:K12982 opsX; heptosyltransferase I [EC:2.4.-.-]	4,12E-12	3,04	4,72E-08
K03972	40	290	ko:K03972 pspE; phage shock protein E	4,20E-12	4,00	4,81E-08
K09697	128	1731	ko:K09697 natA; sodium transport system ATP-binding protein [EC:7.2.2.4]	5,04E-12	2,00	5,77E-08
K03594	265	4439	ko:K03594 bfr; bacterioferritin [EC:1.16.3.1]	5,28E-12	1,59	6,05E-08
K09691	172	2576	ko:K09691 ABC-2.LPSE.A; lipopolysaccharide transport system ATP-binding protein	7,03E-12	1,79	8,06E-08
K07322	63	624	ko:K07322 ytfE, scdA; regulator of cell morphogenesis and NO signaling	7,59E-12	2,81	8,70E-08
K06076	147	2104	ko:K06076 fadL; long-chain fatty acid transport protein	9,42E-12	1,88	1,08E-07
K12287	222	3603	ko:K12287 mshQ; MSHA biogenesis protein MshQ	1,60E-11	1,64	1,83E-07
K03413	263	4451	ko:K03413 cheY; two-component system, chemotaxis family, chemotaxis protein CheY	1,75E-11	1,57	2,01E-07
K02662	105	1351	ko:K02662 pilM; type IV pilus assembly protein PilM	2,30E-11	2,11	2,64E-07
K03744	176	2715	ko:K03744 lemA; LemA protein	4,14E-11	1,73	4,74E-07
K07714	99	1263	ko:K07714 atoC; two-component system, NtrC family, response regulator AtoC	5,22E-11	2,13	5,98E-07
K03768	280	4860	ko:K03768 PPIB, ppiB; peptidyl-prolyl cis-trans isomerase B (cyclophilin B) [EC:5.2.1.8]	5,37E-11	1,53	6,16E-07
K11894	27	160	ko:K11894 impI, vasC; type VI secretion system protein ImpI	1,22E-10	5,08	1,39E-06
K02003	416	7853	ko:K02003 ABC.CD.A; putative ABC transport system ATP-binding protein	1,36E-10	1,40	1,55E-06

K03924	357	6562	ko:K03924 moxR; MoxR-like ATPase [EC:3.6.3.-]	1,39E-10	1,44	1,59E-06
K01990	627	12607	ko:K01990 ABC-2.A; ABC-2 type transport system ATP-binding protein	1,64E-10	1,31	1,88E-06
K08084	119	1661	ko:K08084 fimT; type IV fimbrial biogenesis protein FimT	1,83E-10	1,93	2,09E-06
K09928	78	937	ko:K09928 K09928; uncharacterized protein	3,60E-10	2,27	4,13E-06
K03640	164	2555	ko:K03640 pal; peptidoglycan-associated lipoprotein	3,68E-10	1,71	4,22E-06
K03671	262	4607	ko:K03671 trxA; thioredoxin 1	7,06E-10	1,51	8,09E-06
K00702	23	129	ko:K00702 E2.4.1.20; cellobiose phosphorylase [EC:2.4.1.20]	9,10E-10	5,42	1,04E-05
K15876	26	163	ko:K15876 nrfH; cytochrome c nitrite reductase small subunit	9,36E-10	4,74	1,07E-05
K09696	67	780	ko:K09696 natB; sodium transport system permease protein	1,69E-09	2,35	1,93E-05
K02911	75	918	ko:K02911 RP-L32, MRPL32, rpmF; large subunit ribosomal protein L32	1,73E-09	2,22	1,99E-05
K02851	110	1557	ko:K02851 wecA, tagO, rfe; UDP-GlcNAc:undecaprenyl-phosphate/decaprenyl-phosphate GlcNAc-1-phosphate transferase [EC:2.7.8.33 2.7.8.35]	1,83E-09	1,90	2,09E-05
K06180	228	3940	ko:K06180 rluD; 23S rRNA pseudouridine1911/1915/1917 synthase [EC:5.4.99.23]	2,03E-09	1,54	2,33E-05
K09992	272	4887	ko:K09992 K09992; uncharacterized protein	2,50E-09	1,47	2,87E-05
K03086	197	3303	ko:K03086 rpoD; RNA polymerase primary sigma factor	2,55E-09	1,59	2,92E-05
K13668	60	673	ko:K13668 pimB; phosphatidyl-myo-inositol dimannoside synthase [EC:2.4.1.346]	2,91E-09	2,45	3,34E-05
K02477	213	3643	ko:K02477 K02477; two-component system, LytTR family, response regulator	2,96E-09	1,55	3,40E-05
K03564	216	3711	ko:K03564 BCP, PRXQ, DOT5; thioredoxin-dependent peroxiredoxin [EC:1.11.1.24]	3,31E-09	1,55	3,79E-05
K00368	129	1941	ko:K00368 nirK; nitrite reductase (NO-forming) [EC:1.7.2.1]	3,35E-09	1,78	3,84E-05
K01992	750	15731	ko:K01992 ABC-2.P; ABC-2 type transport system permease protein	3,75E-09	1,25	4,30E-05
K02916	64	747	ko:K02916 RP-L35, MRPL35, rpmI; large subunit ribosomal protein L35	4,21E-09	2,34	4,83E-05
K08976	96	1319	ko:K08976 K08976; putative membrane protein	4,38E-09	1,96	5,01E-05

K09690	122	1817	ko:K09690 ABC-2.LPSE.P; lipopolysaccharide transport system permease protein	4,89E-09	1,80	5,60E-05
K10914	344	6519	ko:K10914 crp; CRP/FNR family transcriptional regulator, cyclic AMP receptor protein	7,02E-09	1,39	8,04E-05
K07031	52	562	ko:K07031 hddA; D-glycero-alpha-D-manno-heptose-7-phosphate kinase [EC:2.7.1.168]	9,23E-09	2,55	1,06E-04
K20333	20	112	ko:K20333 toxD; toxoflavin biosynthesis protein ToxD	1,07E-08	5,43	1,23E-04
K03560	181	3040	ko:K03560 tolR; biopolymer transport protein TolR	1,21E-08	1,58	1,39E-04
K07027	127	1946	ko:K07027 K07027; glycosyltransferase 2 family protein	1,24E-08	1,75	1,42E-04
K03562	235	4183	ko:K03562 tolQ; biopolymer transport protein TolQ	1,34E-08	1,49	1,53E-04
K19302	373	7209	ko:K19302 bcrC; undecaprenyl-diphosphatase [EC:3.6.1.27]	1,38E-08	1,36	1,58E-04
K02282	300	5614	ko:K02282 cpaE, tadZ; pilus assembly protein CpaE	1,93E-08	1,41	2,22E-04
K02650	137	2164	ko:K02650 pilA; type IV pilus assembly protein PilA	2,10E-08	1,69	2,41E-04
K10909	31	255	ko:K10909 luxQ; two-component system, autoinducer 2 sensor kinase/phosphatase LuxQ [EC:2.7.13.3 3.1.3.-]	2,11E-08	3,46	2,41E-04
K01399	6	7	ko:K01399 lasB; pseudolysin [EC:3.4.24.26]	2,19E-08	150,00	2,51E-04
K19411	43	433	ko:K19411 mcsA; protein arginine kinase activator	2,25E-08	2,76	2,58E-04
K05808	92	1290	ko:K05808 yhbH; putative sigma-54 modulation protein	2,31E-08	1,92	2,64E-04
K02655	117	1772	ko:K02655 pilE; type IV pilus assembly protein PilE	2,41E-08	1,77	2,76E-04
K03935	18	96	ko:K03935 NDUFS2; NADH dehydrogenase (ubiquinone) Fe-S protein 2 [EC:7.1.1.2]	2,60E-08	5,77	2,98E-04
K03183	185	3159	ko:K03183 ubiE; demethylmenaquinone methyltransferase / 2-methoxy-6-polyprenyl-1,4-benzoquinol methylase [EC:2.1.1.163 2.1.1.201]	2,67E-08	1,56	3,07E-04
K03272	92	1299	ko:K03272 gmhC, hldE, waaE, rfaE; D-beta-D-heptose 7-phosphate kinase / D-beta-D-heptose 1-phosphate adenosyltransferase [EC:2.7.1.167 2.7.7.70]	3,17E-08	1,91	3,63E-04

K20628	48	522	ko:K20628 exlX; expansin	4,01E-08	2,53	4,59E-04
K02485	45	476	ko:K02485 rssB, hnr; two-component system, response regulator	4,65E-08	2,61	5,33E-04
K03624	126	1974	ko:K03624 greA; transcription elongation factor GreA	4,77E-08	1,70	5,47E-04
K20534	132	2095	ko:K20534 gtrB, csbB; polyisoprenyl-phosphate glycosyltransferase [EC:2.4.-.-]	4,87E-08	1,68	5,58E-04
K00428	165	2772	ko:K00428 E1.11.1.5; cytochrome c peroxidase [EC:1.11.1.5]	5,16E-08	1,58	5,91E-04
K16291	62	765	ko:K16291 erfK; L,D-transpeptidase ErfK/SrfK	5,45E-08	2,20	6,24E-04
K20543	136	2189	ko:K20543 bcsC; cellulose synthase operon protein C	6,87E-08	1,66	7,87E-04
K02887	74	990	ko:K02887 RP-L20, MRPL20, rplT; large subunit ribosomal protein L20	8,29E-08	2,02	9,50E-04
K02437	120	1876	ko:K02437 gcvH, GCSH; glycine cleavage system H protein	8,68E-08	1,71	9,95E-04
K04749	73	975	ko:K04749 rsbV; anti-sigma B factor antagonist	9,45E-08	2,02	1,08E-03
K03179	96	1408	ko:K03179 ubiA; 4-hydroxybenzoate polyprenyltransferase [EC:2.5.1.39]	9,52E-08	1,83	1,09E-03
K01218	155	2593	ko:K01218 gmuG; mannan endo-1,4-beta-mannosidase [EC:3.2.1.78]	9,83E-08	1,59	1,13E-03
K15518	33	303	ko:K15518 dgk; deoxyguanosine kinase [EC:2.7.1.113]	1,08E-07	3,06	1,24E-03
K03060	76	1037	ko:K03060 rpoZ; DNA-directed RNA polymerase subunit omega [EC:2.7.7.6]	1,23E-07	1,98	1,41E-03
K22489	15	74	ko:K22489 hosA; MarR family transcriptional regulator, temperature-dependent positive regulator of motility	1,26E-07	6,36	1,44E-03
K07814	120	1896	ko:K07814 K07814; putative two-component system response regulator	1,50E-07	1,69	1,72E-03
K22391	112	1737	ko:K22391 E3.5.4.16; GTP cyclohydrolase I [EC:3.5.4.16]	1,53E-07	1,72	1,75E-03
K00809	59	736	ko:K00809 DHPS, dys; deoxyhypusine synthase [EC:2.5.1.46]	1,61E-07	2,18	1,85E-03
K00940	97	1445	ko:K00940 ndk, NME; nucleoside-diphosphate kinase [EC:2.7.4.6]	1,66E-07	1,80	1,91E-03
K19668	77	1065	ko:K19668 CBH2, cbhA; cellulose 1,4-beta-cellobiosidase [EC:3.2.1.91]	1,74E-07	1,95	2,00E-03
K13628	63	810	ko:K13628 iscA; iron-sulfur cluster assembly protein	1,84E-07	2,11	2,10E-03
K12506	103	1566	ko:K12506 ispDF; 2-C-methyl-D-erythritol 4-phosphate cytidylyltransferase / 2-C-methyl-D-erythritol 2,4-cyclodiphosphate synthase [EC:2.7.7.60 4.6.1.12]	1,86E-07	1,76	2,14E-03

K02663	67	884	ko:K02663 pilN; type IV pilus assembly protein PilN	1,98E-07	2,05	2,27E-03
K06377	18	110	ko:K06377 spo0M; sporulation-control protein	2,27E-07	4,89	2,60E-03
K06881	59	751	ko:K06881 nrnA; bifunctional oligoribonuclease and PAP phosphatase NrnA [EC:3.1.3.7 3.1.13.3]	3,15E-07	2,13	3,61E-03
K02666	122	1966	ko:K02666 pilQ; type IV pilus assembly protein PilQ	3,26E-07	1,65	3,74E-03
K03271	62	806	ko:K03271 gmhA, lpcA; D-sedoheptulose 7-phosphate isomerase [EC:5.3.1.28]	3,32E-07	2,08	3,80E-03
K07003	242	4518	ko:K07003 K07003; uncharacterized protein	3,41E-07	1,41	3,91E-03
K03530	113	1788	ko:K03530 hupB; DNA-binding protein HU-beta	3,59E-07	1,69	4,11E-03
K03832	506	10514	ko:K03832 tonB; periplasmic protein TonB	3,81E-07	1,26	4,37E-03
K06142	120	1935	ko:K06142 hlpA, ompH; outer membrane protein	4,16E-07	1,65	4,77E-03
K12984	91	1360	ko:K12984 waaE, kdtX; (heptosyl)LPS beta-1,4-glucosyltransferase [EC:2.4.1.-]	4,45E-07	1,79	5,10E-03
K18285	63	835	ko:K18285 mqnE; aminodeoxyfutalosine synthase [EC:2.5.1.120]	5,19E-07	2,04	5,95E-03
K01179	488	10130	ko:K01179 E3.2.1.4; endoglucanase [EC:3.2.1.4]	5,41E-07	1,27	6,20E-03
K08481	58	747	ko:K08481 kaiB; circadian clock protein KaiB	5,74E-07	2,10	6,58E-03
K02914	52	641	ko:K02914 RP-L34, MRPL34, rpmH; large subunit ribosomal protein L34	5,84E-07	2,21	6,69E-03
K21147	156	2697	ko:K21147 moeZR, moeBR; sulfur-carrier protein adenylyltransferase/sulfurtransferase [EC:2.7.7.80 2.7.7.- 2.8.1.11 2.8.1.-]	6,13E-07	1,53	7,02E-03
K05337	96	1475	ko:K05337 fer; ferredoxin	7,38E-07	1,74	8,45E-03
K20074	241	4547	ko:K20074 prpC, phpP; PPM family protein phosphatase [EC:3.1.3.16]	7,73E-07	1,40	8,85E-03
K02237	134	2249	ko:K02237 comEA; competence protein ComEA	7,95E-07	1,58	9,12E-03
K02356	105	1657	ko:K02356 efp; elongation factor P	7,96E-07	1,69	9,13E-03
K10947	88	1323	ko:K10947 padR; PadR family transcriptional regulator, regulatory protein PadR	8,62E-07	1,78	9,88E-03
K12686	80	1169	ko:K12686 apeE, estA, lip-1; outer membrane lipase/esterase	8,93E-07	1,84	1,02E-02
K02612	126	2090	ko:K02612 paaD; ring-1,2-phenylacetyl-CoA epoxidase subunit PaaD	9,22E-07	1,60	1,06E-02

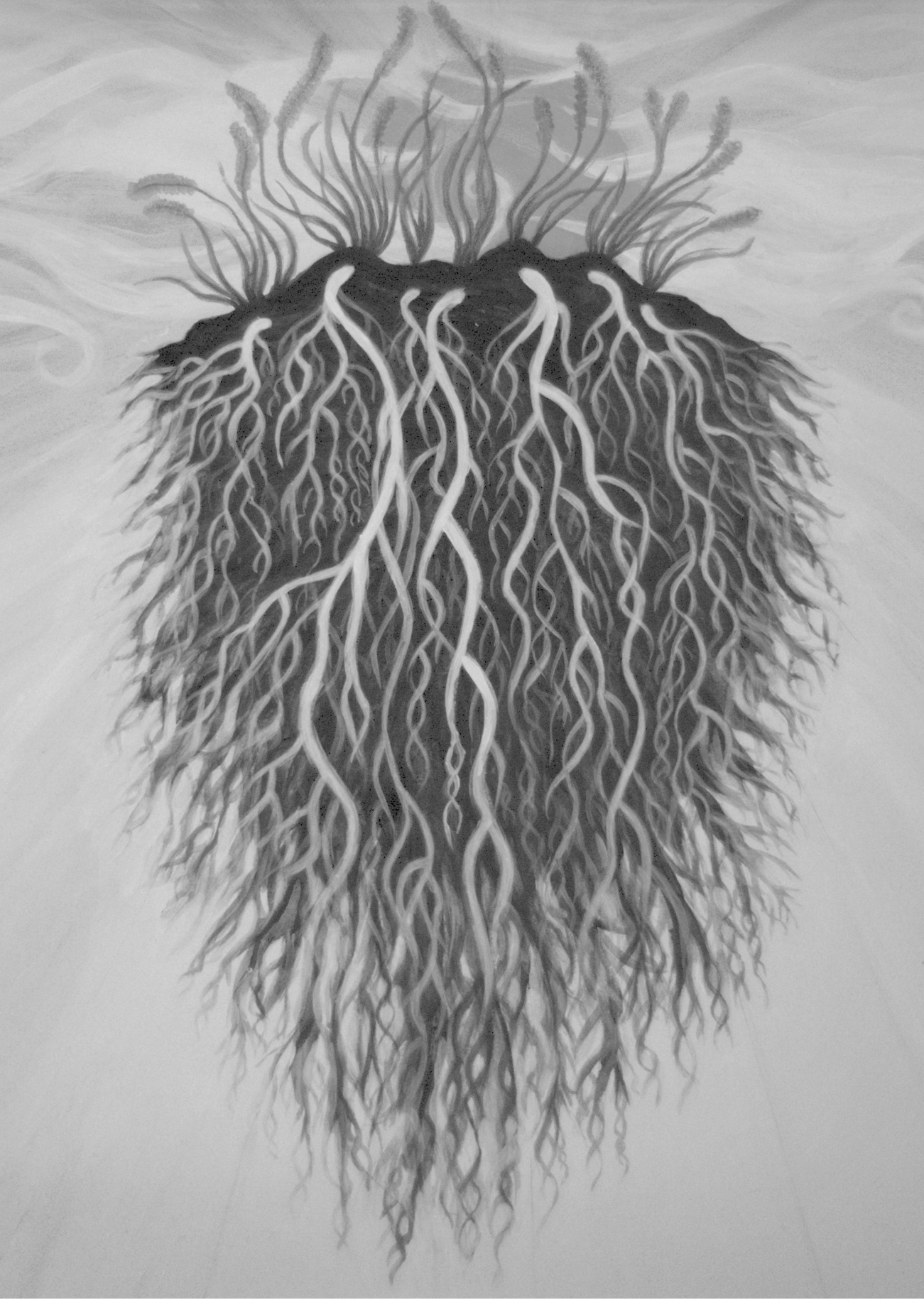
K01512	76	1096	ko:K01512 acyP; acylphosphatase [EC:3.6.1.7]	1,01E-06	1,86	1,16E-02
K13658	19	134	ko:K13658 gumI; beta-1,4-mannosyltransferase [EC:2.4.1.251]	1,04E-06	4,13	1,19E-02
K02110	73	1041	ko:K02110 ATPF0C, atpE; F-type H+-transporting ATPase subunit c	1,08E-06	1,89	1,24E-02
K01953	245	4661	ko:K01953 asnB, ASNS; asparagine synthase (glutamine-hydrolysing) [EC:6.3.5.4]	1,15E-06	1,39	1,32E-02
K01183	155	2710	ko:K01183 E3.2.1.14; chitinase [EC:3.2.1.14]	1,24E-06	1,52	1,42E-02
K08998	142	2437	ko:K08998 K08998; uncharacterized protein	1,27E-06	1,55	1,46E-02
K19342	35	370	ko:K19342 nosL; copper chaperone NosL	1,32E-06	2,61	1,51E-02
K02884	79	1166	ko:K02884 RP-L19, MRPL19, rplS; large subunit ribosomal protein L19	1,51E-06	1,82	1,73E-02
K07778	50	628	ko:K07778 desK; two-component system, NarL family, sensor histidine kinase DesK [EC:2.7.13.3]	1,61E-06	2,16	1,85E-02
K09121	39	439	ko:K09121 larC; pyridinium-3,5-bisthiocarboxylic acid mononucleotide nickel chelatase [EC:4.99.1.12]	1,63E-06	2,44	1,86E-02
K13573	41	473	ko:K13573 pafC; proteasome accessory factor C	1,67E-06	2,37	1,91E-02
K02847	74	1073	ko:K02847 waaL, rfaL; O-antigen ligase [EC:2.4.1.-]	1,68E-06	1,85	1,93E-02
K02653	198	3652	ko:K02653 pilC; type IV pilus assembly protein PilC	1,70E-06	1,43	1,95E-02
K02909	77	1133	ko:K02909 RP-L31, rpmE; large subunit ribosomal protein L31	1,81E-06	1,82	2,08E-02
K07107	291	5737	ko:K07107 ybgC; acyl-CoA thioester hydrolase [EC:3.1.2.-]	2,24E-06	1,34	2,57E-02
K04078	92	1437	ko:K04078 groES, HSPE1; chaperonin GroES	2,39E-06	1,71	2,74E-02
K02066	238	4558	ko:K02066 mlaE, linK; phospholipid/cholesterol/gamma-HCH transport system permease protein	2,54E-06	1,38	2,91E-02
K12340	198	3678	ko:K12340 tolC; outer membrane protein	2,64E-06	1,42	3,03E-02
K18431	54	712	ko:K18431 legF, ptmB; CMP-N,N'-diacetyllegionaminic acid synthase [EC:2.7.7.82]	2,73E-06	2,05	3,12E-02
K20468	26	243	ko:K20468 K20468; putative heme transporter	3,14E-06	3,00	3,60E-02
K03298	41	486	ko:K03298 TC.DME; drug/metabolite transporter, DME family	3,27E-06	2,30	3,75E-02

K07220	92	1449	ko:K07220 K07220; uncharacterized protein	3,33E-06	1,69	3,82E-02
K03116	63	890	ko:K03116 tatA; sec-independent protein translocase protein TatA	4,15E-06	1,90	4,75E-02
K05988	34	373	ko:K05988 dexA; dextranase [EC:3.2.1.11]	4,16E-06	2,51	4,77E-02
K22205	49	632	ko:K22205 K22205; S-adenosyl-L-methionine hydrolase (adenosine-forming) [EC:3.13.1.8]	4,21E-06	2,10	4,82E-02
K04760	66	948	ko:K04760 greB; transcription elongation factor GreB	4,30E-06	1,87	4,93E-02

Table S4. AntiSMASH-predicted occurrences of biosynthetic gene clusters (separated by gene cluster product class according to antiSMASH output) in differentially abundant contigs (more abundant in the suppressive dilutions 25X and 50X) versus the rest of the assembly. Statistical results are based on Fisher exact test, significant results are highlighted in bold.

BGC product	Counts on DE contigs	Counts on NOT DE contigs	ODDS Ratio	P-value
arylpolyene	65	373	1,5145	0,0056
melanin	2	2	inf	0,0150
acyl amino acids	10	157	0,4882	0,0240
ladderane	6	20	3,0757	0,0289
T3PKS	43	260	1,4221	0,0523
NRPS-like	44	278	1,3494	0,0905
betalactone	16	86	1,6404	0,0950
NRPS	69	690	0,7974	0,0988
other	4	15	2,6097	0,1021
T1PKS	18	213	0,6625	0,1055
T2PKS	1	1	inf	0,1225
NAGGN	0	18	0,0000	0,1546
resorcinol	11	59	1,6446	0,1586
proteusin	1	2	7,1766	0,2300
lanthipeptide	4	60	0,5126	0,2343
hglE-KS	7	40	1,5223	0,3282
TfuA-related	3	46	0,5007	0,3610
linaridin	0	11	0,0000	0,3802
phosphonate	6	37	1,3890	0,4478
lassopeptide	15	150	0,7974	0,5238

LAP	2	29	0,5316	0,5699
hserlactone	21	196	0,8612	0,5775
transAT-PKS	0	8	0,0000	0,6070
ectoine	3	38	0,6151	0,6170
butyrolactone	2	14	1,1961	0,6859
bacteriocin	62	486	1,0494	0,7153
indole	3	32	0,7424	0,7907
siderophore	10	89	0,9084	0,8712
terpene	73	605	0,9848	0,9471
CDPS	0	5	0,0000	1,0000
PKS-like	0	7	0,0000	1,0000
transAT-PKS-like	3	30	0,7974	1,0000
amglyccycl	0	4	0,0000	1,0000
microviridin	0	6	0,0000	1,0000
furan	0	2	0,0000	1,0000
thiopeptide	0	5	0,0000	1,0000
cyanobactin	0	3	0,0000	1,0000
phenazine	0	2	0,0000	1,0000
nucleoside	0	1	0,0000	1,0000
oligosaccharide	0	1	0,0000	1,0000
PpyS-KS	0	2	0,0000	1,0000



Chapter 5

Impact of plastic mulch film residues on soil microbiome, disease suppressiveness, and plant growth

Yueling Qi [a, b, *, 1] Adam Ossowicki [b, 1], Étienne Yergeau [c], Gianpiero Vigani [d], Violette Geissen [a], Paolina Garbeva [b]

[a] Soil Physics and Land Management Group, Wageningen University & Research, P.O. Box 47, 6700AA Wageningen, The Netherlands

[b] Department of Microbial Ecology, Netherlands Institute of Ecology (NIOO-KNAW), 6700 AB Wageningen, The Netherlands

[c] Centre Armand-Frappier Santé Biotechnologie, Institut national de la recherche scientifique, Laval, QC, Canada

[d] University of Turin, Plant Physiology Unit, Department of Life Sciences and Systems Biology, 10135 Turin, Italy

[1] These authors contributed equally to this work.

Modified version was submitted for publication

Abstract

Plastic mulch film residues have been accumulating in agricultural soils for decades, but so far, little is known about its consequences on soil microbial communities and functions. Here, we tested the effects of plastic residues of low-density polyethylene and biodegradable mulch films on soil suppressiveness and microbial community. Soil suppressiveness is a microbial-driven phenomenon important for sustainable agriculture. The level of soil suppressiveness, plant biomass and nutrient status and microbial communities in rhizosphere and plastisphere were investigated using a controlled pot experiment in soil suppressive to *Fusarium culmorum*. The addition of 1% plastic residues to the suppressive soil did not affect the level of suppressions and the disease symptoms index. However, we did find that plant biomasses decreased, and that plant nutrient status changed in the presence of plastic residues. We did not observe significant changes in bacterial and fungal rhizosphere communities. Nonetheless, bacterial and fungal communities closely attached to the plastisphere were very different from the rhizosphere communities. The plastisphere revealed a high abundance of specific bacterial phyla (Actinobacteria, Bacteroidetes, and Proteobacteria) and fungal genera (*Rhizoctonia* and *Arthrobotrys*). Our work revealed new insights and raises emerging questions for further studies on the impact of microplastics on the agroecosystems.

Introduction

Soil plays a central role in supporting life and possess the highest microbial diversity known to date. Microbial communities are essential for promoting plant growth and suppressing soil-borne diseases (Cha et al., 2016; Lugtenberg et al., 2017). Plants are exposed to various abiotic and biotic stresses throughout their lives, yet certain soil microbes can help plants to overcome different stresses and improve growth (Gouda et al., 2018; Ilangumaran and Smith, 2017; Jochum et al., 2019).

Along with the abiotic and biotic stresses that can occur sequentially or simultaneously, plants also are challenged by anthropogenic soil pollution. Environmental pollution in soil caused by agrochemicals or the disposal of waste coming from industrial or urban sources may interfere with plant-microbe interactions and communication. One critical type of pollution emerging in agriculture is the increasing load of microplastics (defined as plastic particles < 5 mm) (de Souza Machado et al., 2018). Although, the effect of microplastics on the aquatic ecosystems have been intensively studied, their environmental impacts on the terrestrial ecosystem remain largely unexplored. According to recent literature, agricultural land may store more microplastics than oceans (Nizzetto et al., 2016b, 2016a), likely because there are multiple ways for microplastics to get into the soil (Ng et al., 2018). Plastic mulching is one of the primary sources contributing to the accumulation of microplastics in agroecosystems (Huang et al., 2020).

Plastic mulch films were applied to farmland for several purposes: retaining soil moisture, warming the soil and preventing weeds (Steinmetz et al., 2016). Unfortunately, it is not technically feasible for farmers to remove or recycle most of the mulch films used in the fields because the films are usually very thin (0.01-0.05 mm) (Kasirajan and Ngouajio, 2012). The accumulation of residual plastic mulch films in agricultural soils has raised concerns because it decreases soil productivity by blocking water infiltration, impeding soil gas exchange, and constraining root growth (Hegan et al., 2015; Jiang et al., 2017; Qi et al., 2020a). Plastic pollution is considered to be an emerging threat to soil ecosystem health and function (Dan Zhang et al., 2020). Biodegradable plastics were developed as promising environmentally sustainable alternatives to conventional low-density polyethylene films (Kasirajan and Ngouajio, 2012; Sintim and Flury, 2017). Biodegradable plastics are tilled into the soil where they are expected to be degraded by microbes. However, their impact on i) soil and rhizosphere microbiome, ii) the interactions between beneficial microbes and soil-borne pathogens and iii) the level of soil disease suppressiveness are largely unknown.

Disease suppressive soils protect plants from root pathogens despite the presence of favourable conditions for disease development (Deacon, 1984). Enhancing soil suppressiveness is of great agronomic interest to achieve sustainable management for plant disease control (Ghorbani et al., 2009; Singh and Vyas, 2009). Many previous studies investigated the link between soil disease suppressiveness and the soil microbiome and such findings have been summarized in several review articles (Kinkel et al., 2011; Schlatter et al., 2017b; Weller et al., 2002b). For instance, the presence of some microbial taxa in soil were associated to the development of soil suppressiveness (Gomes Exposito et al., 2017) and the disturbance in microbiome composition lead to losing the ability of microbiome to protect plants (Carrión et al., 2019; Cha et al., 2016).

Recently, we revealed that microplastics could have strong effects on plant growth, the blend of volatiles emitted in the rhizosphere, and the assembly of the rhizosphere communities (Qi et al., 2020b).

The aim of the present study was to understand the impact of microplastic pollution on the level of soil disease suppressiveness, plant growth and nutrient status and on microbial community. Recently, Ossowicki et al. (2020) screened soils from 28 different sites in the Netherlands and Germany for their level of suppressiveness to *Fusarium culmorum*. The microbiological basis of the suppressiveness were characterised in four different field-soils displaying clear and reproducible disease suppressiveness (Ossowicki et al., 2020). In this work, we therefore, tested the effect of plastic residues on i) the level of soil disease suppressiveness (using previously characterized suppressive soil), ii) rhizosphere microbial communities composition and iii) plant growth. Besides, we analysed the microbiome of the so-called plastisphere, which may host a distinct microbial colony on the plastic debris.

Materials and Methods

Growth conditions and materials

A pot experiment was conducted in a growth cabinet (MC 1750 VHO-EVD, Snijders Labs) with photoperiod of 12 h day/12 h night at 20°C and 60% relative humidity. Plants were watered every two days and supplemented weekly with a 0.5 Hoagland solution (1 ml per 80 cc of the soil, 0.5 M $Ca(NO_3)_2 \cdot 4H_2O$, 1 M KNO_3, 1M KH_2PO_4, 0.5 M $MgSO_4 \cdot 7H_2O$ and 98.6 mM ferric EDTA).

The disease-suppressive soil (S11) used in this study was found to be highly suppressive against *F. culmorum* in wheat (Ossowicki et al., 2020). Soil was collected in agricultural field, air-dried at room temperature, homogenized, sieved through a 4 mm sieve, and stored at 4°C. The soil was sandy with an organic matter content of 3.48 ± 0.47% and a pH of 7.28 ± 0.19. We used a gamma-sterilized sand collected near Bergharen, the Netherlands as a standard substrate. More information about the suppressive soil and Bergharen sand is provided in Table S1. Wheat seeds (*Triticum aestivum,* JB Asano variety) were obtained from Agrifirm (the Netherlands). Seeds were surface sterilized and pregerminated on sterile moist filter paper in order to use in the experiment.

Two types of plastic mulch films (PMF) were used in this study: a low-density polyethylene (LDPE) and a starch-based biodegradable plastic (Bio). Two sizes of plastic residues (macro and micro) were prepared as described in a previous study (Qi et al., 2018). Macro-sized plastic pieces were made by cutting PMF into 5 mm × 5 mm squares by hand. The micro-sized powders were obtained through cryogenic grinding, then sieved to obtain a powder size ranging from 50 µm to 1 mm. All plastic materials were sprayed with 70% ethanol and air-dried in a fume cupboard to minimize microbial contamination.

The fungal pathogen *F. culmorum* PV was propagated on 1/4 potato dextrose agar (PDA) and incubated at 20 ºC for two weeks. Plugs with a diameter of 6 mm were cut from the border zone of *F. culmorum* hyphae. One plug was mixed with 10 cc of soil for treatments and, in controls without the pathogen, sterile 1/4 PDA plugs were used instead.

Experimental setup

Prior to the experiment, the soil was “activated” to induce microbial activity by growing wheat for two weeks. Afterwards, plants along with the whole root system were removed and the soil was mixed and prepared as follows. The suppressive soil was mixed 2:1:1 in volume with sterile Bergharen sand and sterile vermiculite (Agra-vermiculite, the Netherlands). Sterile Bergharen sand was mixed with vermiculite 3:1 in volume for negative controls. For each pot, 140 g of the soil mixture, 1.4 g of the plastic residues (except for the controls) and plugs with or without the pathogen were added to pots and manually mixed. One pre-germinated wheat seed was transferred into each pot and grew for three weeks. After this time, disease symptoms were assessed, and rhizosphere samples collected.

Treatments and replicates

Four types of plastic residues were mixed separately with suppressive soil at 1% (w/w). This concentration is environmentally relevant and consistent with our previous studies (Qi *et al.*, 2018). Two positive controls with only suppressive soil and without the addition of plastic residues were used to control for disease suppressiveness (S11_FC and S11_NF). Two negative controls with sterilized Bergharen sand were used to control for the pathogenicity of *F. culmorum* (BS_FC and BS_NF). Eight treatments were tested with 10 replicates in fully randomized design (Table 1).

Table 1 The pot experiment treatments.

Treatment	Plastic residues	*F. culmorum*	Soil
LDPE_Ma	LDPE macro	✓	S11 (Suppressive soil)
LDPE_Mi	LDPE micro	✓	S11 (Suppressive soil)
Bio_Ma	Bio macro	✓	S11 (Suppressive soil)
Bio_Mi	Bio micro	✓	S11 (Suppressive soil)
S11_FC	/	✓	S11 (Suppressive soil)
S11_NF	/	/	S11 (Suppressive soil)
BS_FC	/	✓	Bergharen sand
BS_NF	/	/	Bergharen sand

Disease symptoms assessment and analysis of plant biomass and plant nutrient status

To assess the disease symptoms, the wheat plants were carefully removed, the excess of soil was shaken off, and the roots were cleaned with water. The root system was visually inspected for brown/black lesions or rotting and the stem base/coleoptile was inspected for rotting and the presence of pink-white fungal hyphae. Plants were scored from 0-5 for disease symptoms (Ossowicki et al., 2020). Statistical differences in disease symptoms between treatments and controls were assessed using the chi-square test, with an alpha cutoff of $p < 0.05$.

After the screening, plants were separated into shoots and roots. Dry biomass was recorded after drying at 70 ºC for 48 h. Dried shoot and root tissues were then digested using 65% HNO_3 at 120 ºC. The mineralized samples were transferred into polypropylene test tubes. Samples were diluted 1:40 in MILLI-Q water and the concentration of metal elements was measured by Inductively Coupled Plasma-Mass Spectrometry ICP-MS (BRUKER Aurora- M90 ICP-MS) as previously described (Vigani *et al.*, 2017, Martín-Sánchez *et al.*, 2020). Differences among the mean values of inter-groups were analysed by one-way ANOVA and the post-hoc tests considered were: Tukey HSD (in the case of Levene's test $p > 0.05$) and Tamhane (in the case of Levene's test $p < 0.05$).

DNA extraction for rhizosphere soil and plastisphere

For six randomly selected replicates in each treatment, rhizosphere soil samples were collected. After the plants were taken out of the pots, the excess soil was removed and the root system with adhering soil was placed in a sterile paper bag. Soil particles (rhizosphere) were detached from the roots by rigorously shaking. Rhizosphere soil samples were stored at -4 ºC and the DNA was isolated using a DNeasy PowerSoil Kit (QIAGEN, the Netherlands) within one week.

Six to ten pieces of macroplastics were collected from each pot of treatments LDPE_Ma and Bio_Ma. The plastic pieces were stored in Eppendorf tubes in glycerol stock at -80 ºC before DNA extraction. DNeasy PowerSoil Kit was used to extract the DNA from plastic pieces.

Amplicon sequencing and microbial community analysis

The amplicon library preparation and sequencing was carried out at the McGill University and Genome Québec Innovation Centre (Montréal, Canada). The PCRs of the bacterial 16S rRNA gene V3-V4 region were performed with the primer set 515F (5'-GTGCCAGCMGCCGCGGTAA-3') and 806R (5'-GGACTACHVGGGTWTCTAAT-3'). The PCRs of the fungal rDNA gene ITS region was performed with the primer set ITS1F (5'-CTTGGTCATTTAGAGGAAGTAA-3') and 58A2R (5'-CTGCGTTCTTCATCGAT-3'). Sequencing was carried out on an Illumina MiSeq platform with 4 biological replicates per treatment).

Adapter sequences were removed using cutadapt 2.10 (Martin, 2011) and the quality of reads was evaluated using FastQC 0.11.9 (Andrews, 2015). All the subsequent work on sequencing data was performed in an R (v 4.0.1) environment using packages specified further. Amplicon sequencing variants (ASVs) were constructed using dada2 1.16.0 (Benjamin J Callahan et al., 2016, p. 2) and taxonomically classified based on the SILVA v132 database for bacterial 16S genes or the UNITE v8 database for fungal ITS sequences. Read counts were rarefied for further analysis using a Vegan 2.5-6 package. Analyses of alpha diversity and differential abundance were performed using phyloseq 1.32.0 and DESeq2 1.28.1 packages and visualized using Ampvis2 2.6.0 and ggplot2 3.3.2. The differences in Shannon indexes were assessed using one-way ANOVA, $p < 0.05$.

Results

Effect of plastic residues on the level of disease suppressiveness, plant biomass and plant nutrient status

A significant effect on plant biomass was observed only for shoot biomass in the treatment Bio_Mi as compared to controls without plastic additions (Fig. 1). No significant difference in root biomass was observed.

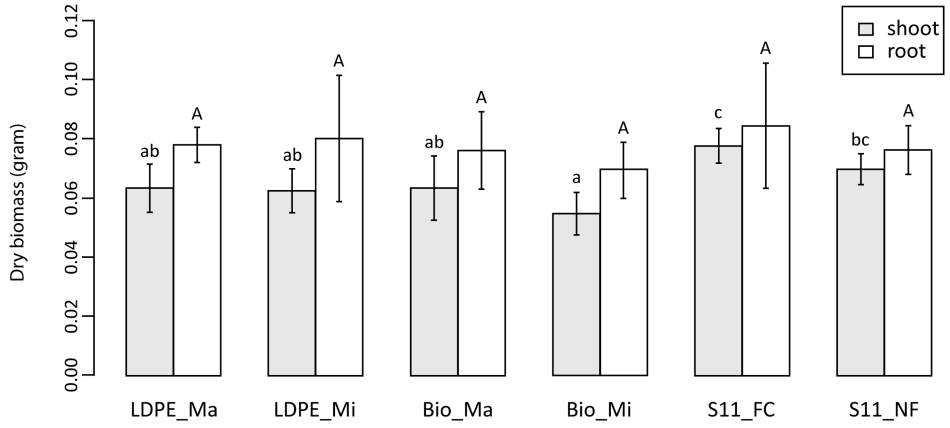


Fig. 1. Shoot and root biomass of wheat in suppressive soil with and without plastic residues. The bars indicate the mean values of each treatment, with the error bars representing the standard deviation. Letters above the bars represent statistically significant differences based on ANOVA, $p < 0.05$.

The results of testing the impact of plastic residues on soil suppressiveness are presented in Fig. 2. It showed that the pathogen was infectious when comparing controls BS_FC to BS_NF and that the soil S11 was suppressive and could significantly reduce disease symptoms (controls BS_FC vs. S11_FC). The presence of plastic residues in suppressive soil did not significantly affect the level of suppressiveness (Fig. 2).

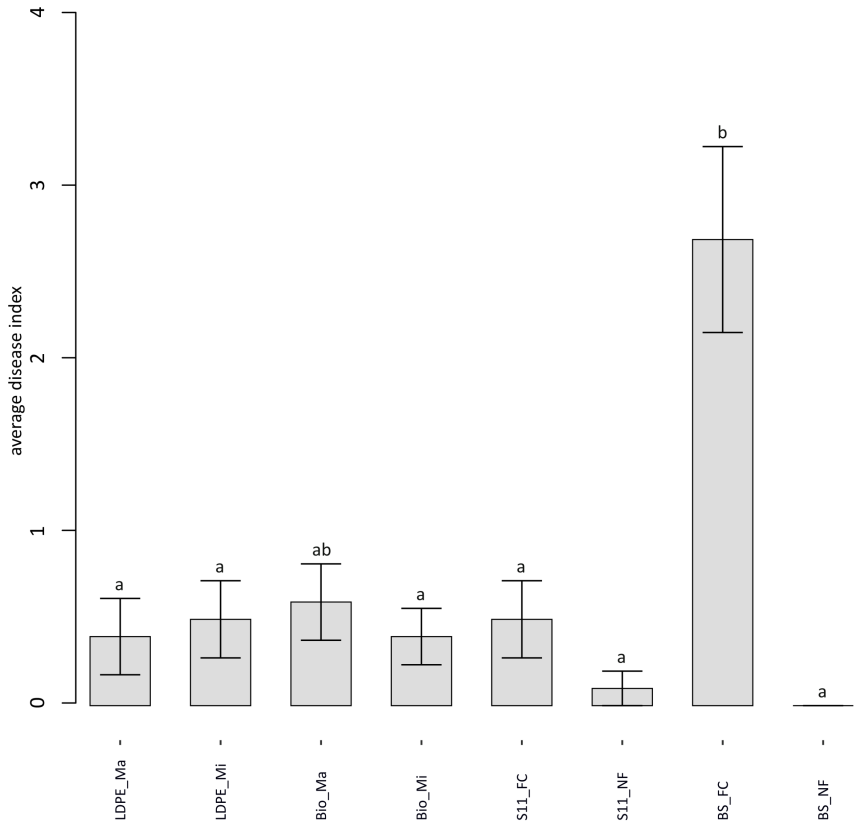


Fig. 2. Disease symptoms observed in wheat inoculated with F. culmorum grown in substrates with plastic and without plastic as controls. The bars indicate the average of the disease symptoms index, with the error bars representing the standard error. Letters above the bars represent significance levels based on the chi-square test.

In addition, we performed an analysis of the mineral nutrient content of shoots and roots, defined as plant ionome. The Principal Component Analysis (PCA) performed on the macronutrient (Mg, K, Ca) content of the shoots revealed a clear separation between LDPE_Ma and LDPE_Mi (Fig. 3a). The PCA performed on the micronutrient (Mn, Fe, Zn, Mo, Cu) content of the shoots revealed separation between LDPE_Ma and LDPE_Mi samples (Fig. 3b). In the shoots, we observed a significant difference in K content between treatments LDPE_Ma and LDPE_Mi and the Mn contents of both treatments were higher than the controls (Table S2). The PCA revealed different macro- and micro- nutrient composition in the roots of the treatment LDPE_Mi (Fig. 3c and 3d). Treatment LDPE_Mi showed higher Cu content in root tissues (Table S3).

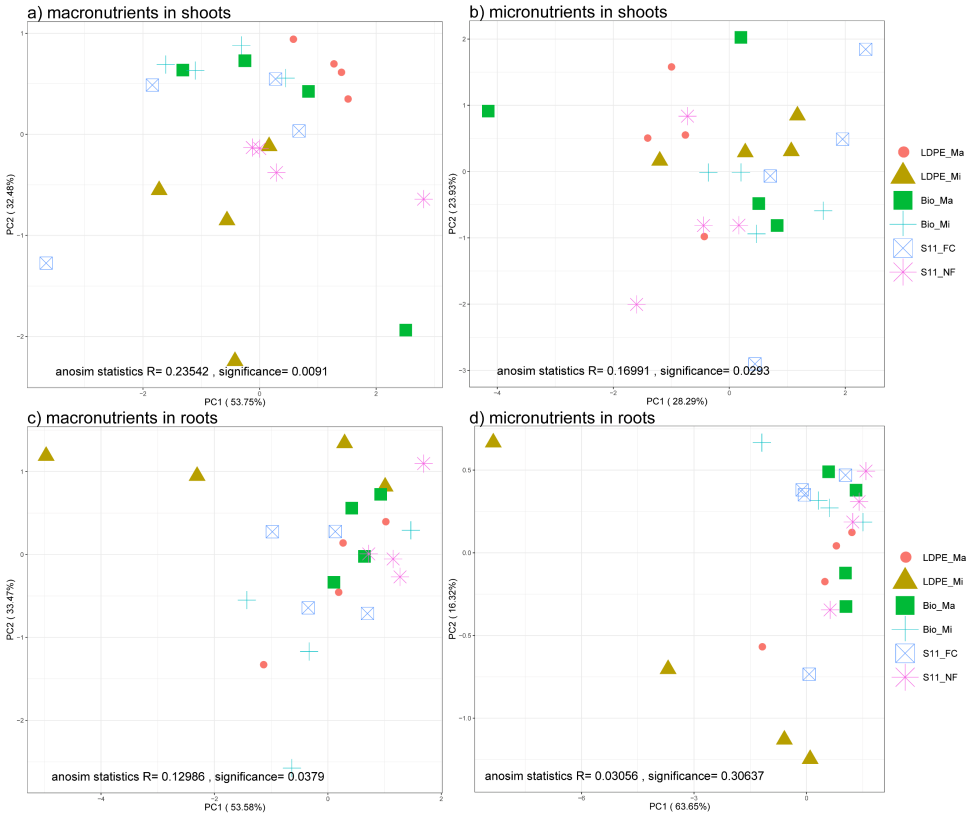


Fig. 3 Principal component analysis (PCA) of the macronutrient and micronutrient content in shoots and roots of wheat. ANOSIM statistics is indicated in the left-bottom corner of each plot.

Effect of plastic residues on the rhizosphere bacterial and fungal communities

The analysis of bacterial and fungal rhizosphere communities was based on 16S rRNA and ITS amplicons sequencing. The effect of the addition of the plastic residues may be seen as a change between treatments (LDPE_Ma, LDPE_Mi, Bio_Ma, Bio_Mi) and control S11_FC – all with pathogenic fungus added.

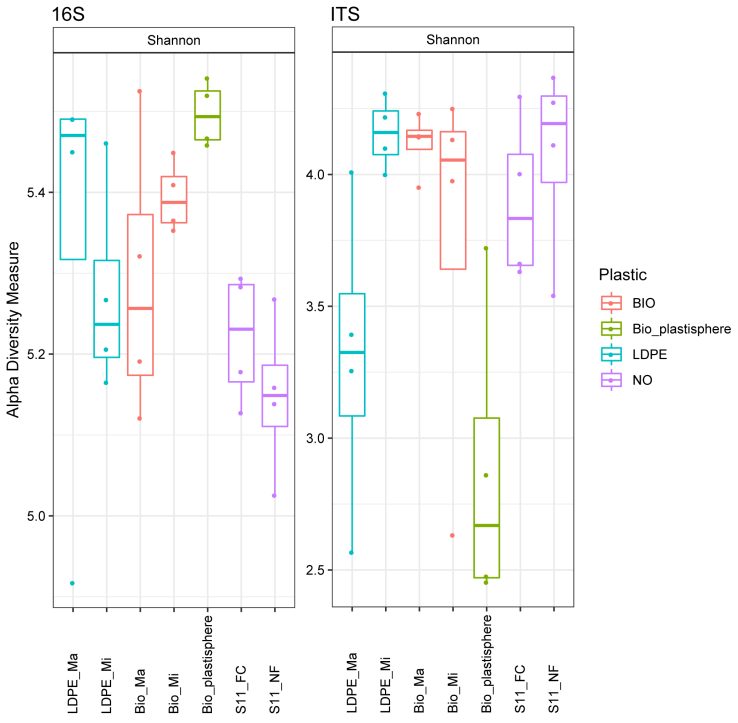


Fig. 4. Alpha diversity of bacterial (16S) and fungal (ITS) communities based on ASVs presented as Shannon index.

The diversity of bacterial and fungal community based on Shannon index revealed that, as compared to control (S11_FC), there was no statistically significant change due to the addition of plastic (Fig. 4, Table S4 and S5). Moreover, looking at the abundance of the major bacteria phyla and fungal genera (Fig.5 and 6 respectively), there was only a small significant change in the abundance *Chloroflexi* between LDPE_Ma treatment and control. Altogether, the addition of LDPE and Bio plastic residues to soil did not have a direct impact on bacterial and fungal rhizosphere community. These results are also supported by PCA analysis (Fig. S1).

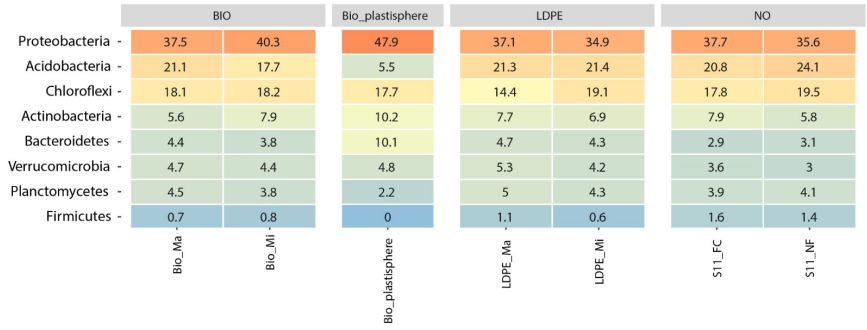


Fig. 5. Heatmap showing the average relative abundance of the top eight bacteria phyla across the samples. The headers of columns indicate the type of plastic used, "NO" indicates controls without the addition of plastic.

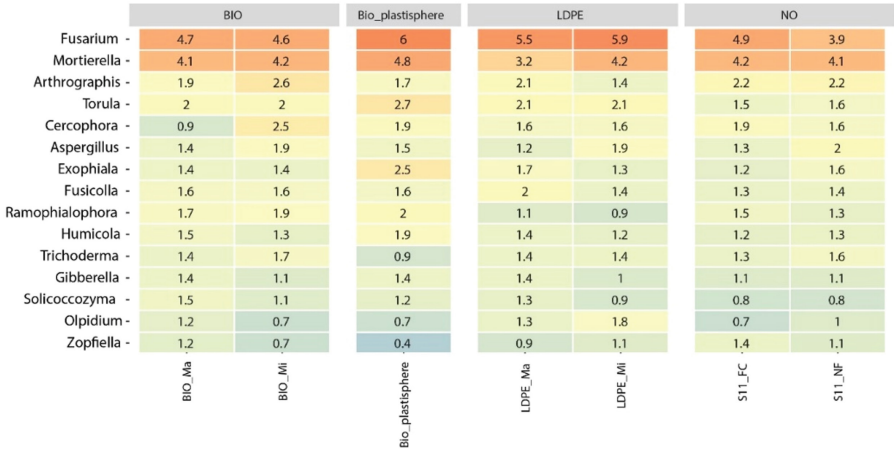


Fig. 6. Heatmap showing the average relative abundance of the top fifteen fungal genera across the samples. The headers of columns indicate the type of plastic used, "NO" indicates controls without the addition of plastic.

Microbial communities in the plastisphere

We compared the bacterial and fungal communities inhabiting the surface of Bio_Ma plastic residues and compared them to the rhizosphere communities of plants from which these residues were extracted. The analysis of bacterial community in the Bio_plastisphere compared to Bio_Ma rhizosphere showed an increase in diversity in "plastisphere" (Fig. 4) and a significantly higher relative abundance of bacteria phyla Actinobacteria, Bacteroidetes, and Proteobacteria and a lower relative abundance of Acidobacteria and Planctomycetes (Fig.7).

We found that the diversity of fungal community (Shannon index) in “plastisphere” was significantly lower comparing to rhizosphere (Fig. 4). The “plastisphere” was vastly dominated by three fungal genera *Rhizoctonia*, *Arthrobotrys* and *Fusarium* (on average around 50% of relative abundance) where the first two genera were significantly enriched compared to the rhizosphere community (Fig. 8). The results of differential abundance comparison revealed also statistically significant higher relative abundance of fungal genera *Torula* and *Exophiala* and lower abundance of *Zoptelia*. Significantly, a higher relative abundance of the fungal genera *Rhizoctonia* and *Arthrobotrys* were measured in the Bio_plastisphere (Fig. 8).

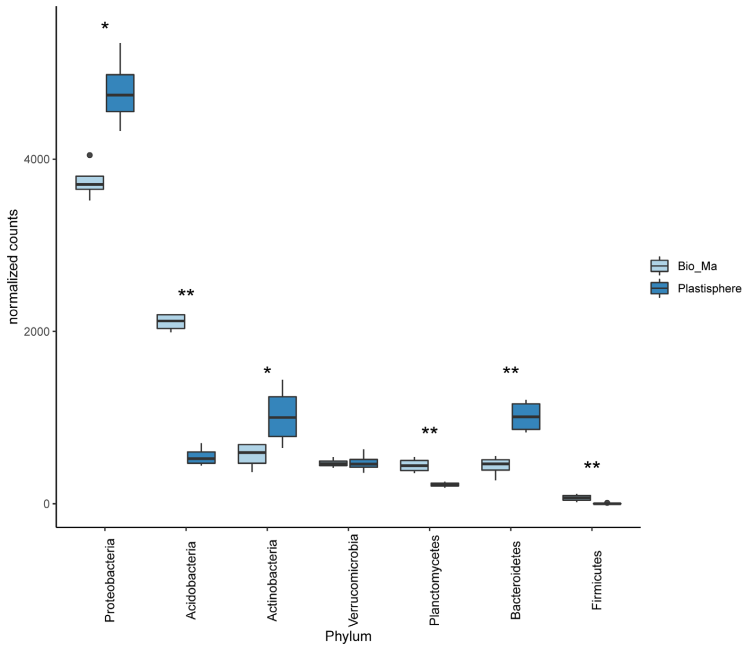


Fig. 7. Boxplots displaying the relative abundance of bacteria phyla between bioplastic plastisphere and the rhizosphere of wheat grown in soil with the addition of bioplastic. Statistically significant differences based on deseq2 analysis are marked with a single asterisk (p<0.05) or with a double asterisk (p<0.01).

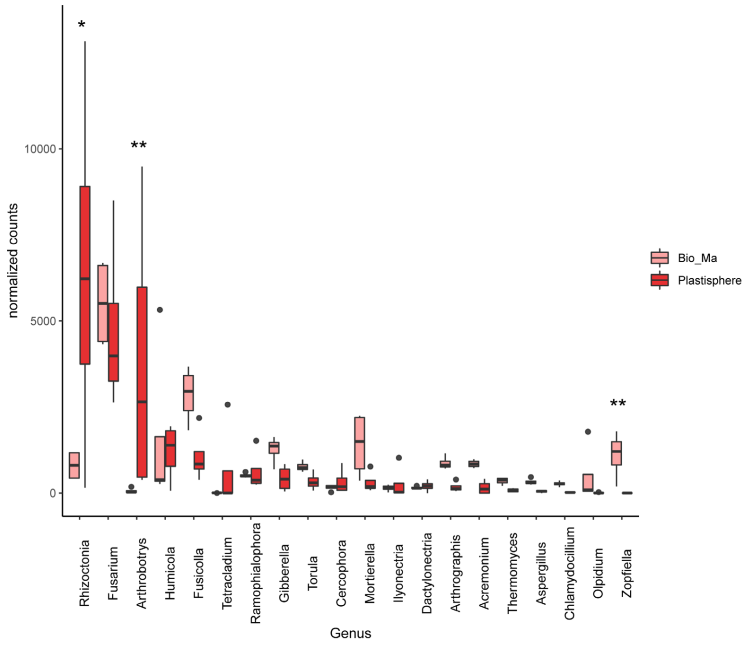


Fig. 8. Boxplots displaying the relative abundance of fungal genera between bioplastic plastisphere and the rhizosphere of wheat grown in soil with the addition of bioplastic. Statistically significant differences based on deseq2 analysis are marked with a single asterisk ($p<0.05$) or with a double asterisk ($p<0.01$).

Discussion

One of the greatest challenges of our generation is to consolidate or even increase current agricultural yields and nutritional quality while reducing the input of fertilizers and pesticides. As a critical agricultural tool, plastic mulch films have made significant contributions to food security and modern agricultural development (Espí et al., 2006; Kasirajan and Ngouajio, 2012). However, we tend to ignore the impact of plastic mulch films residues as pollutants. Plastic residues, especially microplastics, may represent a hidden danger for agriculture affecting soil functions, plants and crop yield (Rillig and Lehmann, 2020; Dan Zhang et al., 2020). Recently, Fuller & Gautam (2016) suggested that background concentrations of microplastics may range from 0.03% to 6.7% in agricultural and industrial soils (Fuller and Gautam, 2016). A promising approach to overcome the accumulation of residual polyethylene mulch films in soils is to use biodegradable mulch films composed of polymers designed to be degraded by soil microorganisms. Biodegradable plastics are a family of various polymers, such as starch blends, poly(lactic acid), poly(butylene adipate terephthalate), polyhydroxyalkonates, etc. In addition, they contain substantial amounts of chemical additives, such as plasticizers, which could be physically and chemically hazardous

to soil (micro)organisms and hence, disturb soil functioning (Zimmermann et al., 2020). Our work is the first to explore the impact of plastic mulch film residues (both LDPE and Biodegradable plastics) on the level of soil disease suppressiveness and plant nutrient status. The results of our study did not reveal major short-term effect of plastic residues on the level of soil suppressiveness against *F. culmorum*.

A significant effect, however, was observed on plant shoot biomass in the treatment Bio_Mi but not in the other treatments, indicating that different types and sizes of plastic residues may cause different effects. For example, the addition of LDPE_Mi affected the macro- and micronutrients composition in the roots. The mineral nutrient content profile of a plant can be considered to be a signature of the nutrient status of plants under stressed conditions (Martín-Sánchez et al., 2020; Pii et al., 2015). Our findings are based on a short-term experiment (two weeks of activation and three weeks of infection) however, it is plausible that in the long-term, the effects on the plant biomass, plant nutrient content and level of soil suppressiveness could be stronger. For example, in our previous study, we observed a significant adverse effect on plant biomass after 2 and 4 months (Qi et al., 2018).

Both soil and plants depend heavily on their microbiome for specific functions and traits (Berg, 2009; Liu et al., 2020). Rhizosphere, the narrow zone surrounding and influencing plant roots, is considered to be one of the most dynamic interfaces on earth (Philippot et al., 2013). Since large parts of the soil have limited nutrient access, the rhizosphere represents an oasis for soil microorganisms due to the release of rhizodeposits by plant roots. These rhizodeposits, defined as the easily available organic nutrients and signaling compounds, include root exudates, border cells and mucilage (D. L. Jones et al., 2009; Philippot et al., 2013; Raaijmakers et al., 2009). We recently observed that the addition of microplastics could have strong effects on the rhizosphere bacterial community (Qi et al., 2020b). In the current study, we did not observe significant changes in bacterial or fungal rhizosphere communities (diversity and assembly) among rhizosphere soil samples. Nonetheless, bacterial and fungal communities that were closely attached to the Bio_Ma "plastisphere" were very different from the rhizosphere communities in the Bio_Ma treatment. The Bio_Ma plastispheres revealed a high abundance of specific bacteria phyla (Actinobacteria, Bacteroidetes, and Proteobacteria) and fungal genera (*Rhizoctonia* and *Arthrobotrys*). By providing a new niche for soil microorganisms, the "plastisphere" could alter the structure and function of soil and rhizosphere microbial community. Despite the increasing interest in "plastisphere", very few studies have been conducted on this topic and they are focused only on aquatic ecosystems (Amaral-Zettler et al., 2020; Yang et al., 2019). In our study, we were able to obtain high-quality DNA only from the plastisphere of the Bio_Ma treatments for amplicon sequencing. However, it would be of great interest to further study the "plastispheres" formed around different types and sizes of plastic. The addition of microplastics to soil could be a source of nutrients and extra surfaces attractive

for certain microbes, and hence, affecting microbial community and function. Taking into consideration that many species belonging to two fungal genera dominating the "plastisphere" (*Rhizoctonia* and *Fusarium*) are pathogenic, we can speculate that this habitat may act as a reservoir of pathogens. Hence, it would be important in the future to study the effect of plastic residues on the abundance of soil borne pathogens.

Conclusions

In the current study, the addition of plastic mulch film residues to suppressive soil, did not reveal significant effects on disease symptoms in wheat inoculated with *F. culmorum*, nor on the plant-associated bacterial and fungal community composition, structure and diversity. However, we observed changes in the plant biomass and mineral nutrient content. Moreover, the analysis of "plastisphere" revealed substantially different bacterial and fungal taxonomic patterns and diversity as compared to the rhizosphere soil. Based on our results, we suggest that the introduction of plastic into the soil would create a new niche "plastisphere" that harbours a distinct microbial community. Such findings highlight the importance to characterize the plastisphere in soil and to unravel its impact on the plant-soil system.

Funding

This research was funded by the Natural Sciences and Engineering Research Council of Canada Discovery grant RGPIN-2014-05274 and Strategic grant for projects STPGP 494702. This work was also supported by the China Scholarship Council (CSC: 201604910510 to Y Qi).

Supplementary Material

Table S1. Detailed information about suppressive soil and Bergharen sand

soil parameters	unit	S11	BS
pH	/	7.28 ± 0.19	7.53 ± 0.05
OM	%	3.48 ± 0.47	0.24 ± 0.04
Fe	mg/kg	0.11	0.19 ± 0.01
K	mg/kg	68.77 ± 1.1	2.02 ± 0.32
Mg	mg/kg	56.43 ± 0.58	0
P	mg/kg	5.43 ± 0.04	0.11 ± 0.03
S	mg/kg	1.17 ± 0.15	0
C	%	1.99 ± 0.88	0.05 ± 0.01
N	%	0.16 ± 0.07	0
C:N	/	12.44	NA

Table S2. Content of some mineral nutrients in shoot of wheat plants. The content of Mg, K and Ca are expressed as mg g^{-1} DW while the content of Mn, Fe, Cu, Zn, Mo are expressed as µg g^{-1} DW. Nutrients displaying significant differences among treatment (p<0.05) are reported in bold.

	LDPE_Ma	LDPE_Mi	Bio_Ma	Bio_Mi	S11_FC	S11_NF
Mg	1.88±0.11	2.06±0.26	1.97±0.51	1.64±0.11	1.77±0.18	2.06±0.23
K	**52.29±1.89 b**	**40.44±2.76a**	**48.38±3.71ab**	**44.12±3.61ab**	**39.98±10.36ab**	**45.51±5.11ab**
Ca	3.67±0.09	3.03±0.31	3.32±0.39	3.20±0.35	3.02±0.58	3.61±0.36
Mn	**19.48±3.90 b**	**21.10±2.05b**	**17.94±2.09ab**	**17.45±4.27ab**	**11.17±1.47a**	**23.54±3.25b**
Fe	154.26±25.42	121.76±40.00	165.48±131.78	95.33±16.73	91.87±17.02	130.03±26.49
Cu	9.15±2.89	6.67±2.47	11.12±7.24	11.59±9.56	8.14±4.13	8.46±2.28
Zn	42.25±1.84	30.45±6.21	37.72±5.16	35.33±2.40	35.05±16.77	42.80±8.15
Mo	11.54±1.90	5.32±0.52	13.68±9.37	9.06±1.24	6.53±2.49	7.03±0.22

Table S3. Content of some mineral nutrients in root of wheat plants. The content of Mg, K and Ca are expressed as mg g^{-1} DW while the content of Mn, Fe, Cu, Zn, Mo are expressed as µg g^{-1} DW. Nutrients displaying significant differences among treatment (p<0.05) are reported in bold.

	LDPE_Ma	LDPE_Mi	Bio_Ma	Bio_Mi	S11_FC	S11_NF
Mg	6.31±3.58	19.51±14.65	5.54±2.16	7.33±5.85	5.19±2.04	3.08±1.41
K	16.71±2.26	15.39±2.23	15.31±1.18	18.42±3.06	16.65±0.94	14.84±1.48

Ca	2.99±0.33	3.96±1.41	2.88±0.21	2.94±0.52	3.40±0.70	2.39±0.19
Mn	51.71±14.81	101.06±69.58	43.80±8.81	58.83±23.78	56.67±8.04	41.27±8.36
Fe	2773.92±1581.59	7516.81±6038.32	2285.71±723.17	3320.64±2228.92	2825.24±728.29	1758.14±633.59
Cu	**18.10±6.61a**	**35.38±7.98b**	**13.94±3.17a**	**13.82±2.40a**	**15.92±5.96a**	**12.45±4.88a**
Zn	46.43±6.40	66.12±19.37	40.40±0.45	49.08±6.25	52.29±6.27	41.44±0.79
Mo	1.28±0.45	0.92±0.31	0.91±0.19	0.87±0.34	0.80±0.37	0.86±0.35

Table S4. One-way ANOVA analysis of bacteria 16S community alpha diversity based on Shannon index.

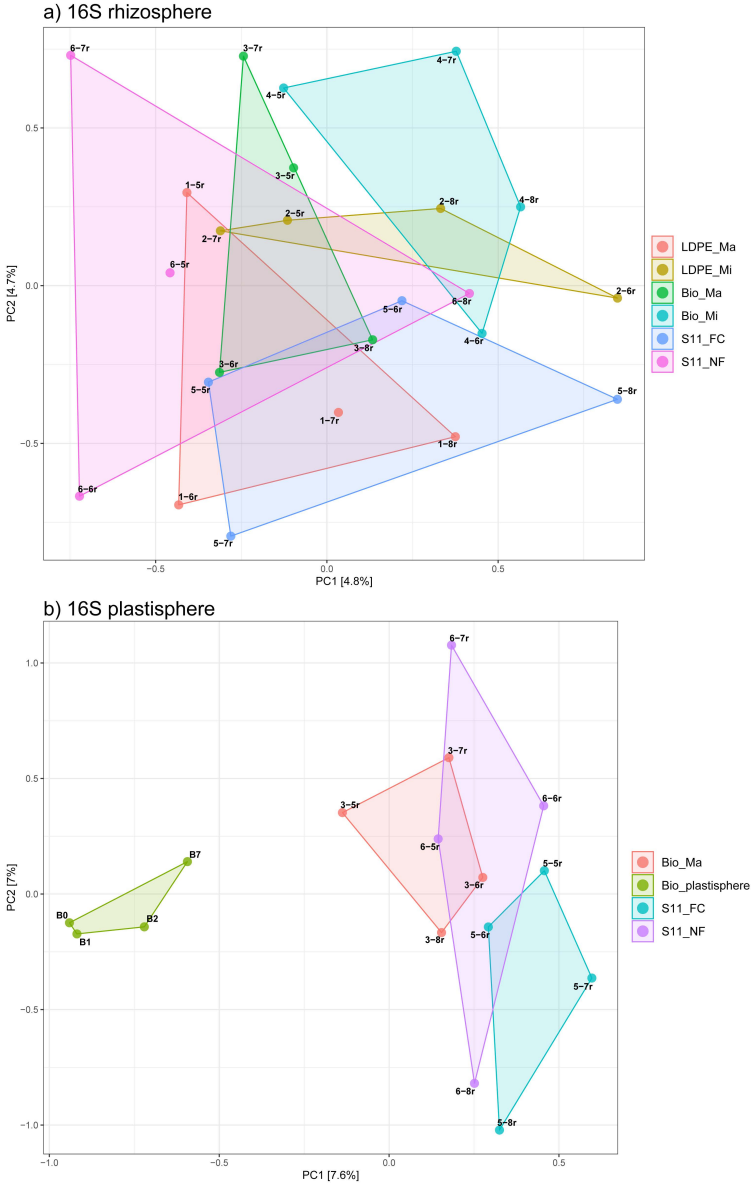
	Df	Sum Sq	Mean Sq	F value	Pr(>F)
Treatments	6	0.3144	0.05240	2.488	0.0561
Residuals	21	0.4422	0.02106		

Table S5. One-way ANOVA and Tuckey posthoc analysis of fungi ITS community alpha diversity based on Shannon index.

	Df	Sum Sq	Mean Sq	F value	Pr(>F)
Treatments	6	5.534	0.9224	4.207	0.00621
Residuals	21	4.604	0.2192		

Treatments	diff	lwr	upr	p adj
LDPE_Mi-LDPE_Ma	0,85	-0,23	1,93	0,19
Bio_Ma-LDPE_Ma	0,81	-0,27	1,89	0,23
Bio_Mi-LDPE_Ma	0,44	-0,63	1,52	0,83
Bio_plastisphere-LDPE_Ma	-0,43	-1,50	0,65	0,85
S11_FC-LDPE_Ma	0,59	-0,48	1,67	0,57
S11_NF-LDPE_Ma	0,77	-0,31	1,84	0,28
Bio_Ma-LDPE_Mi	-0,04	-1,11	1,04	1,00
Bio_Mi-LDPE_Mi	-0,41	-1,48	0,67	0,87
Bio_plastisphere-LDPE_Mi	-1,28	-2,35	-0,20	0,01
S11_FC-LDPE_Mi	-0,26	-1,33	0,82	0,98
S11_NF-LDPE_Mi	-0,08	-1,16	0,99	1,00
Bio_Mi-Bio_Ma	-0,37	-1,45	0,71	0,92
Bio_plastisphere-Bio_Ma	-1,24	-2,32	-0,16	0,02
S11_FC-Bio_Ma	-0,22	-1,30	0,86	0,99
S11_NF-Bio_Ma	-0,04	-1,12	1,03	1,00

Bio_plastisphere-Bio_Mi	-0,87	-1,95	0,21	0,17
S11_FC-Bio_Mi	0,15	-0,93	1,23	1,00
S11_NF-Bio_Mi	0,33	-0,75	1,40	0,95
S11_FC-Bio_plastisphere	1,02	-0,06	2,10	0,07
S11_NF-Bio_plastisphere	1,20	0,12	2,27	0,02
S11_NF-S11_FC	0,18	-0,90	1,25	1,00



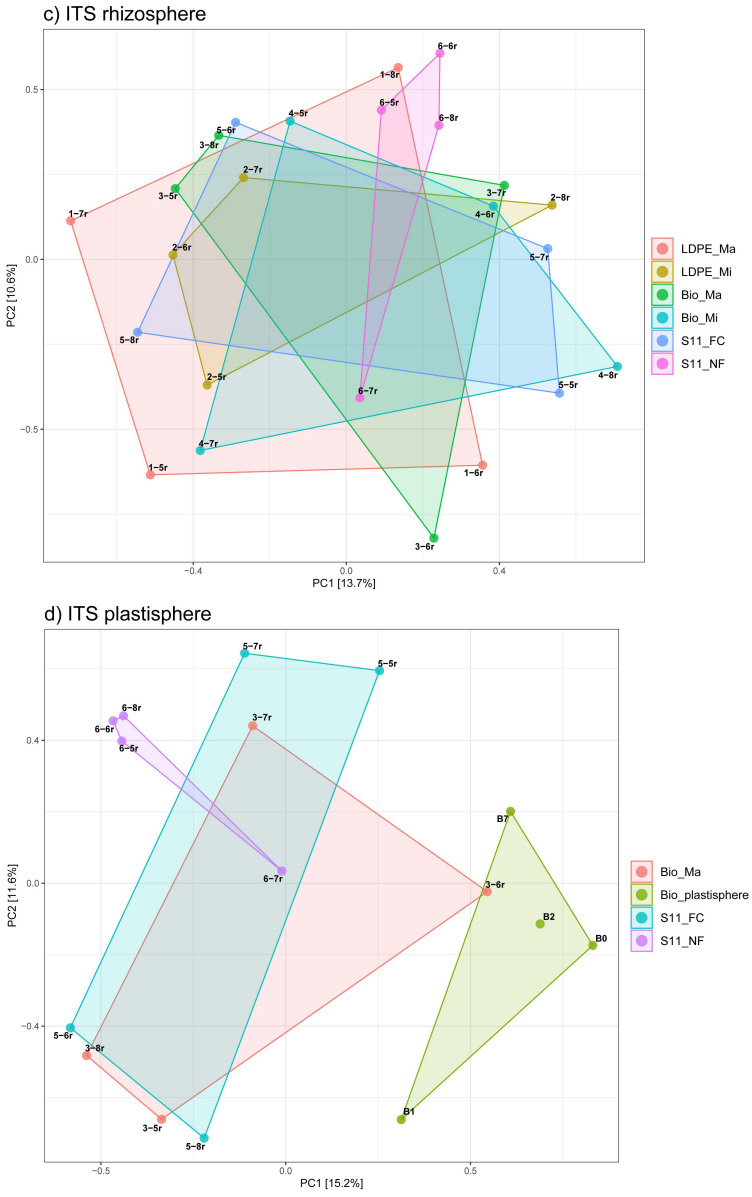
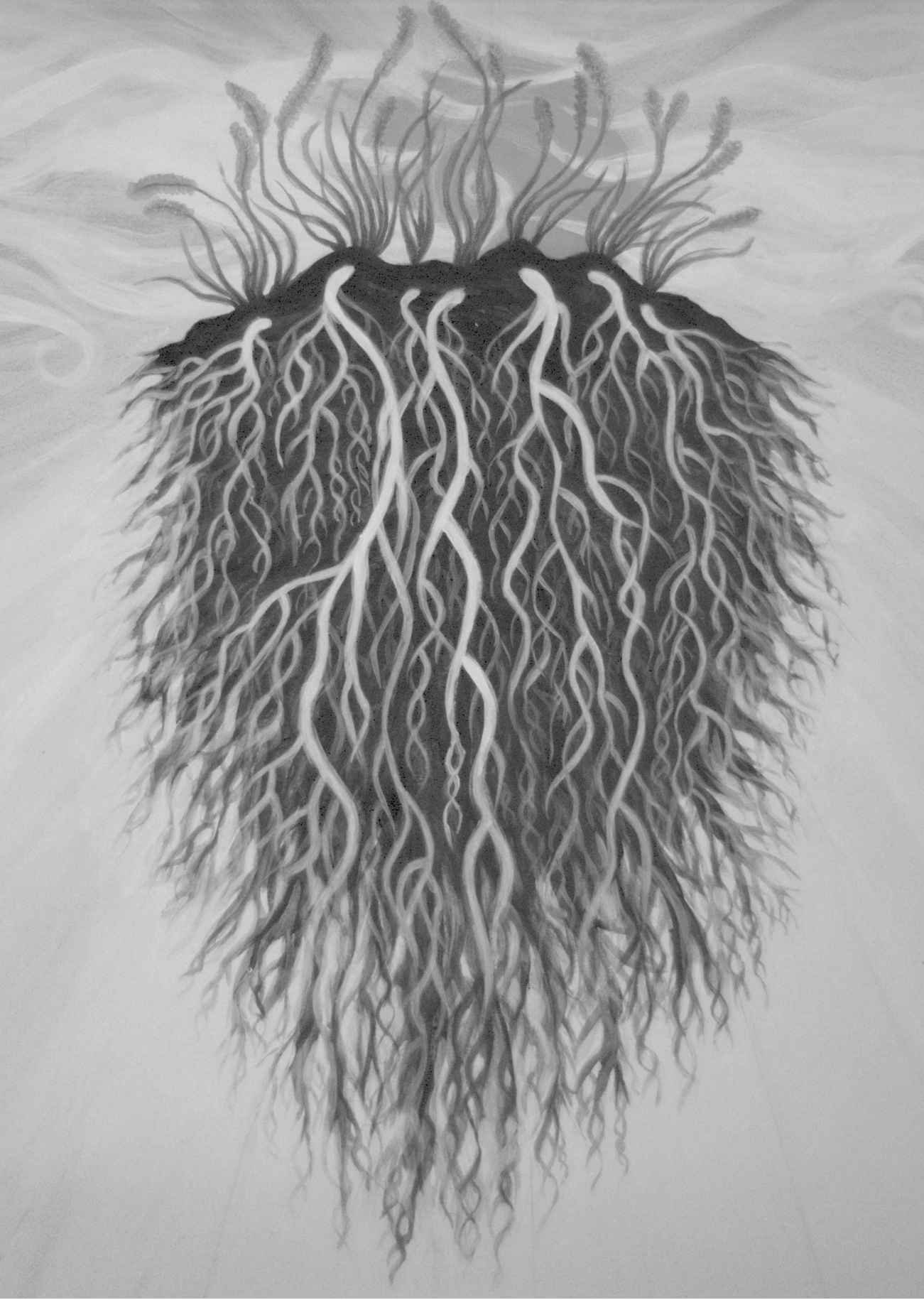


Fig. S1. Principal Component Analysis of bacterial (16S) and fungal (ITS) communities. ANOSIM statistics is indicated in the left-bottom corner of each plot.



Chapter 6

General and summarizing discussion

In 2019, the European Union launched a strategy towards a zero pollution and toxic-free environment ("A European Green Deal," 2019). One of the targets in the so-called "From Farm to Fork" actions for the year 2030 is to reduce the use of chemicals and hazardous pesticides in agriculture by 50%. Hence, one of the great challenges of our generation is to increase agricultural yields and enhance nutritional quality of food crops while reducing the input of fertilizers and pesticides. Soil-borne diseases caused by pathogenic fungi form a major threat for crop production worldwide. Resistance breeding, chemical and cultural control measures have been largely unsuccessful to date for most fungal root pathogens. Hence, 'Learning from Nature' by exploring and exploiting the natural mechanisms of soil disease suppressiveness gives us a profound opportunity to develop effective and sustainable strategies to protect crops from fungal root pathogens. In my thesis, I explored the microbiome-driven phenomenon of soil suppressiveness to *Fusarium culmorum* in wheat, building a basis to identify the responsible microorganisms and to understand the underlying mechanisms of disease suppression (Chapters 2-4). Moreover, I evaluated the impacts of microplastic pollution on disease suppressiveness and the rhizosphere microbiome of wheat (Chapter 5). The main findings of each of the chapters are summarized in figure 1 and discussed in more detail below.

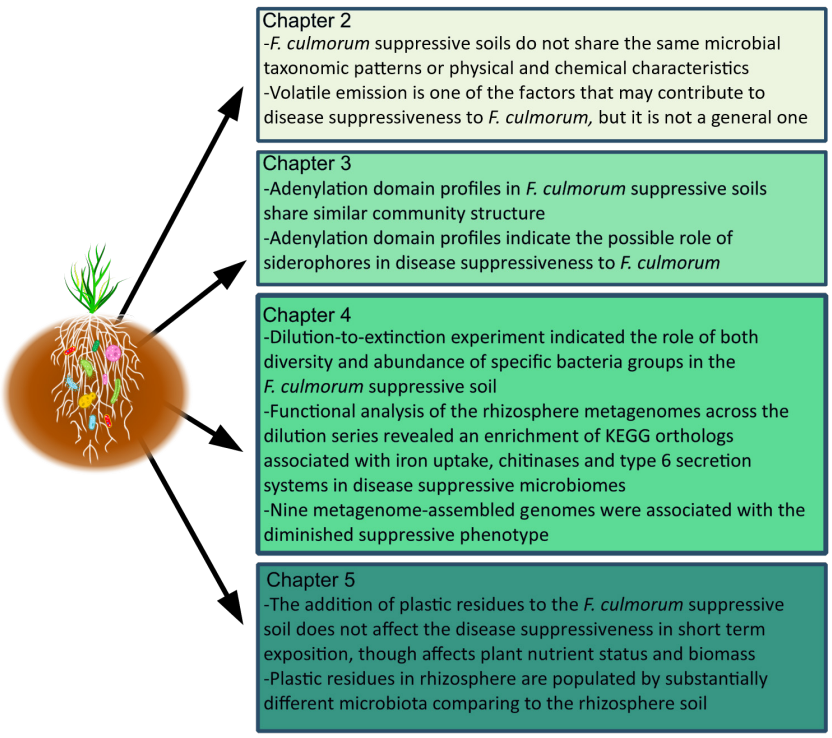


Figure 1. Summary of the main findings presented in the four experimental chapters of this PhD thesis.

The distribution of disease suppressiveness of soils to *Fusarium culmorum*

Natural disease suppressiveness of soils to soil-borne pathogens was recognized worldwide already more than a century ago (Atkinson, 1892; Baker and Cook, 1982; Gomes Exposito et al., 2017; Hornby, 1983; Schlatter et al., 2017a). For most soil-borne pathogens, however, the distribution of disease suppressiveness across multiple agricultural soils is unknown because of a lack of simple diagnostic tools. In *Chapter 2,* we conducted for the first time a large-scale screening of soils from different regions in the Netherlands and Germany for suppressiveness to root rot of wheat caused by the fungal pathogen *Fusarium culmorum*. This economically important pathogen causes significant losses in cereals, mostly in wheat and barley (Dean et al., 2012; Scherm et al., 2013). Because of mycotoxins production, it also contaminates grain making it unfit for human and animal consumption or malting (Antonissen et al., 2014; Nielsen et al., 2014). We found a baseline level of disease suppressiveness to *F. culmorum* in many of the screened soils, but a high level of suppressiveness was found in 4 out of 28 soils tested. In all four, the suppressiveness was eliminated by sterilization and could be transferred to a non-suppressive soil by transplantation (*Chapter 2*). Based on the results presented in *Chapter 2* we concluded that the distribution of *F. culmorum* suppressive soils does not follow a specific geographic pattern or field history. Moreover, we did not find any significant correlation with physical or chemical soil properties. To look for enriched bacteria populations in *Fusarium culmorum* suppressive soils, we performed 16S-based taxonomic profiling of all 28 soils. Based on our results we did not find any specific taxonomic group of bacteria that was significantly enriched in the suppressive soils; however, we found *Acidobacteria* to be hub taxa in some of the suppressive soils based on co-occurrence network analysis. The results presented in *Chapter 3* indicate that co-occurrence patterns of A-domains (functional amplicons) are much better predictors of soil suppressiveness than microbial taxonomy based on 16S amplicon sequencing. This is in line with studies revealing that functional genes involved in secondary metabolite production can be characteristic to disease suppressive microbiomes. For example, the *take-all decline* (TAD) soils show an overrepresentation of 2,4-diacetylphloroglucinol (*phl*) functional genes (Kwak and Weller, 2013; Raaijmakers and Weller, 1998), and *Rhizoctonia solani* AG8 suppressive soils show greater expression of polyketide cyclase genes (Hayden et al., 2018). Additionally, Zhao et al. found that the overrepresentation of non-ribosomal peptide synthases (NRPS) genes in Fusarium wilt suppressive soil is more characteristic for disease suppressiveness than taxonomic microbial community structure and chemical properties (Zhao et al., 2018), which is in line with our results for *F. culmorum* suppressive soils. More specifically, we found an enrichment of NRPS gene clusters in suppressive soils based on co-occurrence networks, and many of these clusters were predicted to encode siderophores. We also predicted, based on

substrate specificity profiles of A-domains, possible enrichment of cyclic and branched lipopeptides in the suppressive soils.

It would be instrumental to be able to diagnose disease suppressiveness in agricultural soils for the purpose of field and crop selection. The perfect diagnostic tool for soil disease suppressiveness should ideally be precise, fast, and easy for interpretation. The sequencing of one or more functional amplicons could possibly meet those criteria but still a more in-depth fundamental understanding of soil suppressiveness is required to develop such tools. The main obstacle is understanding disease suppressiveness at a mechanistic level, which is especially challenging since the phenomenon is complex and diverse. Different approaches to predict soil suppressiveness was presented in the work of Hayden et al. where authors used metabolomics to discriminate between *Rhizoctonia* suppressive and non-suppressive soils (Hayden et al., 2019). Metabolomics allows to study metabolites and their concentrations in biological systems, unlike DNA sequencing that reflects a potential to produce metabolites. Future studies should integrate both NGS sequencing and metabolomics to understand in depth the phenomenon of soil suppressiveness.

Is *Fusarium culmorum* soil suppressiveness general or specific?

Two main models of suppressiveness have been recognized: specific suppression associated with the activity of enriched populations of specific microbes, and general suppression associated with the metabolic activity of the microbial community as a whole. Both types of suppressiveness can be eliminated by soil sterilization but only the specific suppressiveness can be transplanted, by adding small amounts of suppressive soil to conducive soil (Baker and Cook, 1982; Schlatter et al., 2017a).

We show that suppressiveness to *F. culmorum* of the identified soils can be transplanted to non-suppressive soil (Chapter 2) and that rhizosphere suspensions of wheat grown in suppressive soils S11 can be transplanted to a sterile soil (Chapter 4). These results indicate that the observed suppressiveness is specific and associated with the rhizosphere microbiome. Subsequent comparison of the profiles of A-domain functional amplicons between *F. culmorum* suppressive and conducive soils revealed the association of siderophore BGCs with suppressiveness (*Chapter 3*). Soil microorganisms produce siderophores to sequester and solubilize iron that is essential for the functioning of a number of enzymes. It is one of the mechanisms of competition for this limited resource and overall, competition for resources is considered as a general soil suppressiveness phenomenon. Though we have not found any enriched bacterial taxa in *F. culmorum* suppressive soils based on 16S amplicon analyses (*Chapter 2*), we can not exclude the involvement of specific groups of other organisms that we have not tested like, fungi, oomycetes, nematodes, protists or viruses. We also cannot exclude that enriched groups of

microorganisms in the suppressive soils are not taxonomically coherent but rather these are groups of microorganisms collectively expressing certain functions.
All in all, in *F. culmorum* suppressive soils analyzed in this thesis, we found some putative traits associated with specific disease suppressiveness (transferability) but also traits typical for general suppressiveness (competition for iron via siderophores). These results therefore need to be interpreted with caution because they are based on predictions and need future validation experiments. We also can not exclude other traits or involvement of other groups of organisms that we have not tested. It is emphasized in the work of Schlatter et al. that a particular disease suppressive soil can operate in the whole spectrum between specific to general suppressiveness (Schlatter et al., 2017a) and based on our experiments we postulate that *F. culmorum* suppressiveness is one of the examples of intermediate models where both the density of microbial populations and diversity play a role.

Mechanisms of suppressiveness to *Fusarium culmorum*

Up to date, several mechanisms in different disease suppressiveness systems were found (for more details see *Chapter 1*). In *Rhizoctonia solani* suppressive soils, the production of chlorinated lipopeptides nunamycin and thanamycin by *Pseudomonas* was identified as a key mechanism of plant protection (Mendes et al., 2011; Michelsen et al., 2015; Watrous et al., 2012). For the sugar beet – Rhizoctonia suppressive soil, endophytic bacterial genera *Flavobacterium* and *Chitinophaga* provided an additional line of defense (Carrión et al., 2019). In wheat, enriched populations of fluorescent pseudomonads producing 2,4-diacetylphloroglucinol were found responsible, at least in part, in *take-all* suppressive soils (Kwak and Weller, 2013; Raaijmakers and Weller, 1998). For *R. solani* AG8 in wheat, higher frequencies of *Acidobacteria* and *Gemmatimonas* and higher expression of stress related genes and polyketide cyclases were related to suppressiveness (Hayden et al., 2018; Yin et al., 2013). Our work on wheat indicated several possible mechanisms of suppressiveness to *F. culmorum*. These mechanisms are schematically summarized in figure 2 and further described below. We do not know if there is only one dominant mechanism of suppressiveness in this system, but identification of several possible modes of action suggests that the suppressiveness is a synergistic or additive effect of multiple mechanisms that either work simultaneously, in sequence, or in spatially different compartments along the developing plant root system.

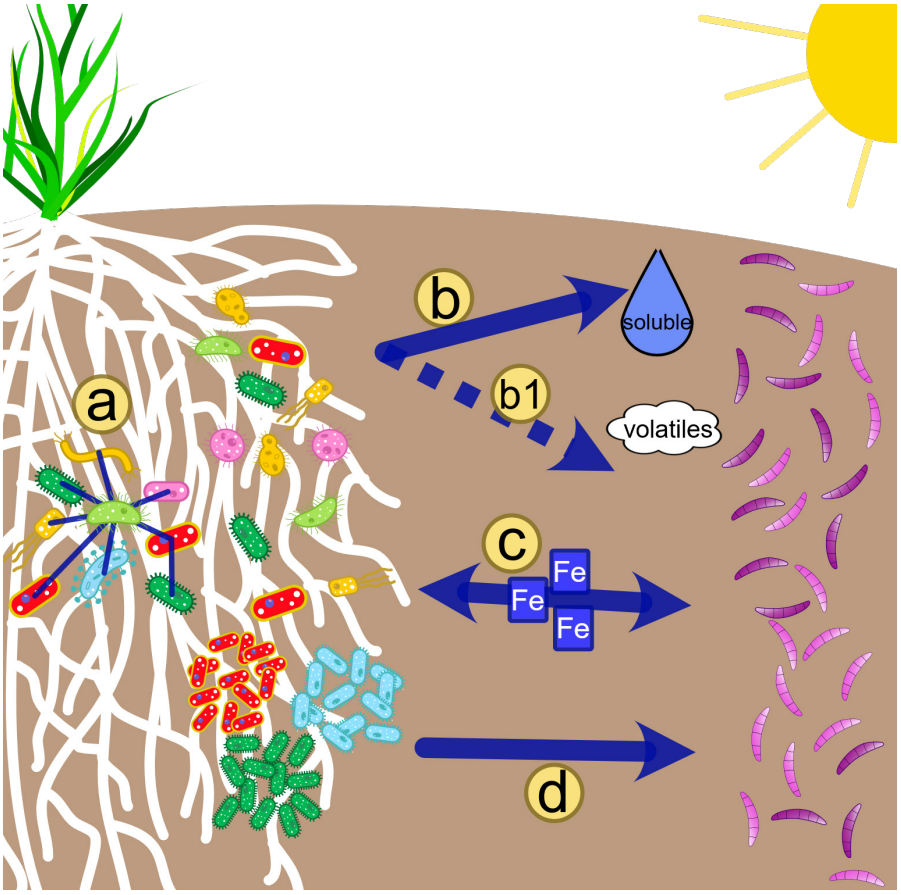


Fig. 2. Proposed mechanisms of Fusarium culmorum disease suppressiveness. The wheat root microbiome is depicted on the left side of the figure and the pathogen is depicted on the right side as spores of F. culmorum. a – Collective activity of the whole microbial community with Acidobacteria as hub taxa (Chapter 2), b- production of secondary metabolites, both soluble and b1 - volatile (Chapters 2, 3 and 4), c- competition for iron (Chapters 3 and 4), d- activity of specific bacteria taxa (Chapter 4).

Collective activity of the microbial community in suppressiveness with Acidobacteria as hub taxa

The high connectivity of Acidobacteria in *F. culmorum* suppressive soils found in the taxonomic analysis (*Chapter 2*) suggests the importance of its interactions with other species for the functioning of the whole bacterial community. The role of Acidobacteria in soil ecosystems is largely elusive despite its ubiquity in soil, mostly because of the difficulties of isolation and *in-vitro* cultivation methods (Eichorst et al., 2018; Kielak et al., 2016).

Nevertheless, sparse cultivation-based and culture-independent functional studies highlight the enormous metabolic potential of this genus, especially in complex carbohydrate metabolism, nitrogen and sulfur turnover and siderophores production (Costa et al., 2020; de Chaves et al., 2019; R. T. Jones et al., 2009; Kalam et al., 2020; Kielak et al., 2016; Lladó et al., 2016). In particular, its role in soil aggregation and in the turnover of exopolysaccharides can have a tremendous effect on soil functioning (Costa et al., 2018). We speculate that in *F. culmorum* suppressive soils Acidobacteria are involved in plant protection by modulating ecological processes and providing crucial ecological services like, nutrients turnover and soil matrix formation. That indirect role is more probable than direct antagonism against the pathogen but considering vast metabolic potential of Acidobacteria we cannot exclude the second scenario. It will be very interesting to further explore the yet unknown roles, if any, of *Acidobacteria* in disease soil suppressiveness.

Involvement of secondary metabolites in disease suppressiveness

Microorganisms execute their beneficial functions through the production of specialized secondary metabolites. These metabolites do not take part in essential cell processes but allow the microorganism to perform auxiliary functions. The synthesis and secretion of secondary metabolites is an energy and resource investment and that is why their production is most of the times controlled by regulation systems in response to external signals. Soil microorganisms are known to produce a plethora of various types of secondary metabolites that constitute a largely untapped resource for novel compounds (Cragg and Newman, 2013). Secondary metabolites allow microorganisms to communicate, acquire nutrients and interact with other (micro)organisms (Raaijmakers et al., 2002; Sharrar et al., 2020). In several cases, the production of microbial secondary metabolites or the potential to produce them (biosynthetic genes) was found to be linked to disease suppressiveness (more in *Chapter 1*). In my thesis (*Chapters 3* and *4*), several gene clusters associated with soil suppressiveness to *F. culmorum* were identified based on sequencing of adenylation domains and based on untargeted shotgun metagenomics. These gene clusters encoded mostly lipopeptides, polyketides and siderophores, groups of compounds that are known for their antifungal activities through direct antagonism or through competition for resources. Substantial genetic diversity of the gene clusters combined with limited prediction of their functions, in most of the cases, allows us only to speculate about their precise roles. Nevertheless, the association with the disease suppressive phenotype makes them a good target for further studies.

In general, the identification of gene cluster functions requires isolation of the microorganism carrying that cluster followed by site-directed mutagenesis or by cloning and expression of the gene cluster in a different host, in case the corresponding microbial species is difficult to culture or to transform (Cui et al., 2018; Gomez-Escribano and Bibb,

2011). With the mutants at hand, these can then be compared to their wild type strain for their ability to suppress the target fungal pathogen *in vitro* and/or *in planta*. One of the best examples of functional identification of a gene cluster followed by identification of its function in suppressive soils comes from the work on thanamycin. The gene cluster encoding this compound was identified to be crucial for antifungal activity against *R. solani* by transposon mutagenesis in *Pseudomonas* sp. strain SH-C52 isolated from a suppressive soil (Mendes et al., 2011). Later the encoded metabolite was identified as a chlorinated 9-AA lipopeptide and characterized for its antifungal activity and for its production by nanoDESI mass spectrometry in live microbial colonies (Watrous et al., 2012). Our findings about the biosynthetic genes in *F. culmorum* suppressive soils in *Chapters 3* and *4* allow us to generate a number of hypotheses about the role of secondary metabolites in the soil suppressiveness that we can further validate in a similar manner.

Potential role of volatile metabolites in suppressiveness

A number of studies have demonstrated the role of volatile compounds emitted by soil bacteria in antagonism towards plant pathogens *in-vitro* (Garbeva et al., 2014b; Hammerbacher et al., 2019; Hunziker et al., 2015; Ossowicki et al., 2017) including strains isolated from suppressive soils (Carrion et al., 2018; Cho et al., 2017; V. Cordovez et al., 2015; Gómez Expósito et al., 2015). Nevertheless, the exact role of this group of compounds in disease suppressiveness is still unclear. In the work presented in *Chapter 2* we have made the first attempt to elucidate this role. Based on our results the overall volatile emissions by the soil microbiome provided some level of protection against the pathogen. Volatile-mediated soil suppressiveness was observed for four soils, including two suppressive and two conducive soils. Hence, volatile emission is one of the factors that may contribute to disease suppressiveness to *F. culmorum*, but it is not a general one. In our work we did not focus on isolating pure cultures of bacteria and testing their *in-vitro* activity but rather tested the suppressive effect of overall soil volatile emissions on plant health. There are often discrepancies between *in-vitro* experiments with single isolates and experiments including soil and plants. Gómez Expósito et al. described the antifungal *in-vitro* activity (including volatiles) of *Lysobacter* spp. isolated from a *Rhizoctonia*-suppressive soil showing plant growth-promoting traits of these strains, but when introduced into the soil the *Lysobacter* isolates were not able to protect plant against infection (Gómez Expósito et al., 2015). Recent *in-vitro* and *in-situ* studies indicated that the production of volatiles in natural environment is related to the composition of microbial communities and that reduced microbial diversity increased the volatile emission but decreased the number of emitted volatiles (Abis et al., 2020). In a perspective article, Brilli et al. highlighted the need to further explore volatile emissions in soil to improve sustainable plant protection strategies for agriculture (Brilli et al., 2019). Our findings indicating the potential role of volatiles in soil

suppressiveness to *F. culmorum* require follow-up experiments to identify the volatile compounds with suppressive activity and the microorganisms emitting them.

Competition for iron

The availability of iron is soils is generally low and while this element is essential for living organisms it is often a limiting resource in this environment. Microorganisms, under low iron conditions, produce siderophores allowing them to sequester and take up iron. Production of siderophores is often recognized as a mechanism of competition between (micro)organisms (Ahmed and Holmström, 2014; Saha et al., 2016). The profound example of the key role of competition for iron in soil suppressiveness comes from the work on *Fusarium oxysporum* suppressive soils in the Châteaurenard region in France. The central role of competition for iron and involvement of siderophore-producing Pseudomonads was demonstrated as one of the key mechanisms of suppression (summarized in *Chapter 1*). The pathogen used in the French work is related to *F. culmorum*, which is why we presumed some similarities between these two suppressiveness soil systems. Indeed, we found overrepresentation of siderophore biosynthetic gene clusters (BGC) in *F. culmorum*-suppressive soils based on adenylation domain profiles (*Chapter 3*) and enrichment of iron uptake functional genes based on a dilution-to-extinction experiment (*Chapter 4*). Iron-limiting conditions, where the production of siderophores is triggered, are most likely to prevail in soil environments. That is why the production of siderophores is often identified in soil microorganisms, including the microorganisms related to disease suppression and plant growth promotion (for review: (Ahmed and Holmström, 2014; Höfte and Bakker, 2007)). It has also been shown that some siderophores can trigger systemic resistance in plants, constituting another line of defense against pathogens (Audenaert et al., 2002; Chae et al., 2020; Pieterse et al., 2014; Sousa and Olivares, 2016). In three out of four *F. culmorum* suppressive soils found in our work the concentration of bioavailable iron is very low (0.02 to 0.11 mg/kg) and on the remaining one it reaches 0.45 mg/kg what is related to a low pH of this soil (*Chapter 2)*. That suggests that in most of the suppressive soils tested here, we can expect competition of iron via siderophores. That is in line with the data obtained in *Chapter 3* where we see the overrepresentation of siderophore BGCs in suppressive soils. All in all our results suggest that siderophores take part in direct antagonism against pathogens causing iron starvation, but also may trigger ISR in wheat, making it a possible dual action mechanism of soil suppressiveness. Additional experiments are needed to validate the role of competition for iron in disease suppressiveness. In previous works on other soil suppressiveness systems the involvement of this competition was tested by modifying iron availability in soil using surplus of iron or chelators (Almario et al., 2014; Scher and Baker, 1982). This simple yet elegant approach is also planned in the continuation of our work.

Activity of specific bacteria taxa

The screening of 28 soils described in *Chapter 2* did not reveal any common enriched bacterial taxa within suppressive soils but the extensive analysis of suppressive soil S11 in *Chapter 4* suggested that several taxa possibly play a role in disease suppressiveness (Acidobacteria, Verrucomicrobia and Streptomycetes). There could be two main reasons for this apparent discrepancy: soil suppressiveness in different soils may not share the same mechanisms or the microbial basis of the activity may be more similar functionally than taxonomically. Moreover, in *Chapter 4* we used a deep shotgun metagenomic that can provide more detailed taxonomic representation of microbial community than 16S amplicon sequencing used in *Chapter 2*. Using high volume metagenomes, we can often find the differences between datasets at lower taxonomic levels (Schöler et al., 2017; Tessler et al., 2017). Comparison of shotgun metagenomes obtained in a dilution-to-extinction experiment revealed that several bacterial taxa significantly decreased in abundance as the soil lost disease suppressiveness upon dilutions of the extracted microbiome (*Chapter 4*). Among these taxa we found again Acidobacteria, but also Streptomycetes, previously associated with suppressiveness, and Verrucomicrobiota, previously associated with soil fertility (Navarrete et al., 2015). *Streptomyces* isolated from *Streptomyces scabies* suppressive soils (Liu et al., 2011), from *Fusarium oxysporum* suppressive soils (Cha et al., 2016) and from *Rhizoctonia* suppressive soil (V. Cordovez et al., 2015) exhibited antagonistic activities against pathogens. In general, the biosynthetic potential and biocontrol traits of *Streptomyces* are prominent (Belknap et al., 2020; Nicault et al., 2020; Sousa and Olivares, 2016; van der Meij et al., 2017). In the metagenomic analysis of suppressive soil S11 (*Chapter 4*) we found a number of biosyntetic gene clusters taxonomically assigned to Streptomycetes encoding siderophores (discussed above), melanins that appear to play a role in colonization of plant roots by Streptomycetes (Chewning et al., 2019) and possibly novel compounds of unknown functions belonging to terpenes, polyketides and non-ribosomal peptides.

The future efforts in this study will be focused on the integration of the metagenomic approach, with metabolomics and culturomics. In the course of the dilution-to-extinction experiments on suppressive soil S11 (*Chapter 4*) from the collected rhizosphere samples, we have additionally extracted metabolites for mass spectrometry analysis (MS) and preserved a bacterial collection of 184 strains, which were also subjected to sequencing. Successive steps will be identifying the changing trends in the abundance of natural products across the dilution series and linking these products to BGCs and taxa identified in this study. Having this information, we can further use selective isolation and molecular identification approaches (PCR, DNA probes or sequencing) to recognize producers of these natural products in the bacterial isolate collection from soil S11. Following this path, we can further identify functions and mechanisms provided by key taxa and elucidate their role in

soil suppressiveness. Extensive knowledge about the microbial community of suppressive soil S11 and bacterial collection will allow us to construct synthetic microbial communities that we can test for protection against Fusarium and possibly other pathogens in wheat or other plants. Altogether, the follow up studies will allow us to not only predict the mechanisms of the soil disease suppression but also validate the findings.

The impact of plastic on soil microbiomes and disease suppressiveness

Agriculture is a substantial producer of waste products, and in the last decade, also of plastic waste (Millati et al., 2019). Nowadays, accumulation of plastic is becoming a global threat, but the use of plastic in agriculture is becoming increasingly popular. One of the main sources of plastic in agriculture is the use of mulching films. It was demonstrated by Zhao et al. that fields that use mulching contain significantly more plastic residues then fields that do not (Zhou et al., 2020). The impact of plastic on terrestrial ecosystems is not only the problem for agriculture but our knowledge on how it affects farming is insufficient (Rillig, 2020; Rillig and Lehmann, 2020). In the last years the answer from the industry for the demand of more environmentally friendly solutions has been manufacturing all kinds of "bioplastics". In principle these materials have similar physical properties to conventional, fossil fuel-based plastic, but they degrade in the environment much faster. In practice, there are no clear international guidelines defining what is a "bioplastic", which causes a lot of misconceptions. Often "bioplastics" are composed of bio-based (for example cellulose-based) polymers mixed with conventional plastic. Recent work of Qi et al. show that both conventional plastics and "bioplastic" have a negative impact on the growth of wheat and a significant impact on rhizosphere microbial communities (Qi et al., 2019, 2018). We have found that the soil suppressiveness to *F. culmorum* has a microbial basis (*Chapter 2*) and subsequently we wanted to evaluate if the addition of plastic to a suppressive soil can influence the ability of the microbiome to protect the plant. Although we have not seen a significant impact on the protective effect of suppressive soil in our short-term experiment, we have found an impact on the plant nutrient status and microbiome. We see in our experiments that the "bioplastic" we tested, may cause a significant shift in the microbial community as it creates a new niche in the soil inhabited by different microbiota. The difference in this microbiota manifested mainly as the high relative abundance of fungal genera such as *Rhizoctonia* and *Fusarium.* We can speculate that in the long term it can have an impact enrichment of economically relevant pathogens as many of them belong to these genera, but further experiments are needed to investigate this (Chapter 5). What seems to be an environmentally friendly alternative to conventional plastic may be actually harmful to soil health. This problem may get more pressing as global climate changes affect the ability to grow crops (Godfray et al., 2010; Wang et al., 2017). Increasing temperature and drought may force farmers to use more plastic mulching to maintain food production at the

same level. Global warming and drought can also directly have an impact on soil microbiomes, causing unforeseen effects in food production (Ochoa-Hueso, 2017). Our work highlights the importance of healthy soil microbiomes and gives the basis for improving the sustainability of agriculture in the future.

Concluding remarks and future perspectives

Overall, the research presented in this thesis constitutes the first extensive screening of suppressiveness to *Fusarium culmorum* across numerous agricultural field soils, the essential groundwork to establish the microbial basis of disease suppressiveness, and the first integration of a dilution-to-extinction approach with untargeted metagenomics to deconstruct the mechanistic basis of suppressiveness. We also evaluated the impact of plastic on disease suppressiveness, plant growth and soil microbial communities that addresses current global environmental concerns. This work builds a foundation for further research on this intriguing phenomenon and a methodological base for plant-associated microbiome studies. We suggested several possible mechanisms of soil suppressiveness and proposed the ways to validate them. In the course of our work on disease suppressiveness to *F. culmorum*, we have also pointed out several putative mechanisms of suppressiveness that were not yet experimentally validated. Considering the high abundance of various pathogenic and non-pathogenic Fusaria in soils (Moretti, 2009; Summerell et al., 2010) and that the main distinction between these groups is the ability of producing mycotoxins and other pathogenicity factors (Perincherry et al., 2019; Wachowska et al., 2017), studying the effects of a disease suppressive microbiome on the production of pathogenicity factors by *F. culmorum* will be part of these validation experiments.

Another step in research on disease suppressiveness is the implementation of metatranscriptomics and metabolomics. The current study indicated a metabolic potential of the rhizosphere microbiome of wheat to produce a number of metabolites that may play an important role in soil suppressiveness, nevertheless linking this data with information about produced metabolites necessitates confirmation and validation. Moreover, the data on bacterial taxa that were proposed to play a role in suppressiveness in *Chapter 4* should be used for selective isolation and characterization including site-directed mutagenesis and functional bioassays. Altogether, these approaches can be used to further pinpoint key microbial taxa and traits which in turn provides a framework to design a synthetic microbial community that recreates the natural protection against *F. culmorum* observed in the field soils (Carrión et al., 2019; Tsolakidou et al., 2019). Having a deep understanding of functioning of soil suppressiveness, we can utilize this knowledge in designing biological plant protection agents or in steering soil microbial communities towards developing disease suppressiveness (Arif et al., 2020; Kumar and Dubey, 2020; Orozco-Mosqueda et al., 2018).

References

A European Green Deal [WWW Document], 2019. . Eur. Comm. - Eur. Comm. URL https://ec.europa.eu/info/strategy/priorities-2019-2024/european-green-deal_en (accessed 12.18.20).

Ahmed, E., Holmström, S.J.M., 2014. Siderophores in environmental research: roles and applications. Microb. Biotechnol. 7, 196–208. https://doi.org/10.1111/1751-7915.12117

Alabouvette, C., 1999. Fusarium wilt suppressive soils: an example of disease-suppressive soils. Australas. Plant Pathol. 28, 57–64. https://doi.org/10.1071/AP99008

Alabouvette, C., 1986. Fusarium-Wilt Suppressive Soils from the Chateaurenard Region - Review of a 10-Year Study. Agronomie 6, 273–284. https://doi.org/DOI 10.1051/agro:19860307

Alabouvette, C., Olivain, C., Migheli, Q., Steinberg, C., 2009. Microbiological control of soil-borne phytopathogenic fungi with special emphasis on wilt-inducing Fusarium oxysporum. New Phytol. 184, 529–544. https://doi.org/10.1111/j.1469-8137.2009.03014.x

Al-Babili, S., Bouwmeester, H.J., 2015. Strigolactones, a Novel Carotenoid-Derived Plant Hormone. Annu. Rev. Plant Biol. 66, 161–186. https://doi.org/10.1146/annurev-arplant-043014-114759

Almario, J., Muller, D., Défago, G., Moënne-Loccoz, Y., 2014. Rhizosphere ecology and phytoprotection in soils naturally suppressive to Thielaviopsis black root rot of tobacco. Environ. Microbiol. 16, 1949–1960. https://doi.org/10.1111/1462-2920.12459

Amaral-Zettler, L.A., Zettler, E.R., Mincer, T.J., 2020. Ecology of the plastisphere. Nat. Rev. Microbiol. 18, 139–151. https://doi.org/10.1038/s41579-019-0308-0

Andrade, O., Campillo, R., Peyrelongue, A., Barrientos, L., 2011. Soils suppressive against Gaeumannomyces graminis var. tritici identified under wheat crop monoculture in southern Chile. Cienc. E Investig. Agrar. 38, 345–356. https://doi.org/10.4067/S0718-16202011000300004

Andrade, O.A., Mathre, D.E., Sands, D.C., 1994. Suppression of Gaeumannomyces graminis var. tritici in Montana soils and its transferability between soils. Soil Biol. Biochem. 26, 397–402. https://doi.org/10.1016/0038-0717(94)90289-5

Andrews, S., 2015. FastQC: A Quality Control Tool for High Throughput Sequence Data [Online] [WWW Document]. URL https://qubeshub.org/resources/fastqc

AntiSMASH results [WWW Document], 2021. URL https://bioinformatics.nl/~traca001/rhizo_antismash/antismash_de_contigs/ (accessed 1.19.21).

Antonissen, G., Martel, A., Pasmans, F., Ducatelle, R., Verbrugghe, E., Vandenbroucke, V., Li, S.J., Haesebrouck, F., Van Immerseel, F., Croubels, S., 2014. The Impact of Fusarium Mycotoxins on Human and Animal Host Susceptibility to Infectious Diseases. Toxins 6, 430–452. https://doi.org/10.3390/toxins6020430

Arif, I., Batool, M., Schenk, P.M., 2020. Plant Microbiome Engineering: Expected Benefits for Improved Crop Growth and Resilience. Trends Biotechnol. 38, 1385–1396. https://doi.org/10.1016/j.tibtech.2020.04.015

Atkinson, G.F., 1892. Some Diseases of Cotton. Agricultural Experiment Station of the Agricultural and Mechanical College.

Audenaert, K., Pattery, T., Cornelis, P., Höfte, M., 2002. Induction of systemic resistance to Botrytis cinerea in tomato by Pseudomonas aeruginosa 7NSK2: role of salicylic acid, pyochelin, and pyocyanin. Mol. Plant-Microbe Interact. MPMI 15, 1147–1156. https://doi.org/10.1094/MPMI.2002.15.11.1147

Ayuso-Sacido, A., Genilloud, O., 2005. New PCR primers for the screening of NRPS and PKS-I systems in actinomycetes: detection and distribution of these biosynthetic gene sequences in major taxonomic groups. Microb Ecol 49, 10–24. https://doi.org/10.1007/s00248-004-0249-6

Babalola, O.O., 2010. Beneficial bacteria of agricultural importance. Biotechnol. Lett. 32, 1559–1570. https://doi.org/10.1007/s10529-010-0347-0

Baker, K.F., Cook, R.J., 1982. Biological Control of Plant Pathogens. American Phytopathological Society.

Baker, R., Elad, Y., Sneh, B., 1986. Physical, Biological and Host Factors in Iron Competition in Soils, in: Swinburne, T.R. (Ed.), Iron, Siderophores, and Plant Diseases, NATO ASI Series. Springer US, Boston, MA, pp. 77–84. https://doi.org/10.1007/978-1-4615-9480-2_10

Bakker, P.A.H.M., Berendsen, R.L., Doornbos, R.F., Wintermans, P.C.A., Pieterse, C.M.J., 2013. The rhizosphere revisited: root microbiomics. Front. Plant Sci. 4. https://doi.org/10.3389/fpls.2013.00165

Bakker, P.A.H.M., Ran, L.X., Pieterse, C.M.J., Loon, L.C. van, 2003. Understanding the involvement of rhizobacteria-mediated induction of systemic resistance in biocontrol of plant diseases. Can. J. Plant Pathol. 25, 5–9. https://doi.org/10.1080/07060660309507043

Barghouthi, S., Young, R., Olson, M.O., Arceneaux, J.E., Clem, L.W., Byers, B.R., 1989. Amonabactin, a novel tryptophan- or phenylalanine-containing phenolate siderophore in Aeromonas hydrophila. J. Bacteriol. 171, 1811–1816.

Barnett, S., Zhao, S., Ballard, R., Franco, C., 2017. Selection of microbes for control of Rhizoctonia root rot on wheat using a high throughput pathosystem. Biol. Control 113, 45–57. https://doi.org/10.1016/j.biocontrol.2017.07.003

Belknap, K.C., Park, C.J., Barth, B.M., Andam, C.P., 2020. Genome mining of biosynthetic and chemotherapeutic gene clusters in Streptomyces bacteria. Sci. Rep. 10, 2003. https://doi.org/10.1038/s41598-020-58904-9

Berg, G., 2009. Plant-microbe interactions promoting plant growth and health: perspectives for controlled use of microorganisms in agriculture. Appl. Microbiol. Biotechnol. 84, 11–18. https://doi.org/10.1007/s00253-009-2092-7

Berg, G., Köberl, M., Rybakova, D., Müller, H., Grosch, R., Smalla, K., 2017. Plant microbial diversity is suggested as the key to future biocontrol and health trends. FEMS Microbiol. Ecol. 93. https://doi.org/10.1093/femsec/fix050

Berg, G., Smalla, K., 2009. Plant species and soil type cooperatively shape the structure and function of microbial communities in the rhizosphere. FEMS Microbiol. Ecol. 68, 1–13. https://doi.org/10.1111/j.1574-6941.2009.00654.x

Bergsma-Vlami, M., Prins, M.E., Raaijmakers, J.M., 2005. Influence of plant species on population dynamics, genotypic diversity and antibiotic production in the rhizosphere by indigenous Pseudomonas spp. FEMS Microbiol. Ecol. 52, 59–69. https://doi.org/10.1016/j.femsec.2004.10.007

Blaser, M.J., 2016. Antibiotic use and its consequences for the normal microbiome. Science 352, 544–545. https://doi.org/10.1126/science.aad9358

Blin, K., Shaw, S., Kautsar, S.A., Medema, M.H., Weber, T., 2020. The antiSMASH database version 3: increased taxonomic coverage and new query features for modular enzymes. Nucleic Acids Res. https://doi.org/10.1093/nar/gkaa978

Blin, K., Shaw, S., Steinke, K., Villebro, R., Ziemert, N., Lee, S.Y., Medema, M.H., Weber, T., 2019. antiSMASH 5.0: updates to the secondary metabolite genome mining pipeline. Nucleic Acids Res. 47, W81–W87. https://doi.org/10.1093/nar/gkz310

Blom, D., Fabbri, C., Eberl, L., Weisskopf, L., 2011. Volatile-Mediated Killing of Arabidopsis thaliana by Bacteria Is Mainly Due to Hydrogen Cyanide. Appl. Environ. Microbiol. 77, 1000–1008. https://doi.org/10.1128/Aem.01968-10

Bohac, T.J., Fang, L., Giblin, D.E., Wencewicz, T.A., 2019. Fimsbactin and Acinetobactin Compete for the Periplasmic Siderophore Binding Protein BauB in Pathogenic Acinetobacter baumannii. ACS Chem. Biol. 14, 674–687. https://doi.org/10.1021/acschembio.8b01051

Bokulich, N.A., Kaehler, B.D., Rideout, J.R., Dillon, M., Bolyen, E., Knight, R., Huttley, G.A., Caporaso, J.G., 2018. Optimizing taxonomic classification of marker-gene amplicon sequences with QIIME 2 ' s q2-feature-classifier plugin. Microbiome 6. https://doi.org/10.1186/s40168-018-0470-z

Bolger, A.M., Lohse, M., Usadel, B., 2014. Trimmomatic: a flexible trimmer for Illumina sequence data. Bioinformatics 30, 2114–2120. https://doi.org/10.1093/bioinformatics/btu170

Bolyen, E., Rideout, J.R., Dillon, M.R., Bokulich, N.A., Abnet, C.C., Al-Ghalith, G.A., Alexander, H., Alm, E.J., Arumugam, M., Asnicar, F., Bai, Y., Bisanz, J.E., Bittinger, K., Brejnrod, A., Brislawn, C.J., Brown, C.T., Callahan, B.J., Caraballo-Rodríguez, A.M., Chase, J., Cope, E.K., Da Silva, R., Diener, C., Dorrestein, P.C., Douglas, G.M., Durall, D.M., Duvallet, C., Edwardson, C.F., Ernst, M., Estaki, M., Fouquier, J., Gauglitz, J.M., Gibbons, S.M., Gibson, D.L., Gonzalez, A., Gorlick, K., Guo, J., Hillmann, B., Holmes, S., Holste, H., Huttenhower, C., Huttley, G.A., Janssen, S., Jarmusch, A.K., Jiang, L., Kaehler, B.D., Kang, K.B., Keefe, C.R., Keim, P., Kelley, S.T., Knights, D., Koester, I., Kosciolek, T., Kreps, J., Langille, M.G.I., Lee, J., Ley, R., Liu, Y.-X., Loftfield, E., Lozupone, C., Maher, M., Marotz, C., Martin, B.D., McDonald, D., McIver, L.J., Melnik, A.V., Metcalf, J.L., Morgan, S.C., Morton, J.T., Naimey, A.T., Navas-Molina, J.A., Nothias, L.F., Orchanian, S.B., Pearson, T., Peoples, S.L., Petras, D., Preuss, M.L., Pruesse, E., Rasmussen, L.B., Rivers, A., Robeson, M.S., Rosenthal, P., Segata, N., Shaffer, M., Shiffer, A., Sinha, R., Song, S.J., Spear, J.R., Swafford, A.D., Thompson, L.R., Torres, P.J., Trinh, P., Tripathi, A., Turnbaugh, P.J., Ul-Hasan, S., van der Hooft, J.J.J., Vargas, F., Vázquez-Baeza, Y.,

Vogtmann, E., von Hippel, M., Walters, W., Wan, Y., Wang, M., Warren, J., Weber, K.C., Williamson, C.H.D., Willis, A.D., Xu, Z.Z., Zaneveld, J.R., Zhang, Y., Zhu, Q., Knight, R., Caporaso, J.G., 2019. Reproducible, interactive, scalable and extensible microbiome data science using QIIME 2. Nat. Biotechnol. 37, 852–857. https://doi.org/10.1038/s41587-019-0209-9

Bosland, P.W., 1988. Fusarium Oxysporum, a Pathogen of Many Plant Species, in: Sidhu, G.S. (Ed.), Advances in Plant Pathology, Genetics of Plant Pathogenic Fungi. Academic Press, pp. 281–289. https://doi.org/10.1016/B978-0-12-033706-4.50023-2

Boyer, F., Fichant, G., Berthod, J., Vandenbrouck, Y., Attree, I., 2009. Dissecting the bacterial type VI secretion system by a genome wide in silico analysis: what can be learned from available microbial genomic resources? BMC Genomics 10, 104. https://doi.org/10.1186/1471-2164-10-104

Brilli, F., Loreto, F., Baccelli, I., 2019. Exploiting Plant Volatile Organic Compounds (VOCs) in Agriculture to Improve Sustainable Defense Strategies and Productivity of Crops. Front. Plant Sci. 10. https://doi.org/10.3389/fpls.2019.00264

Brussaard, L., 2012. Ecosystem Services Provided by the Soil Biota, Soil Ecology and Ecosystem Services. Oxford University Press.

Buchfink, B., Xie, C., Huson, D.H., 2015. Fast and sensitive protein alignment using DIAMOND. Nat. Methods 12, 59–60. https://doi.org/10.1038/nmeth.3176

Bushnell, B., n.d. BBMap [WWW Document]. URL sourceforge.net/projects/bbmap/

Callahan, B. J., McMurdie, P.J., Rosen, M.J., Han, A.W., Johnson, A.J.A., Holmes, S.P., 2016. DADA2: High-resolution sample inference from Illumina amplicon data. Nat. Methods 13, 581. https://doi.org/10.1038/Nmeth.3869

Callahan, Benjamin J, McMurdie, P.J., Rosen, M.J., Han, A.W., Johnson, A.J.A., Holmes, S.P., 2016. DADA2: High resolution sample inference from Illumina amplicon data. Nat. Methods 13, 581–583. https://doi.org/10.1038/nmeth.3869

Campbell, B., Beare, D., Bennett, E., Hall-Spencer, J., Ingram, J., Jaramillo, F., Ortiz, R., Ramankutty, N., Sayer, J., Shindell, D., 2017. Agriculture production as a major driver of the Earth system exceeding planetary boundaries. Ecol. Soc. 22. https://doi.org/10.5751/ES-09595-220408

Caporaso, J.G., Kuczynski, J., Stombaugh, J., Bittinger, K., Bushman, F.D., Costello, E.K., Fierer, N., Pena, A.G., Goodrich, J.K., Gordon, J.I., Huttley, G.A., Kelley, S.T., Knights, D., Koenig, J.E., Ley, R.E., Lozupone, C.A., McDonald, D., Muegge, B.D., Pirrung, M., Reeder, J., Sevinsky, J.R., Tumbaugh, P.J., Walters, W.A., Widmann, J., Yatsunenko, T., Zaneveld, J., Knight, R., 2010. QIIME allows analysis of high-throughput community sequencing data. Nat. Methods 7, 335–336. https://doi.org/10.1038/nmeth.f.303

Carrion, V.J., Cordovez, V., Tyc, O., Etalo, D.W., de Bruijn, I., de Jager, V.C.L., Medema, M.H., Eberl, L., Raaijmakers, J.M., 2018. Involvement of Burkholderiaceae and sulfurous volatiles in disease-suppressive soils. ISME J 12, 2307–2321. https://doi.org/10.1038/s41396-018-0186-x

Carrión, V.J., Perez-Jaramillo, J., Cordovez, V., Tracanna, V., Hollander, M. de, Ruiz-Buck, D., Mendes, L.W., Ijcken, W.F.J. van, Gomez-Exposito, R., Elsayed, S.S., Mohanraju, P., Arifah, A., Oost, J. van der, Paulson, J.N., Mendes, R., Wezel, G.P.

van, Medema, M.H., Raaijmakers, J.M., 2019. Pathogen-induced activation of disease-suppressive functions in the endophytic root microbiome. Science 366, 606–612. https://doi.org/10.1126/science.aaw9285

Cawoy, H., Debois, D., Franzil, L., Pauw, E.D., Thonart, P., Ongena, M., 2015. Lipopeptides as main ingredients for inhibition of fungal phytopathogens by Bacillus subtilis/amyloliquefaciens. Microb. Biotechnol. 8, 281–295. https://doi.org/10.1111/1751-7915.12238

Cha, J.Y., Han, S., Hong, H.J., Cho, H., Kim, D., Kwon, Y., Kwon, S.K., Crusemann, M., Lee, Y.B., Kim, J.F., Giaever, G., Nislow, C., Moore, B.S., Thomashow, L.S., Weller, D.M., Kwak, Y.S., 2016. Microbial and biochemical basis of a Fusarium wilt-suppressive soil. ISME J 10, 119–129. https://doi.org/10.1038/ismej.2015.95

Chae, D.-H., Kim, D.-R., Cheong, M.S., Lee, Y.B., Kwak, Y.-S., 2020. Investigating the Induced Systemic Resistance Mechanism of 2,4-Diacetylphloroglucinol (DAPG) using DAPG Hydrolase-Transgenic Arabidopsis. Plant Pathol. J. 36, 255–266. https://doi.org/10.5423/PPJ.OA.02.2020.0031

Chaparro, J.M., Sheflin, A.M., Manter, D.K., Vivanco, J.M., 2012. Manipulating the soil microbiome to increase soil health and plant fertility. Biol. Fertil. Soils 48, 489–499. https://doi.org/10.1007/s00374-012-0691-4

Chapelle, E., Mendes, R., Bakker, P.A.H., Raaijmakers, J.M., 2016. Fungal invasion of the rhizosphere microbiome. ISME J. 10, 265–268. https://doi.org/10.1038/ismej.2015.82

Charlop-Powers, Z., Owen, J.G., Reddy, B.V.B., Ternei, M., Guimaraes, D.O., de Frias, U.A., Pupo, M.T., Seepe, P., Feng, Z.Y., Brady, S.F., 2015. Global Biogeographic Sampling of Bacterial Secondary Metabolism. Elife 4. https://doi.org/10.7554/eLife.05048

Chen, Q.-L., An, X.-L., Li, H., Zhu, Y.-G., Su, J.-Q., Cui, L., 2017. Do manure-borne or indigenous soil microorganisms influence the spread of antibiotic resistance genes in manured soil? Soil Biol. Biochem. 114, 229–237. https://doi.org/10.1016/j.soilbio.2017.07.022

Chen, Q.-L., An, X.-L., Zheng, B.-X., Gillings, M., Peñuelas, J., Cui, L., Su, J.-Q., Zhu, Y.-G., 2019. Loss of soil microbial diversity exacerbates spread of antibiotic resistance. Soil Ecol. Lett. 1, 3–13. https://doi.org/10.1007/s42832-019-0011-0

Chen, Q.-L., Ding, J., Zhu, Y.-G., He, J.-Z., Hu, H.-W., 2020. Soil bacterial taxonomic diversity is critical to maintaining the plant productivity. Environ. Int. 140, 105766. https://doi.org/10.1016/j.envint.2020.105766

Chewning, S.S., Grant, D.L., O'Banion, B.S., Gates, A.D., Kennedy, B.J., Campagna, S.R., Lebeis, S.L., 2019. Root-Associated Streptomyces Isolates Harboring melC Genes Demonstrate Enhanced Plant Colonization. Phytobiomes J. 3, 165–176. https://doi.org/10.1094/PBIOMES-01-19-0005-R

Chng, S., Cromey, M.G., Dodd, S.L., Stewart, A., Butler, R.C., Jaspers, M.V., 2015. Take-all decline in New Zealand wheat soils and the microorganisms associated with the potential mechanisms of disease suppression. Plant Soil 397, 239–259. https://doi.org/10.1007/s11104-015-2620-4

Cho, G., Kim, J., Park, C.G., Nislow, C., Weller, D.M., Kwak, Y.S., 2017. Caryolan-1-ol, an antifungal volatile produced by Streptomyces spp., inhibits the endomembrane system of fungi. Open Biol. 7. https://doi.org/ARTN 170075 10.1098/rsob.170075

Chong, J., Soufan, O., Li, C., Caraus, I., Li, S.Z., Bourque, G., Wishart, D.S., Xia, J.G., 2018. MetaboAnalyst 4.0: towards more transparent and integrative metabolomics analysis. Nucleic Acids Res. 46, W486–W494. https://doi.org/10.1093/nar/gky310

Cook, R.J., Baker, K.F., 1983. The Nature and Practice of Biological Control of Plant Pathogens. American Phytopathological Society.

Cook, R.J., Rovira, A.D., 1976. The role of bacteria in the biological control of Gaeumannomyces graminis by suppressive soils. Soil Biol. Biochem. 8, 269–273. https://doi.org/10.1016/0038-0717(76)90056-0

Cook, R.J., Schillinger, W.F., Christensen, N.W., 2002. Rhizoctonia root rot and take-all of wheat in diverse direct-seed spring cropping systems. Can. J. Plant Pathol. 24, 349–358. https://doi.org/10.1080/07060660209507020

Cordero, R.J., Casadevall, A., 2017. Functions of fungal melanin beyond virulence. Fungal Biol. Rev. 31, 99–112. https://doi.org/10.1016/j.fbr.2016.12.003

Cordovez, V., Carrion, V.J., Etalo, D.W., Mumm, R., Zhu, H., van Wezel, G.P., Raaijmakers, J.M., 2015. Diversity and functions of volatile organic compounds produced by Streptomyces from a disease-suppressive soil. Front Microbiol 6. https://doi.org/ARTN 1081 10.5589/fmicb.2015.01081

Cordovez, Viviane, Carrion, V.J., Etalo, D.W., Mumm, R., Zhu, H., van Wezel, G.P., Raaijmakers, J.M., 2015. Diversity and functions of volatile organic compounds produced by Streptomyces from a disease-suppressive soil. Front. Microbiol. 6. https://doi.org/10.3389/fmicb.2015.01081

Cordovez, V., Dini-Andreote, F., Carrión, V.J., Raaijmakers, J.M., 2019. Ecology and Evolution of Plant Microbiomes. Annu. Rev. Microbiol. 73, 69–88. https://doi.org/10.1146/annurev-micro-090817-062524

Costa, O.Y.A., de Hollander, M., Pijl, A., Liu, B., Kuramae, E.E., 2020. Cultivation-independent and cultivation-dependent metagenomes reveal genetic and enzymatic potential of microbial community involved in the degradation of a complex microbial polymer. Microbiome 8, 76. https://doi.org/10.1186/s40168-020-00836-7

Costa, O.Y.A., Raaijmakers, J.M., Kuramae, E.E., 2018. Microbial Extracellular Polymeric Substances: Ecological Function and Impact on Soil Aggregation. Front. Microbiol. 9. https://doi.org/10.3389/fmicb.2018.01636

Coulthurst, S.J., 2013. The Type VI secretion system – a widespread and versatile cell targeting system. Res. Microbiol., Bacterial secretion systems: function and structural biology 164, 640–654. https://doi.org/10.1016/j.resmic.2013.03.017

Cragg, G.M., Newman, D.J., 2013. Natural products: A continuing source of novel drug leads. Biochim. Biophys. Acta BBA - Gen. Subj. 1830, 3670–3695. https://doi.org/10.1016/j.bbagen.2013.02.008

Crits-Christoph, A., Diamond, S., Butterfield, C.N., Thomas, B.C., Banfield, J.F., 2018. Novel soil bacteria possess diverse genes for secondary metabolite biosynthesis. Nature 558, 440–444. https://doi.org/10.1038/s41586-018-0207-y

Cui, W., Han, L., Suo, F., Liu, Z., Zhou, L., Zhou, Z., 2018. Exploitation of Bacillus subtilis as a robust workhorse for production of heterologous proteins and beyond. World J. Microbiol. Biotechnol. 34, 145. https://doi.org/10.1007/s11274-018-2531-7

Cycoń, M., Mrozik, A., Piotrowska-Seget, Z., 2019. Antibiotics in the Soil Environment—Degradation and Their Impact on Microbial Activity and Diversity. Front. Microbiol. 10. https://doi.org/10.3389/fmicb.2019.00338

de Boer, W., Klein Gunnewiek, P.J.A., Lafeber, P., Janse, J.D., Spit, B.E., Woldendorp, J.W., 1998. Anti-fungal properties of chitinolytic dune soil bacteria. Soil Biol. Biochem. 30, 193–203. https://doi.org/10.1016/S0038-0717(97)00100-4

de Chaves, M.G., Silva, G.G.Z., Rossetto, R., Edwards, R.A., Tsai, S.M., Navarrete, A.A., 2019. Acidobacteria Subgroups and Their Metabolic Potential for Carbon Degradation in Sugarcane Soil Amended With Vinasse and Nitrogen Fertilizers. Front. Microbiol. 10. https://doi.org/10.3389/fmicb.2019.01680

de Souza Machado, A.A., Lau, C.W., Till, J., Kloas, W., Lehmann, A., Becker, R., Rillig, M.C., 2018. Impacts of Microplastics on the Soil Biophysical Environment. Environ. Sci. Technol. 52, 9656–9665. https://doi.org/10.1021/acs.est.8b02212

Deacon, J.W., 1984. The Nature and Practice of Biological-Control of Plant-Pathogens - Cook,Rj, Baker,Kf. Nature 309, 732–732. https://doi.org/DOI 10.1038/309732a0

Dean, R., Van Kan, J.A., Pretorius, Z.A., Hammond-Kosack, K.E., Di Pietro, A., Spanu, P.D., Rudd, J.J., Dickman, M., Kahmann, R., Ellis, J., Foster, G.D., 2012. The Top 10 fungal pathogens in molecular plant pathology. Mol Plant Pathol 13, 414–30. https://doi.org/10.1111/j.1364-3703.2011.00783.x

del Barrio-Duque, A., Ley, J., Samad, A., Antonielli, L., Sessitsch, A., Compant, S., 2019. Beneficial Endophytic Bacteria-Serendipita indica Interaction for Crop Enhancement and Resistance to Phytopathogens. Front. Microbiol. 10. https://doi.org/10.3389/fmicb.2019.02888

Díaz-Zorita, M., Perfect, E., Grove, J.H., 2002. Disruptive methods for assessing soil structure. Soil Tillage Res., Soil Fragmentation and Seedbed Characterization 64, 3–22. https://doi.org/10.1016/S0167-1987(01)00254-9

Dong, X., Rao, D., Tian, L., Wang, Q., Yang, K., 2020. A slurry microcosm study on the interaction between antibiotics and soil bacterial community. Heliyon 6, e03348. https://doi.org/10.1016/j.heliyon.2020.e03348

Donn, S., Almario, J., Mullerc, D., Moenne-Loccoz, Y., Gupta, V.V.S.R., Kirkegaard, J.A., Richardson, A.E., 2014. Rhizosphere microbial communities associated with Rhizoctonia damage at the field and disease patch scale. Appl. Soil Ecol. 78, 37–47. https://doi.org/10.1016/j.apsoil.2014.02.001

Duijff, B.J., Bakker, P.A.H.M., Schippers, B., 1994. Suppression of fusarium wilt of carnation by Pseudomonas putida WCS358 at different levels of disease incidence and iron availability. Biocontrol Sci. Technol. 4, 279–288. https://doi.org/10.1080/09583159409355336

Duijff, B.J., Recorbet, G., Bakker, P.A.H.M., Loper, J.E., Lemanceau, P., 1999. Microbial antagonism at the root level is involved in the suppression of Fusarium wilt by the combination of nonpathogenic Fusarium oxysporum Fo47 and Pseudomonas putida WCS358. Phytopathology 89, 1073–1079. https://doi.org/Doi 10.1094/Phyto.1999.89.11.1073

Duran, P., Jorquera, M., Viscardi, S., Carrion, V.J., Mora, M.D., Pozo, M.J., 2017. Screening and Characterization of Potentially Suppressive Soils against Gaeumannomyces graminis under Extensive Wheat Cropping by Chilean Indigenous Communities. Front Microbiol 8. https://doi.org/ARTN 1552 10.3389/fmicb.2017.01552

Effmert, U., Kalderas, J., Warnke, R., Piechulla, B., 2012. Volatile Mediated Interactions Between Bacteria and Fungi in the Soil. J. Chem. Ecol. 38, 665–703. https://doi.org/10.1007/s10886-012-0135-5

Eichorst, S.A., Trojan, D., Roux, S., Herbold, C., Rattei, T., Woebken, D., 2018. Genomic insights into the Acidobacteria reveal strategies for their success in terrestrial environments. Environ. Microbiol. 20, 1041–1063. https://doi.org/10.1111/1462-2920.14043

El-Gebali, S., Mistry, J., Bateman, A., Eddy, S.R., Luciani, A., Potter, S.C., Qureshi, M., Richardson, L.J., Salazar, G.A., Smart, A., Sonnhammer, E.L.L., Hirsh, L., Paladin, L., Piovesan, D., Tosatto, S.C.E., Finn, R.D., 2019. The Pfam protein families database in 2019. Nucleic Acids Res. 47, D427–D432. https://doi.org/10.1093/nar/gky995

El-Naggar, N.E.-A., El-Ewasy, S.M., 2017. Bioproduction, characterization, anticancer and antioxidant activities of extracellular melanin pigment produced by newly isolated microbial cell factories Streptomyces glaucescens NEAE-H. Sci. Rep. 7. https://doi.org/10.1038/srep42129

Eren, A.M., Esen, Ö.C., Quince, C., Vineis, J.H., Morrison, H.G., Sogin, M.L., Delmont, T.O., 2015. Anvi'o: an advanced analysis and visualization platform for 'omics data. PeerJ 3, e1319. https://doi.org/10.7717/peerj.1319

Espí, E., Salmerón, A., Fontecha, A., García, Y., Real, A.I., 2006. PLastic Films for Agricultural Applications. J. Plast. Film Sheeting 22, 85–102. https://doi.org/10.1177/8756087906064220

Felnagle, E.A., Jackson, E.E., Chan, Y.A., Podevels, A.M., Berti, A.D., McMahon, M.D., Thomas, M.G., 2008. Nonribosomal Peptide Synthetases Involved in the Production of Medically Relevant Natural Products. Mol. Pharm. 5, 191–211. https://doi.org/10.1021/mp700137g

Food and Agriculture Organisation of the United Nations [WWW Document], 2020. . http://faostat.fao.org/. URL http://faostat.fao.org/

Francino, M.P., 2016. Antibiotics and the Human Gut Microbiome: Dysbioses and Accumulation of Resistances. Front. Microbiol. 6. https://doi.org/10.3389/fmicb.2015.01543

Fuller, S., Gautam, A., 2016. A Procedure for Measuring Microplastics using Pressurized Fluid Extraction. Environ. Sci. Technol. 50, 5774–5780. https://doi.org/10.1021/acs.est.6b00816

Garbeva, P., Hol, W.H.G., Termorshuizen, A.J., Kowalchuk, G.A., de Boer, W., 2011. Fungistasis and general soil biostasis - A new synthesis. Soil Biol. Biochem. 43, 469–477. https://doi.org/10.1016/j.soilbio.2010.11.020

Garbeva, P., Hordijk, C., Gerards, S., de Boer, W., 2014a. Volatiles produced by the mycophagous soil bacterium Collimonas. Fems Microbiol. Ecol. 87, 639–649. https://doi.org/10.1111/1574-6941.12252

Garbeva, P., Hordijk, C., Gerards, S., de Boer, W., 2014b. Volatiles produced by the mycophagous soil bacterium Collimonas. FEMS Microbiol Ecol 87, 639–649. https://doi.org/10.1111/1574-6941.12252

Garbeva, P., Postma, J., van Veen, J.A., van Elsas, J.D., 2006. Effect of above-ground plant species on soil microbial community structure and its impact on suppression of Rhizoctonia solani AG3. Environ. Microbiol. 8, 233–246. https://doi.org/10.1111/j.1462-2920.2005.00888.x

Garbeva, P., van Veen, J.A., van Elsas, J.D., 2004. Microbial diversity in soil: selection microbial populations by plant and soil type and implications for disease suppressiveness. Annu. Rev. Phytopathol. 42, 243–270. https://doi.org/10.1146/annurev.phyto.42.012604.135455

Garland, J.L., Lehman, R.M., 1999. Dilution/extinction of community phenotypic characters to estimate relative structural diversity in mixed communities. FEMS Microbiol. Ecol. 30, 333–343. https://doi.org/10.1111/j.1574-6941.1999.tb00661.x

Gerlagh, M., 1968. Introduction of Ophiobolus graminis into new polders and its decline. Neth. J. Plant Pathol. 74, 1–97. https://doi.org/10.1007/BF02019999

Geudens, N., Martins, J.C., 2018. Cyclic Lipodepsipeptides From Pseudomonas spp. – Biological Swiss-Army Knives. Front. Microbiol. 9. https://doi.org/10.3389/fmicb.2018.01867

Ghorbani, R., Wilcockson, S., Koocheki, A., Leifert, C., 2009. Soil Management for Sustainable Crop Disease Control: A Review, in: Environmental Chemistry Letters. pp. 177–201. https://doi.org/10.1007/978-1-4020-9654-9_10

Girard, L., Höfte, M., Mot, R.D., 2020. Lipopeptide families at the interface between pathogenic and beneficial *Pseudomonas* -plant interactions. Crit. Rev. Microbiol. 46, 397–419. https://doi.org/10.1080/1040841X.2020.1794790

Godfray, H.C.J., Beddington, J.R., Crute, I.R., Haddad, L., Lawrence, D., Muir, J.F., Pretty, J., Robinson, S., Thomas, S.M., Toulmin, C., 2010. Food Security: The Challenge of Feeding 9 Billion People. Science 327, 812–818. https://doi.org/10.1126/science.1185383

Gomes Exposito, R., de Bruijn, I., Postma, J., Raaijmakers, J.M., 2017. Current Insights into the Role of Rhizosphere Bacteria in Disease Suppressive Soils. Front Microbiol 8. https://doi.org/ARTN 2529 10.3389/fmicb.2017.02529

Gómez Expósito, R., Postma, J., Raaijmakers, J.M., De Bruijn, I., 2015. Diversity and Activity of Lysobacter Species from Disease Suppressive Soils. Front. Microbiol. 6, 1243. https://doi.org/10.3389/fmicb.2015.01243

Gomez-Escribano, J.P., Bibb, M.J., 2011. Engineering Streptomyces coelicolor for heterologous expression of secondary metabolite gene clusters. Microb. Biotechnol. 4, 207–215. https://doi.org/10.1111/j.1751-7915.2010.00219.x

Goswami, R.S., Kistler, H.C., 2004. Heading for disaster: Fusarium graminearum on cereal crops. Mol. Plant Pathol. 5, 515–525. https://doi.org/10.1111/j.1364-3703.2004.00252.x

Gouda, S., Kerry, R.G., Das, G., Paramithiotis, S., Shin, H.-S., Patra, J.K., 2018. Revitalization of plant growth promoting rhizobacteria for sustainable development in agriculture. Microbiol. Res. 206, 131–140. https://doi.org/10.1016/j.micres.2017.08.016

Haas, D., Défago, G., 2005. Biological control of soil-borne pathogens by fluorescent pseudomonads. Nat. Rev. Microbiol. 3, 307–319. https://doi.org/10.1038/nrmicro1129

Hammerbacher, A., Coutinho, T.A., Gershenzon, J., 2019. Roles of plant volatiles in defence against microbial pathogens and microbial exploitation of volatiles. Plant Cell Environ. 42, 2827–2843. https://doi.org/10.1111/pce.13602

Han, A.W., Sandy, M., Fishman, B., Trindade-Silva, A.E., Soares, C.A.G., Distel, D.L., Butler, A., Haygood, M.G., 2013. Turnerbactin, a novel triscatecholate siderophore from the shipworm endosymbiont Teredinibacter turnerae T7901. PloS One 8, e76151. https://doi.org/10.1371/journal.pone.0076151

Hancock, E.N., Brown, M.K., 2021. Ladderane Natural Products: From the Ground Up. Chem. – Eur. J. 27, 565–576. https://doi.org/10.1002/chem.202002866

Harman, G.E., Howell, C.R., Viterbo, A., Chet, I., Lorito, M., 2004. Trichoderma species — opportunistic, avirulent plant symbionts. Nat. Rev. Microbiol. 2, 43–56. https://doi.org/10.1038/nrmicro797

Hartmann, A., Schmid, M., Tuinen, D. van, Berg, G., 2009. Plant-driven selection of microbes. Plant Soil 321, 235–257. https://doi.org/10.1007/s11104-008-9814-y

Hayden, H.L., Rochfort, S.J., Ezernieks, V., Savin, K.W., Mele, P.M., 2019. Metabolomics approaches for the discrimination of disease suppressive soils for Rhizoctonia solani AG8 in cereal crops using 1H NMR and LC-MS. Sci. Total Environ. 651, 1627–1638. https://doi.org/10.1016/j.scitotenv.2018.09.249

Hayden, H.L., Savin, K.W., Wadeson, J., Gupta, V., Mele, P.M., 2018. Comparative Metatranscriptomics of Wheat Rhizosphere Microbiomes in Disease Suppressive and Non-suppressive Soils for Rhizoctonia solani AG8. Front Microbiol 9, 859. https://doi.org/10.3389/fmicb.2018.00859

Hegan, D., Tong, L., Zhiquan, H., Qinming, S., Ru, L., 2015. Determining time limits of continuous film mulching and examining residual effects on cotton yield and soil properties. J. Environ. Biol. 36, e677–e684.

Herlemann, D.P.R., Labrenz, M., Jurgens, K., Bertilsson, S., Waniek, J.J., Andersson, A.F., 2011. Transitions in bacterial communities along the 2000 km salinity gradient of the Baltic Sea. Isme J. 5, 1571–1579. https://doi.org/10.1038/ismej.2011.41

Hjort, K., Presti, I., Elväng, A., Marinelli, F., Sjöling, S., 2014. Bacterial chitinase with phytopathogen control capacity from suppressive soil revealed by functional metagenomics. Appl. Microbiol. Biotechnol. 98, 2819–2828. https://doi.org/10.1007/s00253-013-5287-x

Hofer, U., 2018. The majority is uncultured. Nat. Rev. Microbiol. 16, 716–717. https://doi.org/10.1038/s41579-018-0097-x

Höfte, M., Bakker, P.A.H.M., 2007. Competition for Iron and Induced Systemic Resistance by Siderophores of Plant Growth Promoting Rhizobacteria, in: Varma, A., Chincholkar, S.B. (Eds.), Microbial Siderophores, Soil Biology. Springer, Berlin, Heidelberg, pp. 121–133. https://doi.org/10.1007/978-3-540-71160-5_6

Hol, W.H.G., Garbeva, P., Hordijk, C., Hundscheid, M.P.J., Gunnewiek, P.J.A.K., Agtmaal, M. van, Kuramae, E.E., Boer, W. de, 2015. Non-random species loss in bacterial communities reduces antifungal volatile production. Ecology 96, 2042–2048. https://doi.org/10.1890/14-2359.1

Hoper, H., Alabouvette, C., 1996. Importance of physical and chemical soil properties in the suppressiveness of soils to plant diseases. Eur. J. Soil Biol. 32, 41–58.

Hornby, D., 1983. Suppressive Soils. Annu Rev Phytopathol 21, 65–85. https://doi.org/DOI 10.1146/annurev.py.21.090183.000433

Hover, B.M., Kim, S.-H., Katz, M., Charlop-Powers, Z., Owen, J.G., Ternei, M.A., Maniko, J., Estrela, A.B., Molina, H., Park, S., Perlin, D.S., Brady, S.F., 2018. Culture-independent discovery of the malacidins as calcium-dependent antibiotics with activity against multidrug-resistant Gram-positive pathogens. Nat. Microbiol. 3, 415–422. https://doi.org/10.1038/s41564-018-0110-1

Huang, Y., Liu, Q., Jia, W., Yan, C., Wang, J., 2020. Agricultural plastic mulching as a source of microplastics in the terrestrial environment. Environ. Pollut. 260, 114096. https://doi.org/10.1016/j.envpol.2020.114096

Hunziker, L., Bonisch, D., Groenhagen, U., Bailly, A., Schulz, S., Weisskopf, L., 2015. Pseudomonas Strains Naturally Associated with Potato Plants Produce Volatiles with High Potential for Inhibition of Phytophthora infestans. Appl. Environ. Microbiol. 81, 821–830. https://doi.org/10.1128/Aem.02999-14

Hyatt, D., Chen, G.-L., LoCascio, P.F., Land, M.L., Larimer, F.W., Hauser, L.J., 2010. Prodigal: prokaryotic gene recognition and translation initiation site identification. BMC Bioinformatics 11, 119. https://doi.org/10.1186/1471-2105-11-119

Ilangumaran, G., Smith, D.L., 2017. Plant Growth Promoting Rhizobacteria in Amelioration of Salinity Stress: A Systems Biology Perspective. Front. Plant Sci. 8. https://doi.org/10.3389/fpls.2017.01768

Janvier, C., Villeneuve, F., Alabouvette, C., Edel-Hermann, V., Mateille, T., Steinberg, C., 2007. Soil health through soil disease suppression: Which strategy from descriptors to indicators? Soil Biol. Biochem. 39, 1–23. https://doi.org/10.1016/j.soilbio.2006.07.001

Jiang, X.J., Liu, W., Wang, E., Zhou, T., Xin, P., 2017. Residual plastic mulch fragments effects on soil physical properties and water flow behavior in the Minqin Oasis, northwestern China. Soil Tillage Res. 166, 100–107. https://doi.org/10.1016/j.still.2016.10.011

Jochum, M.D., McWilliams, K.L., Borrego, E.J., Kolomiets, M.V., Niu, G., Pierson, E.A., Jo, Y.-K., 2019. Bioprospecting Plant Growth-Promoting Rhizobacteria That Mitigate Drought Stress in Grasses. Front. Microbiol. 10. https://doi.org/10.3389/fmicb.2019.02106

Johnson, K.B., 1994. Dose-Response Relationship and Inundative Biological Control. Phytopathology.

Jones, D.L., Nguyen, C., Finlay, R.D., 2009. Carbon flow in the rhizosphere: carbon trading at the soil–root interface. Plant Soil 321, 5–33. https://doi.org/10.1007/s11104-009-9925-0

Jones, R.T., Robeson, M.S., Lauber, C.L., Hamady, M., Knight, R., Fierer, N., 2009. A comprehensive survey of soil acidobacterial diversity using pyrosequencing and clone library analyses. ISME J. 3, 442–453. https://doi.org/10.1038/ismej.2008.127

Jousset, A., Schulz, W., Scheu, S., Eisenhauer, N., 2011. Intraspecific genotypic richness and relatedness predict the invasibility of microbial communities. ISME J. 5, 1108–1114. https://doi.org/10.1038/ismej.2011.9

Jurburg, S.D., Nunes, I., Brejnrod, A., Jacquiod, S., Priemé, A., Sørensen, S.J., Van Elsas, J.D., Salles, J.F., 2017a. Legacy Effects on the Recovery of Soil Bacterial Communities from Extreme Temperature Perturbation. Front. Microbiol. 8. https://doi.org/10.3389/fmicb.2017.01832

Jurburg, S.D., Nunes, I., Stegen, J.C., Le Roux, X., Priemé, A., Sørensen, S.J., Salles, J.F., 2017b. Autogenic succession and deterministic recovery following disturbance in soil bacterial communities. Sci. Rep. 7. https://doi.org/10.1038/srep45691

Kalam, S., Basu, A., Ahmad, I., Sayyed, R.Z., El-Enshasy, H.A., Dailin, D.J., Suriani, N.L., 2020. Recent Understanding of Soil Acidobacteria and Their Ecological Significance: A Critical Review. Front. Microbiol. 11. https://doi.org/10.3389/fmicb.2020.580024

Kanehisa, M., Furumichi, M., Tanabe, M., Sato, Y., Morishima, K., 2017. KEGG: new perspectives on genomes, pathways, diseases and drugs. Nucleic Acids Res. 45, D353–D361. https://doi.org/10.1093/nar/gkw1092

Kang, D., Li, F., Kirton, E.S., Thomas, A., Egan, R.S., An, H., Wang, Z., 2019. MetaBAT 2: an adaptive binning algorithm for robust and efficient genome reconstruction from metagenome assemblies (No. e27522v1). PeerJ Inc. https://doi.org/10.7287/peerj.preprints.27522v1

Kasirajan, S., Ngouajio, M., 2012. Polyethylene and biodegradable mulches for agricultural applications: a review. Agron. Sustain. Dev. 32, 501–529. https://doi.org/10.1007/s13593-011-0068-3

Kautsar, S.A., Blin, K., Shaw, S., Navarro-Muñoz, J.C., Terlouw, B.R., van der Hooft, J.J.J., van Santen, J.A., Tracanna, V., Suarez Duran, H.G., Pascal Andreu, V., Selem-Mojica, N., Alanjary, M., Robinson, S.L., Lund, G., Epstein, S.C., Sisto, A.C., Charkoudian, L.K., Collemare, J., Linington, R.G., Weber, T., Medema, M.H., 2020. MIBiG 2.0: a repository for biosynthetic gene clusters of known function. Nucleic Acids Res. 48, D454–D458. https://doi.org/10.1093/nar/gkz882

Kaymak, H.Ç., Güvenç, I., Yarali, F., Dönmez, M.F., 2009. The Effects of Bio-priming with PGPR on Germination of Radish (Raphanus sativus L.) Seeds under Saline Conditions [WWW Document]. undefined. URL /paper/The-Effects-of-Bio-priming-with-PGPR-on-Germination-Kaymak-G%C3%BCven%C3%A7/949056e344d291f93dc86a3315f4bf5845445473 (accessed 11.10.20).

Kenters, N., Henderson, G., Jeyanathan, J., Kittelmann, S., Janssen, P.H., 2011. Isolation of previously uncultured rumen bacteria by dilution to extinction using a new liquid culture medium. J. Microbiol. Methods 84, 52–60. https://doi.org/10.1016/j.mimet.2010.10.011

Kielak, A.M., Barreto, C.C., Kowalchuk, G.A., van Veen, J.A., Kuramae, E.E., 2016. The Ecology of Acidobacteria: Moving beyond Genes and Genomes. Front. Microbiol. 7. https://doi.org/10.3389/fmicb.2016.00744

Kim, D., Paggi, J.M., Park, C., Bennett, C., Salzberg, S.L., 2019. Graph-based genome alignment and genotyping with HISAT2 and HISAT-genotype. Nat. Biotechnol. 37, 907–915. https://doi.org/10.1038/s41587-019-0201-4

Kinkel, L.L., Bakker, M.G., Schlatter, D.C., 2011. A Coevolutionary Framework for Managing Disease-Suppressive Soils. Annu. Rev. Phytopathol. 49, 47–67. https://doi.org/10.1146/annurev-phyto-072910-095232

Kinkel, L.L., Schlatter, D.C., Bakker, M.G., Arenz, B.E., 2012. Streptomyces competition and co-evolution in relation to plant disease suppression. Res. Microbiol. 163, 490–499. https://doi.org/10.1016/j.resmic.2012.07.005

Kloepper, J.W., Leong, J., Teintze, M., Schroth, M.N., 1980. Enhanced plant growth by siderophores produced by plant growth-promoting rhizobacteria. Nature 286, 885–886. https://doi.org/10.1038/286885a0

Korenblum, E., Dong, Y., Szymanski, J., Panda, S., Jozwiak, A., Massalha, H., Meir, S., Rogachev, I., Aharoni, A., 2020. Rhizosphere microbiome mediates systemic root metabolite exudation by root-to-root signaling. Proc. Natl. Acad. Sci. https://doi.org/10.1073/pnas.1912130117

Kramer, J., Özkaya, Ö., Kümmerli, R., 2020. Bacterial siderophores in community and host interactions. Nat. Rev. Microbiol. 18, 152–163. https://doi.org/10.1038/s41579-019-0284-4

Kruijt, M., Tran, H., Raaijmakers, J.M., 2009. Functional, genetic and chemical characterization of biosurfactants produced by plant growth-promoting Pseudomonas putida 267. J. Appl. Microbiol. 107, 546–556. https://doi.org/10.1111/j.1365-2672.2009.04244.x

Kumar, A., Dubey, A., 2020. Rhizosphere microbiome: Engineering bacterial competitiveness for enhancing crop production. J. Adv. Res. 24, 337–352. https://doi.org/10.1016/j.jare.2020.04.014

Kurm, V., Geisen, S., Gera Hol, W.H., 2019. A low proportion of rare bacterial taxa responds to abiotic changes compared with dominant taxa. Environ. Microbiol. 21, 750–758. https://doi.org/10.1111/1462-2920.14492

Kwak, M.J., Kong, H.G., Choi, K., Kwon, S.K., Song, J.Y., Lee, J., Lee, P.A., Choi, S.Y., Seo, M., Lee, H.J., Jung, E.J., Park, H., Roy, N., Kim, H., Lee, M.M., Rubin, E.M., Lee, S.W., Kim, J.F., 2018. Rhizosphere microbiome structure alters to enable wilt resistance in tomato (vol 36, pg 1100, 2018). Nat. Biotechnol. 36, 1117–1117. https://doi.org/DOI 10.1038/nbt1118-1117

Kwak, Y.S., Han, S., Thomashow, L.S., Rice, J.T., Paulitz, T.C., Kim, D., Weller, D.M., 2011. Saccharomyces cerevisiae Genome-Wide Mutant Screen for Sensitivity to 2,4-Diacetylphloroglucinol, an Antibiotic Produced by Pseudomonas fluorescens. Appl. Environ. Microbiol. 77, 1770–1776. https://doi.org/10.1128/Aem.02151-10

Kwak, Y.S., Weller, D.M., 2013. Take-all of Wheat and Natural Disease Suppression: A Review. Plant Pathol. J. 29, 125–135. https://doi.org/10.5423/Ppj.Si.07.2012.0112

Lacombe-Harvey, M.-È., Brzezinski, R., Beaulieu, C., 2018. Chitinolytic functions in actinobacteria: ecology, enzymes, and evolution. Appl. Microbiol. Biotechnol. 102, 7219–7230. https://doi.org/10.1007/s00253-018-9149-4

Lagier, J.-C., Hugon, P., Khelaifia, S., Fournier, P.-E., Scola, B.L., Raoult, D., 2015. The Rebirth of Culture in Microbiology through the Example of Culturomics To Study Human Gut Microbiota. Clin. Microbiol. Rev. 28, 237–264. https://doi.org/10.1128/CMR.00014-14

Lam, K.N., Spanogiannopoulos, P., Soto-Perez, P., Alexander, M., Nalley, M.J., Bisanz, J.E., Yu, F.B., Turnbaugh, P.J., 2020. Phage-delivered CRISPR-Cas9 for strain-specific depletion and genomic deletions in the gut microbiota. bioRxiv 2020.07.09.193847. https://doi.org/10.1101/2020.07.09.193847

Landa, B.B., Mavrodi, O.V., Raaijmakers, J.M., Gardener, B.B.M., Thomashow, L.S., Weller, D.M., 2002. Differential ability of genotypes of 2,4-diacetylphloroglucinol-producing Pseudomonas fluorescens strains to colonize the roots of pea plants. Appl. Environ. Microbiol. 68, 3226–3237. https://doi.org/10.1128/Aem.68.7.3226-3237.2002

Lankenau, M.A., Patel, R., Liyanarachchi, S., Maharry, S.E., Hoag, K.W., Duggan, M., Walker, C.J., Markowitz, J., Carson, W.E., Eisfeld, A.K., de la Chapelle, A., 2015. MicroRNA-3151 inactivates TP53 in BRAF-mutated human malignancies. Proc Natl Acad Sci U A 112, E6744-51. https://doi.org/10.1073/pnas.1520390112

Larkin, R.P., 2015. Soil Health Paradigms and Implications for Disease Management. Annu. Rev. Phytopathol. 53, 199–221. https://doi.org/10.1146/annurev-phyto-080614-120357

Lee, S.-M., Kong, H.G., Song, G.C., Ryu, C.-M., 2020. Disruption of Firmicutes and Actinobacteria abundance in tomato rhizosphere causes the incidence of bacterial wilt disease. ISME J. https://doi.org/10.1038/s41396-020-00785-x

Lehmann, S., Serrano, M., L'Haridon, F., Tjamos, S.E., Metraux, J.-P., 2015. Reactive oxygen species and plant resistance to fungal pathogens. Phytochemistry, In Memory of G. Paul Bolwell: Plant Cell Wall Dynamics 112, 54–62. https://doi.org/10.1016/j.phytochem.2014.08.027

Lemanceau, P., Bakker, P., Jandekogel, W., Alabouvette, C., Schippers, B., 1993. Antagonistic Effect of Nonpathogenic Fusarium-Oxysporum Fo47 and Pseudobactin 358 Upon Pathogenic Fusarium-Oxysporum F-Sp Dianthi. Appl. Environ. Microbiol. 59, 74–82. https://doi.org/10.1128/AEM.59.1.74-82.1993

Lemanceau, P., Bakker, P.A., Kogel, W.J.D., Alabouvette, C., Schippers, B., 1992. Effect of pseudobactin 358 production by Pseudomonas putida WCS358 on suppression of fusarium wilt of carnations by nonpathogenic Fusarium oxysporum Fo47. Appl. Environ. Microbiol. 58, 2978–2982.

Lemanceau, P., Expert, D., Gaymard, F., Bakker, P.A.H.M., Briat, J.F., 2009. Role of Iron in Plant-Microbe Interaction. Adv. Bot. Res. 51, 491–549. https://doi.org/10.1016/S0065-2296(09)51012-9

Letunic, I., Bork, P., 2019. Interactive Tree Of Life (iTOL) v4: recent updates and new developments. Nucleic Acids Res. 47, W256–W259. https://doi.org/10.1093/nar/gkz239

Li, D., Luo, R., Liu, C.-M., Leung, C.-M., Ting, H.-F., Sadakane, K., Yamashita, H., Lam, T.-W., 2016. MEGAHIT v1.0: A fast and scalable metagenome assembler driven by advanced methodologies and community practices. Methods, Pan-omics analysis of biological data 102, 3–11. https://doi.org/10.1016/j.ymeth.2016.02.020

Li, H., Handsaker, B., Wysoker, A., Fennell, T., Ruan, J., Homer, N., Marth, G., Abecasis, G., Durbin, R., 1000 Genome Project Data Processing Subgroup, 2009. The Sequence Alignment/Map format and SAMtools. Bioinformatics 25, 2078–2079. https://doi.org/10.1093/bioinformatics/btp352

Libis, V., Antonovsky, N., Zhang, M., Shang, Z., Montiel, D., Maniko, J., Ternei, M.A., Calle, P.Y., Lemetre, C., Owen, J.G., Brady, S.F., 2019. Uncovering the biosynthetic potential of rare metagenomic DNA using co-occurrence network analysis of targeted sequences. Nat. Commun. 10, 3848. https://doi.org/10.1038/s41467-019-11658-z

Liu, D., Anderson, N.A., Kinkel, L.L., 2011. Selection and characterization of strains of Streptomyces suppressive to the potato scab pathogen. Can. J. Microbiol. https://doi.org/10.1139/m96-066

Liu, H., Brettell, L.E., Qiu, Z., Singh, B.K., 2020. Microbiome-Mediated Stress Resistance in Plants. Trends Plant Sci. 25, 733–743. https://doi.org/10.1016/j.tplants.2020.03.014

Lladó, S., Žifčáková, L., Větrovský, T., Eichlerová, I., Baldrian, P., 2016. Functional screening of abundant bacteria from acidic forest soil indicates the metabolic potential of Acidobacteria subdivision 1 for polysaccharide decomposition. Biol. Fertil. Soils 52, 251–260. https://doi.org/10.1007/s00374-015-1072-6

López-Ráez, J.A., Bouwmeester, H., 2008. Fine-tuning regulation of strigolactone biosynthesis under phosphate starvation. Plant Signal. Behav. 3, 963–965. https://doi.org/10.4161/psb.6126

Love, M.I., Huber, W., Anders, S., 2014. Moderated estimation of fold change and dispersion for RNA-seq data with DESeq2. Genome Biol. 15, 550. https://doi.org/10.1186/s13059-014-0550-8

Lozupone, C., Knight, R., 2005. UniFrac: a new phylogenetic method for comparing microbial communities. Appl. Environ. Microbiol. 71, 8228–8235. https://doi.org/10.1128/Aem.71.12.8228-8235.2005

Lugtenberg, B., Rozen, D.E., Kamilova, F., 2017. Wars between microbes on roots and fruits. F1000Research 6. https://doi.org/10.12688/f1000research.10696.1

MacMillan, J., 2001. Occurrence of Gibberellins in Vascular Plants, Fungi, and Bacteria. J. Plant Growth Regul. 20, 387–442. https://doi.org/10.1007/s003440010038

Mallon, C.A., Elsas, J.D. van, Salles, J.F., 2015. Microbial Invasions: The Process, Patterns, and Mechanisms. Trends Microbiol. 23, 719–729. https://doi.org/10.1016/j.tim.2015.07.013

Martin, M., 2011. Cutadapt removes adapter sequences from high-throughput sequencing reads. EMBnet.journal 17, 10–12. https://doi.org/10.14806/ej.17.1.200

Martínez-Núñez, M.A., López, V.E.L. y., 2016. Nonribosomal peptides synthetases and their applications in industry. Sustain. Chem. Process. 4, 13. https://doi.org/10.1186/s40508-016-0057-6

Martín-Sánchez, L., Ariotti, C., Garbeva, P., Vigani, G., 2020. Investigating the effect of belowground microbial volatiles on plant nutrient status: perspective and limitations. J. Plant Interact. 15, 188–195. https://doi.org/10.1080/17429145.2020.1776408

Mazurier, S., Corberand, T., Lemanceau, P., Raaijmakers, J.M., 2009. Phenazine antibiotics produced by fluorescent pseudomonads contribute to natural soil suppressiveness to Fusarium wilt. ISME J. 3, 977–991. https://doi.org/10.1038/ismej.2009.33

Mazzola, M., 2002. Mechanisms of natural soil suppressiveness to soilborne diseases. Antonie Van Leeuwenhoek Int. J. Gen. Mol. Microbiol. 81, 557–564. https://doi.org/Doi 10.1023/A:1020557523557

McDonald, B.A., Stukenbrock, E.H., 2016. Rapid emergence of pathogens in agro-ecosystems: global threats to agricultural sustainability and food security. Philos. Trans. R. Soc. B Biol. Sci. 371, 20160026. https://doi.org/10.1098/rstb.2016.0026

Medema, M.H., Cimermancic, P., Sali, A., Takano, E., Fischbach, M.A., 2014. A Systematic Computational Analysis of Biosynthetic Gene Cluster Evolution: Lessons for Engineering Biosynthesis. PLoS Comput. Biol. 10, e1004016. https://doi.org/10.1371/journal.pcbi.1004016

Mehrabi, Z., McMillan, V.E., Clark, I.M., Canning, G., Hammond-Kosack, K.E., Preston, G., Hirsch, P.R., Mauchline, T.H., 2016. Pseudomonas spp. diversity is negatively associated with suppression of the wheat take-all pathogen. Sci. Rep. 6, 29905. https://doi.org/10.1038/srep29905

Meleshko, D., Mohimani, H., Tracanna, V., Hajirasouliha, I., Medema, M.H., Korobeynikov, A., Pevzner, P.A., 2019. BiosyntheticSPAdes: reconstructing biosynthetic gene clusters from assembly graphs. Genome Res. 29, 1352–1362. https://doi.org/10.1101/gr.243477.118

Mendes, R., Garbeva, P., Raaijmakers, J.M., 2013. The rhizosphere microbiome: significance of plant beneficial, plant pathogenic, and human pathogenic microorganisms. FEMS Microbiol. Rev. 37, 634–663. https://doi.org/10.1111/1574-6976.12028

Mendes, R., Kruijt, M., Bruijn, I. de, Dekkers, E., Voort, M. van der, Schneider, J.H.M., Piceno, Y.M., DeSantis, T.Z., Andersen, G.L., Bakker, P.A.H.M., Raaijmakers, J.M., 2011. Deciphering the Rhizosphere Microbiome for Disease-Suppressive Bacteria. Science 332, 1097–1100. https://doi.org/10.1126/science.1203980

Michelsen, C.F., Watrous, J., Glaring, M.A., Kersten, R., Koyama, N., Dorrestein, P.C., Stougaard, P., 2015. Nonribosomal Peptides, Key Biocontrol Components for Pseudomonas fluorescens In5, Isolated from a Greenlandic Suppressive Soil. mBio 6. https://doi.org/10.1128/mBio.00079-15

Millati, R., Cahyono, R.B., Ariyanto, T., Azzahrani, I.N., Putri, R.U., Taherzadeh, M.J., 2019. Agricultural, Industrial, Municipal, and Forest Wastes: An Overview, in: Taherzadeh, M.J., Bolton, K., Wong, J., Pandey, A. (Eds.), Sustainable Resource Recovery and Zero Waste Approaches. Elsevier, pp. 1–22. https://doi.org/10.1016/B978-0-444-64200-4.00001-3

Minz, D., Ofek, M., Hadar, Y., 2013. Plant Rhizosphere Microbial Communities, in: Rosenberg, E., DeLong, E.F., Lory, S., Stackebrandt, E., Thompson, F. (Eds.), The Prokaryotes: Prokaryotic Communities and Ecophysiology. Springer, Berlin, Heidelberg, pp. 56–84. https://doi.org/10.1007/978-3-642-30123-0_38

Mistry, J., Finn, R.D., Eddy, S.R., Bateman, A., Punta, M., 2013. Challenges in homology search: HMMER3 and convergent evolution of coiled-coil regions. Nucleic Acids Res. 41, e121–e121. https://doi.org/10.1093/nar/gkt263

Mm, Y., Ss, W., Dv, M., Ov, M., D, von W., Ls, T., Jh, G., Dm, W., 2014. Biological control of wheat root diseases by the CLP-producing strain Pseudomonas fluorescens HC1-07. Phytopathology 104, 248–256. https://doi.org/10.1094/phyto-05-13-0142-r

Monjarás Feria, J., Valvano, M.A., 2020. An Overview of Anti-Eukaryotic T6SS Effectors. Front. Cell. Infect. Microbiol. 10, 584751. https://doi.org/10.3389/fcimb.2020.584751

Morella, N.M., Weng, F.C.-H., Joubert, P.M., Metcalf, C.J.E., Lindow, S., Koskella, B., 2020. Successive passaging of a plant-associated microbiome reveals robust habitat and host genotype-dependent selection. Proc. Natl. Acad. Sci. 117, 1148–1159. https://doi.org/10.1073/pnas.1908600116

Moretti, A., 2009. Taxonomy of Fusarium genus: A continuous fight between lumpers and splitters. Zb. Matice Srp. Za Prir. Nauke 7–13. https://doi.org/10.2298/ZMSPN0917007M

Mulwa, L.S., Jansen, R., Praditya, D.F., Mohr, K.I., Wink, J., Steinmann, E., Stadler, M., 2018. Six Heterocyclic Metabolites from the Myxobacterium Labilithrix luteola. Mol. Basel Switz. 23. https://doi.org/10.3390/molecules23030542

Navarrete, A.A., Soares, T., Rossetto, R., van Veen, J.A., Tsai, S.M., Kuramae, E.E., 2015. Verrucomicrobial community structure and abundance as indicators for changes in chemical factors linked to soil fertility. Antonie Van Leeuwenhoek 108, 741–752. https://doi.org/10.1007/s10482-015-0530-3

Naylor, D., Fansler, S., Brislawn, C., Nelson, W.C., Hofmockel, K.S., Jansson, J.K., McClure, R., 2020. Deconstructing the Soil Microbiome into Reduced-Complexity Functional Modules. mBio 11, e01349-20, /mbio/11/4/mBio.01349-20.atom. https://doi.org/10.1128/mBio.01349-20

NCBI Resource Coordinators, 2016. Database resources of the National Center for Biotechnology Information. Nucleic Acids Res. 44, D7-19. https://doi.org/10.1093/nar/gkv1290

Ng, E.-L., Huerta Lwanga, E., Eldridge, S.M., Johnston, P., Hu, H.-W., Geissen, V., Chen, D., 2018. An overview of microplastic and nanoplastic pollution in agroecosystems. Sci. Total Environ. 627, 1377–1388. https://doi.org/10.1016/j.scitotenv.2018.01.341

Nicault, M., Tidjani, A.-R., Gauthier, A., Dumarcay, S., Gelhaye, E., Bontemps, C., Leblond, P., 2020. Mining the Biosynthetic Potential for Specialized Metabolism of a Streptomyces Soil Community. Antibiotics 9. https://doi.org/10.3390/antibiotics9050271

Nielsen, L.K., Cook, D.J., Edwards, S.G., Ray, R.V., 2014. The prevalence and impact of Fusarium head blight pathogens and mycotoxins on malting barley quality in UK. Int. J. Food Microbiol. 179, 38–49. https://doi.org/10.1016/j.ijfoodmicro.2014.03.023

Nizzetto, L., Futter, M., Langaas, S., 2016a. Are Agricultural Soils Dumps for Microplastics of Urban Origin? Environ. Sci. Technol. 50, 10777–10779. https://doi.org/10.1021/acs.est.6b04140

Nizzetto, L., Langaas, S., Futter, M., 2016b. Pollution: Do microplastics spill on to farm soils? Nature 537, 488–488. https://doi.org/10.1038/537488b

Ochoa-Hueso, R., 2017. Global Change and the Soil Microbiome: A Human-Health Perspective. Front. Ecol. Evol. 5. https://doi.org/10.3389/fevo.2017.00071

Omoboye, O.O., Geudens, N., Duban, M., Chevalier, M., Flahaut, C., Martins, J.C., Leclère, V., Oni, F.E., Höfte, M., 2019a. Pseudomonas sp. COW3 Produces New

Bananamide-Type Cyclic Lipopeptides with Antimicrobial Activity against Pythium myriotylum and Pyricularia oryzae. Mol. Basel Switz. 24. https://doi.org/10.3390/molecules24224170

Omoboye, O.O., Oni, F.E., Batool, H., Yimer, H.Z., De Mot, R., Höfte, M., 2019b. Pseudomonas Cyclic Lipopeptides Suppress the Rice Blast Fungus Magnaporthe oryzae by Induced Resistance and Direct Antagonism. Front. Plant Sci. 10, 901. https://doi.org/10.3389/fpls.2019.00901

Oni, F.E., Geudens, N., Onyeka, J.T., Olorunleke, O.F., Salami, A.E., Omoboye, O.O., Arias, A.A., Adiobo, A., Neve, S.D., Ongena, M., Martins, J.C., Höfte, M., n.d. Cyclic lipopeptide-producing Pseudomonas koreensis group strains dominate the cocoyam rhizosphere of a Pythium root rot suppressive soil contrasting with P. putida prominence in conducive soils. Environ. Microbiol. n/a. https://doi.org/10.1111/1462-2920.15127

Orozco-Mosqueda, M. del C., Rocha-Granados, M. del C., Glick, B.R., Santoyo, G., 2018. Microbiome engineering to improve biocontrol and plant growth-promoting mechanisms. Microbiol. Res. 208, 25–31. https://doi.org/10.1016/j.micres.2018.01.005

Ossowicki, A., Jafra, S., Garbeva, P., 2017. The antimicrobial volatile power of the rhizospheric isolate Pseudomonas donghuensis P482. PloS One 12.

Ossowicki, A., Tracanna, V., Petrus, M.L.C., van Wezel, G., Raaijmakers, J.M., Medema, M.H., Garbeva, P., 2020. Microbial and volatile profiling of soils suppressive to Fusarium culmorum of wheat. Proc. R. Soc. B Biol. Sci. 287, 20192527. https://doi.org/10.1098/rspb.2019.2527

Ou, Y., Penton, C.R., Geisen, S., Shen, Z., Sun, Y., Lv, N., Wang, B., Ruan, Y., Xiong, W., Li, R., Shen, Q., 2019. Deciphering Underlying Drivers of Disease Suppressiveness Against Pathogenic Fusarium oxysporum. Front. Microbiol. 10, 2535. https://doi.org/10.3389/fmicb.2019.02535

Owen, J.G., Reddy, B.V.B., Ternei, M.A., Charlop-Powers, Z., Calle, P.Y., Kim, J.H., Brady, S.F., 2013. Mapping gene clusters within arrayed metagenomic libraries to expand the structural diversity of biomedically relevant natural products. Proc. Natl. Acad. Sci. https://doi.org/10.1073/pnas.1222159110

Pande, S., Kost, C., 2017. Bacterial Unculturability and the Formation of Intercellular Metabolic Networks. Trends Microbiol. 25, 349–361. https://doi.org/10.1016/j.tim.2017.02.015

Pandey, S.S., Patnana, P.K., Rai, R., Chatterjee, S., 2017. Xanthoferrin, the α-hydroxycarboxylate-type siderophore of Xanthomonas campestris pv. campestris, is required for optimum virulence and growth inside cabbage. Mol. Plant Pathol. 18, 949–962. https://doi.org/10.1111/mpp.12451

Park, Y.S., Dutta, S., Ann, M., Raaijmakers, J.M., Park, K., 2015. Promotion of plant growth by Pseudomonas fluorescens strain SS101 via novel volatile organic compounds. Biochem. Biophys. Res. Commun. 461, 361–365. https://doi.org/10.1016/j.bbrc.2015.04.039

Parks, D.H., Chuvochina, M., Chaumeil, P.-A., Rinke, C., Mussig, A.J., Hugenholtz, P., 2020. A complete domain-to-species taxonomy for Bacteria and Archaea. Nat. Biotechnol. 38, 1079–1086. https://doi.org/10.1038/s41587-020-0501-8

Paulson, J.N., Stine, O.C., Bravo, H.C., Pop, M., 2013. Differential abundance analysis for microbial marker-gene surveys. Nat. Methods 10, 1200. https://doi.org/10.1038/Nmeth.2658

Pedregosa, F., Varoquaux, G., Gramfort, A., Michel, V., Thirion, B., Grisel, O., Blondel, M., Prettenhofer, P., Weiss, R., Dubourg, V., Vanderplas, J., Passos, A., Cournapeau, D., Brucher, M., Perrot, M., Duchesnay, E., 2011. Scikit-learn: Machine Learning in Python. J. Mach. Learn. Res. 12, 2825–2830.

Pérez-Victoria, I., Oves-Costales, D., Lacret, R., Martín, J., Sánchez-Hidalgo, M., Díaz, C., Cautain, B., Vicente, F., Genilloud, O., Reyes, F., 2019. Structure elucidation and biosynthetic gene cluster analysis of caniferolides A–D, new bioactive 36-membered macrolides from the marine-derived Streptomyces caniferus CA-271066. Org. Biomol. Chem. 17, 2954–2971. https://doi.org/10.1039/C8OB03115K

Perincherry, L., Lalak-Kańczugowska, J., Stępień, Ł., 2019. Fusarium-Produced Mycotoxins in Plant-Pathogen Interactions. Toxins 11. https://doi.org/10.3390/toxins11110664

Peter, H., Beier, S., Bertilsson, S., Lindström, E.S., Langenheder, S., Tranvik, L.J., 2011. Function-specific response to depletion of microbial diversity. ISME J. 5, 351–361. https://doi.org/10.1038/ismej.2010.119

Philippot, L., Raaijmakers, J.M., Lemanceau, P., van der Putten, W.H., 2013. Going back to the roots: the microbial ecology of the rhizosphere. Nat. Rev. Microbiol. 11, 789–799. https://doi.org/10.1038/nrmicro3109

Pierik, R.L.M., 1997. Germination of orchid seeds, in: Pierik, R.L.M. (Ed.), In Vitro Culture of Higher Plants. Springer Netherlands, Dordrecht, pp. 149–158. https://doi.org/10.1007/978-94-011-5750-6_16

Pieterse, C.M.J., Zamioudis, C., Berendsen, R.L., Weller, D.M., Van Wees, S.C.M., Bakker, P.A.H.M., 2014. Induced Systemic Resistance by Beneficial Microbes. Annu. Rev. Phytopathol. 52, 347–375. https://doi.org/10.1146/annurev-phyto-082712-102340

Pii, Y., Cesco, S., Mimmo, T., 2015. Shoot ionome to predict the synergism and antagonism between nutrients as affected by substrate and physiological status. Plant Physiol. Biochem. PPB 94, 48–56. https://doi.org/10.1016/j.plaphy.2015.05.002

Pluskal, T., Castillo, S., Villar-Briones, A., Oresic, M., 2010. MZmine 2: Modular framework for processing, visualizing, and analyzing mass spectrometry-based molecular profile data. BMC Bioinformatics 11. https://doi.org/10.1186/1471-2105-11-395

Qi, Y., Beriot, N., Gort, G., Huerta Lwanga, E., Gooren, H., Yang, X., Geissen, V., 2020a. Impact of plastic mulch film debris on soil physicochemical and hydrological properties. Environ. Pollut. 266, 115097. https://doi.org/10.1016/j.envpol.2020.115097

Qi, Y., Ossowicki, A., Yang, X., Huerta Lwanga, E., Dini-Andreote, F., Geissen, V., Garbeva, P., 2020b. Effects of plastic mulch film residues on wheat rhizosphere and soil properties. J. Hazard. Mater. 387, 121711. https://doi.org/10.1016/j.jhazmat.2019.121711

Qi, Y., Ossowicki, A., Yang, X., Lwanga, E.H., Dini-Andreote, F., Geissen, V., Garbeva, P., 2019. Effects of plastic mulch film residues on wheat rhizosphere and soil properties. J. Hazard. Mater. 121711.

Qi, Y., Yang, X., Pelaez, A.M., Huerta Lwanga, E., Beriot, N., Gertsen, H., Garbeva, P., Geissen, V., 2018. Macro- and micro- plastics in soil-plant system: Effects of plastic mulch film residues on wheat (Triticum aestivum) growth. Sci. Total Environ. 645, 1048–1056. https://doi.org/10.1016/j.scitotenv.2018.07.229

Qian, J., Comin, M., 2019. MetaCon: unsupervised clustering of metagenomic contigs with probabilistic k-mers statistics and coverage. BMC Bioinformatics 20, 367. https://doi.org/10.1186/s12859-019-2904-4

Raaijmakers, J.M., Bonsall, R.E., Weller, D.M., 1999. Effect of population density of Pseudomonas fluorescens on production of 2,4-diacetylphloroglucinol in the rhizosphere of wheat. Phytopathology 89, 470–475. https://doi.org/Doi 10.1094/Phyto.1999.89.6.470

Raaijmakers, J.M., De Bruijn, I., Nybroe, O., Ongena, M., 2010. Natural functions of lipopeptides from *Bacillus* and *Pseudomonas* : more than surfactants and antibiotics. FEMS Microbiol. Rev. 34, 1037–1062. https://doi.org/10.1111/j.1574-6976.2010.00221.x

Raaijmakers, J.M., Mazzola, M., 2012. Diversity and Natural Functions of Antibiotics Produced by Beneficial and Plant Pathogenic Bacteria. Annu. Rev. Phytopathol. 50, 403–424. https://doi.org/10.1146/annurev-phyto-081211-172908

Raaijmakers, J.M., Mazzola, M., 2011. Diversity and Natural Functions of Antibiotics Produced by Beneficial and Plant Pathogenic Bacteria. Annu. Rev. Phytopathol. 50, 403–424. https://doi.org/10.1146/annurev-phyto-081211-172908

Raaijmakers, J.M., Paulitz, T.C., Steinberg, C., Alabouvette, C., Moënne-Loccoz, Y., 2009. The rhizosphere: a playground and battlefield for soilborne pathogens and beneficial microorganisms. Plant Soil 321, 341–361. https://doi.org/10.1007/s11104-008-9568-6

Raaijmakers, J.M., Vlami, M., de Souza, J.T., 2002. Antibiotic production by bacterial biocontrol agents. Antonie Van Leeuwenhoek 81, 537. https://doi.org/10.1023/A:1020501420831

Raaijmakers, J.M., Weller, D.M., 1998. Natural Plant Protection by 2,4-Diacetylphloroglucinol-Producing Pseudomonas spp. in Take-All Decline Soils. Mol. Plant-Microbe Interactions® 11, 144–152. https://doi.org/10.1094/MPMI.1998.11.2.144

Ramachandran, G., Bikard, D., 2019. Editing the microbiome the CRISPR way. Philos. Trans. R. Soc. B Biol. Sci. 374, 20180103. https://doi.org/10.1098/rstb.2018.0103

Ramankutty, N., Mehrabi, Z., Waha, K., Jarvis, L., Kremen, C., Herrero, M., Rieseberg, L.H., 2018. Trends in Global Agricultural Land Use: Implications for Environmental Health and Food Security. Annu. Rev. Plant Biol. 69, 789–815. https://doi.org/10.1146/annurev-arplant-042817-040256

Records, A.R., 2011. The type VI secretion system: a multipurpose delivery system with a phage-like machinery. Mol. Plant-Microbe Interact. MPMI 24, 751–757. https://doi.org/10.1094/MPMI-11-10-0262

Reddy, B.V.B., Milshteyn, A., Charlop-Powers, Z., Sean F. Brady, 2014. eSNaPD: a versatile, web-based bioinformatics platform for surveying and mining natural product biosynthetic diversity from metagenomes. Chem. Biol. 21, 1023–1033. https://doi.org/10.1016/j.chembiol.2014.06.007

Riah-Anglet, W., Trinsoutrot-Gattin, I., Martin-Laurent, F., Laroche-Ajzenberg, E., Norini, M.-P., Latour, X., Laval, K., 2015. Soil microbial community structure and function relationships: A heat stress experiment. Appl. Soil Ecol. 86, 121–130. https://doi.org/10.1016/j.apsoil.2014.10.001

Rice, P., Longden, I., Bleasby, A., 2000. EMBOSS: the European Molecular Biology Open Software Suite. Trends Genet. TIG 16, 276–277. https://doi.org/10.1016/s0168-9525(00)02024-2

Rillig, M.C., 2020. Plastic and plants. Nat. Sustain. 3, 887–888. https://doi.org/10.1038/s41893-020-0583-9

Rillig, M.C., Lehmann, A., 2020. Microplastic in terrestrial ecosystems. Science 368, 1430–1431. https://doi.org/10.1126/science.abb5979

Rillig, M.C., Muller, L.A., Lehmann, A., 2017. Soil aggregates as massively concurrent evolutionary incubators. ISME J. 11, 1943–1948. https://doi.org/10.1038/ismej.2017.56

Rillig, M.C., Mummey, D.L., 2006. Mycorrhizas and soil structure. New Phytol. 171, 41–53. https://doi.org/10.1111/j.1469-8137.2006.01750.x

Rodriguez-R, L.M., Gunturu, S., Tiedje, J.M., Cole, J.R., Konstantinidis, K.T., 2018. Nonpareil 3: Fast Estimation of Metagenomic Coverage and Sequence Diversity. mSystems 3. https://doi.org/10.1128/mSystems.00039-18

Roesch, L.F.W., Fulthorpe, R.R., Riva, A., Casella, G., Hadwin, A.K.M., Kent, A.D., Daroub, S.H., Camargo, F.A.O., Farmerie, W.G., Triplett, E.W., 2007. Pyrosequencing enumerates and contrasts soil microbial diversity. ISME J. 1, 283–290. https://doi.org/10.1038/ismej.2007.53

Roget, D.K., 1995. Decline in root rot (Rhizoctonia solani AG-8) in wheat in a tillage and rotation experiment at Avon, South Australia. Aust. J. Exp. Agric. 35, 1009–1013. https://doi.org/10.1071/ea9951009

Saha, M., Sarkar, S., Sarkar, B., Sharma, B.K., Bhattacharjee, S., Tribedi, P., 2016. Microbial siderophores and their potential applications: a review. Environ. Sci. Pollut. Res. 23, 3984–3999. https://doi.org/10.1007/s11356-015-4294-0

Saleem, M., Arshad, M., Hussain, S., Bhatti, A.S., 2007. Perspective of plant growth promoting rhizobacteria (PGPR) containing ACC deaminase in stress agriculture. J. Ind. Microbiol. Biotechnol. 34, 635–648. https://doi.org/10.1007/s10295-007-0240-6

Savary, S., Willocquet, L., Pethybridge, S.J., Esker, P., McRoberts, N., Nelson, A., 2019. The global burden of pathogens and pests on major food crops. Nat. Ecol. Evol. 3, 430–439. https://doi.org/10.1038/s41559-018-0793-y

Scher, F.M., Baker, R., 1982. Effect of Pseudomonas putida and a Synthetic Iron Chelator on Induction of Soil Suppressiveness to Fusarium Wilt Pathogens. 1982 72, 1567–1573. https://doi.org/10.1094/Phyto-72-1567.

Scher M., B.R., 1982. Effect of *Pseudomonas putida* and a Synthetic Iron Chelator on Induction of Soil Suppressiveness to Fusarium Wilt Pathogens. Phytopathology 72, 1567. https://doi.org/10.1094/Phyto-72-1567

Scherm, B., Balmas, V., Spanu, F., Pani, G., Delogu, G., Pasquali, M., Migheli, Q., 2013. Fusarium culmorum: causal agent of foot and root rot and head blight on wheat. Mol Plant Pathol 14, 323–41. https://doi.org/10.1111/mpp.12011

Schillinger, W.F., Paulitz, T.C., 2013. Natural Suppression of Rhizoctonia Bare Patch in a Long-Term No-Till Cropping Systems Experiment. Plant Dis. 98, 389–394. https://doi.org/10.1094/PDIS-04-13-0420-RE

Schlatter, D., Kinkel, L., Thomashow, L., Weller, D., Paulitz, T., 2017a. Disease Suppressive Soils: New Insights from the Soil Microbiome. Phytopathology 107, 1284–1297. https://doi.org/10.1094/Phyto-03-17-0111-Rvw

Schlatter, D., Kinkel, L., Thomashow, L., Weller, D., Paulitz, T., 2017b. Disease Suppressive Soils: New Insights from the Soil Microbiome. Phytopathology 107, 1284–1297. https://doi.org/10.1094/Phyto-03-17-0111-Rvw

Schmidt, Y., van der Voort, M., Crüsemann, M., Piel, J., Josten, M., Sahl, H.-G., Miess, H., Raaijmakers, J.M., Gross, H., 2014. Biosynthetic origin of the antibiotic cyclocarbamate brabantamide A (SB-253514) in plant-associated Pseudomonas. Chembiochem Eur. J. Chem. Biol. 15, 259–266. https://doi.org/10.1002/cbic.201300527

Schöler, A., Jacquiod, S., Vestergaard, G., Schulz, S., Schloter, M., 2017. Analysis of soil microbial communities based on amplicon sequencing of marker genes. Biol. Fertil. Soils 53, 485–489. https://doi.org/10.1007/s00374-017-1205-1

Schöner, T.A., Gassel, S., Osawa, A., Tobias, N.J., Okuno, Y., Sakakibara, Y., Shindo, K., Sandmann, G., Bode, H.B., 2016. Aryl Polyenes, a Highly Abundant Class of Bacterial Natural Products, Are Functionally Related to Antioxidative Carotenoids. ChemBioChem 17, 247–253. https://doi.org/10.1002/cbic.201500474

Schulz-Bohm, K., Zweers, H., de Boer, W., Garbeva, P., 2015. A fragrant neighborhood: volatile mediated bacterial interactions in soil. Front. Microbiol. 6. https://doi.org/10.3389/fmicb.2015.01212

Schwartz, D.J., Langdon, A.E., Dantas, G., 2020. Understanding the impact of antibiotic perturbation on the human microbiome. Genome Med. 12, 82. https://doi.org/10.1186/s13073-020-00782-x

Shannon, P., Markiel, A., Ozier, O., Baliga, N.S., Wang, J.T., Ramage, D., Amin, N., Schwikowski, B., Ideker, T., 2003. Cytoscape: a software environment for integrated models of biomolecular interaction networks. Genome Res. 13, 2498–2504. https://doi.org/10.1101/gr.1239303

Sharrar, A.M., Crits-Christoph, A., Méheust, R., Diamond, S., Starr, E.P., Banfield, J.F., 2020. Bacterial Secondary Metabolite Biosynthetic Potential in Soil Varies with Phylum, Depth, and Vegetation Type. mBio 11. https://doi.org/10.1128/mBio.00416-20

Shen, Z., Ruan, Y., Xue, C., Zhong, S., Li, R., Shen, Q., 2015. Soils naturally suppressive to banana Fusarium wilt disease harbor unique bacterial communities. Plant Soil 393, 21–33.

Sieber, C.M.K., Probst, A.J., Sharrar, A., Thomas, B.C., Hess, M., Tringe, S.G., Banfield, J.F., 2018. Recovery of genomes from metagenomes via a dereplication, aggregation

and scoring strategy. Nat. Microbiol. 3, 836–843. https://doi.org/10.1038/s41564-018-0171-1

Siegel-Hertz, K., Edel-Hermann, V., Chapelle, E., Terrat, S., Raaijmakers, J.M., Steinberg, C., 2018a. Comparative Microbiome Analysis of a Fusarium Wilt Suppressive Soil and a Fusarium Wilt Conducive Soil From the Chateaurenard Region. Front Microbiol 9. https://doi.org/ARTN 568 10.3389/fmicb.2018.00568

Siegel-Hertz, K., Edel-Hermann, V., Chapelle, E., Terrat, S., Raaijmakers, J.M., Steinberg, C., 2018b. Comparative Microbiome Analysis of a Fusarium Wilt Suppressive Soil and a Fusarium Wilt Conducive Soil From the Chateaurenard Region. Front. Microbiol. 9. https://doi.org/10.3389/fmicb.2018.00568

Singh, P., Vyas, D., 2009. Biocontrol of plant diseases and sustainable agriculture. Proc. Natl. Acad. Sci. India Sect. B - Biol. Sci. 79, 110–128.

Sinninghe Damsté, J.S., Rijpstra, W.I.C., Geenevasen, J.A.J., Strous, M., Jetten, M.S.M., 2005. Structural identification of ladderane and other membrane lipids of planctomycetes capable of anaerobic ammonium oxidation (anammox). FEBS J. 272, 4270–4283. https://doi.org/10.1111/j.1742-4658.2005.04842.x

Sintim, H.Y., Flury, M., 2017. Is Biodegradable Plastic Mulch the Solution to Agriculture's Plastic Problem? Environ. Sci. Technol. 51, 1068–1069. https://doi.org/10.1021/acs.est.6b06042

Soil Microbiology, Ecology and Biochemistry, 2015. . Elsevier. https://doi.org/10.1016/C2011-0-05497-2

Sousa, J.A. de J., Olivares, F.L., 2016. Plant growth promotion by streptomycetes: ecophysiology, mechanisms and applications. Chem. Biol. Technol. Agric. 3, 24. https://doi.org/10.1186/s40538-016-0073-5

Stachelhaus, T., Mootz, H.D., Marahiel, M.A., 1999. The specificity-conferring code of adenylation domains in nonribosomal peptide synthetases. Chem. Biol. 6, 493–505. https://doi.org/10.1016/S1074-5521(99)80082-9

Steinmetz, Z., Wollmann, C., Schaefer, M., Buchmann, C., David, J., Tröger, J., Muñoz, K., Frör, O., Schaumann, G.E., 2016. Plastic mulching in agriculture. Trading short-term agronomic benefits for long-term soil degradation? Sci. Total Environ. 550, 690–705. https://doi.org/10.1016/j.scitotenv.2016.01.153

Stingl, U., Cho, J.-C., Foo, W., Vergin, K.L., Lanoil, B., Giovannoni, S.J., 2008. Dilution-to-extinction culturing of psychrotolerant planktonic bacteria from permanently ice-covered lakes in the McMurdo Dry Valleys, Antarctica. Microb. Ecol. 55, 395–405. https://doi.org/10.1007/s00248-007-9284-4

Summerell, B.A., Laurence, M.H., Liew, E.C.Y., Leslie, J.F., 2010. Biogeography and phylogeography of Fusarium: a review. Fungal Divers. 44, 3–13. https://doi.org/10.1007/s13225-010-0060-2

Tamietti, G., Alabouvette, C., 1986. Studies on the Disease Suppressiveness of Soil .13. Role of Nonpathogenic Fusarium-Oxysporum in the Wilt-Suppression Mechanisms of a Soil Form Noirmoutier. Agronomie 6, 541–548. https://doi.org/DOI 10.1051/agro:19860606

Tecon, R., Or, D., 2017. Biophysical processes supporting the diversity of microbial life in soil. FEMS Microbiol. Rev. 41, 599–623. https://doi.org/10.1093/femsre/fux039

Tejman-Yarden, N., Robinson, A., Davidov, Y., Shulman, A., Varvak, A., Reyes, F., Rahav, G., Nissan, I., 2019. Delftibactin-A, a Non-ribosomal Peptide With Broad Antimicrobial Activity. Front. Microbiol. 10. https://doi.org/10.3389/fmicb.2019.02377

Tessler, M., Neumann, J.S., Afshinnekoo, E., Pineda, M., Hersch, R., Velho, L.F.M., Segovia, B.T., Lansac-Toha, F.A., Lemke, M., DeSalle, R., Mason, C.E., Brugler, M.R., 2017. Large-scale differences in microbial biodiversity discovery between 16S amplicon and shotgun sequencing. Sci. Rep. 7, 6589. https://doi.org/10.1038/s41598-017-06665-3

The Natural Product Domain Seeker NaPDoS: A Phylogeny Based Bioinformatic Tool to Classify Secondary Metabolite Gene Diversity [WWW Document], n.d. URL https://journals.plos.org/plosone/article?id=10.1371/journal.pone.0034064 (accessed 8.2.20).

Tracanna, V., Ossowicki, A., Petrus, M.L.C., Overduin, S., Terlow, B.R., Lund, G., Robinson, S.L., Warris, S., Schijlen, E.G.W.M., van Wezel, G.P., Raaijmakers, J.M., Garbeva, P., Medema, M.H., n.d. Dissecting disease suppressive rhizosphere microbiomes by functional amplicon sequencing and 10X metagenomics. mSystems. https://doi.org/submitted

Traxler, M.F., Watrous, J.D., Alexandrov, T., Dorrestein, P.C., Kolter, R., 2013. Interspecies Interactions Stimulate Diversification of the Streptomyces coelicolor Secreted Metabolome. mBio 4. https://doi.org/10.1128/mBio.00459-13

Trunk, K., Peltier, J., Liu, Y.-C., Dill, B.D., Walker, L., Gow, N.A.R., Stark, M.J.R., Quinn, J., Strahl, H., Trost, M., Coulthurst, S.J., 2018. The Type VI secretion system deploys anti-fungal effectors against microbial competitors. Nat. Microbiol. 3, 920–931. https://doi.org/10.1038/s41564-018-0191-x

Tsolakidou, M.-D., Stringlis, I.A., Fanega-Sleziak, N., Papageorgiou, S., Tsalakou, A., Pantelides, I.S., 2019. Rhizosphere-enriched microbes as a pool to design synthetic communities for reproducible beneficial outputs. FEMS Microbiol. Ecol. 95. https://doi.org/10.1093/femsec/fiz138

Tyc, O., de Jager, V.C.L., van den Berg, M., Gerards, S., Janssens, T.K.S., Zaagman, N., Kai, M., Svatos, A., Zweers, H., Hordijk, C., Besselink, H., de Boer, W., Garbeva, P., 2017. Exploring bacterial interspecific interactions for discovery of novel antimicrobial compounds. Microb. Biotechnol. 10, 910–925. https://doi.org/10.1111/1751-7915.12735

Tyc, O., van den Berg, M., Gerards, S., van Veen, J.A., Raaijmakers, J.M., de Boer, W., Garbeva, P., 2014. Impact of interspecific interactions on antimicrobial activity among soil bacteria. Front. Microbiol. 5, 567. https://doi.org/10.3389/fmicb.2014.00567

Valverde-Bogantes, E., Bianchini, A., Herr, J.R., Rose, D.J., Wegulo, S.N., Hallen-Adams, H.E., 2019. Recent population changes of Fusarium head blight pathogens: drivers and implications. Can. J. Plant Pathol. 42, 3,315-329. https://doi.org/10.1080/07060661.2019.1680442

van Agtmaal, M., Straathof, A.L., Termorshuizen, A., Lievens, B., Hoffland, E., de Boer, W., 2018. Volatile-mediated suppression of plant pathogens is related to soil

properties and microbial community composition. Soil Biol. Biochem. 117, 164–174. https://doi.org/10.1016/j.soilbio.2017.11.015

van Bruggen, A.H.C., Sharma, K., Kaku, E., Karfopoulos, S., Zelenev, V.V., Blok, W.J., 2015. Soil health indicators and Fusarium wilt suppression in organically and conventionally managed greenhouse soils. Appl. Soil Ecol. 86, 192–201. https://doi.org/10.1016/j.apsoil.2014.10.014

van der Meij, A., Worsley, S.F., Hutchings, M.I., van Wezel, G.P., 2017. Chemical ecology of antibiotic production by actinomycetes. FEMS Microbiol. Rev. 41, 392–416. https://doi.org/10.1093/femsre/fux005

van der Voort, M., Kempenaar, M., van Driel, M., Raaijmakers, J.M., Mendes, R., 2016. Impact of soil heat on reassembly of bacterial communities in the rhizosphere microbiome and plant disease suppression. Ecol. Lett. 19, 375–382. https://doi.org/10.1111/ele.12567

van Elsas, J.D., Chiurazzi, M., Mallon, C.A., Elhottovā, D., Krištůfek, V., Salles, J.F., 2012. Microbial diversity determines the invasion of soil by a bacterial pathogen. Proc. Natl. Acad. Sci. U. S. A. 109, 1159–1164. https://doi.org/10.1073/pnas.1109326109

Veliz, E.A., Martínez-Hidalgo, P., Hirsch, A.M., 2017. Chitinase-producing bacteria and their role in biocontrol. AIMS Microbiol. 3, 689–705. https://doi.org/10.3934/microbiol.2017.3.689

Verbon, E.H., Trapet, P.L., Stringlis, I.A., Kruijs, S., 2017. Iron and Immunity 24.

Vittorio Tracanna, 2020. Project title: dom2bgc [WWW Document]. URL https://git.wageningenur.nl/traca001/dom2bgc

Vos, M., Wolf, A.B., Jennings, S.J., Kowalchuk, G.A., 2013. Micro-scale determinants of bacterial diversity in soil. FEMS Microbiol. Rev. 37, 936–954. https://doi.org/10.1111/1574-6976.12023

Wachowska, U., Packa, D., Wiwart, M., 2017. Microbial Inhibition of Fusarium Pathogens and Biological Modification of Trichothecenes in Cereal Grains. Toxins 9. https://doi.org/10.3390/toxins9120408

Wagg, C., Bender, S.F., Widmer, F., van der Heijden, M.G.A., 2014. Soil biodiversity and soil community composition determine ecosystem multifunctionality. Proc. Natl. Acad. Sci. 111, 5266–5270. https://doi.org/10.1073/pnas.1320054111

Wang, P., Marsh, E.L., Ainsworth, E.A., Leakey, A.D.B., Sheflin, A.M., Schachtman, D.P., 2017. Shifts in microbial communities in soil, rhizosphere and roots of two major crop systems under elevated CO 2 and O 3. Sci. Rep. 7, 15019. https://doi.org/10.1038/s41598-017-14936-2

Watrous, J., Roach, P., Alexandrov, T., Heath, B.S., Yang, J.Y., Kersten, R.D., van der Voort, M., Pogliano, K., Gross, H., Raaijmakers, J.M., Moore, B.S., Laskin, J., Bandeira, N., Dorrestein, P.C., 2012. Mass spectral molecular networking of living microbial colonies. Proc. Natl. Acad. Sci. U. S. A. 109, E1743-1752. https://doi.org/10.1073/pnas.1203689109

Watson, A.G., Ford, E.J., 1972. Soil Fungistasis - Reappraisal. Annu. Rev. Phytopathol. Vol 50 10, 327. https://doi.org/10.1146/annurev.py.10.090172.001551

Weissman, K.J., Müller, R., 2009. A brief tour of myxobacterial secondary metabolism. Bioorg. Med. Chem. 17, 2121–2136. https://doi.org/10.1016/j.bmc.2008.11.025

Weller, D.M., Raaijmakers, J.M., Gardener, B.B.M., Thomashow, L.S., 2002a. Microbial populations responsible for specific soil suppressiveness to plant pathogens. Annu Rev Phytopathol 40, 309-+. https://doi.org/10.1146/annurev.phyto.40.030402.110010

Weller, D.M., Raaijmakers, J.M., Gardener, B.B.M., Thomashow, L.S., 2002b. Microbial populations responsible for specific soil suppressiveness to plant pathogens. Annu. Rev. Phytopathol. Vol 50 40, 309. https://doi.org/10.1146/annurev.phyto.40.030402.110010

Wheeler, T.J., Eddy, S.R., 2013. nhmmer: DNA homology search with profile HMMs. Bioinformatics 29, 2487–2489. https://doi.org/10.1093/bioinformatics/btt403

Wiese, M.V., 1987. Compendium of wheat diseases, 2nd ed, The Disease compendium series of the American Phytopathological Society. APS Press, St. Paul, Minn.

Wiseman, B.M., Neate, S.M., Keller, K.O., Smith, S.E., 1996. Suppression of Rhizoctonia solani anastomosis group 8 in Australia and its biological nature. Soil Biol. Biochem. 28, 727–732. https://doi.org/10.1016/0038-0717(95)00178-6

Wood, D.E., Lu, J., Langmead, B., 2019. Improved metagenomic analysis with Kraken 2. Genome Biol. 20, 257. https://doi.org/10.1186/s13059-019-1891-0

Wu, Y.-W., Simmons, B.A., Singer, S.W., 2016. MaxBin 2.0: an automated binning algorithm to recover genomes from multiple metagenomic datasets. Bioinformatics 32, 605–607. https://doi.org/10.1093/bioinformatics/btv638

Yair, S., Yaacov, D., Susan, K., Jurkevitch, E., 2009. Small Eats Big: Ecology and Diversity of Bdellovibrio and Like Organisms, and their Dynamics in Predator-Prey Interactions, in: Lichtfouse, E., Navarrete, M., Debaeke, P., Véronique, S., Alberola, C. (Eds.), Sustainable Agriculture. Springer Netherlands, Dordrecht, pp. 275–284. https://doi.org/10.1007/978-90-481-2666-8_18

Yamamoto, E., Muramatsu, H., Nagai, K., 2014. Vulgatibacter incomptus gen. nov., sp. nov. and Labilithrix luteola gen. nov., sp. nov., two myxobacteria isolated from soil in Yakushima Island, and the description of Vulgatibacteraceae fam. nov., Labilitrichaceae fam. nov. and Anaeromyxobacteraceae fam. nov. Int. J. Syst. Evol. Microbiol. 64, 3360–3368. https://doi.org/10.1099/ijs.0.063198-0

Yan, Y., Kuramae, E.E., de Hollander, M., Klinkhamer, P.G.L., van Veen, J.A., 2017. Functional traits dominate the diversity-related selection of bacterial communities in the rhizosphere. ISME J. 11, 56–66. https://doi.org/10.1038/ismej.2016.108

Yan, Y., Kuramae, E.E., Klinkhamer, P.G.L., Veen, J.A. van, 2015. Revisiting the Dilution Procedure Used To Manipulate Microbial Biodiversity in Terrestrial Systems. Appl. Environ. Microbiol. 81, 4246–4252. https://doi.org/10.1128/AEM.00958-15

Yang, Y., Liu, G., Song, W., Ye, C., Lin, H., Li, Z., Liu, W., 2019. Plastics in the marine environment are reservoirs for antibiotic and metal resistance genes. Environ. Int. 123, 79–86. https://doi.org/10.1016/j.envint.2018.11.061

Yin, C., Hulbert, S.H., Schroeder, K.L., Mavrodi, O., Mavrodi, D., Dhingra, A., Schillinger, W.F., Paulitz, T.C., 2013. Role of Bacterial Communities in the Natural Suppression of Rhizoctonia solani Bare Patch Disease of Wheat (Triticum aestivum L.). Appl. Environ. Microbiol. 79, 7428–7438. https://doi.org/10.1128/AEM.01610-13

Youdkes, D., Helman, Y., Burdman, S., Matan, O., Jurkevitch, E., 2020. Potential Control of Potato Soft Rot Disease by the Obligate Predators Bdellovibrio and Like Organisms. Appl. Environ. Microbiol. 86. https://doi.org/10.1128/AEM.02543-19

Yu, X., Polz, M.F., Alm, E.J., 2019. Interactions in self-assembled microbial communities saturate with diversity. ISME J. 13, 1602–1617. https://doi.org/10.1038/s41396-019-0356-5

Yuan, J., Wen, T., Zhang, H., Zhao, M., Penton, C.R., Thomashow, L.S., Shen, Q., 2020. Predicting disease occurrence with high accuracy based on soil macroecological patterns of Fusarium wilt. ISME J. 1–15. https://doi.org/10.1038/s41396-020-0720-5

Zegeye, E.K., Brislawn, C.J., Farris, Y., Fansler, S.J., Hofmockel, K.S., Jansson, J.K., Wright, A.T., Graham, E.B., Naylor, D., McClure, R.S., Bernstein, H.C., 2019. Selection, Succession, and Stabilization of Soil Microbial Consortia. mSystems 4. https://doi.org/10.1128/mSystems.00055-19

Zehnder, G.W., Murphy, J.F., Sikora, E.J., Kloepper, J.W., 2001. Application of Rhizobacteria for Induced Resistance. Eur. J. Plant Pathol. 107, 39–50. https://doi.org/10.1023/A:1008732400383

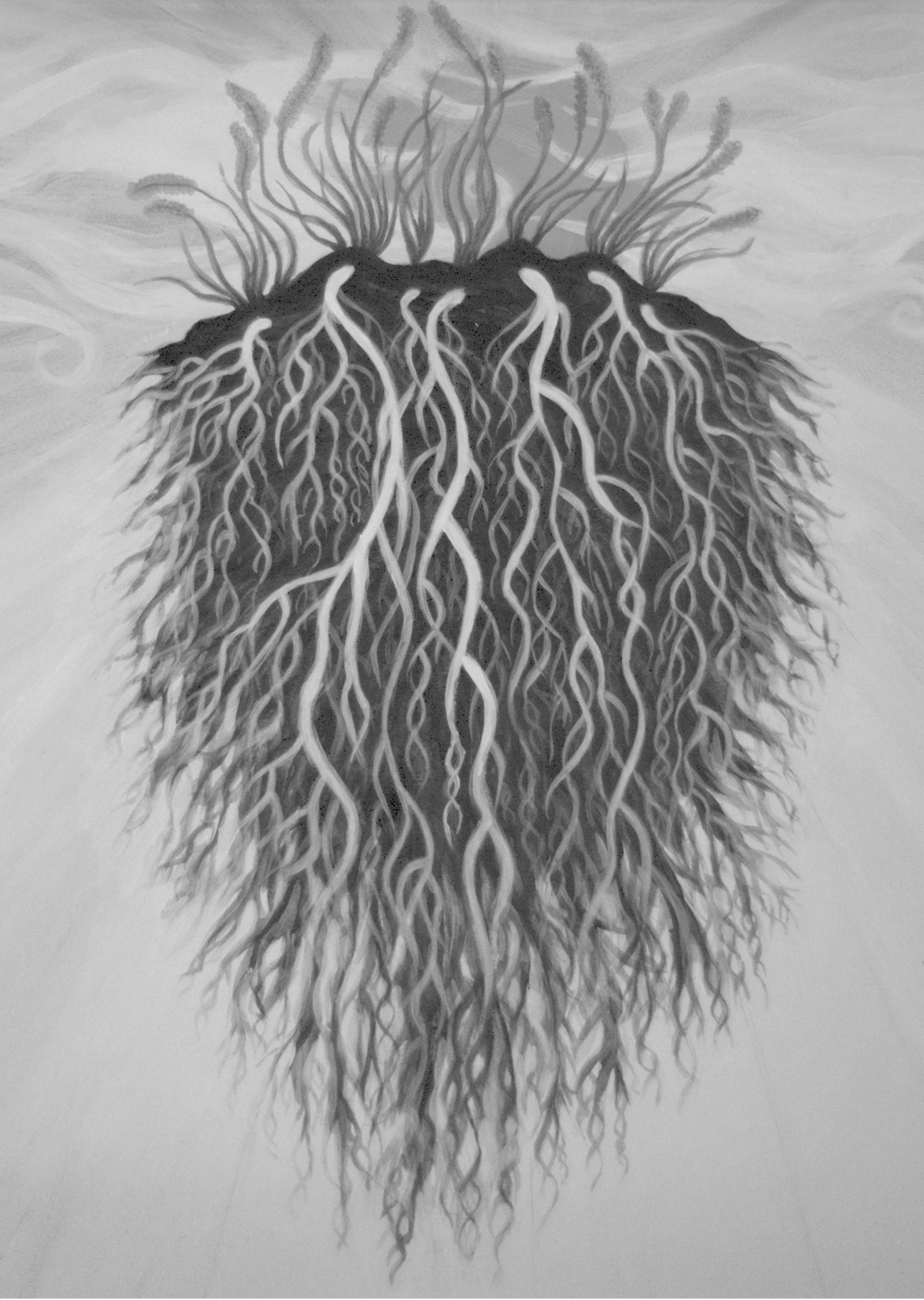
Zhang, Dong, Lu, Y., Chen, H., Wu, C., Zhang, H., Chen, L., Chen, X., 2020. Antifungal peptides produced by actinomycetes and their biological activities against plant diseases. J. Antibiot. (Tokyo) 73, 265–282. https://doi.org/10.1038/s41429-020-0287-4

Zhang, Dan, Ng, E.L., Hu, W., Wang, H., Galaviz, P., Yang, H., Sun, W., Li, C., Ma, X., Fu, B., Zhao, P., Zhang, F., Jin, S., Zhou, M., Du, L., Peng, C., Zhang, X., Xu, Z., Xi, B., Liu, X., Sun, S., Cheng, Z., Jiang, L., Wang, Y., Gong, L., Kou, C., Li, Y., Ma, Y., Huang, D., Zhu, J., Yao, J., Lin, C., Qin, S., Zhou, L., He, B., Chen, D., Li, H., Zhai, L., Lei, Q., Wu, S., Zhang, Y., Pan, J., Gu, B., Liu, H., 2020. Plastic pollution in croplands threatens long-term food security. Glob. Change Biol. 26, 3356–3367. https://doi.org/10.1111/gcb.15043

Zhao, M.L., Yuan, J., Zhang, R.F., Dong, M.H., Deng, X.H., Zhu, C.Z., Li, R., Shen, Q.R., 2018. Microflora that harbor the NRPS gene are responsible for Fusarium wilt disease-suppressive soil. Appl. Soil Ecol. 132, 83–90. https://doi.org/10.1016/j.apsoil.2018.08.022

Zhou, B., Wang, J., Zhang, H., Shi, H., Fei, Y., Huang, S., Tong, Y., Wen, D., Luo, Y., Barceló, D., 2020. Microplastics in agricultural soils on the coastal plain of Hangzhou Bay, east China: Multiple sources other than plastic mulching film. J. Hazard. Mater. 388, 121814. https://doi.org/10.1016/j.jhazmat.2019.121814

Zimmermann, L., Dombrowski, A., Völker, C., Wagner, M., 2020. Are bioplastics and plant-based materials safer than conventional plastics? In vitro toxicity and chemical composition. Environ. Int. 145, 106066. https://doi.org/10.1016/j.envint.2020.106066



Summary

Soil holds an enormous diversity of microbial life that is essential for the functioning of terrestrial ecosystems. Bacteria, fungi, protists, viruses and other organisms living is the soil colonise plant roots in response to root exudates and form a rhizosphere – a remarkable ecosystem where microorganisms live in close association with plant roots. The rhizosphere microbiome is known to provide beneficial services to plants like nutrient acquisition, growth promotion or directly and indirectly protecting against biotic and abiotic stresses. In contrast to beneficial plant-associated microorganisms, plant pathogens are a major threat causing reduced yields and contaminated food products. Their control requires the application of environmentally hazardous pesticides. Cereals and also other crops suffer severely from pathogenic fungi from the genus *Fusarium*. Those pathogens not only significantly reduce the yield but contaminate the harvest with mycotoxins making it unfit for consumption. In my thesis, I studied soils that are suppressive to *Fusarium culmorum* of wheat. These soils provide a natural protection against root infections which is mediated by the activity of soil microbial community. Those soils are recognised worldwide but, in most cases, the exact mechanisms of microbiome-based crop protection are unclear. The overall aim of my thesis was to disentangle the microorganisms and mechanisms involved in disease suppressiveness to *F. culmorum* of wheat.

We started the investigation on soil suppressiveness by performing a phenotypic screening of 28 field soils from the Netherlands and Germany to identify suppressive soils. Four soils exhibited a high level of disease suppressiveness to *F. culmorum* and via soil sterilization and soil transplantation we showed that the protective effect observed in the four suppressive soils is (micro)biological in nature. After comparing bacterial taxonomy profiles, physical and chemical parameters we found that different *F. culmorum* suppressive soils do not share the same microbial taxonomic patterns nor physical or chemical characteristics. Our results further showed that the emissions of volatiles from the soil microbiome may contribute to disease suppressiveness of some soils, but not for all. Subsequently we analyzed the profiles of adenylation domain (A-domain) functional genes. Those genes are part of biosynthetic genes clusters encoding secondary metabolites like polyketides, non-ribosomal peptides or terpenes, metabolites often associated with microbial interactions and suppression of plant pathogens in suppressive soils. Based on A-domain profiles we found that the *F. culmorum* suppressive soils share a similar A-domain community structure. These bioinformatic analyses further suggested a possible role of siderophores and competition for iron in disease suppressiveness. The microbiome of suppressive soil showing the highest level of protection – soil S11, was then subjected to perturbation by dilution-to-extinction by transferring serial dilutions of an extracted suppressive soil S11

microbiome to a sterile soil. In the wheat-Fusarium bioassays with diluted microbiomes, we showed the transferability of suppressiveness and a non-linear relationship between suppressiveness and microbiome dilution. Subsequent analysis of wheat rhizosphere metagenomes along the dilution trajectory revealed a significant reduction of genetic diversity and significant changes in microbial community composition. Bacterial taxa previously associated with suppressiveness and soil fertility (ex. Streptomycetes, Acidobacteria and Verrucomicrobia) significantly decreased in relative abundance with higher dilutions of the microbiome. Moreover, in low dilutions that still conferred suppressiveness, we found an enrichment of genes related to iron uptake, chitinases and elements of type six secretion system. Furthermore, we discovered an association between suppressiveness and nine metagenome-assembled bacterial genomes carrying various novel biosynthetic gene clusters. Altogether, the dilution-to-extinction approach pointed to several mechanisms of disease suppression that need to be validated in future research. Finally, we evaluated the impact of plastic film residues on the soil microbiome, disease suppressiveness and plant growth. We found that the addition of plastic to the soil in short term does not affect the soil suppressiveness to *F. culmorum* but has a negative impact on plant biomass and nutrient status. We also found that plastic residues in soil create a new niche populated by significantly different microbiota that, in a longer term, may affect soil microbiome diversity and functioning.

In conclusion, this thesis presents the identification of disease suppressive soils, putative microbes, mechanisms, genes and metabolites associated with suppressiveness, as well as the environmental impact of microplastics on the soil microbiome, plant growth and plant health. Based on the results obtained, several new hypotheses were generated to further disentangle plant-associated microbiome functioning in the context of protection against biotic stress and the exposure to microplastic pollution of soil ecosystems.

Streszczenie

Gleba jest siedliskiem zróżnicowanych mikroorganizmów będących niezbędnymi do funkcjonowania ekosystemów lądowych. Bakterie, grzyby, protisty, wirusy i inne mikroorganizmy żyjące w glebie zasiedlają korzenie roślin w odpowiedzi na związki chemiczne wydzielanie przez nie tworząc ryzosferę – nadzwyczajny ekosystem, w którym mikroorganizmy żyją w ścisłej współpracy z roślinami. Pula mikroorganizmów (mikrobiom) zasiedlających ryzosferę pełni funkcje mające korzystny wpływ na rośliny takie jak: udział w pobieraniu związków pokarmowych, wydziałanie związków promujących wzrost roślin lub też pośredni albo bezpośredni udział w ochronie rośliny przed czynnikami biologicznymi (np. patogenami) lub fizycznymi. W przeciwieństwie do mikrobiomu pełniącego korzystne funkcje względem roślin w glebie występują też mikroorganizmy patogenne które wywołując choroby stanowią istotny element redukujący plony lub czyniący plon niezdatnym do użytku poprzez kontaminację produktami swojego metabolizmu (np. toksynami). Zwykle ochrona upraw przed chorobami wymaga stosowania środków ochrony roślin, które wywierają zgubny wpływ na środowisko jak i obniżają jakość upraw. Szczególnie zboża, ale także inne uprawy, są często ofiarą patogennych grzybów z rodzaju *Fusarium.* Patogeny te nie tylko znacząco obniżają plony, ale także zanieczyszczają ziarno mykotoksynami powodują ich niezdatność do spożycia. W mojej pracy, zajmowałem się tak zwanymi glebami hamującymi, których unikalny mikrobiom nie dopuszczają do wykształcenia symptomów chorobowych pomimo obecności patogenu oraz sprzyjających warunków do wystąpienia choroby. Dokładnie, glebami hamującymi na których pszenica nie przejawiała symptomów chorobowych wywołanych przez patogen grzybowy *Fusarium culmorum*. Gleby hamujące są rozpoznawane na całym świecie, niemniej jednak w większości przypadków, pomimo rozpoznania biologicznych podstaw aktywności, dokładne mechanizmy ich działania są niejasne. Głównym celem mojej pracy jest rozwikłanie mechanizmów biologicznej aktywności gleb hamujących zaangażowanych w ochronę pszenicy przed *F. culmorum*.

Rozpoczęliśmy naszą pracę od przesiewowego badania gleb znajdujących się na terenie Holandii i Niemiec pod kątem fenotypu gleby hamującej. Wśród 28 przetestowanych przez nas prób, w 4 znaleźliśmy wysoki poziom hamowania *F. culmorum,* po czym poprzez sterylizację i transplantację gleby wykazaliśmy, że hamowanie to ma podłoże (mikro)biologiczne. Po przeanalizowaniu profili taksonomicznych mikrobiomów wszystkich analizowanych przez nas gleb jak i ich właściwości fizyko-chemicznych, wykazaliśmy, że gleby hamujące z naszej kolekcji nie wykazują znaczących podobieństw w ani w profilu taksonomicznym mikrobiomu, ani w charakterystyce fizyko-chemicznej. Nasze kolejne badania wykazały, że związki lotne emitowane przez mikroorganizmy zasiedlające badane

przez nas gleby hamujące mogą mieć związek z obserwowaną ochroną pszenicy, ale nie w każdym przypadku. Następnie, przeanalizowaliśmy profile genów funkcyjnych domen adenylacji. Są one elementami klastrów genów biosyntezy metabolitów wtórnych takich jak: poliketydy, peptydy pochodzenia nierybosomalnego czy terpeny. Produkcja tych metabolitów jest często powiązana z mechanizmami ochrony roślin występującymi w glebach hamujących. Analiza profili domen adenylacji wykazała, że badane przez nas gleby hamujące posiadają podobną strukturę sieci tych domen. Dalsze analizy bioinformatyczne oparte o te profile sugerują istotną rolę sideroforów oraz konkurencji o żelazo w badanych przez nas glebach hamujących. Mikrobiom gleby hamującej wykazującej najwyższy poziom ochrony przed patogenem – gleby S11, został przez nas poddany analizie z udziałem perturbacji poprzez jego ekstrakcję, seryjne rozcieńczenie oraz wprowadzenie do sterylnej gleby. W testach fenotypowych wykazaliśmy, że mikrobiom gleby S11 poddany takiej perturbacji nadal jest w stanie chronić pszenicę przed patogenem jednak traci tą zdolność wraz ze wzrastającym rozcieńczeniem w sposób nieliniowy. Następnie, przeanalizowaliśmy dane metagenomowe uzyskane z sekwencjonowania mikrobiomów ryzosfery pszenicy hodowanej w tym eksperymencie wykazując, znaczące zmiany w różnorodności genetycznej oraz strukturze mikrobiomu pomiędzy rozcieńczeniami. Grupy bakterii uprzednio powiązane z żyznością gleby oraz glebami hamującymi (np. Streptomycetes, Acidobacteria and Verrucomicrobia) znacząco zmniejszyły swój względny udział w mikrobiomie przy wyższych rozcieńczeniach. Ponadto, przy niższych rozcieńczeniach, które wciąż znacząco chroniły pszenicę przed patogenem, znaleźliśmy wysoki udział genów związanych z pobieraniem żelaza przez mikroorganizmy, chitynaz oraz elementów systemu sekrecji typu szóstego. Znaleźliśmy także związek pomiędzy hamowaniem patogenu, a obecnością dziewięciu genomów bakterii uzyskanych z metagenomów, które posiadają szereg nowych, nie-opisanych wcześniej biosyntetycznych klastrów genów. W końcu, zbadaliśmy wpływ plastiku w glebie hamującej na jej mikrobiom, wzrost roślin oraz hamowanie patogenu. Wykazaliśmy, że pomimo braku wpływu plastiku na przeciwdziałanie rozwojowi choroby, ma on negatywny wpływ na biomasę rośliny oraz jej stan odżywienia. Ponadto, obecność cząstek plastiku w glebie tworzy nową niszę ekologiczną która może mieć dalekosiężny wpływ na bioróżnorodność oraz funkcjonowanie gleby.

Podsumowując, praca ta zawiera identyfikację gleb hamujących oraz domniemanych mikroorganizmów, genów, metabolitów i mechanizmów leżących u podstaw ich funkcjonowania, jak również badania nad wpływem plastiku w glebie na jej mikrobiom, funkcjonowanie i zdrowie roślin. W oparciu o uzyskane wyniki udało nam się wygenerować szereg hipotez których weryfikacja będzie prowadziła do przybliżenia rozwikłania biologicznych mechanizmów aktywności gleb hamujących oraz wpływu plastiku na ekosystemy lądowe.

Curriculum Vitae



Adam Stanisław Ossowicki was born on 26th of March 1988 in Gdynia, Poland. After finishing high school (Pierwsze Akademickie Liceum Ogólnokształcące in Gdynia) in 2007, he decided to study biotechnology at the Intercollegiate Faculty of Biotechnology UG&MUG what resulted in BSc (2010) and MSc degree (2012). After defending the MSc thesis, he started working in Laboratory of Biological Plant Protection IFB UG&MUG under supervision of his MSc thesis promoter Prof. UG dr hab. Sylwia Jafra on biocontrol traits of Pseudomonads. In the course of his academic education, Adam did internships in the Institute of Oceanology Polish Academy of Science working on characterisation of marine bacteriophages; Centre of Biomolecular Sciences, University of Nottingham working on the molecular biology and metabolomics of Pseudomonads and two internships in the Netherlands Institute of Ecology NIOO-KNAW. One of these internships resulted in moving to the Netherlands and starting his PhD in the group of dr Paolina Garbeva in 2016. Starting with the MSc project Adam has been working in soil microbiology field what continues until the present day together with fascination with little forms of life and big mountains. He will now continue his career as a postdoc in the lab of dr Roey Angel in Biologické centrum AVČR in České Budějovice, Czechia working on interactions between Actinobacteria and soil fauna.

Publications

Czajkowski, R., Ozymko, Z., Siwinska, J., **Ossowicki, A.**, de Jager, V., Narajczyk, M., & Lojkowska, E. (2015). The complete genome, structural proteome, comparative genomics and phylogenetic analysis of a broad host lytic bacteriophage φD3 infecting pectinolytic Dickeya spp. *Standards in Genomic Sciences*, *10*(1), 68.

Czajkowski, R., Ozymko, Z., de Jager, V., Siwinska, J., Smolarska, A., **Ossowicki, A.**, … Lojkowska, E. (2015). Genomic, proteomic and morphological characterization of two novel broad host lytic bacteriophages ΦPD10. 3 and ΦPD23. 1 infecting pectinolytic Pectobacterium spp. and Dickeya spp. *PLoS One*, *10*(3).

Krzyżanowska, D. M., **Ossowicki, A.**, Rajewska, M., Maciąg, T., Jabłońska, M., Obuchowski, M., … Jafra, S. (2016). When genome-based approach meets the "old but good": revealing genes involved in the antibacterial activity of Pseudomonas sp. P482 against soft rot pathogens. *Frontiers in Microbiology*, *7*, 782.

Ossowicki, A., Jafra, S., & Garbeva, P. (2017). The antimicrobial volatile power of the rhizospheric isolate Pseudomonas donghuensis P482. *PloS One*, *12*(3).

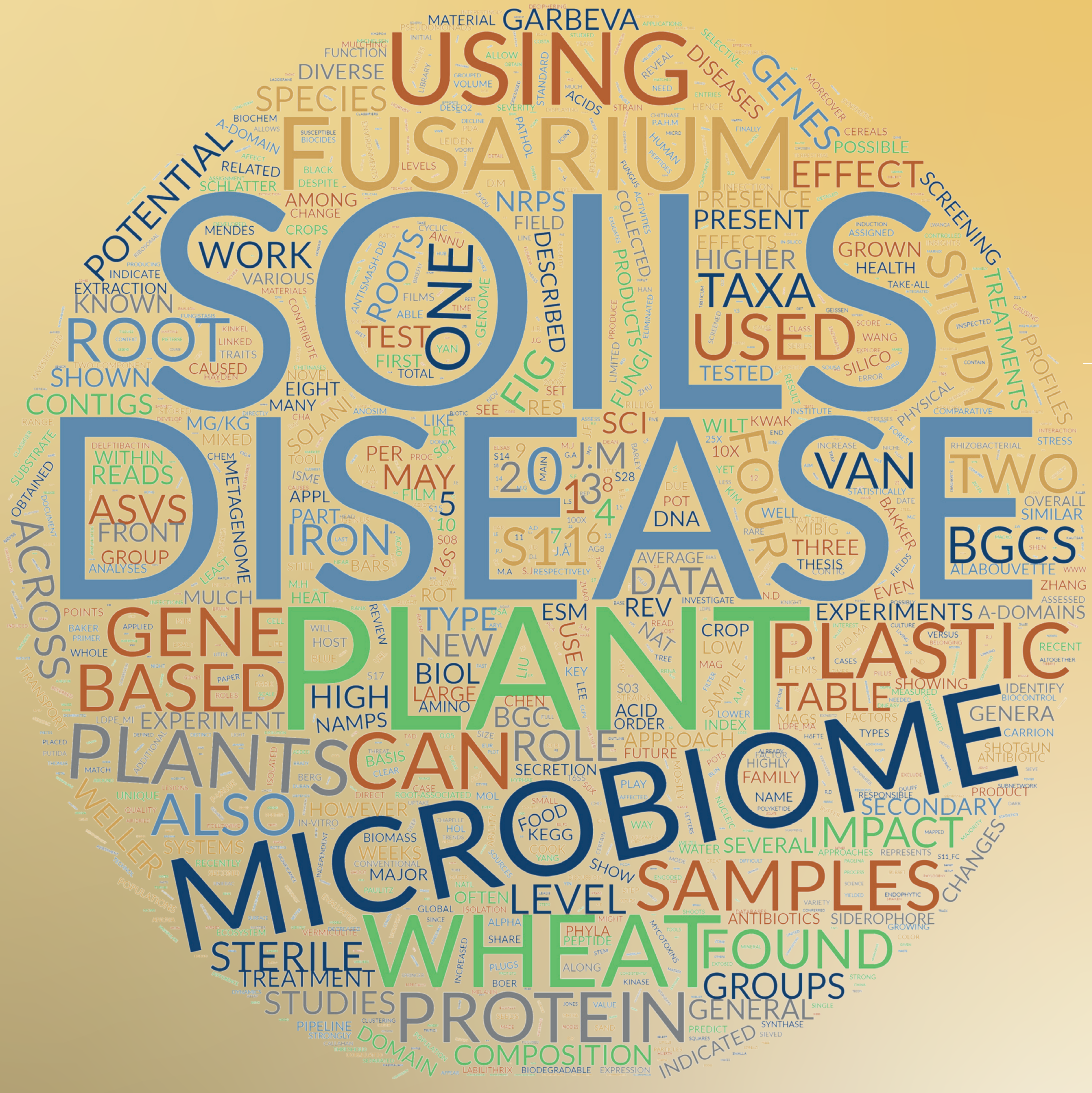
Krzyżanowska, D. M., Maciąg, T., **Ossowicki, A.**, Rajewska, M., Kaczyński, Z., Czerwicka, M., … Jafra, S. (2019). Ochrobactrum quorumnocens sp. nov., a quorum quenching bacterium from the potato rhizosphere, and comparative genome analysis with related type strains. *PloS One*, *14*(1).

Qi, Y., **Ossowicki, A.**, Yang, X., Lwanga, E. H., Dini-Andreote, F., Geissen, V., & Garbeva, P. (2019). Effects of plastic mulch film residues on wheat rhizosphere and soil properties. *Journal of Hazardous Materials*, 121711.

Ossowicki, A.*, Tracanna, V., Petrus, M. L. C., van Wezel, G., Raaijmakers, J. M., Medema, M. H., & Garbeva, P. (2020). Microbial and volatile profiling of soils suppressive to Fusarium culmorum of wheat. *Proceedings of the Royal Society B: Biological Sciences*, *287*(1921), 20192527.

Tracanna, V., **Ossowicki, A*.**, Petrus, M.L.C., Overduin, S., Terlouw, B.R., Lund, G., Robinson, S.L., Warris, S., Schijlen, E.G.W.M., van Wezel, G.P., Raaijmakers, J.M., Garbeva, P., Medema, M.H. (2021) Dissecting disease-suppressive rhizosphere microbiomes by functional amplicon sequencing and 10X metagenomics. mSystems in press.

*shared first authorship


SOILS
DISEASE
MICROBIOME
PLANT
PLASTIC
FUSARIUM
WHEAT
SAMPLES
PROTEIN
USING
GENE
BASED
PLANTS
SCAN
ROLE
IMPACT
SECONDARY
FOUND
GROUPS
TAXA
USED
EFFECT
STUDY
ROOT
IRON
ACROSS
ALSO
STERILE
TREATMENT
LEVEL
COMPOSITION
GARBEVA
SPECIES
POTENTIAL
ONE
TWO
VAN
BGCS
DATA
TABLE
EXPERIMENTS
A-DOMAINS
GENERA
SHOTGUN
ANTIBIOTIC
CARRION
IDENTIFY
BIOCONTROL
SIDEROPHORE
ANTIBIOTICS
CHANGES
SEVERAL
WATER
FAMILY
NAME
RESPONSIBLE
PRODUCT
SHOWING
RECENT
ASSESSED
ZHANG
ALABOUVETTE
OVERALL
SIMILAR
BAKKER
EVEN
THREE
THESIS
AVERAGE
DNA
POT
FOUR
WILT
KWAK
PHYSICAL
SILICO
WANG
GROWN
HEALTH
TAKE-ALL
PRESENCE
PRESENT
HIGHER
EFFECTS
TREATMENTS
PROFILES
STRESS
RHIZOBACTERIAL
COMPARATIVE
INSTITUTE
INCREASE
10X
25X
YET
WELL
RARE
MIBIG
STATISTICALLY
DATE
FIELDS
SHEN
WWW
ASSESSED
VERSUS
CULTURE
CASES
HEMS
MEASURES
FACTORS
TYPES
INDUCTION
ASSIGNED
SCORE
INSPECTED
CONTAIN
ENDOPHYTIC
GROWING
SYNTHASE
SILVELD
INDICATED
PREDICT
GENERAL
SINGLE
KINASE
STRONG
BOER
PLUGS
ALONG
PEPTIDE
PHYLA
SHARE
ALPHA
ISOLATION
GLOBAL
SINCE
VARIETY
OFTEN
SHOW
MAJOR
WEEKS
BIOMASS
HOWEVER
WELLER
SYSTEMS
FOOD
KEGG
MAGS
LOWER
INDEX
ORDER
ACID
APPROACH
FUTURE
SECRETION
HIGHLY
PLAY
WAY
APPROACHES
REPRESENTS
S11
FC
NAMPS
BGC
HIGH
AMINO
LARGE
BIOL
NEW
TYPE
ESM
REV
NAT
CROP
LOW
SAMPLE
KEY
USEY
LIU
CHEN
S03
EXPERIMENT
MULCH
HEAT
ROT
REVIEW
HOST
WHOLE
POINTS
APPLIED
WILL
517
PAPER
DOI
MI
PLASTIC
MATCH
UNIQUE
BASIS
CLEAR
CASE
DIRECT
IN-VITRO
MOL
MAG
HOL
BIOMASS
SHARE
PEPTIDE
PHYLA